Efficacité thérapeutique de l'association radiothérapie+inhibiteur de KRASG12C MRTX1257 (Mirati Labs) sur modèle pré-clinique muté KRASG12C

Marina Milic

THÈSE DE DOCTORAT

NNT : 2023UPASL152

université PARIS-SACLAY

Therapeutic efficacy of the combination radiotherapy+ KRAS^{G12C} inhibitor MRTX1257 (Mirati Labs) in preclinical KRAS^{G12C} mutant models

Efficacité thérapeutique de l'association radiothérapie+inhibiteur de KRAS^{G12C} MRTX1257 (Mirati Labs) sur modèle pré-clinique muté KRAS^{G12C}

Thèse de doctorat de l'université Paris-Saclay

École doctorale n°582, Cancérologie : Biologie – Médecine – Santé (CBMS)
Spécialité de doctorat : Sciences du Cancer
Graduate School : Sciences de la vie et santé. Référent : Faculté de Médecine

Thèse préparée dans l'unité de recherche Radiothérapie Moléculaire et Innovation Thérapeutique (Institut Gustave Roussy, INSERM),
sous la direction du Professeur **Éric DEUTSCH**

Thèse soutenue à Paris-Saclay, le 12 décembre 2023, par

Marina MILIC

Composition du Jury

Membres du jury avec voix délibérative

Pr Christophe Massard Professeur, HDR, Université Paris Saclay	Président
Pr Nicolas Magné Professeur, Centre Bergonié Bordeaux	Rapporteur & Examinateur
Dr Martin Forster MD, Associate Professor, University College London	Rapporteur & Examinateur
Dr Céline Mirjolet PhD, HDR, Centre GF Leclerc, Dijon	Examinatrice

université PARIS-SACLAY | ÉCOLE DOCTORALE Cancérologie : biologie - médecine - santé (CBMS)

Titre : ***Efficacité thérapeutique de l'association radiothérapie+inhibiteur de KRAS^{G12C} MRTX1257 (Mirati Labs) sur modèle pré-clinique muté KRAS^{G12C}***

Mots clés : radiothérapie, KRAS^{G12C}, inhibiteurs de KRAS , MRTX1257, radio-sensibilisation

Résumé : Les mutations activatrices du gène KRAS sont les plus fréquents drivers oncogéniques et sont corrélées avec la radiorésistance dans de multiples cancers y compris le cancer bronchique non à petites cellules (CBNPC) et le cancer colorectal. Même si KRAS était considéré comme impossible à cibler jusqu'à très récemment, plusieurs inhibiteurs de KRAS ont atteint le stade de développement clinique et deux d'entre eux, sotorasib (AMG510, Amgen) et adagrasib (MRTX849, Mirati Therapeutics) ont été autorisés par la FDA dans le traitement des cancers CBNPC KRAS^{G12C} mutés.

MRTX849 a montré des résultats cliniques encourageants dans le traitement de patients sélectionnés atteints de cancers bronchiques et colorectaux, cependant très peu de données sur la combinaison radiothérapie (RT) et inhibition de KRAS dans les tumeurs KRAS mutées sont disponibles actuellement.

Dans ce travail, nous avons démontré que MRTX1257, inhibiteur covalent de KRAS^{G12C}, et similaire à MRTX849, était en mesure d'augmenter l'effet cytotoxique de la RT dans différents modèles cellulaires *KRAS^{G12C}* ainsi que dans les modèles murins, mais pas chez leurs homologues *KRAS^{G12C}* wild type (WT).

Les effets radiosensibilisants à la fois *in vitro* et *in vivo* ont été observés de manière temps et dose dépendante. De plus, l'utilisation de la RT et MRTX1257 chez les souris BALB/c portant des tumeurs CT26 KRAS$^{G12C+/+}$ a permis d'obtenir un taux de guérison de 20%. L'analyse du microenvironment immunitaire tumoral des tumeurs murines CT26 KRAS$^{G12C+/+}$ après RT et MRTX1257 a montré une augmentation de la proportion de plusieurs sous-types cellulaires, y compris lymphocytes CD4^{+} conventionnels, cellules dendritiques de type 2 (cDC2) et monocytes inflammatoires. De plus, l' expression de PD-L1 était drastiquement diminuée au sein des cellules tumorales et cellules myéloides , illustrant la polarization du microenvironnement tumoral vers un phénotype pro-inflammatoire suite à la combinaison.

Title : Therapeutic efficacy of the combination radiotherapy+ KRAS^{G12C} inhibitor MRTX1257 (Mirati Labs) in preclinical KRAS^{G12C} mutant models

Keywords : radiotherapy, KRAS^{G12C}, KRAS inhibitors, MRTX1257, radio-sensitizing

Abstract : *KRAS* activating mutations are considered the most frequent oncogenic drivers and are correlated with radio-resistance in multiple cancers including non-small cell lung cancer (NSCLC) and colorectal cancer. Although KRAS was considered undruggable until recently, several KRAS inhibitors have reached clinical development and two of them, sotorasib (AMG510, Amgen) and adagrasib (MRTX849, Mirati Therapeutics) have been approved in 2022 by the FDA for the treatment of *KRAS^{G12C}* mutant NSCLC.

MRTX849 showed encouraging clinical outcomes for the treatment of selected patients with NSCLC and colorectal cancers, however, only scarce data exploring the combination of radiotherapy (RT) and KRAS inhibition in *KRAS* mutated tumors are available.

In this work, we demonstrated that MRTX1257, a potent covalent KRAS^{G12C} inhibitor similar to MRTX849, was able to increase the cytotoxic effect of RT in different *KRAS^{G12C}* mutated cell lines and murine tumors, but not in their *KRAS^{G12C}* wild type (WT) counterparts.

Both *in vitro* and *in vivo* radio-sensitizing effects were observed in a time and dose dependent manner. Moreover, the use of RT and MRTX1257 in BALB/c mice bearing CT26 KRAS$^{G12C+/+}$ tumors resulted in an observable cure rate of 20%. The analysis of the tumor immune microenvironment of murine CT26 KRAS$^{G12C+/+}$ tumors following RT and MRTX1257 showed an increase in the proportion of various cell subtypes including conventional CD4^{+} T cells, dendritic cells type 2 (cDC2) and inflammatory monocytes. Moreover, the expression of PD-L1 was dramatically reduced within tumor cells and myeloid cells, thus illustrating the polarization of the tumor microenvironment towards a pro-inflammatory phenotype following the combination.

REMERCIEMENTS / ACKNOWLEDGEMENTS

Je tiens tout d'abord à remercier chacun des membres du jury d'avoir accepté d'évaluer mon travail de thèse.

Je veux ensuite exprimer mes remerciements particulièrement appuyés à mon Directeur de thèse. Son leadership et sa vision m'ont accompagnés tout au long de mon parcours et m'ont fait grandir.

Je remercie mon équipe U1030 pour leur accueil et pour leur soutien tout au long de ce travail entrepris avant la pandémie et qui s'achève pendant mon clinicat entre Paris et Londres. Tout comme la vie, ce ne fut pas une longue route tranquille, mais un marathon riche en surprises, expériences et parfois parcours d'obstacles, mais qui en valait la peine.

Je tiens particulièrement à remercier mon conjoint pour son soutien sans faille surtout dans les moments de doute, sa logistique infaillible, et mon fils pour sa patience du haut de ses trois ans. Ce travail est le résultat de votre soutien et compréhension.

COMMUNICATIONS

Publications

How to improve SBRT outcomes in NSCLC: from pre-clinical modeling to successful clinical translation.

Marina Milic, Michele Mondini, Eric Deutsch
Cancers (Basel). 2022 Mar 27;14(7):1705.
doi: 10.3390/cancers14071705.

$KRAS^{G12C}$ inhibition using MRTX1257: a novel radio-radiosensitizing partner.

Pierre-Antoine Laurent[1], Marina Milic[1], Clément Quévrin, Lydia Meziani, Winchygh Liu, Daphné Morel, Nicolas Signolle, Céline Clémenson, Antonin Lévy, Michele Mondini, Eric Deutsch
Journal of Translational Medicine (2023) 21:773
doi: 10.1186/s12967-023-04619-0

1. equal contributors

Presentations

Poster at ESMO 2023, Madrid, Spain

RESUME DETAILLE

La radiothérapie joue un rôle central dans le traitement des cancers. Pendant leur parcours thérapeutique, près de 50% des patients atteints de cancers ont une indication de traitement par radiothérapie, et ce 34% à visée curative et 14% à visée palliative et symptomatique. La radiosensibilité est multifactorielle, la probabilité de contrôle de la croissance tumorale et la survie globale sont en effet intrinsèquement liées. La radiosensibilité est un facteur clé mais pas unique de la probabilité de contrôle de la croissance tumorale et guérison. Parmi les autres facteurs, l'activation d'oncogènes et de voies de signalisation sont des paramètres déterminants. Les mutations activatrices de l'oncogène RAS (*Rat sarcoma viral oncogene homolog*) sont considérées comme étant les mutations oncogéniques les plus fréquentes. L'isoforme KRAS (*Kirsten rat sarcoma viral oncogene*) est impliqué dans 75% des cancers RAS mutés. Les mutations de KRAS sont présentes dans 20-25% des cancers bronchiques non à petites cellules (CBNPC), 80% des adénocarcinomes du pancréas et 30% des cancers colorectaux et des voies biliaires. L'isoforme $KRAS^{G12C}$ est présent dans 14% des CBNPC et 3-4% des cancers colorectaux. Les mutations de KRAS sont corrélées à la radiorésistance de multiples cancers. Jusqu'à très récemment, la protéine KRAS était considérée comme impossible à cibler. Les progrès récents ont permis la mise au point d'inhibiteurs covalents et sélectifs de $KRAS^{G12C}$ dont les principaux candidats Sotorasib (AMG-510, Amgen) et Adagrasib (MRTX849, Mirati) ont donné des résultats thérapeutiques encourageants dans le cadre d'essais cliniques précoces chez les patients prétraités porteurs de tumeurs solides $KRAS^{G12C}$ mutées. Très peu de données sont actuellement disponibles sur la combinaison thérapeutique radiothérapie et inhibiteurs de $KRAS^{G12C}$.

Dans ce contexte, notre projet explore l'effet radio-sensibilisant de la combinaison thérapeutique radiothérapie et inhibiteur de $KRAS^{G12C}$, MRTX1257 (Mirati Labs) dans le modèle préclinique CT26 $KRAS^{G12C}$ muté. Il s'agit d'un analogue préclinique de MRTX849 (Adagrasib). Dans un premier temps nous avons exploré in vitro l'action radio-sensibilisante de MRTX1257 dans les modèles CT26 $KRAS^{G12C+/+}$, CT26 WT, LL2 WT et LL2 NRAS KO (LL2 $NRAS^{-/-}$). Dans un second temps, nous avons testé in vivo la combinaison MRTX1257 avec la radiothérapie dans le modèle sous-cutané murin syngénique CT26 $KRAS^{G12C+/+}$.

MRTX1257 a montré une réduction significative de la croissance tumorale résultant en 20% de guérisons durables dans le groupe combinaison MRTX1257 et radiothérapie.

Enfin, nous avons exploré l'influence de MRTX1257 seul ou en combinaison avec l'irradiation sur la modulation du microenvironnement tumoral montrant une augmentation de la proportion de lymphocytes CD4+, cellules dendritiques de type 2, et monocytes inflammatoires. De plus nous avons démontré une régulation à la baisse de l'expression de PD-L1 à la fois dans les cellules tumorales et myéloides, illustrant une polarisation pro-inflammatoire du microenvironnement tumoral.

Ce travail est le premier à notre connaissance à démontrer in vitro et in vivo l'effet radio-sensibilisant de MRTX1257 dans le modèle préclinique CT26 $KRAS^{G12C}$ et représente une étape importante vers le développement de nouvelles combinaisons thérapeutiques dans les tumeurs $KRAS^{G12C}$ mutées.

1 SUMMARY OF CONTENTS

2 TABLE OF ILLUSTRATIONS

3 LIST OF TABLES

Table 4. Current $KRAS^{G12C}$ combination therapies

4 LIST OF ABBREVIATIONS

AKT: Serine/threonine-protein kinase
ANOVA: Analysis of variance
cDC2: Conventional dendritic cell type 2
3D-CT: Conformal 3D Radiotherapy 3D-CT
CT26: Colon tumor 26 cell line
EGFR: Epithelial growth factor receptor
FoxP3: Forkhead box P3
GDP: Guanosine diphosphate
GTP: Guanosine triphosphate
IMRT : Intensity modulated radiotherapy
LC: Local Control
LL2: Lewis Lung carcinoma cell line
MAPK: Microtubule associated protein kinase
MHC II: Major histocompatibility complex II
OARs : Organs at risk
NSCLC: Non-small cell lung cancer
ORR: Objective response rate
OS: Overall survival
PD-L1: Programmed cell-death ligand 1
PFA: Paraformaldehyde
PFS: Progression-free survival
PI3K: Phosphatidylinositol 3-kinase
RAS: Rat sarcoma viral oncogene homolog
RT: Radiotherapy
SBRT: Sterotactib Body Radiothearapy
SEM: Standard error to the mean
Tregs: T regulator lymphocytes
VMAT: volumetric arc therapy
WT: Wild-type

5 INTRODUCTION

The discovery of X-rays as a new type of radiation in 1895 by Wilhelm Conrad Röntgen ("Über eine neue Art von Strahlung. (Vorläufige Mitteilung)") followed shortly after by the study of radioactivity by Pierre and Marie Curie in 1898, have opened a new therapeutic era by the first years of the 20th century (Lederman, 1981). With the story unfolding, radiotherapy has been an effective tool for treating cancer for more than 100 years.
Of the 10.9 million people diagnosed with cancer worldwide each year (International Agency for Research on Cancer), around 50% require radiotherapy, 60% of whom are treated with curative intent

Currently radiotherapy plays a central role in cancer treatment. It is indicated in the treatment of more than 50% of solid tumors (Barton et al., 2014a) in most developed countries either alone or in combination with other treatment modalities, chemotherapy, immunotherapy or targeted therapy.

It has been shown to provide significant local control (LC) and overall survival (OS) benefits as part of evidence-based cancer care. Hanna, et al.(Hanna et al., 2018) in their population based study reporting on the benefit of radiotherapy in high-income countries , found that 48% of all cancers have indications for RT, 34% curative and 14% palliative. RT provided a 5-year local control LC benefit in 10.4% of all cancer patients and a 5-year OS benefit in 2.4% (T. P. Hanna et al., 2018a).

The benefit of curative RT among patients with curative indications was for 5-year LC 31.9%.

As expected, the local control benefit with radiotherapy alone was highest in cancer types where RT was most commonly used including cervix 33%, head and neck 32% and prostate 26%. However, the 5-year LC benefit was almost inexistant in unknown primary, pancreas, ovary, liver, kidney, gallbladder and colon. (T. P. Hanna et al., 2018a)

Fig 1. Radiotherapy Population 5-year local control benefit. Ordered by magnitude of radiotherapy alone absolute proportional benefit. Radiotherapy benefit is separated into radiotherapy alone benefit and chemoradiation benefit.

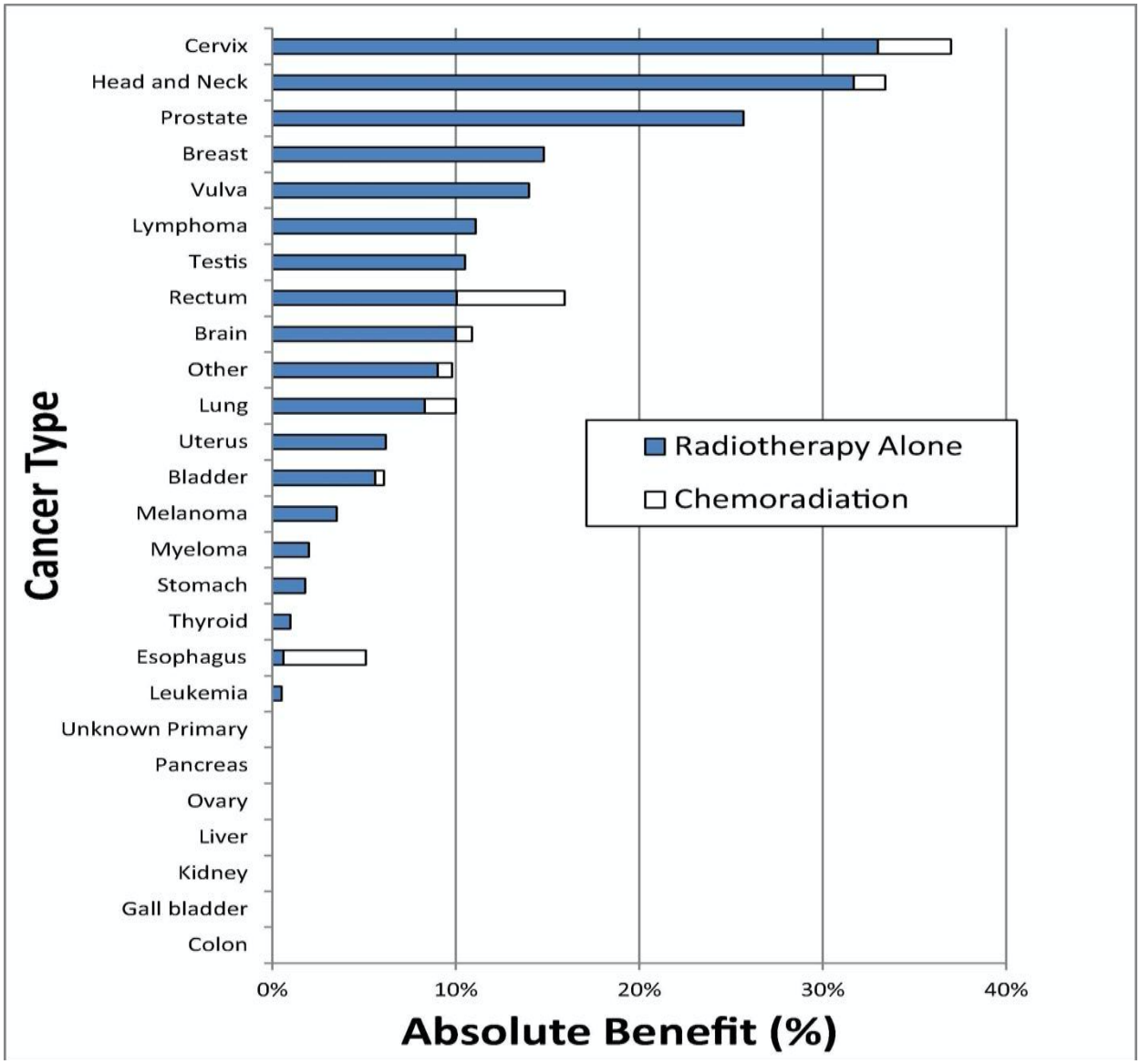

https://doi.org/10.1016/j.radonc.2017.11.004

More specifically, radiotherapy is the standard approach for the definitive treatment of early-stage lung and colorectal cancers. Its role has dramatically changed over the last decades. Despite technological advances and novel radiotherapy techniques, such as conformal radiotherapy and image-guidance

of stereotactic-body radiotherapy (SBRT) or IMRT, resistance to RT and disease recurrence remain major limitations.

Therefore, despite RT being a highly effective treatment modality, radiation resistance which results in local or distant relapse, cancer recurrence and poor prognosis remains a major obstacle calling for new treatment approaches.

Factors contributing to disease relapse and radioresistance are multiple, including but not limited to tumor heterogeneity, tumor microenvironment or numerous gene alterations. (Kim et al., 2015)(Olivares-Urbano et al., 2020).

A more profound understanding of molecular mechanisms underpinning radioresistance and interactions with the tumor microenvironment are needed in order to identify new treatment strategies and improve clinical outcomes.

6 RADIOTHERAPY GENERAL PRINCIPLES AND TECHNIQUES

6.1 RADIOTHERAPY TECHNIQUES

6.1.1 3D-CRT

Before the advent of computed tomography (CT), treatment plans were carried out using 2-dimensional treatment planning for a short time resulting in large volumes of normal tissue being irradiated. Computed tomography (CT) came into wide use around 1972 and started to be used in radiation treatment planning. The availability of CT based treatment planning has allowed for direct identification and delineation of relevant target volumes in 3D. This combined with multi-level collimators has enabled 3D conformal radiotherapy (3D-CRT) development leading to increased treatment accuracy and reduction in normal tissue irradiation.

6.1.2 Intensity modulated RT (IMRT) vs. 3D conformal RT.

Intensity-modulated radiotherapy (IMRT), and volumetric arc therapy (VMAT) represent recent developments offering improved dose conformality therefore allowing lower doses to organs at risk (OARs).(Cilla et al., 2012) (Dröge et al., 2015).

They have been increasingly used for pelvis radiotherapy and support the delivery of concavely shaped dose distributions. They are based on the delivery of highly modulated dose fluence from multiple directions limiting high dose volume outside the treatment target. This results in lower radiation induced toxicities.

Dosimetric studies showed that bowel volume receiving 45-50 Gy was significantly reduced with IMRT which could potentially reduce bowel toxicity. (Tseng et al., 2019).

However, one of the limitations is that most studies were small scale or dosimetric in nature. Some of the shortcomings of these techniques include organ motion, volume variability or dose inhomogeneity, hence raising the potential concern of underdosing. This could be attributed to a rapid drop-off of dose beyond target volumes. Therefore, more prospectively generated data are needed.

6.1.3 Standard RT techniques in Colorectal cancer

According to the World Health Organization (WHO), colorectal cancer is the third most common cancer worldwide, accounting for approximately 10% of all cases. About two-thirds occur in the sigmoid colon or rectum and are stage II or above at diagnosis requiring chemoradiotherapy in addition to surgery.

The current standard is 3-dimension 3D conformal radiotherapy allowing localization and dose analysis of organs at risk (OARs) via 3D planning and dose-volume histograms.

Fig 2. Dose distributions of (a) 3D conformal radiotherapy, (b) intensity-modulated radiotherapy and (c) spot-scanning proton therapy plans. The 50 Gy (red), 40 Gy (yellow) and 20 Gy (blue) isodose lines are highlighted. The planning target volume is shown in green.

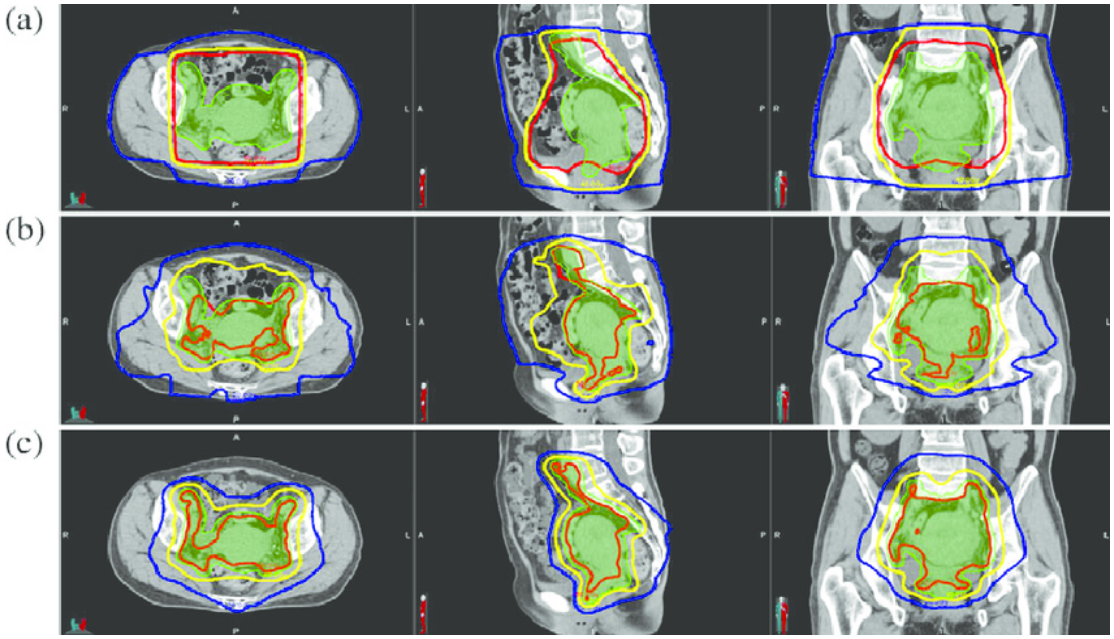

July 2016 Journal of Radiation Research 57(5) DOI:10.1093/jrr/rrw052

Fig 3. Dose distribution for 3D conformal radiotherapy (left) and IMRT (right). Prescription dose 50.4 Gy. IMRT, intensity-modulated radiotherapy

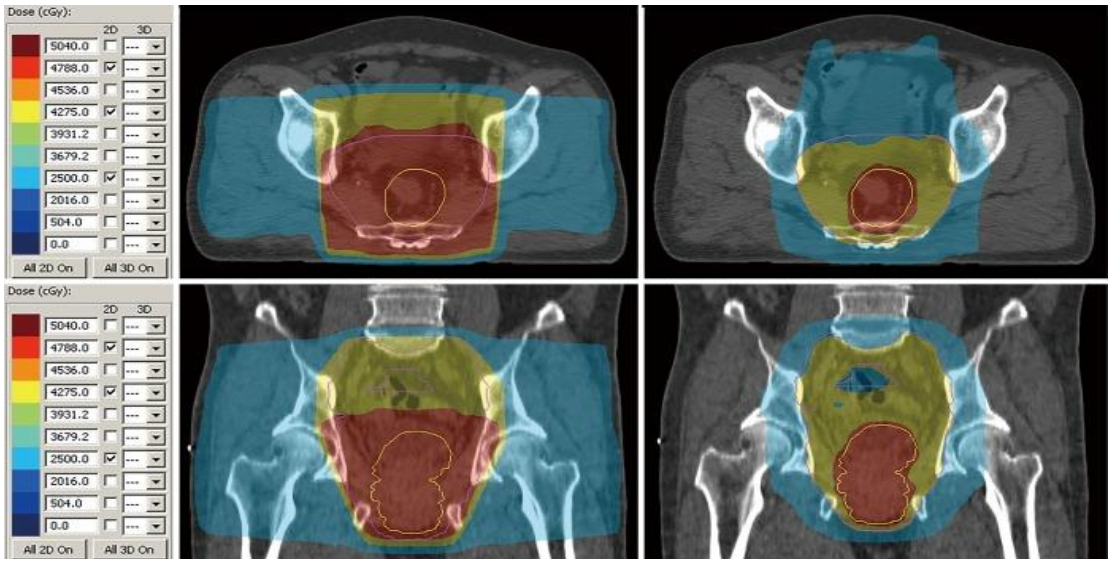

J Gastrointest Oncol.2019 Dec ;10(6) :1238-1250

6.1.4 Conventional fractionated RT vs. Stereotactic Body Radiotherapy (SBRT)

Conventional radiation is delivered via multiple fractions of low-dose radiation.

In contrast, SBRT is described as a high-precision external beam radiotherapy technique using numerous beams all converging in a small target volume, allowing the accurate delivery of high doses per fraction (>6-7 Gy) in very few treatment fractions to an extracranial target (Guckenberger et al., 2014). Its main indications include small or solitary lesions, oligometastatic disease or painful metastasis.

It is worth pointing out that detailed understanding of the radiobiology of SBRT is still lacking.

6.2 CLINICAL ROLE OF RADIOTHERAPY

6.2.1 Curative setting

Curative intent radiotherapy is given in patients with early and locally advanced disease. Its aim is to improve local control and survival benefit.
It is estimated that RT contributes to 40% of all cancer cures worldwide.

As dose constraints are placed on organs at risk (OARs) and normal tissues to avoid acute and late toxicity, the dose of radiation delivered to the tumor is therefore often limited by the dose that can be safely delivered to the normal tissues. This can represent a real challenge in situations with large volume disease or disease close to critical normal structures. As it has been shown that local control correlates with improved survival, this could potentially translate in a poorer outcome (Aupérin et al., 2010) (Machtay et al., 2012).
The last two decades have seen the development of great advancements in radiotherapy technology (Diwanji et al., 2017).

One of those is conformal three-dimensional RT (3D-CRT) where CT planning allows improved tumor coverage and reduction in dose to organs at risk (OARs) has been established as the gold standard for radical RT since the 1990's. Improved conformal treatment has become possible with the advent of intensity modulated radiotherapy (IMRT), a high precision radiotherapy mode using linear accelerators to deliver precise radiation doses to a tumor whilie minimizing the dose to surrounding normal tissues.

Subsequent 4D planning incorporating tumor motion into the planning process has further facilitated a reduction in tumor margins and therefore dose delivered to normal tissue (Brown et al., 2019).

Fig 4. Improved conformity of the high-dose region to the target volume and improved sparing of organs at risk with intensity-modulated radiation therapy compared to 3-dimensional conformal radiation therapy

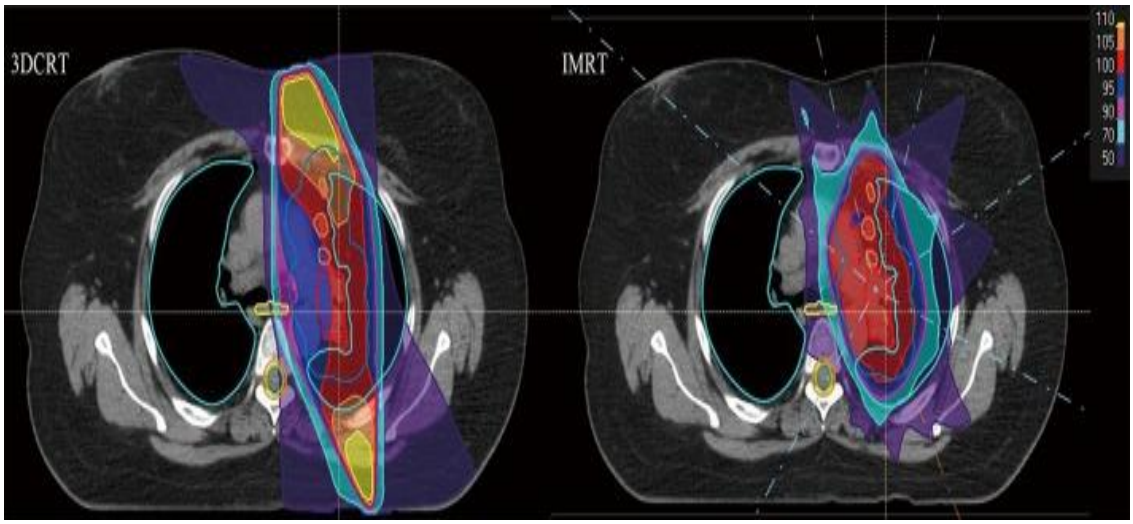

Gross tumor volume including nodal disease is depicted by the red/orange contour. Spinal cord is depicted by the green contour. Esophagus is depicted by the yellow contour. The relative isodose is depicted in colorwash as per the color scale in the picture.
Transl Lung Cancer Res. 2017 Apr; 6(2): 131–147.
doi: 10.21037/tlcr.2017.04.04

Fig 5. Example of RT planning and dose distribution to organs at risk

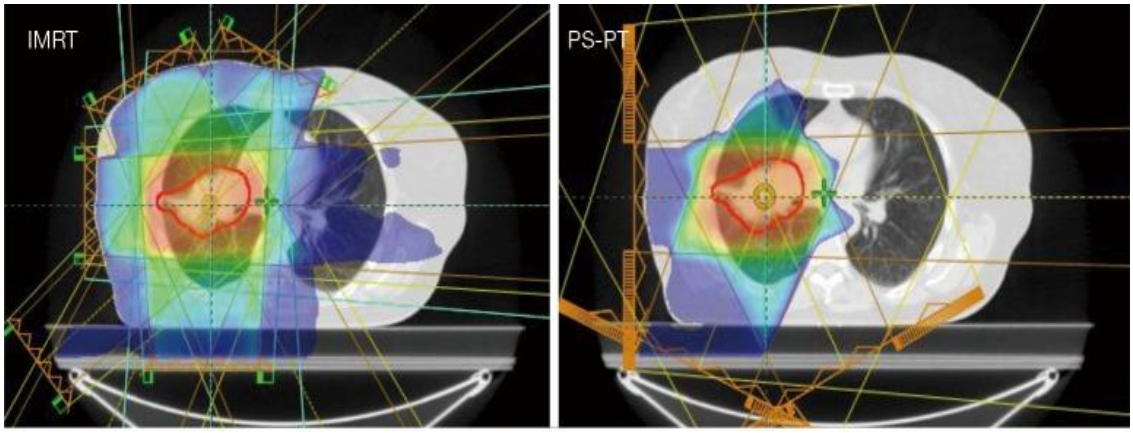

Dose to organ at risk	IMRT	PS-PT
Mean lung dose	24.2 Gy	18.6 Gy
Lung V5	78.8%	44.6%
Lung V20	41.4%	38%
Mean heart dose	14.7 Gy	5.3 Gy

Five-field intensity-modulated radiation therapy (IMRT) plan vs. three-field passive scatter proton therapy (PS-PT) plan for a large stage IIIA non-small cell lung cancer treated with definitive chemoradiation therapy to 60 Gy in 2 Gy per fraction. Unlike PS-PT, IMRT distributes significant exit dose to the left lung and heart. As a result, PS-PT leads to decreased mean lung dose, lung volume receiving at least 5 Gy (V5), and mean heart dose. Both plans depict the 10 Gy colorwash on lung windows on the average scan of the 4-dimensional computed tomography simulation. The red contour outlines the gross tumor volume.

J Thorac Dis. 2018 Aug; 10(Suppl 21): S2474–S2491.
doi: 10.21037/jtd.2018.07.29

6.2.2 Oligometastatic setting

For a long time, the focus of treatment in the metastatic setting has been palliative systemic therapy with low-dose radiotherapy being used only for palliation of symptoms. The hypothesis that patients with a small volume of metastatic disease can benefit from ablation of all metastasis with some achieving long-term disease control or even cure started emerging in the late 1930's (Barney and Churchill, 1939).

While surgery has long been considered as the primary modality for metastasis-directed treatment, stereotactic ablative radiotherapy (SABR) has emerged as a newer and less-invasive option (Palma et al., 2020).
Palma et al, (Palma et al., 2020) have shown that patients with a limited burden of metastatic disease derive a benefit in long-term outcomes with metastasis-directed treatment, whether surgical resection or stereotactic ablative radiotherapy (SABR).

Fig. 6. Example of SABR planning on a metastatic bone lesion

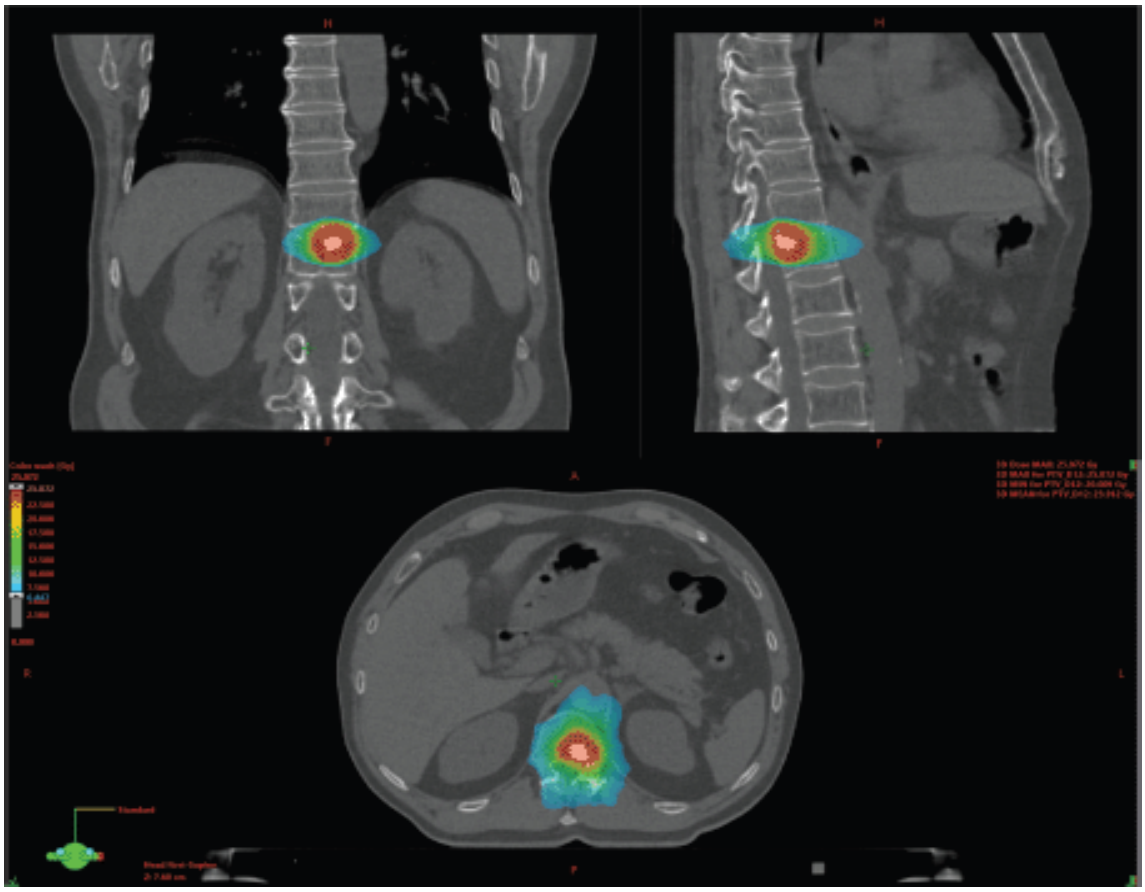

https://doi.org/10.3332/ecancer.2020.1036

Gradually accumulating evidence has helped define the oligometastatic state as a separate entity, a transitional state between localized and widespread disease.

The Hellman's spectrum theory (Hellman, et al.) hypothesizes that "the metastatic spread is a continuum reflecting a step-wise process leading to the transformation of localized disease to a widespread one". Based on this theory, cancer is a continuum of diseases ranging from being a local disease to one that metastasizes. The oligometastatic disease could be seen as « an intermediate state both quantitatively and qualitatively between the two extremes, almost as an epiphenomenon of restricted virulence resulting in limited metastatic capacity ».(Miglietta, et al).

Fig 7. Oligometastatic breast cancer

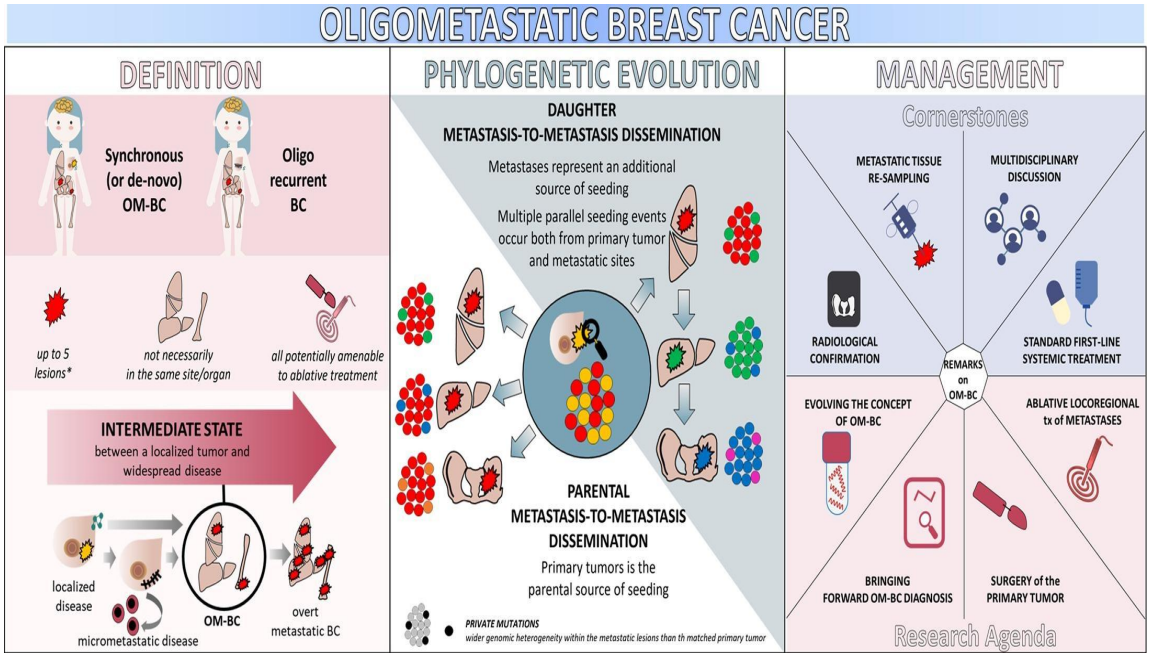

Cancer Treatment Reviews Volume 110 (November 2022)
DOI: 10.1016/j.ctrv.2022.102462

Even tough randomized phase III data are still awaited, growing evidence is suggesting that SABR can improve long-term outcomes in patients with a limited burden of metastatic disease.

The SABR-COMET phase II randomized trial (Palma et al., 2020) enrolled 99 patients with a controlled primary tumor (breast, lung, colorectal or prostate) and 1-5 metastatic lesions all amenable to SABR showing showed a 5-year OS rate of 17.7% (95% CI, 6% to 34%).

in the standard of care arm vs. 42.3 months (95% CI, 28% to 56%; stratified log-rank *P* = .006) in the SOC plus SABR arm. There was no detrimental impact on QOL or new safety signals.

Other phase II trials have suggested benefits in the setting of colorectal cancer liver metastasis (Ruers et al., 2012), in non-small-cell lung cancer (NSCLC) (Gomez et al., 2019), and in prostate cancer (Ost et al., 2018).

Data from phase III trials will aim to confirm outcome benefits and develop biomarkers predictive of benefit with SABR.

6.2.3 Metastatic setting

Palliative radiotherapy

Radiotherapy is known to have beneficial effects in the palliative treatment of cancer, and some data even suggest some survival improvement (Mac Manus et al., 2006).

Local RT is an established option to achieve rapid, effective palliation of symptomatic metastases with few side effects. Oncological emergencies and cancer-related severe symptoms are two clinical scenarios in which timely radiation therapy is crucial.

The manifestations of oncological emergencies are diverse ranging from mechanical obstruction such as SVCO, metastatic spinal cord compression (MSCC), hemoptysis, brain metastasis with impending herniation, etc.

In addition to short-term symptom palliation, radiotherapy provided better survival by improving Performance Status (ECOG PS) and potentially opening the door to consideration of more aggressive systemic treatment options

6.2.4 ASTRO Clinical guidelines

ASTRO clinical guidelines (Wo et al., 2021) recommend neo-adjuvant RT for patients with stage II-III rectal cancer, with either conventional fractionation with concurrent 5-FU or capecitabine or short-course RT. Pre-operative RT is recommended over post-operative.

For patients with clinical stage II-III rectal cancer, there is strong evidence to recommend neoadjuvant RT. Multiple prospective trials have demonstrated that neoadjuvant RT decreases the risk of local recurrence, even in the era of total mesorectal excision (TME). (Folkesson et al., 2005)(Roh et al., 2009)(Sauer et al., 2012)

These results were confirmed by several meta-analyses, which consistently found that the hazard ratio for local recurrence with RT was approximately 0.5 compared with surgery alone. (Abraha et al., 2018)(Cammà et al., 2000)

Despite the strong evidence supporting the use of neoadjuvant RT for patients with stage II-III rectal cancer, a subset of patients may be at low risk for locoregional recurrence based on proximal tumor location and MRI-determined "safe" circumferential resection margin.(Ruppert et al., 2018)(Taylor et al., 2014).

Based on this moderate evidence, a conditional recommendation may be made to omit neoadjuvant RT in favor of upfront surgery for patients in clinical stage IIA (cT3a/b N0) when the cancer is located >10 cm from the anal verge and there is a predicted circumferential resection margin ≥2 mm and the absence of extramural vascular invasion as determined by MRI with rectal cancer protocol.

Three prospective trials randomizing patients between preoperative and postoperative chemoradiation demonstrated improvements in disease-free survival and/or local recurrence-free survival with the preoperative approach. (Roh et al., 2009) (Sauer et al., 2012) (Sebag-Montefiore et al., 2009)

Therefore, when RT is indicated for rectal cancer, the evidence strongly supports a recommendation favoring pre-operative over post-operative treatment.

Preoperative RT can be conditionally omitted in selected patients with lower risk of locoregional recurrence.
Addition of chemotherapy before or after chemoradiation or after short-course RT is conditionally recommended.

Shared decision making and improved stratification of risk within stage II-III rectal cancer in required to individualize the use of neoadjuvant RT.

7 RADIOBIOLOGY

7.1 RADIATION RESPONSE CURVES AND DOSE VOLUME CONSTRAINTS

The aim of RT is to deliver a sufficient dose of radiation to the tumor cells to destroy them without irradiating normal tissue to a dose that would lead to severe toxicity or normal tissue damage. The probability of achieving tumor control and developing healthy tissue complications as a function of radiation dose was first theorized in 1936 by Hermann Holthusen.The principle is generally represented by two sigmoid curves, one for the tumor control probability, and one for the probability of normal tissue damage.

Fig 8. Radiation response curves

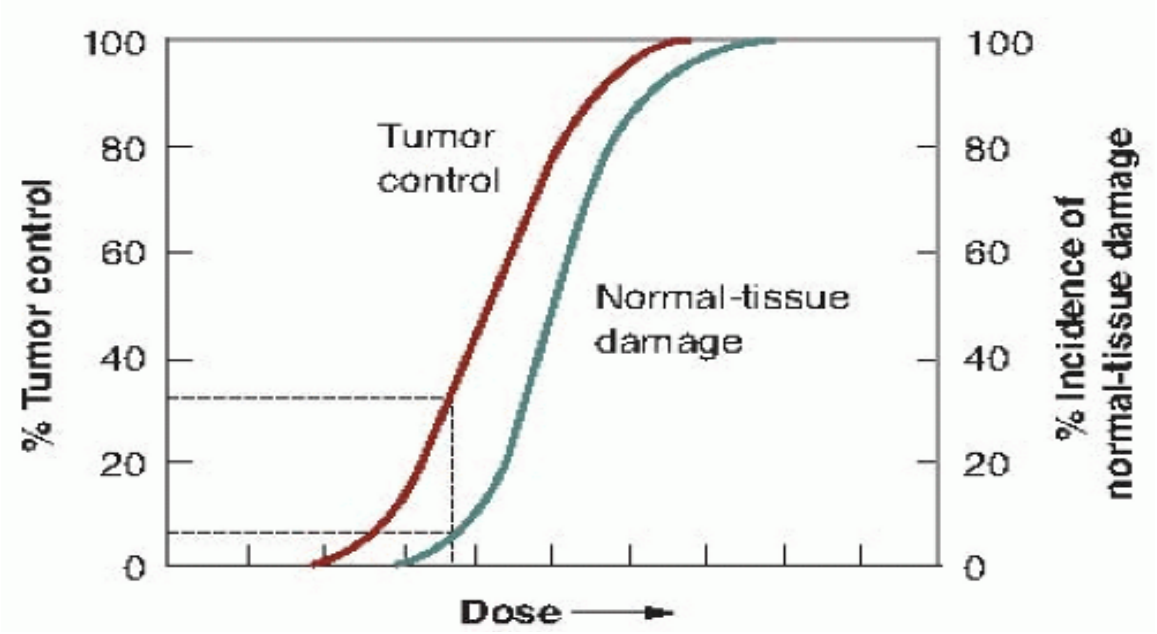

Radiotherapy planning can be seen as a precision exercise or careful balancing act between optimal tumor control and limitation of damage to normal tissue. In order to avoid toxicity on the normal tissue, dose constraints are placed on the normal tissues or organs at risk (OARs) such as heart, esophagus, lungs, spinal cord to avoid functional damage.

Table 1. Example of general volume constraints for adult patients – organ nomenclature based on the Global Quality Assurance of Radiation Therapy Clinical Trials Harmonization Group (GHG) contouring guidelines. (Mir, et al.)

Organ	**Constraints** **(conventional fractionation)**	**Constraints (Hypofractionation)**			
		1 fraction	3 fractions	5 fractions	8 fractions
Bowel	$V_{15\ Gy}$ < 120 cm^3; $V_{45\ Gy}$ < 195 cm^3 (A) (Bisello, et al.)			For primary prostate SBRT only: $V_{18.1\ Gy}$ < 5 cm^3; $V_{30\ Gy}$ < 1 cm^3 (mandatory)	
Brainstem	Brainstem PRV: D_{MAX} < 54 Gy; $D_{1–10\ cm^3}$ < 59 Gy (peripheral edge)	$D_{MAX(0.035\ cm^3)}$ < 15 Gy(mandatory); $D_{MAX(0.035\ cm^3)}$ < 10 Gy(optimal); (A)	$D_{Max\ (0.035\ cm^3)}$ < 23.1 Gy(mandatory); $D_{MAX(0.035\ cm^3)}$ < 18 Gy(optimal); (A)	$D_{MAX(0.035\ cm^3)}$ < 31 Gy(mandatory); $D_{MAX\ (0.035\ cm^3)}$ < 23 Gy(optimal); (A)	
Cauda equina		$D_{MAX(0.035\ cm^3)}$ < 16 Gy(mandatory) (Diez et al., 2022)(A); $V_{14\ Gy}$ < 5 cm^3(optimal); (Benedict et al., 2010) (A)	$D_{MAX\ (0.035\ cm^3)}$ < 24 Gy(mandatory) (Diez et al., 2022) (A); $D_{5\ cm^3}$ < 21.9 Gy(optimal); (Benedict et al., 2010) (A)	$D_{MAX\ (0.035\ cm^3)}$ < 32 Gy(mandatory) (Diez et al., 2022) (A); $D_{5\ cm^3}$ < 30 Gy(optimal);	
Heart	D_{MEAN} < 26–30 Gy $V_{25\ Gy}$ < 10%; $V_{30\ Gy}$ ≤ 30%;	$D_{MAX(0.03\ cm^3)}$ < 22 Gy(mandatory) (Benedict et al., 2010) *; $D_{15\ cm^3}$ < 16 Gy(optimal); [(Benedict et al., 2010)] (A)	$D_{MAX(0.5\ cm^3)}$ < 26 Gy(mandatory); $D_{MAX(0.5\ cm^3)}$ < 24 Gy(optimal); (G. G. Hanna et al., 2018) (A) D_{MAX} < 30 Gy(mandatory) [25] (A); $D_{15\ cm^3}$ < 24 Gy (Benedict et al., 2010) (A); $V_{21\ Gy}$ < 5 cm^3 (Grimm et al., 2011) (B)	$D_{MAX(0.5\ cm^3)}$ < 29 Gy(mandatory); $D_{MAX(0.5\ cm^3)}$ < 27 Gy(optimal); (G. G. Hanna et al., 2018) (A) $D_{15\ cm^3}$ < 32 Gy (Benedict et al., 2010) (A) Avoid 105% of PTV prescription*	D_{MAX}(0.5 cm3) <60 Gy (mandatory); D_{MAX}(0.5 cm3) < 50 Gy (optimal); (G. G. Hanna et al., 2018) (A)
Lung	$V_{40\ Gy}$ ≤ 10%; $V_{30\ Gy}$ ≤ 15%; $V_{20\ Gy}$ ≤ 20%; $V_{10\ Gy}$ ≤ 40%; $V_{5\ Gy}$ ≤ 50%; D_{MEAN} < 20 Gy	Lungs and Lungs–ITV: $V_{20\ Gy}$ < 15% (mandatory); D_{MEAN} < 8 Gy (optimal); $V_{20\ Gy}$ < 10% (optimal); (Diez et al., 2022) (A) $D_{1500\ cm^3}$ < 7 Gy; $D_{1000\ cm^3}$ < 7.4 Gy; (Benedict et al., 2010)(A)	Lungs and Lungs–ITV: $V_{20\ Gy}$ < 15% (mandatory); D_{MEAN} < 8 Gy (optimal); $V_{20\ Gy}$ < 10% (optimal); (Diez et al., 2022) (A) $D_{1500\ cm^3}$ < 11.6 Gy; $D_{1000\ cm^3}$ < 12.4 Gy; (Benedict et al., 2010) (A)	Lungs and Lungs–ITV: $V_{20\ Gy}$ < 15% (mandatory); D_{MEAN} < 8 Gy (optimal); $V_{20\ Gy}$ < 10% (optimal); (Diez et al., 2022) (A) $D_{1500\ cm^3}$ < 12.5 Gy; $D_{1000\ cm^3}$ < 13.5 Gy; [(Benedict et al., 2010)](A)	Lungs and Lungs–ITV: $V_{20\ Gy}$ < 15% (mandatory); D_{MEAN} < 8 Gy (optimal); $V_{20\ Gy}$ < 10% (optimal); (Diez et al., 2022) (A)

Key: D = dose received (by % of the organ volume / by cubic centimeter of the organ volume); D_{Max}: Maximum Dose received by the organ; D_{Mean}: Mean Dose received by the organ; Gy: Gray; PRV: planning risk volume; SBRT: stereotactic body radiation therapy; V = Volume receiving a dose ≥ Gy; Volumes and doses were expressed as percentage (%) or absolute values (cm^3 or Gy, respectively). (A) source of recommendation : international guidelines.
* : NCNN Practice Guidelines in Oncology-Non-small cell lung cancer. Version 5.2022.

Bisello, et al.
Curr Oncol. 2022 Oct; 29(10): 7021–7050.
doi: 10.3390/curroncol29100552

As seen in the table above, the dose or radiation delivered to the tumor is often limited by the dose that can be safely delivered to the normal tissues.

With the advent of IMRT where treatment can be delivered using non-uniform dose distributions aiming to reduce the dose to critical organs-at-risk, new dose-volume constraints have become increasingly necessary. However, the low doses cover more healthy volume.

A similar situation is encountered with SBRT as published dose constraints are obtained using different methods including BED conversion and different clinical and dosimetric parameters leading to a lack of consistency with each other . The failure to take into account the variation in those factors could potentially lead to suboptimal treatment, highlighting the need for validated dose tolerance limits (Xue et al., 2016).

7.2 THE THERAPEUTIC RATIO

The development of IGRT and IMRT have allowed to achieve a substantial gain in the therapeutic ratio, that is the balance between the probability of cure and probability of treatment related toxicity.
Conventional fractionated radiotherapy focuses on attempting to maximize the therapeutic ratio.

There are two main mathematical formulations of therapeutic ratio; the equal dose and the equal effect equation.

The equal dose equation is defined as the ratio of damage to the tumor cells to damage to normal cells for the same dose.

Therapeutic Ratio = Damage to tumor cells/damage to normal cells at Equal dose

Therapeutic Ratio= Dose to normal cells/Dose to tumor cells Equal Effect

With improved cancer cure rates, survivorship issues such as long-term toxicities are becoming increasingly important.

Fractionated radiotherapy was developed in an attempt to achieve optimal killing of the tumor cells while keeping to a minimum damage to surrounding normal tissues and OARs.

While single high-doses of radiation are associated with poor elimination of hypoxic cells and exposure of cells within resistant phases of the cell cycle, radiation fractionation allows tumor cells to redistribute into more radio-sensitive phases and reduces hypoxia by reoxygenation (Withers, 1975).

Radiotherapy fractionation attempts to maximize the therapeutic ratio, offering the best trade-off between probability of cure and probability of adverse reaction.
However, technical advances and altered dose fractionation alone won't be sufficient in attempting to maximize toxicity free survival, unless taken in conjunction with new drug combinations and radiosensitivity (Barnett et al., 2009).

7.2.1 The linear quadratic model

The Linear Quadratic model (LQ) is a mathematical model providing a simple relationship between cell survival and the radiation dose delivered: $S = e^{-\alpha D - \beta D2}$. (McMahon, 2018) It describes the radiation response of the tumor, in which the α/β ratio is used to characterize the sensitivity of a particular tissue type to fractionation (Jones and Dale, 2018).
It has been considered the standard method of modelling for decades and has been used to predict response to radiation both in vitro and in vivo.

The classical theory of radiation action emerged with the help of Douglas Lea (Lea D.E. Action of radiation on living cells. In: ASIN: B0007JLWKQ. 1st Edition (1946), 2nd edition (1962): The British Institute of Radiology.; 1962) who expressed the average yield of severe chromosomal aberrations per cell (E) in

the form of a linear-quadratic relationship with single-dose d and radiosensitivity parameters α and β:

$$E = \alpha d + \beta d^2$$

Where: E (logarithmic cell kills) is the fraction of cells killed by an absorbed dose d; α is the linear component of cell kills related to DSBs caused by a single hit of radiation; β describes double hits (the quadratic) component of cell kills. (Lea, 1946)

The most common expression of the LQ model used is: $S = e^{-\alpha D - \beta D2}$
It describes the probability of cell survival following exposure to a single dose of radiation S where D is the dose delivered α and β are parameters of cell radiosensitivity.
Survival is generally plotted on a log scale, giving a quadratic response curve.

The α/β ratio expressed in Gy is generally defined as the degree of curvature and corresponds to the dose at which the linear α and quadratic β contributions are equal.(McMahon, 2018)

Fig 9. Illustration of LQ curves

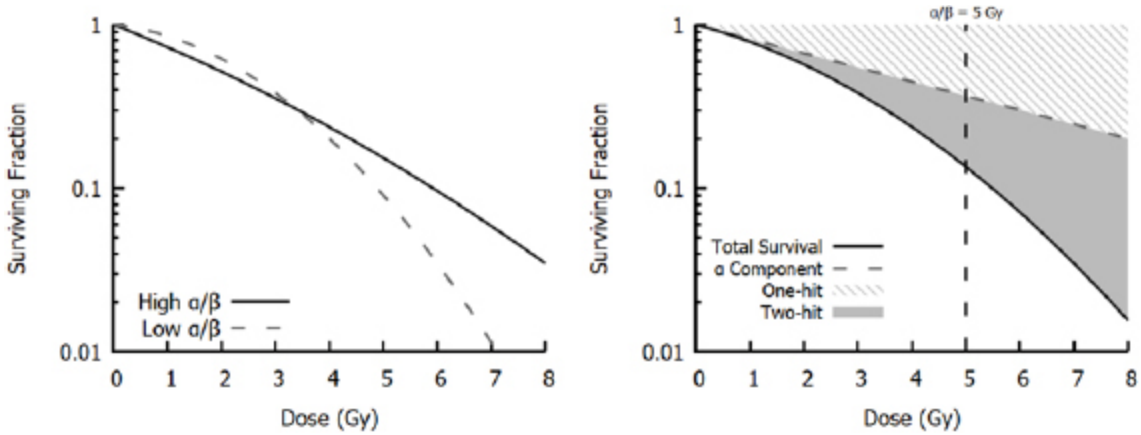

Left: Responses for cell lines with high and low α/β ratios. High α/β cell lines (10 Gy) have nearly-constant rates of cell killing with increasing dose, while low α/β lines (3 Gy) show a pronounced curvature, with greater killing per unit dose at higher doses. Right: Separation into one- and two-hit kinetics. At low doses, response is dominated by one-hit events, while at higher doses multi-hit killing is more important.

These effects are equal when the dose matches the α/β ratio of the cell line (5 Gy).

Stephen Joseph McMahon 2019 *Phys. Med. Biol.* **64** 01TR01
DOI 10.1088/1361-6560/aaf26a

The applicability and validity of the LQ model is increasingly becoming scrutinized in light of increasing complexity of underlying biology of new radiotherapy techniques and a deeper understanding of intrinsic and extrinsic factors modulating radiosensitivity.

7.2.2 Biological effective dose (BED)

The Biologically effective dose (BED) term was introduced in 1989 (Fowler, 1989) based on the LQ model and indicates the biological effect of a radiation treatment. It takes into account the dose per fraction, total dose and includes the time factor as opposed to previous formulas.
In clinical practice, the use of BED requires careful interpretation of modelling results before making treatment decisions and can involve the use of multiple parameters in some situations. (Jones et al., 2001). For instance, this is particularly true in cases where the dose per fraction is being modified due to concerns about normal tissue tolerance, those with a large planning target volume (PTV) or those including combinations of radiotherapy treatments or different histological subtypes of cancer (Jones et al., 2001).

7.3 BIOLOGICAL EFFECTS OF RADIOTHERAPY ON CANCER CELLS

While reponse to radiation is largely mediated by cytotoxic DNA damage, multiple radiation-induced effects on both tumor cells and the tumor microenvironment are in play.

Current data indicate that radiotherapy can activate multiple cell signaling pathways which lead to the induction of senescence, apoptosis, autophagy (leading to cell death or survival) and/or cell cycle checkpoint activation and DNA repair (Chen et al., 2019)(Havaki et al., 2015)(Santivasi and Xia, 2014) (Schmukler et al., 2013)(Nguyen et al., 2018).

Fig 10. Cellular response to radiation-induced damage

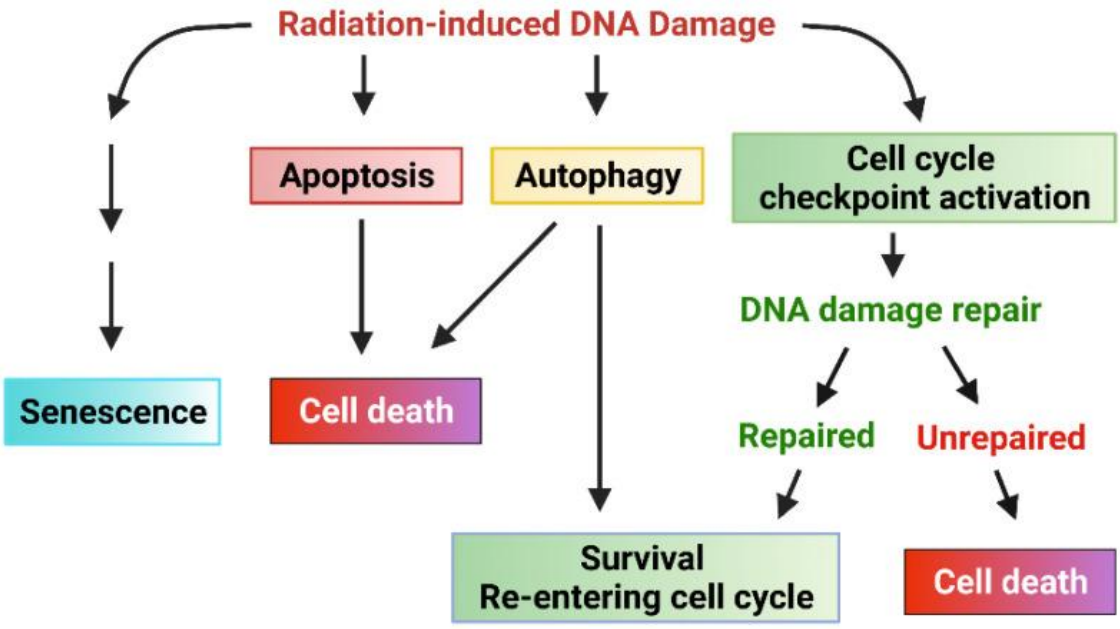

Cellular response to radiation-induced DNA damage. Ionizing radiation (IR) induces DNA damage in cancer cells in the form of either single-strand breaks (SSB) or double-strand breakes (DSB). DNA damage sensed by cells results in various cellular responses/senescence, apoptosis, autophagy, cell cycle arrest, and DNA repair. Signaling pathways that promote cell cycle checkpoint activation /DNA repair and inhibition of apoptosis can protect cancer cells drom IR-induced cytotoxicity, promoting survival and the subsequent radiation resistance of cancer cells.

Diagnostics (Basel). 2022 Mar; 12(3): 656.
Published online 2022 Mar 8. doi: 10.3390/diagnostics12030656

Ionizing radiation's cytotoxicity or ability to control tumors is mainly the result of direct DNA damage which in turn activates a number of damage response and repair (DDR) signaling cascades that control cell cycle arrest, DNA repair and the cell's fate.(Santivasi, et al.) (Raleigh and Haas-Kogan).

DNA double-strand breaks (DSBs) generated by IR represent the most lethal form of damage and are repaired either via homologous recombination (HR) or nonhomologous end-joining (NHEJ) pathways. (Raleigh and Haas-Kogan, 2013).

7.3.1 Types of radiation induced DNA damage

DNA damage is considered to be the primary target for cell inactivation by ionizing radiation, and cell death induced by radiation is largely the result of lack of repair or mis-repair of complex DNA lesions.
DNA lesions are reported to affect a significant number of cells in the human body, occurring at a reported rate of 10 000 to 1,000,000 molecular lesions per cell per day (Friedberg, 2019). If unrepaired, or incorrectly repaired this damage can lead to serious genome aberrations or mutations resulting in cell death.(Jackson and Bartek, 2009).
It is estimated that ionizing radiation produces about 1000 single-strand breaks (SSBs) and 25-40 double-strand breaks (DSBs) per diploid cell per gray regardless of cell type (except in hypoxic cells or cells deficient in GSH) (Olive, 1998).

Fig 11. Types of DNA damage induced by ionizing radiation

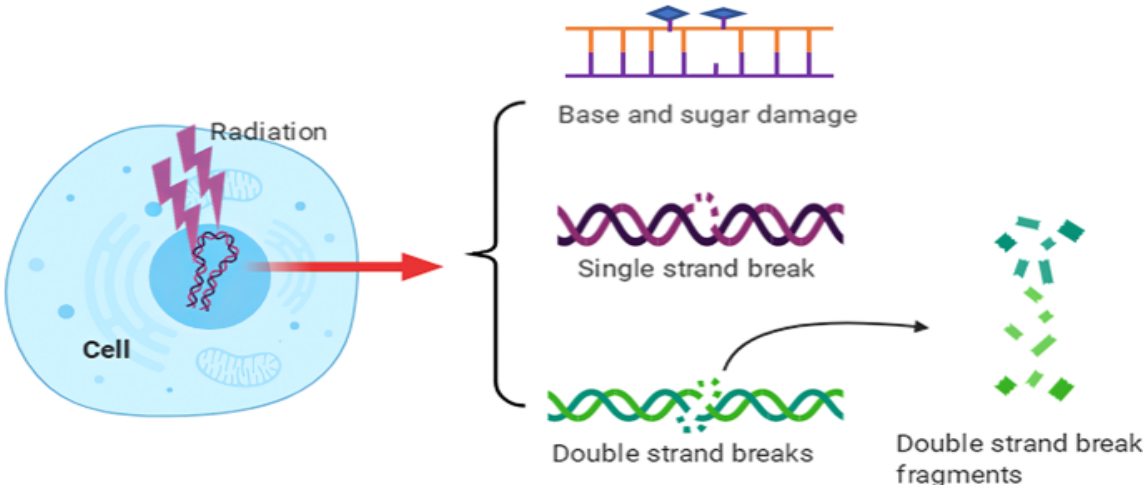

The major types of DNA damage induced by IR include base and sugar damage, single strand double-strand breaks, double-strand breaks, clustered DNA damage, and covalent intra-strand or inter-strand crosslinking.

Signal Transduction and Targeted Therapy
(Sig Transduct Target Ther) ISSN 2059-3635 (online)
https://doi.org/10.1038/s41392-020-0150-x

Irradiation can induce a great variety of DNA damage including single-strand breaks (SSBs), double DNA strand breaks (DSBs) and base modifications such as oxidation, alkylation deamination, loss of bases residues to produce apurinic or apyrimidinic sites (AP sites), all of which can indirectly lead to SSBs and/or DSB's. (Huang and Zhou, 2020).

There are also crosslinks formed involving DNA-DNA and DNA-protein interactions.

Radiation causes formation of ROS (Reactive Oxygen Species) which are indirectly involved in DNA damage. These ROS generate apurinic or apyriminidic sites (abasic sites) in the DNA, SSBs, sugar modifications and deaminated adducted bases (Redon et al., 2010)(Aparicio et al., 2014).

Collectively all these changes induce cell death and mitotic failure.

While IR does induce a variety to DNA lesions, double-strand breaks are considered the lesion responsible for lethality of tumor cells, but also for the genomic instability that leads to development of secondary cancers among normal cells.

7.3.2 Double-strand breaks (DSBs)

DSBs are considered the most critical lesion in terms of lethality and mutation probability, they are viewed as a form of complex DNA damage, also called clustered damage. (Ward, 1994).

Following irradiation with X-rays or Gamma-rays, clustered DNA lesions are reported to be 3-4 times more abundant than single-strand damage. (Nikitaki et al., 2016)(Sage and Shikazono, 2017).

Complex DNA damage is commonly described as two or more lesions within one or two helical turns of the DNA arising from a single radiation track and distinct from endogenous DNA damage (Goodhead, 1994). IR causes DNA lesions by direct interaction with DNA or indirectly via the generation of reactive species (ROS).

While simple single strand breaks are generally rapidly repaired by base excision repair (BER), complex DSBs are more slowly and inefficiently repaired resulting in genomic instability (Li et al., 2016)(Goldstein and Kastan, 2015). Additionally, once complex DSBs form, the repair processes occur slowly and chromosomal aberrations can cause cell death or delayed mitosis without further repair.(Nikitaki et al., 2016)(Stewart, 2018)

Double-strand breaks generated by irradiation are by far the most deleterious form of DNA damage, leading to cell death and viable chromosomal rearrangements.

7.3.3 The DNA damage response (DDR)

Over time, cells have developed an efficient and rapid DDR to maintain genomic integrity. DDR is a major determinant of cancer cell responses to radiotherapy and hence radiosensitivity.

The DDR components can be divided in three groups: sensors, signal transducers, and effectors.

DNA damage sensors are generally described as response proteins that can first detect DNA damage and recruit transducer proteins triggering cell signaling transduction signals to enzymes to respond to the break (Schuch et al., 2013) (Kouranti and Peyroche, 2012). Signal transducers are often seen as functional partners of DNA damage sensors (Ciccia and Elledge)(Heijink, et al). As DNA damage sensors and transducers usually coexist, it is difficult to classify them. That said, signal transducers have kinase activity triggering the activity of downstream effectors (Hau and Tsao, 2017).

The effector pathways include proteins involved in cell cycle control, DNA repair and apoptosis (Nakanishi et al., 2006).

7.3.3.1 DNA damage sensor proteins

One of the first DNA sensor proteins identified was Rad24p by Ford et al.in 1994. It is required for DNA damage checkpoint activation and is essential for cell proliferation (Voicu et al., 2007).

To date a series of DNA sensor proteins have since been identified including γH2AX, Rad50, 53BP1, Nbs1, BRCA1/2, or Ku (Ku70/Ku80 heterodimer).

They share some common characteristics: they localize to the sites of DSBs within seconds or minutes after IR exposure, they can recruit other proteins to sites of damage, and can also regulate each other.

γH2AX

γH2AX is a typical example of a marker that has been translated from bench to bedside and has been used as a predictive biomarker for radiotherapy sensitivity in certain cancer types (Siddiqui et al., 2015). The expression of gamma-H2AX has been established as a sensitive indicator of DSBs.

Phosphorylation of H2AX histone at the S139 site to form gamma-H2AX is a known marker of DSBs induced by irradiation and occurs at a very early time at the sites of those DSBs leading to visible γH2AX nuclear foci.(Rogakou et al., 1998).
As indicated by Siddiqui et al, (Siddiqui et al ,2015), γH2AX persisted after exposure to IR under treatment with various radiosensitizing drugs, indicating that this sensor could be used to monitor cancer therapy.

More than a decade ago, Kuo and Yang (Kuo and Yang, 2008) suggested that γH2AX foci could be used as a biomarker for DNA damage as they represent DSBs in a 1:1 ratio.

Of particular interest is the fact that the disappearance of γH2AX foci occurs earlier than that of other IR exposure response proteins. Therefore, γH2AX constitutes a useful and widely used tool to measure irradiation or cytotoxics-induced DNA damage due to its high sensitivity.

Table 2. Summary of a few main DNA damage sensors induced by IR (human versions)

	Length	**Subcellular location**	**Interaction partners**
γH2AX	143	Nucleus (Kobayashi, et al.) chromosome	Several other proteins (Kobayashi et al., 2002) (Stewart et al., 2003)
Nbs1	754	Nucleus (Lee, et al.) ; telomere, chromosome	MCM9 (Lee et al., 2015); BRCA1, MSH2, MSH6, MLH1, ATM, BLM, RAD50, MRE11, and NBN (Wang et al., 2015)
Mre11	708	Nucleus, telomere, chromosome (Lee et al., 2015)	MCM9 (Lee et al., 2015)(Trujillo et al., 1998)
Rad50	1312	Nucleus, telomere, chromosome (Lee et al., 2015)	MCM8 and MCM9 (Lee,et al.), BRCA1 (Zhong et al., 1999), MSH2, MSH6, MLH1, ATM, BLM, RAD50, MRE11, NBN
MDC1	2089	Nucleus, chromosome (Becherel et al., 2010)	MRE11, RAD50 and NBN, CHEK2, the BRCA1-BARD1 complex, SMC1A and TP53BP1, ATM and FANCD2
53BP1	1972	Nucleus (Drané et al., 2017), chromosome	P53 /TP53 (Derbyshire, 2002), H2AFX (Stewart et al., 2003), CHEK2 (Wang et al., 2000) RIF1, PAXIP1, IFI202A and SHLD2
BRCA1	1863	Nucleus (Wu et al., 2016), cytoplasm (Hiraike et al., 2010)	BARD1, UIMC1/RAP80, ARBRAXAS1, BRCC3/BRCC36, BABAM2 and BABAM1/NBA1

Available from https://www.uniprot.org

Fig 12. Damage sensors and their functional complexes in response to DNA double-strand breaks

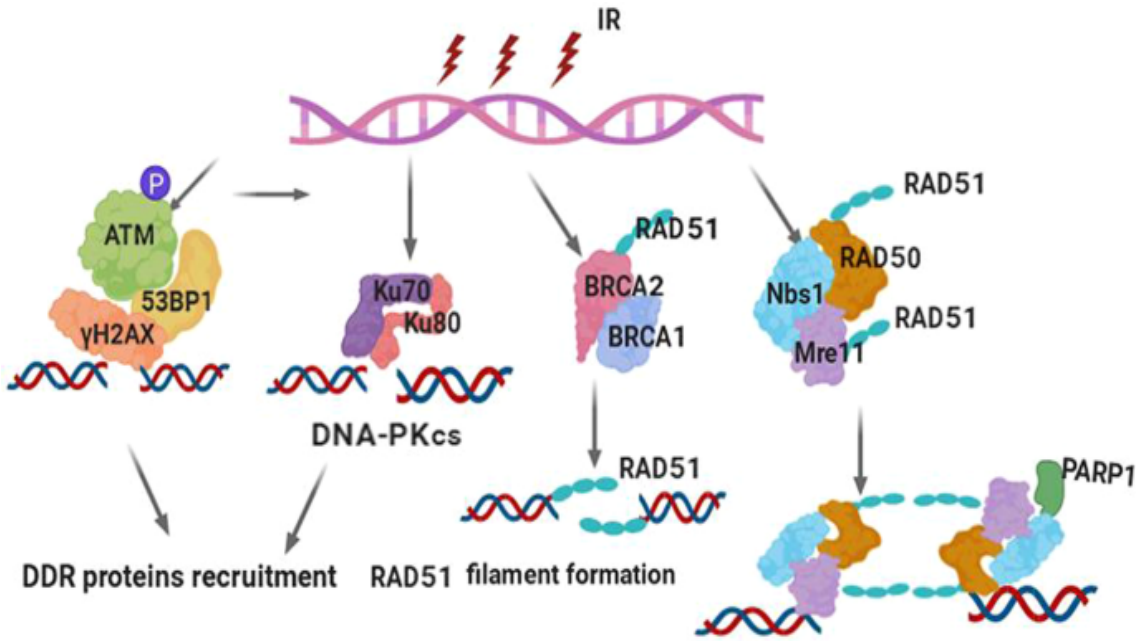

Damage sensors and their functional complexes in response to DNA double-strand breaks. (1) Upon DSB occurrence, the core histone protein variant H2AX is instantaneously phosphorylated on its S139 position to form γH2AX foci, which can be detected at the DSB site. γH2AX provides a platform to recruit DDR proteins, such as 53BP1, MDC1, and ATM, to DSBs to initiate DDR signal transduction. (2) DNA-dependent protein kinase (DNA-PK), composed of Ku70, Ku80, and the catalytic subunit DNA-PKcs, is a classical DSB-sensing and -binding complex. DSB binding by DNA-PK protects the broken DNA end from degradation by endogenous nucleases; on the other hand, it recruits and activates the downstream components in the NHEJ pathway of DSB repair. (3) BRCA1 and BRCA2 are key proteins involved in DSB binding and initiating the HR pathway and later repair processing. BRCA2 directly recruits RAD51 to sites of DNA damage through interaction with conserved BRCT motifs to stabilize the RAD51 nucleoprotein filament on the ssDNA end of DSBs. Following end resection of the DSBs, BRCA1 activates RAD51 to promote gene conversion of homologous recombination. (4) The MRN complex (Mre11-Rad50-Nbs1) is the primary sensor of DSBs and localizes to damage sites to initiate end resection and HR processing. The MRN complex also promotes the recruitment and activation of ATM and PARP-1. PARP-1 produces poly(ADP-ribose) polymers and extends DNA damage signaling

Signal Transduct Target Ther. 2020; 5: 60.
Published online 2020 May 1. doi: 10.1038/s41392-020-0150-x

P53

P53 protein is a crucial tumor suppressor encoded by the TP53 gene. It is activated and phosphorylated on serine-15 in response to cellular stress (Horn and Vousden, 2007).

The p53 pathway is a key player in determining cells fate via involvement in DNA repair, induction of permanent or transient cell cycle arrest and induction of apoptosis (Purvis et al., 2012).

In response to cell stress such as telomere shortening and radiation, ataxia telangiectasia mutated (ATM) protein kinase phosphorylates p53 leading to its stabilization and transcriptional activation of p21 (CDKN1A)-mediated cell cycle arrest. Other kinases involved in checkpoint control, such as ataxia-telangiectasia and Rad3-related protein (ATR), checkpoint kinase 1 (CHK1), and checkpoint kinase 2 (CHK2), also target p53 (Harris and Levine, 2005).

Fig 13. Factors that might determine the outcome of p53 activation by IR

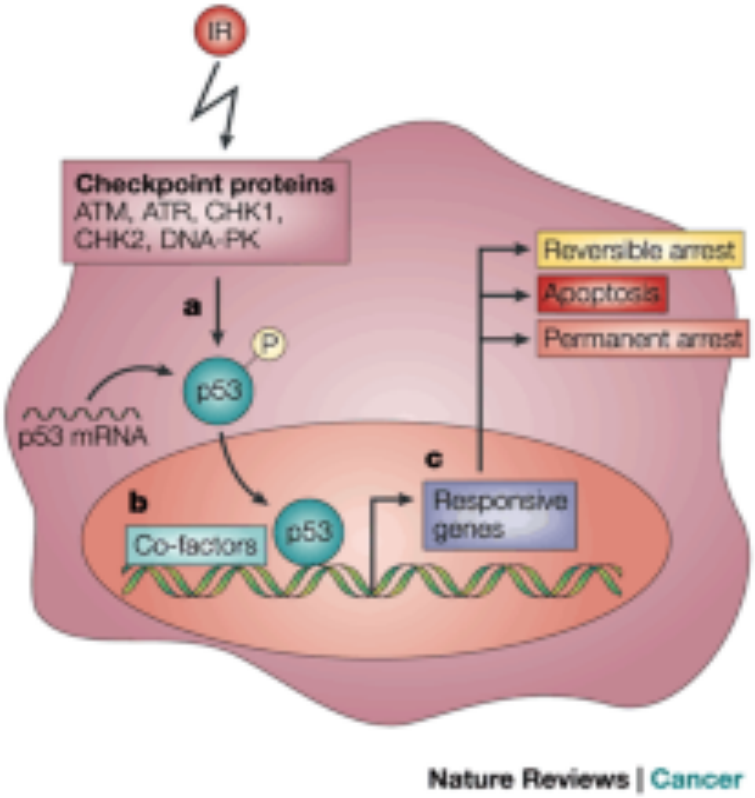

Gudkov, A., Komarova, E. The role of p53 in determining sensitivity to radiotherapy. *Nat Rev Cancer* **3**, 117–129 (2003). https://doi.org/10.1038/nrc992

7.3.4 Signaling pathways of DDR and repair

7.3.4.1 The IR-induced DNA damage response

As seen earlier, IR leads to cell death via the induction of DSBs in cancer cell DNA resulting in genomic instability, indirectly via induction of ROS, (Smith et al., 2017) apoptosis, cell cycle checkpoint alteration or post-mitotic death.

When DNA damage occurs, the repair machinery stops the cell cycle at specific control checkpoints to repair DNA damage and prevent continuation of the cell cycle. Intrinsic radiosensitivity of tumor cells is strongly influenced by the cells DSB repair capacity (Mladenov et al., 2013).
If the radiation damage can be efficiently repaired by tumor cells, this leads to development of radiation resistance enabling cells to survive and replicate. In the event that the damage remains unrepaired, these mechanisms induce programmed cell death or apoptosis to prevent accumulation of mutations in daughter cells (Deckbar et al., 2011).

The major repair pathways used by cells for dealing with DSBs are homologous recombination repair (HRR) non-homologous end-joining (NHEJ), and alternative NHEJ, operating as a backup. The goal of these is to handle different forms of DNA lesions eventually achieving DSB removal and maintaining genomic integrity (Iliakis et al., 2019). Importantly, their function represents a major mechanism of radiation resistance in tumor cells.

Fig 14. Major DNA double-strand break repair pathways

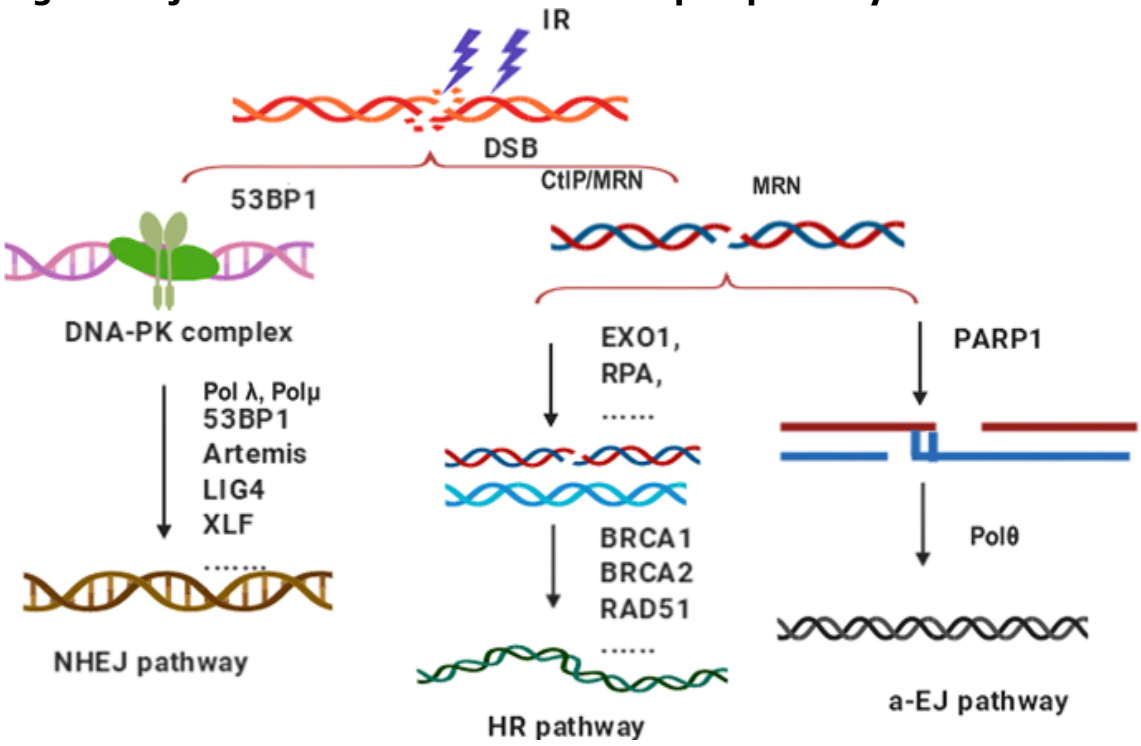

The pathways of DNA double-strand break repair. The nonhomologous end-joining (NHEJ) pathway is an error-prone repair pathway that functions through the cell cycle. The homologous recombination pathway is an error-free repair pathway that requires intact homologous DNA as a repair template and is active in the later S and G2 phases. The alternative end-joining (a-EJ) pathway, which repairs DNA double-strand breaks (DSBs), is initiated by end resection that generates 3′ single strand.

The HR repair pathway was the first to be discovered and named due to the close proximity of homologous strands during mitosis. It is specifically triggered in the later S and G2/M phases (Resnick, 1976).

In 1980's , the DNA end-joining pathway was discovered. The NHEJ pathway is triggered in the G0/G1 phase as well as G2/M phases (Lodovichi et al., 2020) and is supposed to be predominant in mammalian cells compared to microorganisms. (Roth et al., 1985)

The HR repair pathway requires a template, is slow but highly accurate. It is only initiated at the later G2 and S phases, can repair both one and tow-ended breaks, and can repair protein-blocked ends. (Turan and Oktay, 2020).

.

The HR pathway has also been used as a genome editing tool, an example being the clustered regularly interspaced short palindromic repeats (CRISPR)-Cas9 technique.(Knott and Doudna, 2018).

Importantly, the HR pathway is associated with radioresistance.

A recent study by Jin et al.(Jin et al., 2019) found that *Deinococcus* shows high resistance to IR exposure due to a combination of defense mechanisms such as self-repair of DNA damage through the HR pathway. (Lopez Perez et al., 2019) reported that glioblastoma cells exposed to carbon ions initiated the HR repair pathway with significant cell cycle delays, predominantly in G2 phase.

In clinical practice both HR and NHEJ pathways are important for repairing irradiation-induced DSB's.

For example, GSK212, a MEK1/2 inhibitor functionally repressed both HR and NHEJ repair pathways leading to delayed DNA repair and persistent increased expression of gH2AX as a way to modulate radiosensitivity (Estrada-Bernal et al., 2015).

As such, upregulation of DNA repair pathways or up-regulation of DDR genes (BRCA1, RAD51, FANCG) are recognized as a primary acquired mechanism through which cancer cells may become radioresistant (Young et al., 2014). Additionally, DDR alterations also alter the TME and the inflammatory cascade (Khalil et al., 2016).

7.3.5 Activation of cell cycle checkpoints

The cell cycle is essential for cell growth, proliferation and reproduction. It allows cellular components to be replicated and delivered to the next generation of cells (Barnum and O'Connell, 2014). It involves a large number of regulatory proteins.

Cell cycle checkpoints, maintain genomic integrity and ensure an ordered succession of cell cycle events. These checkpoints are critical for protecting cells from progressing into the next phase of the cell cycle before resolution of prior molecular events such as DNA damage or spindle structure disruption has taken place (Wang et al., 2015).

Radiotherapy induced DNA damage triggers cell cycle checkpoints activation to block cell cycle progression therefore allowing time for cells to repair the damage.

Depending on the phase of the cell cycle the damage is sensed, the cells can be blocked at the G1/S or G2/M phase of the cell cycle. (Fig 15)

Fig 15. Irradiation and celle cycle checkpoints

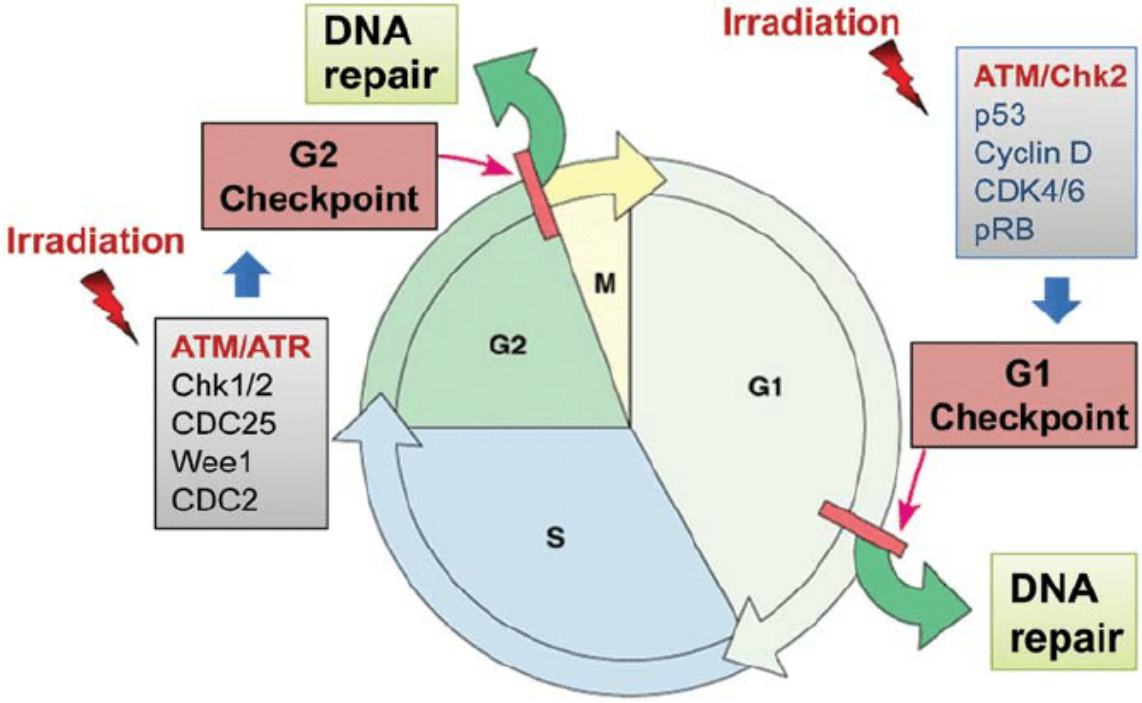

Irradiation induces G1 and G2 cell cycle checkpoint activation and DNA repair. Most cancer cells are defective in G1 checkpoint, commonly due to the mutations/alterations of the key regulators of the G1 checkpoint (in blue), but contain a functional G2 checkpoint.
Irradiation induced DNA damage is one of the major triggers for the activation of a number of DNA structure checkpoints, leading to cell cycle arrest at various stages called G1 /S phase arrest, S-phase arrest and G2/M arrest, spindle checkpoint arrest and M-phase arrest.
Int J Oncol. 2014 Nov; 45(5): 1813–1819.
Published online 2014 Aug 20. doi: 10.3892/ijo.2014.2614

7.3.5.1 G1/S checkpoint

In G1/S arrest, the cyclin D-CDK4/6 complex phosphorylates pRB, leading to the release of transcription factor E2F from pRB and activation of cyclin E

transcription. Cyclin E forms a complex with CDK2, which further phosphorylates pRB in a positive feedback loop and promotes the transition from G1 to S phase. (Finkielstein et al., 2002)(Peng et al., 2020a).

Irradiation may contribute to transient delays or interruption of the G1/S transition, resulting in S phase arrest. Theoretically, a G1/S arrest would give cells with radiation exposure more time to perform DNA damage repair. Transcription factor p53 has been shown to regulate the cell cycle (Kotteman and Bale) mainly by monitoring G1 and G2/M checkpoints (Barnum and O'Connell). P53 is required for the arrest in G1 phase and G1 arrest is consequently associated with its status.

The crucial p53 protein is encoded by the TP53 gene. The p53 pathway determines the fate of the cell via involvement in DNA repair, induction of permanent or transient cell cycle arrest and induction of apoptosis.

Ataxia telangiectasia mutated (ATM) kinase ATM functions as an important initiator of the DNA damage response and activates p53 a strong tumor suppressor.
ATM is activated under several cellular stress condition including radiation, oxidative stress or hypoxia. (Khoronenkova and Dianov, 2015)(Chow et al., 2019) Once activated, it phosphorylates p53 leading to its stabilization and transcriptional activation of p21 cyclin-dependent kinase inhibitor-mediated cell cycle arrest.

In their study, Nagasawa et al. have shown the absence of G1/S arrest in cancer cells expressing normal p53 synchronized by mitotic selection following irradiation. Subsequent data point that p53 is regulated at post-translational level by a series of protein interactions (Fabbro et al., 2004) and phosphorylation.
As a result, phosphorylation of p53 serves to monitor G1/S arrest by inducing the cyclin-dependent kinase inhibitor, p21.

Regulation of p53 in response to irradiation is complex, therefore recovery or activation of p53 could be a strategy for overcoming radiation resistance.

7.3.5.2 S-phase arrest

During IR induced cell damage response, S-phase arrest is activated to inhibit DNA synthesis (Wang). Several DNA damage patterns can trigger S-phase

arrest including DSBs, DNA crosslinks and DNA adducts.(Barnum and O'Connell, 2014)(Deckbar et al., 2011).

Deficiencies in S-phase checkpoints accelerate DNA synthesis in case of DSBs in patients with ataxia -teleangiectasia or other chromosomal syndromes. Additionally, ATM phosphorylates both Nbs1 and CHK2 leading to S-phase checkpoint activation following irradiation.

Regulation of the S-phase checkpoint is complex as it involves multiple pathways.

7.3.5.3 The G2/M checkpoint

The G2/M checkpoint is considered crucial in preventing premature mitosis in cells with damaged DNA especially in cells with p53 functional deficiency. (Cuddihy and O'Connell, 2003).

G2/M arrest prevents cells from entering the Mitosis phase in presence of DSBs (Wang et al., 2015). There is high variability in the duration and level of cell cycle arrest and recovery time among different cell lines. G2/M arrest often occurs 0.5 to 4h post irradiation in mammalian cells and then resolves. (Peng et al., 2020b)

It is generally considered that the higher the dose of IR, the more obvious the G2/M arrest, and the more delayed the recovery effect.

In response to DNA damage caused by IR, cancer cells are arrested in proliferation and increased apoptosis. However, radiation resistant cells are able to overcome the cell cycle block and proceed to proliferation.

In their study, Peng et al. (Peng et al., 2020a)show that radioresistant cells show a recoverable G2/M phase during prolonged cell cycle and manifested lower apoptosis rate and more colony formation.

Fig 16. Functional complexes and cyclin-dependent kinases (CDKs) and the signaling pathways involved in the regulation of cell cycle checkpoints in response to IR-induced DNA damage.

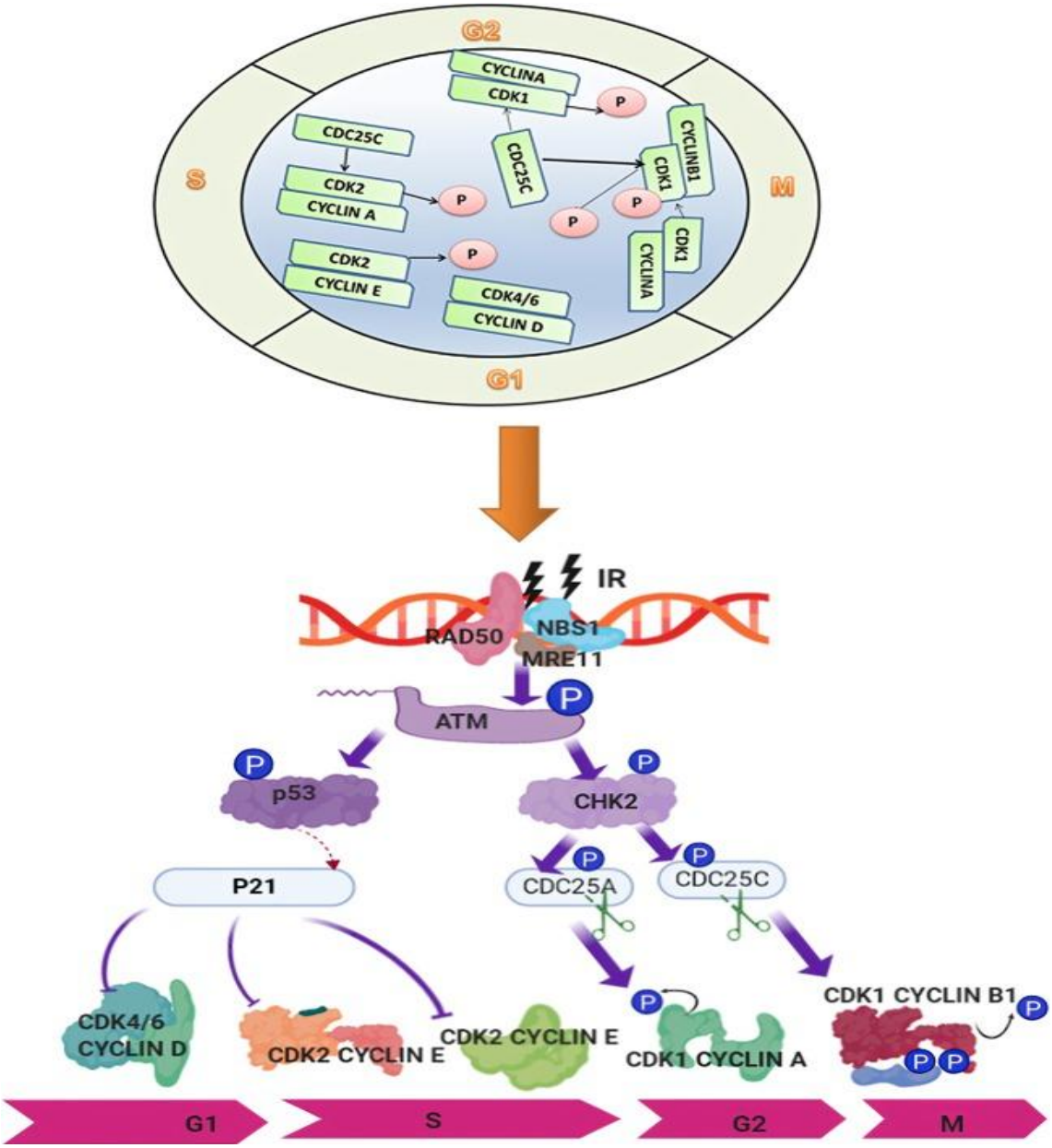

Signal Transduct Target Ther. 2020; 5: 60.
Published online 2020 May 1. doi: 10.1038/s41392-020-0150-x

Targeting DNA damage repair in order to sensitize cancer cells to irradiation remains a promising therapeutic approach. However most DNA damage pathway inhibitors lack toxicity assessments and require estimation of the risk of carcinogenesis prior to clinical application.

The idea of inhibiting kinases involved in the cell cycle checkpoint control responsible for cell cycle progression and DNA damage repair is a promising approach to overcoming radioresistance. (Vlatkovic et al., 2022).

7.4 From the 4 to the 6 R's of Radiotherapy

Whiters et al. defined the 4 R's of radiotherapy in 1975. The classical 4 R's "Repair, Redistribution, Repopulation, Reoxygenation" were mainly used in order to understand the differential response from one patient to another to RT and to explain the effect of RT fractionation on the treatment efficacy.

Later, a key 5th "R" or Radiosensitivity (Steel et al., 1989) has emerged in the form of intrinsic radiosensitivity as a probable result of our inability to explain at the mechanistic level the different radio-curabilities of malignancies like lymphomas, seminomas or gliomas or melanomas.

Each « R » can be viewed as a double-edged sword, such that changes can occur in either direction to increase or decrease the net therapeutic effect (Chew et al., 2021).

It is now widely accepted that the immune response could play a critical role in RT response leading to the emergence of a 6th R: Reactivation (of the anti-tumor immune response). (Boustani et al., 2019)(Fig 17).

Fig 17. The 6 R's of radiotherapy

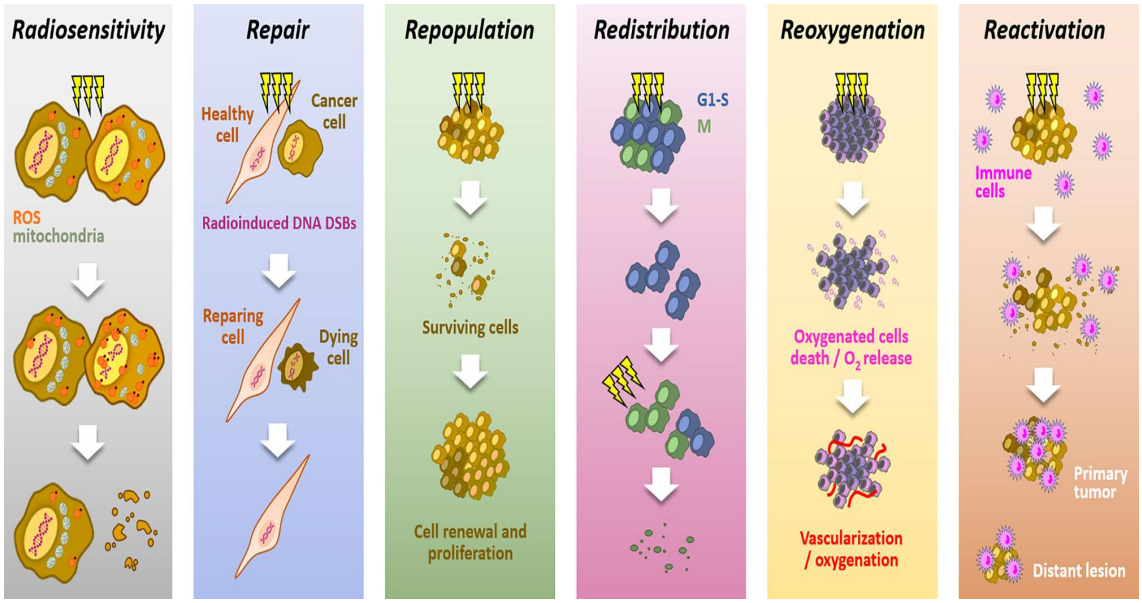

The six "Rs" dictating the response to radiotherapy.

Radiotherapy response depends on six parameters: *Radiosensitivity*, refers to the cell-intrinsic mechanisms (*e.g.*, metabolic adaption, ROS detoxification), explaining differences in cell responses to irradiations; *Repair*, refers to the cell capacity to survive by repairing radio-induced damages (particularly DSBs), in theory, more characteristic of healthy cells; *Repopulation*, refers to the tumor cells capacity to grow following a radiotherapy fraction; *Redistribution*, refers to the progression of cancer cells from radioresistant cell cycle phases (*i.e.*, G1/S) toward more radiosensitive phases (*i.e.*, G2/M), between radiotherapy fractions; *Reoxygenation*, refers to the oxygen level recovery following irradiation, due to well-oxygenated cells death and tumor vascularization; *Reactivation*, refers to the triggering of a systemic anti-tumor immune response following irradiation-induced immunogenic cell deaths.

https://doi.org/10.3389/fendo.2021.742215

7.4.1 Repair

Ionizing radiation causes DNA damage, as a result, cell survival following radiation depends on its ability to repair itself and on the type of DNA lesion. In the event the DNA lesions are irreparable, cell activate death programs (Schultz, et al.). In case of post-irradiation survival, tumor cells continue to proliferate (Brown et al., 2019).
Different DNA repair mechanisms are involved including base excision repair (BER), nucleotide excision repair and DNA DSB repair. Homologous recombination repair (occurs in late S/G2 phase) uses undamaged sister chromatin as template and represents a slow process, while nonhomologous

end joining is a fast but error prone and potentially mutagenic process occurring in G1 phase.

7.4.2 Redistribution through the division cycle

Cells are likely to be in different phases of the cell cycles during irradiation and exhibit different levels of radiosensitivity during the cell cycle as discussed earlier. Cells in the S phase are more radioresistant and cells in G2/M more radiosensitive. During the fractionated radiation cells in the G2/M phase are preferentially killed. The time between the two fractions allows resistant cells from the S-phase to redistribute into cell cycle phases in which cells are more radiosensitive.

7.4.3 Repopulation

"Repopulation" is the process of renewal and increase in cell division seen in surviving normal and malignant cells in between irradiation fractions. It represents one of the main reasons for failure of conventionally fractionated radiotherapy.
The time of onset and rate of repopulation after irradiation vary with the tissue.

Some tumors exhibit accelerated repopulation, a marked increase in their growth fraction and doubling time and decrease in cell cycle time at 4 weeks, such as in SCC head and neck or cervix. It can be countered if treatment time extends over 5 weeks.

Extensive data support the role of cancer stem cells (CSCs) in cancer progression and post-radiothrapy recurrence (Liu et al., 2020). and their subsequent association with hypoxia (Phillips et al., 2006)(Najafi et al., 2020). An important characteritstic of somatic stem cells, whether normal or malignant is their ability to perform asymmetric cell divisions which give rise to a daughter stem cell and a committed progenitor cell (Chhabra and Booth, 2021). In a symmetric cell division in contrast, stem cells divide into two committed progenitor cells or two daughter stem cells.

The asymmetric cell division is key to tissue homeostasis (Yamashita et al., 2010) as even small changes in the way stem cells divide have huge impact on organization of a tissue or tumor and are thought to be behind the mechanism of accelerated repopulation.

7.4.4 Re-oxygenation

The sensitivity of radiation increases in well oxygenate tissues.Hypoxia is a consequence of the high tumor cell proliferation rate and the abnormal structure of the tumor vasculature (Rey et al., 2017).

Pre-clinical data suggest that tumor cells in a hypoxic environment have a higher probability of surviving after irradiation.

Reoxygenation refers to the fact that between radiotherapy fractions, well-oxygenated cells death leads to oxygen release, reduction in oxygen demand and tumor shrinkage which in turn allows better oxygen diffusion and angiogenesis.(Rakotomalala et al., 2021).

While reoxygenation turns initially hypoxic areas to a more radiosensitive state, the process leads to oxidative stress and paradoxically stabilizes HIF-1. (Harada et al., 2009).

Numerous studies have shown that reoxygenation of tumors may occur only 24 to 72h after irradiation (Crokart et al., 2005) (Harada et al., 2009)

Harada et al,(Harada et al., 2009) show that tissue reoxygenation leads to an increase of HIF-1 (hypoxia inducible factor-1) activity through AKT/mTOR signaling activation.

At present, the role of reoxygenation in response to RT remains ambiguous. While the oxygen level increase radiosensitizes tumor cells via the so called "oxygen effect", reoxygenation induces radioresistance through hypoxia-related signaling (HIF-1 stabilization mediated by oxidative stress) (Kabakov and Yakimova, 2021).

Fig 18. Reoxygenation

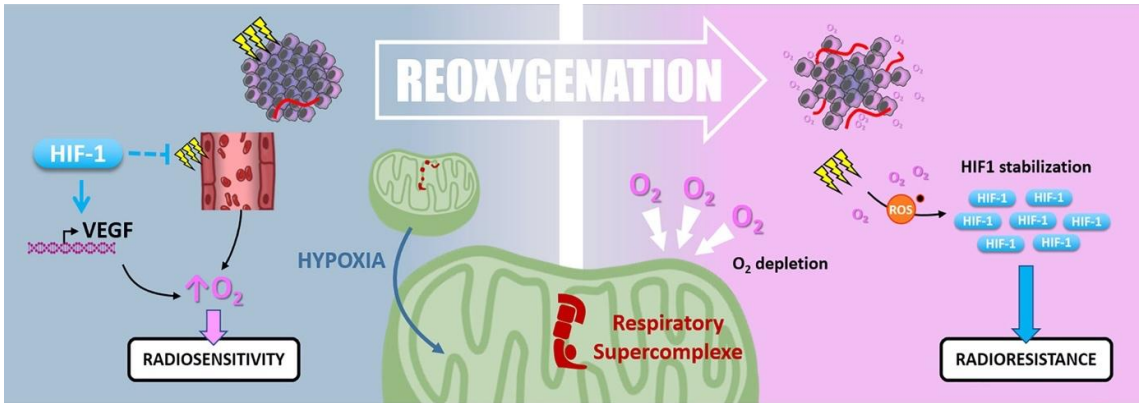

Radiotherapy induces tissue reoxygenation through O_2 release and angiogenesis. Hypoxia also favors reoxygenation since HIF1 protects endothelial cells from irradiation and promotes VEGF expression. Nevertheless, hypoxia induces mitochondrial respiratory supercomplexes formation, which could persist after reoxygenation and cause high O_2 consumption and depletion. Oxidative stress due to irradiation and reoxygenation stabilizes HIF-1, which can maintain radioresistance

Front. Endocrinol.;02 September 2021 Sec. Cellular Endocrinology
Volume 12-2021
https://doi.org/10.3389/fendo.2021.742215

Different mechanisms contribute to the process of re-oxygenation. Oxygen availability is closely linked with the microvascular network. While Grogan, et al.(Grogan et al., 2017) used 3-D vessel network representations, various models have been developed to study the dynamics of hypoxia and the effect of reoxygenation in fractionated radiotherapy (Kempf et al., 2015)(Harting et al., 2007).

Hami et al, (5), developed a multi-scale model considering the spatio-temporal evolution of oxygen during radiotherapy treatment as well as the whole 5 R's of radiotherapy to predict the effects of radiation on tumor growth.

7.4.5 Radiosensitivity

A fifths factor was added by Steel: radiosensitivity, in recognition of the fact that the intrinsic vulnerability of cancer cells differs markedly, as well as individual radiosensitivity. (Steel et al., 1989).

In conventional radiotherapy therefore, the relative biologic effectiveness of radiation is influenced by the '5Rs'. A linear quadratic model prevails to describe the radiation response of the tumor in which the alpha/beta ratio is used to characterize the sensitivity of a particular tissue type to fractionation.

7.4.6 Reactivation

While radiotherapy was long considered immunosuppressive, the last two decades have shed some new light.

Radiotherapy leads to immunogenic cell death (ICD) by inducing critical events for DC activation and effector T cell priming : the cell translocation of calreticulin, the extracellular release of high-mobility group protein B1 HMGB1 and the release of ATP (Kroemer et al., 2013).

In addition to this, RT can modulate the expression of several receptors and cytokines by cancer cells and tumor stroma resulting in modifications of the TME that can be harvested to enhance the effect of immunotherapy (Demaria et al., 2005).

It has been shown that RT promotes the cytotoxic CD8 and Th1 cells recruitment to TME by the induction of chemokines CXCL9, CXCL10 and CXCL16 (Matsumura, et al.)

While reshaping of the TME undoubtedly includes immunosuppressive effects such as MDSC, T-regs, M2- like marcrophage polarization, up-regulation od PD-L1 and CTLA-4, , RT also induces immunostimulatory effects. Those modifications including DC, CD8+ Tcells and NK cells activation, interferon type I and II response or Fas apoptotic cell death, contribute to an increase in the ability of tumor cells to be recognized by the immune system and to the activation of the adaptive and innate immunity effectors leading to a specific anti-tumor response. Therefore, the irradiated tumor becomes an in-situ vaccine contributing to a systemic anti-tumor response in addition to the local RT effect.

Fig 19. Reactivation

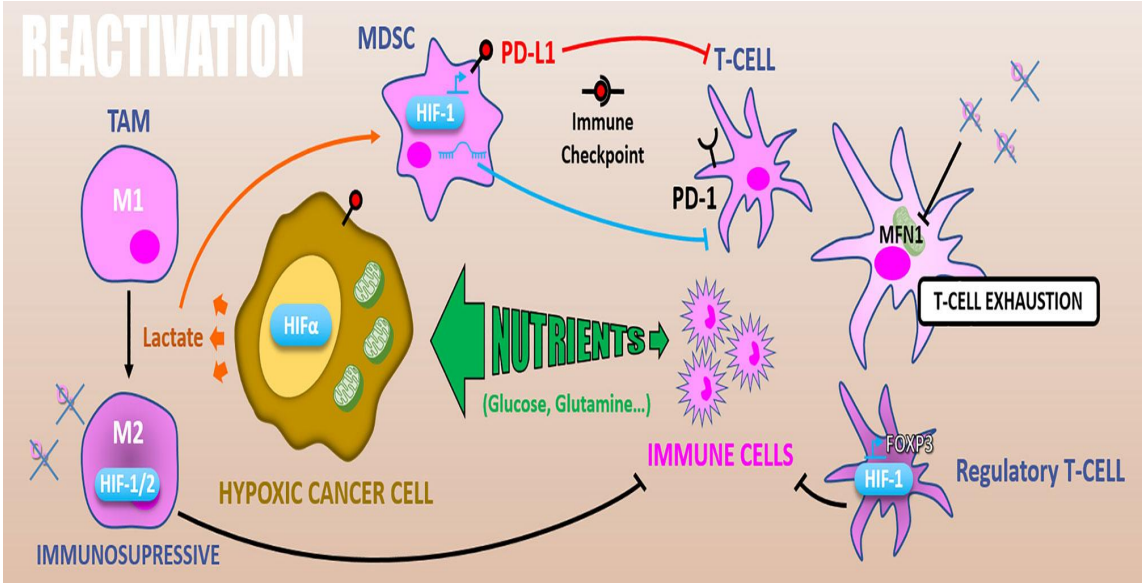

Because of exacerbated metabolism, hypoxic cancer cells consume nutrients from the microenvironment and starve immune cells. In addition, glycolytic metabolism produces lactate which polarizes TAMs in M2 immuno-suppressive and activates MDSCs inhibiting T-cells. HIFs expression in TAMs increases their immunosuppressive activity. Also, in MDSCs HIF-1 promotes PD-L1 expression that inhibits T-cell through PD-1/PD-L1 immune checkpoint. HIF-1α differentiates T-cells into immunosuppressive regulatory T-cells *via* FOXP3 expression. Finally, hypoxia can cause T-cells exhaustion by reducing their energetic metabolism through MFN1 down-regulation.

Front. Endocrinol.;02 September 2021 Sec. Cellular Endocrinology
Volume 12-2021
https://doi.org/10.3389/fendo.2021.742215

8 FACTORS INFLUENCING RADIOSENSITIVITY

Radiosensitivity can be influenced both by factors intrinsic and extrinsic to a cancer cell.

8.1 EXTRINSIC FACTORS

8.1.1 Hypoxia

One of the factors in the tumor microenvironment (TME) extrinsic to the cancer cell that can influence radiosensitivity is oxygenation.

In vivo, it is generally accepted that radiosensitivity of a tumor depends on the complex interaction between the intrinsic sensitivity of the cancer cells, and that of the tumor microenvironment, with hypoxia representing a major modulator of radiosensitivity (Vaupel, 2004).
Ambient air is 21% O_2 (150 mm Hg); however, most mammalian tissues exist at 2%-9% O_2 (on average 40 mm Hg). Hypoxia is usually defined as ≤ 2% O_2.(Bertout et al., 2008)

Research into hypoxia's role in tumor biology started in the early 20th century by Otto Warburg who demonstrated that tumor cells favor glycolysis unlike normal cells. Increased glycolysis and subsequent CO2 production result in acidification of the tumor microenvironment (Vaupel et al., 2019). This hypoxic and acidic environment can in turn make cells resistant to both radiation and chemotherapy (Cairns et al., 2006).

Following Warburg's observation, first research attempts looked at determining whether hypoxic or anoxic cells can be found in mammalian tumors and how these cells affected radiotherapy. (Bertout et al., 2008)
In 1940's Lacassagne and Evans et al. demonstrated the radioprotective effect of anoxia in normal tissues using whole body anoxia in newborn rodents (reviewed in {Gray, 1953 #6395}). Since then, it has been largely demonstrated that molecular oxygen significantly modifies the effectiveness of radiotherapy.(Evans and Koch, 2003)(Wilson and Hay, 2011). More precisely, the response of anoxic regions of the tumor to irradiation is 2.5-3 times weaker (Zdrowowicz et al., 2022) compared to that of their well-oxygenated ccounterparts, known as the oxygen enhancement ratio. (Hall and Giaccia, 2006)(Bertout et al., 2008).

Low tissue oxygenation influences the response to several treatment modalities by contributing to to chemoresistance, radioresistance, angiogenesis, vasculogenesis, invasiveness, resistance to cell death, altered metabolism and genomic instability. (Wilson and Hay, 2011). Hypoxia is considered to be a negative prognostic and predictive indicator as hypoxic tumors are more biologically aggressive and more likely to recur locally and metastasize.

Indeed, other elements in the TME such as stromal cells and the expression of factors such as VEGF and hypoxia-inducible factor-1 (HIF-1) may influence tumor radiosensitivity.

8.1.2 Hypoxia Inducible factors (HIFs)

HIFs are heterodimeric transcription factors consisting of an α and a β sub-unit.

HIF1 is found in mammalian cells cultured in hypoxic conditions and is required for transcriptional activation mediated by the erythropoietin gene enhancer in hypoxic cells.(Wang et al., 1995)

Fig 20. Genes activated by hypoxia-inducible factors involved in tumor progression

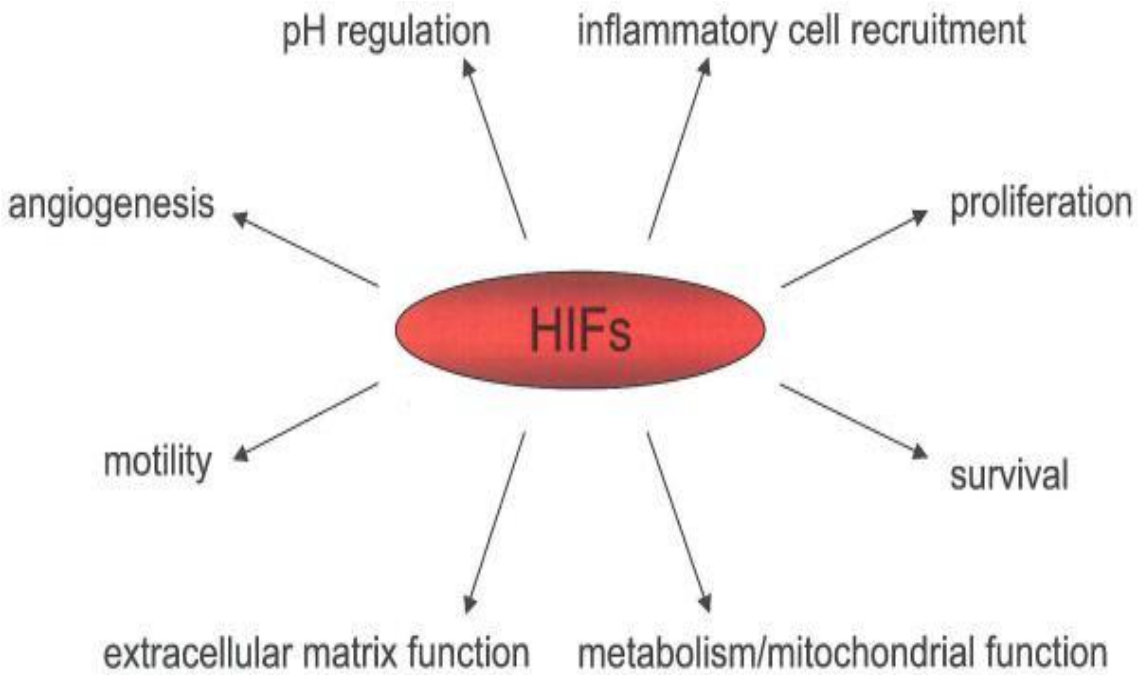

Genes encoding proteins involved in numerous aspects of tumor initiation, growth and metastasis are transcriptionally activated by either HIF-1α or HIF-2α. Examples include: inflammatory cell recruitment (SDF-1α, CXCR4), proliferation (cyclin-D2, IGF-2), survival (VEGF, erythropoietin), metabolism/mitochondrial function (glycolytic enzymes, PDK-1), extracellular matrix function (fibronectin-1, collagen type-5), motility (c-MET, SPF-1α), angiogenesis (VEGF, PDGF), and pH regulation (carbonic anhydrase-9).

Nat Rev Cancer. 2008 Dec; 8(12): 967–975.
Published online 2008 Nov 6. doi: 10.1038/nrc2540

8.2 INTRINSIC FACTORS

Law of Bergonie and Tribondeau

The law of Bergonie and Tribondeau states that the "The radiosensitivity of a cell is directly proportional to its reproductive rate and is inversely proportional to its degree of differentiation."

This means that radiosensitivity increases with:

- Increased rate of cell division
- Low degree of specialization (stem cells are very radiosensitive)
- Higher metabolic rate
- Increased oxygenation
- Increased length of time they are actively proliferating

8.2.1 Intrinsic radiosensitivity

Radiosensitivity is correlated to the ability of cells to detect and repair or not the irradiation induced DNA damages.

In vivo, radiosensitivity of a tumor depends on the complex interaction between the intrinsic sensitivity of the cancer cells, and that of the tumor microenvironment, with hypoxia representing a major modulator of radiosensitivity (Vaupel) as seen earlier.

Normal cell radiosensitivity

The first evidence for a genetic basis of individual sensitivity to radiation came from the observation that people with ataxia telangiectasia were very sensitive to radiation in vitro.

Taylor et al. described that extreme normal-cell radiosensitivity in those patients played a role in severe radiotherapy toxicity and morbidity (Taylor, et al).

By the end of 1980's, extensive evidence was accumulating showing that there was variation in in vitro sensitivity to radiation of cells cultured from patients without any genetic syndrome (Malaise et al. 1987).

Tumour cell radiosensitivity

Early in the 20th century Studies by West et al.(West et al., 1989) (West et al., 1993) highlighted the potential prognostic role of of tumour cell radiosensitivity measurements in assessing response to radiotherapy. They measured intrinsic radiosensitivity of cervical carcinoma using a clonogenic assay in patients undergoing radical radiotherapy showing that the 3 year patient survival rate was higher for those with SF3.5 values less than median.

In 1993 Girinsky et al. (Girinsky et al., 1993) studied radiosensitivity in biopsies obtained from head and neck cancer patients undergoing surgery and radiotherapy or radiotherapy alone suggesting in vitro parameters might be useful in predicting treatment outcomes.

It is now widely accepted that intrinsic radiosensitivity is defined by multiple factors including radiation physics, comorbidities, treatment, Poisson statistics (chance that a cell in irradiated normal tissue sustains lethal damage), inherited genetic basis, epigenetics or inter-individual variability.

However, tumour sterilization by irradiation depends above all upon intrinsic radiosensitivity of tumour cells and factors affecting it, such as hypoxia, proportion of cells in S phase, loss of repair pathways integrity.

8.2.2 The cell cycle effect

Role of the cell cycle in mediating sensitivity to radiotherapy

Three major radiation-induced checkpoints exist, in G1, S and G2 phases. Following DNA damage, cell cycle checkpoints are activated to block cell cycle progression and prevent propagation of cells with damaged DNA.

Cell cycle blockage in the G1 phase after irradiation is believed to allow time for recognition/repair of DNA damage prior to the initiation of DNA synthesis.

The G1 checkpoint is mediated mainly by ATM resulting in activation of P53 tumor suppressor transcriptional activity which is often deficient or lacking in tumor cells.
Tumor cells may therefore rely more on the S and G2 checkpoints for repair of radiation damage compared to normal cells.

Radiation resistance in the S phase is thought to be due to an elevated amount of DNA synthesis and repair enzymes, as well as high intracellular levels of glutathione (a free radical scavenger). Cells in S-phase at the time of radiation have a slower DNA synthesis which is mediated by two distinct pathways, ATM/NBS1/SMC1 and ATM/CHK2/CDC25A/CDK2. (Kastan and Bartek, 2004).

Cells are most sensitive in the G2/M phase of the cell cycle, partly due to the lack of time for adequate repair before chromosome segregation takes place. (Sharda et al., 2002) Encyclopedia of Cancer (second edition 2002).

A checkpoint arrest in G2 is not dependent on ATM, p53 or p21, in contrast to checkpoint response in G1 phase. Activation of the G2 checkpoint in response to DNA damage prevents entry of cells into mitosis and is initiated by ATM-mediated activation of ChK1 and ChK2. While ATM is the initial activator of this pathway, ATR activation and Chk1 are essential to checkpoint maintenance (Liu et al., 2000)(Flynn and Zou, 2011).

Fig 21. Cell cycle phases with the most and least radiosensitive phases.

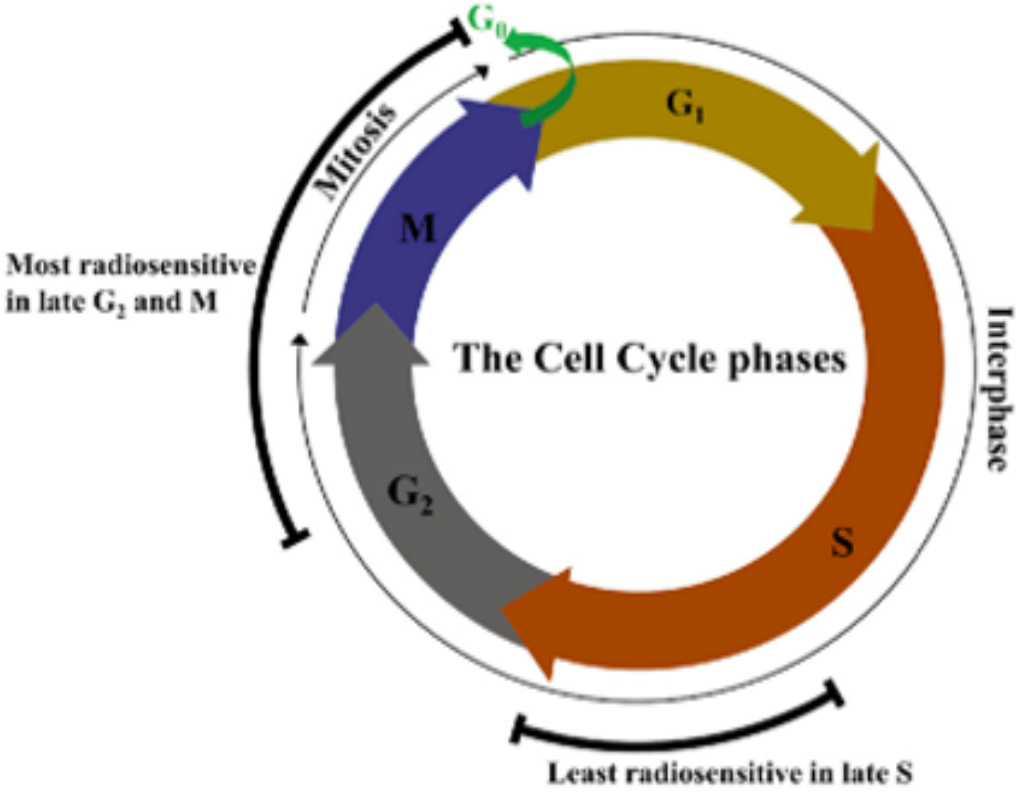

https://doi.org/10.1016/j.radphyschem.2020.108994

In the late 1960's studies started to examine the dependence of the radiation response on the phase of the cell cycle. It has since then been known that cells in different cell cycle phases display different radiosensitivity.
Cell survival data have shown that cells were most sensitive to irradiation during mitosis M and G2 phase, less sensitive in G1 and least sensitive during the late phase S (Sinclair and Morton, 1963)(Sinclair, 2012).

Synchronization studies were performed in different cell lines (e.g.; HeLa cells, Yoshida sarcoma cells, mouse fibroblasts or L cells) (Terasima and Tolmach, 1963a) (Therasima and Tolmach Science), (Mak and Till, 1963) and during those early experiments methods used include excess thymidine, serum starvation, mitotic "shake-off" or hydroxyurea (Sinclair and Morton, 1966)(Terasima and Tolmach, 1963b)(Sinclair, 1967). More recently, lovastatin or fluorescence activated cell sorting were some of the methods used to isolate phase-specific cell populations. (Wlodek and Hittelman, 1988)(Herzenberg et al., 2002).

As a general rule, the method of synchronization used determines the phase of the cell cycle that cells are arrested in. For example, excess thymidine blocks the cell cycle in the S phase, and lovastatin in early G1 phase. Regardless of the method used, maximal radiosensitivity has been generally found in the mitosis phase with resistance during the S phase reaching a maximum in the late part of the S phase (Sinclair, 2012) (Sinclair, 1968). Following those findings, the concept of cell cycle synchronization has emerged as a potentially important way to enhance RT efficacy (Formenti et al., 1999)(Hennequin et al., 1996) (Kano et al., 1998)(Zoli et al., 1999).

Despite extensive progress made in understanding the cell-cycle phase, the therapeutic application of synchronization remains limited. This is partly due to the fact that timing of synchronization varies in different cell lines and that optimal synchronization is seldom achieved (Pawlik and Keyomarsi, 2004). Synchrony of cell populations is difficult to maintain and many human tumors display a kinetic heterogeneity even after synchronization (Steel, 1994). Additionally, the synchronization of cell populations before each RT fraction would be difficult to achieve, given the average cell cycle time and the heterogeneity of most cancer cells.

Nonetheless, cell type and organ specific variations in intrinsic radiosensitivity exist and are to be taken into consideration. Deschavanne and Fertil (Deschavanne and Fertil, 1996) showed that in vitro radiosensitivity varied depending on the cell type and organ. Biade et al. studied the effects of RT on ovarian OVCAR10 and HT29 colon cells showing that both cell lines exhibited a maximal radioresistance near the G1-S phase boundary but HT29 cells remained relatively radioresistant in th G2 phase, while ovarian cells became more radiosensitive (Biade et al., 1997).

8.2.3 Ability to repair DNA damage

Exposure to RT induces activation of a complex signal transduction network, the DNA damage repair (DDR).
DDR pathways are also part of some hereditary syndromes and oncogenesis and are not limited to post-irradiation. (Knijnenburg et al., 2018).

Fig 22. Genomic and molecular landscape of DNA Damage Repair Deficiency across the Cancer Genome Atlas

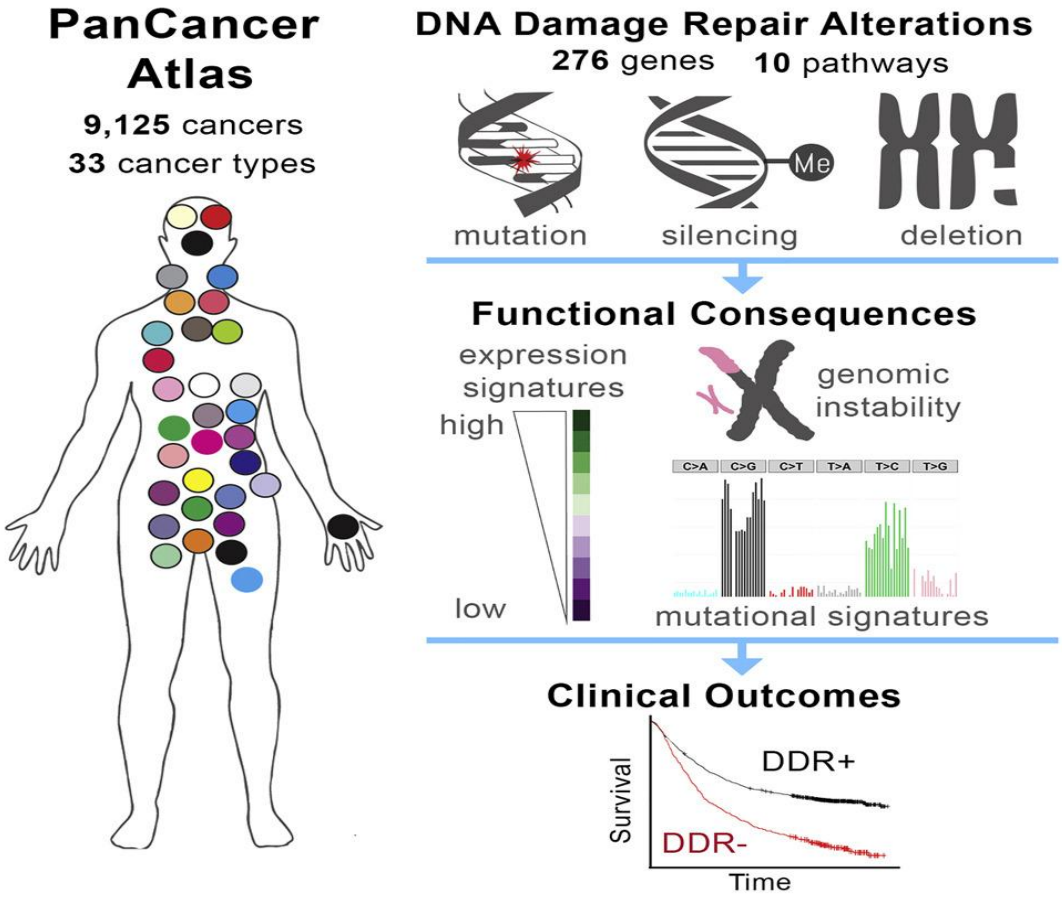

Genomic and molecular landscape of DNA Damage Repair Deficiency across the Cancer Genome Atlas
https://doi.org/10.1016/j.celrep.2018.03.076

The ability of tumor cells to elicit a DNA damage response following radiation via activation of DNA repair and cell cycle checkpoints promotes radioresistance and tumor cell survival.

Fig 23. The effects of radiation-induced DNA damage

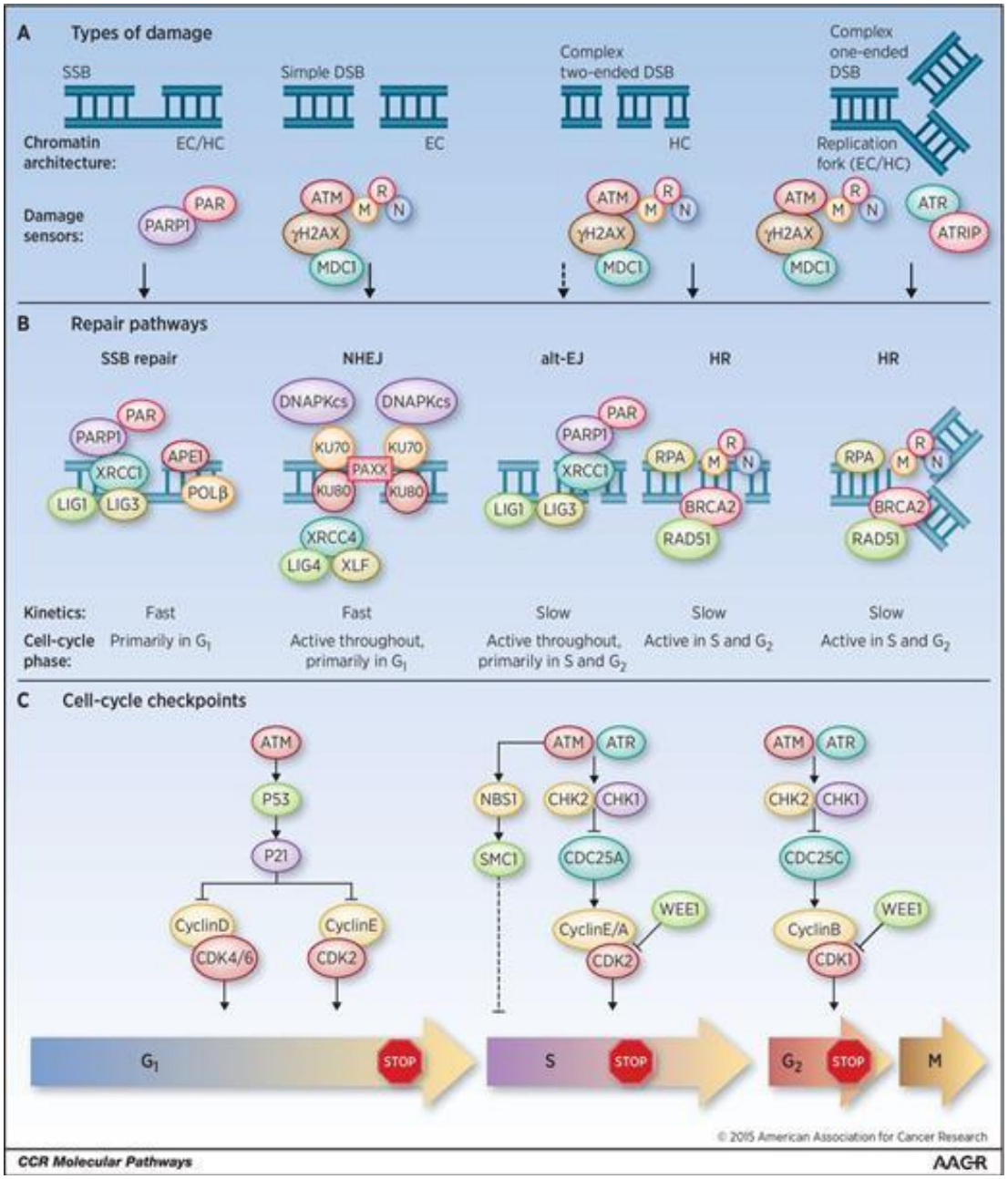

A, major types of radiation-induced DNA damage with respective DNA damage sensor proteins are illustrated. Radiation induces SSBs either directly or indirectly as intermediates of BER. Simple DSBs involve two broken DNA ends in close proximity and occur in euchromatin (EC). Complex DSBs involve two broken DNA ends (i.e., two-ended DSB) in proximity to additional DNA damage (e.g., cross-links, SSBs, etc.) or within heterochromatin (HC), or a DSB within a replication fork (one-ended DSB).

B, SSBs and simple DSBs are repaired with fast kinetics by SSB repair and NHEJ pathways, respectively. Alt-EJ is a slow, compensatory repair pathway activated when DNA-PKcs is absent or when NHEJ/HR attempt, but fail to complete

repair. Alt-EJ likely contributes to repair of complex two-ended DSBs. HR operates under slow kinetics and is partly responsible for repair of complex two-ended DSBs and exclusively responsible for repair of one-ended DSBs. These repair pathways function in a cell-cycle–dependent manner, as illustrated.

C, cell-cycle checkpoints are activated in response to DNA damage to prevent propagation of cells with damaged DNA and to permit time for DNA repair. The major checkpoints include those occurring in G_1, S, and G_2. While ATM activation is the initial response to radiation-induced DNA DSBs, ATR is subsequently activated and contributes to a sustained cell-cycle checkpoint response. Dashed lines
represent incompletely understood pathways. ATRIP, ATR interacting protein.

Clin Cancer Res (2015) 21 (13): 2898–2904.
https://doi.org/10.1158/1078-0432.CCR-13-3229

Multiple agents targeting the DNA damage response and therefore preventing repair or cell cycle checkpoints in response to radiation have been under development. The majority of those are effective radiosensitizers. However an outstanding issue remains tumor cell selectivity.

Table 3. Agents targeting the DNA damage response in clinical and pre-clinical development

Target	Agent	Single agent development stage	Combination agent development stage	Reference or clinical trial identifier number(s)
ATM	KU55933, KU59403	Pre-clinical	Pre-clinical (RT, chemo)	(Cremona and Behrens, 2014)
	AZ32	-	Pre-clinical (RT)	(Karlin et al., 2014)
ATR	AZD6738	Phase 1	Phase 1 (RT, chemo[1])	NCT02223923, NCT02264678
	VE-821/VE-822, VX-970	Pre-clinical	Phase 1 (chemo[2])	NCT02157792
			Pre-clinical (RT)	(Fokas et al., 2012).
CHK1	LY2606368 (Chk1/2)	Phase 2	Phase 1 (chemo[3])	NCT02124148
	LY2603618	Phase 2	Phase 2 (chemo[4])	NCT01139775, NCT00839332
	MK8776	Phase 1	Phase 2 (chemo[5])	NCT01870596, NCT00779584
DNA-PK	CC-115 (DNA-PK & mTOR)	Phase 1	-	NCT01343625
	ZSTK474 (PI3 kinase)	Phase 2	-	NCT01682473
LIG4	SCR7	Pre-clinical	Pre-clinical (RT, chemo)	(Srivastava et al., 2012)
PARP	Olaparib	Approved	Phase 1 (RT, chemoRT[6])	NCT01460888, NCT01562210
			Phase 3 (chemo[7])	NCT01924533
	Veliparib	Phase 3	Phase 1 (RT)	NCT01264432, NCT01589419
			Phase 2 (chemoRT[8])	NCT01514201, NCT01386385
			Phase 3 (chemo[9])	NCT02163694, NCT02152982
	Niraparib	Phase 3	Phase 1 (chemo[10])	NCT01847274, NCT02044120
RAD51	RI-1	Pre-clinical	Pre-clinical (chemo)	(Budke et al., 2012)
	B02	Pre-clinical	Pre-clinical (chemo)	(Huang and Mazin, 2014)
RPA	Compound 8	Pre-clinical	-	(Frank et al., 2013)
	HAMNO	Pre-clinical	Pre-clinical (chemo)	(Glanzer et al., 2014)
	SMI MCI13E	Pre-clinical	Pre-clinical (chemo)	(Neher et al., 2011)
WEE1	AZD1775	Phase 1	Phase 1/2 (RT, chemoRT)	NCT01922076, NCT02037230
			Phase 2 (chemo)	NCT02272790, NCT01076400

As monotherapy, PARP inhibition in BRCA1/2 mutant cancers probably represent the historical example of synthetic lethality between a molecule and a gene involved in the DNA damage response. Various other cases of synthetic lethal interactions have been described, including ATM defective cancers that are susceptible to DNA-PK or ATR inhibition (Riabinska et al., 2013)(Reaper et al., 2011).

Likewise, ATR pathway inhibition has been shown to be synthetically lethal in cancers with ERCC1 deficiency (Mohni et al., 2014).

The search for further synthetic interactions beyond DDR genes is ongoing, such as KRAS and MYC.
In case of deregulation, those oncogenes lead to replication stress, genomic instability, endogenous DNA damage and increased reliance on DNA damage response pathways such as those mediated by ATR/CHK1. (Gilad et al., 2010) Gilad et al. showed that ATR inhibition in combination with oncogenic Ras expression synergistically increased genomic instability.

Many cancers expressing oncogenic Ras also harbor p53 mutations which is reported to produce an increased sensitivity to ATR/Chk1 pathway inhibition.(Lapenna and Giordano, 2009)(Zhou and Bartek, 2004).

8.2.4 Differential gene expression

Cell cycle dependent radiation sensitivity has also been shown to depend on the genetic background.

Wechselbaum et al. observed that cells from the same tissue of origin, but from different patients can show varying radiation sensitivities, therefore tumors from different patients with the same histologic diagnosis can show different responses to irradiation. This has also been observed within a single tumor.

In their paper Weichselbaum et al. reported that four different cell lines clonally derived from the same tumour source showed different radiation sensitivities

Tutt, et al. (Tutt et al., 2003) found that BRCA2 mutation has little effect on cells irradiated in quiescence, but sensitized proliferating cells to ionizing radiation on a p53(-/-) background. BRCA2's role in mediating cell survival occurred in the S and G2 phases of the cell cycle.

It appears therefore that both gene status and origin of cell line account for variations in intrinsic radiosensitivity and should be taken into prospect when addressing radioresistance.

8.3 RADIOTHERAPY-INDUCED SIGNAL TRANSDUCTION AND RADIORESISTANCE

PI3K/AKT/mTOR pathway is a key cascade downstream of several protein kinases, especially membrane-bound receptor protein-kinases, including EGFR family members.

Hyperactivation of the PI3K/AKT pathway has been widely observed (Valerie et al., 2007) and is correlated with tumor development, progression, poor prognosis and resistance to cancer therapies including radiotherapy.(Toulany and Rodemann, 2015).

Radiation causes a rapid ROS dependent activation of ERBB family and other tyrosine kinases, leading to activation of RAS proteins and multiple protective downstream signaling pathways (e.i. AKT and ERK1/2) which alter apoptotic treshold of cells.

Therefore, activation of Ras/PI3K/AKT/mTOR pathway is one of the factors implicated in radioresistance (Gupta et al., 2001)(Grana et al., 2002) PI3K pathway activation can occur via loss of PTEN, by RAS mutation or by increased expression of EGFR.

Multiple groups have demonstrated that the PI3K/AKT/mTOR pathway activation in response to radiotherapy is a major mechanism of radioresistance. (Chen et al., 2015)(Yu et al., 2017) (Toulany and Rodemann, 2015).

PI3K/Akt pathway is constitutively active in tumor cells presenting mutation in one of the components of the EGFR downstream pathways, such as phosphatase and tensin homolog (PTEN), PIK3CA and RAS (Cengel et al., 2007)(McKenna et al., 2003).

Fig 24. Involvement of PI3K/Akt/mTOR signaling pathways in development of cancers.

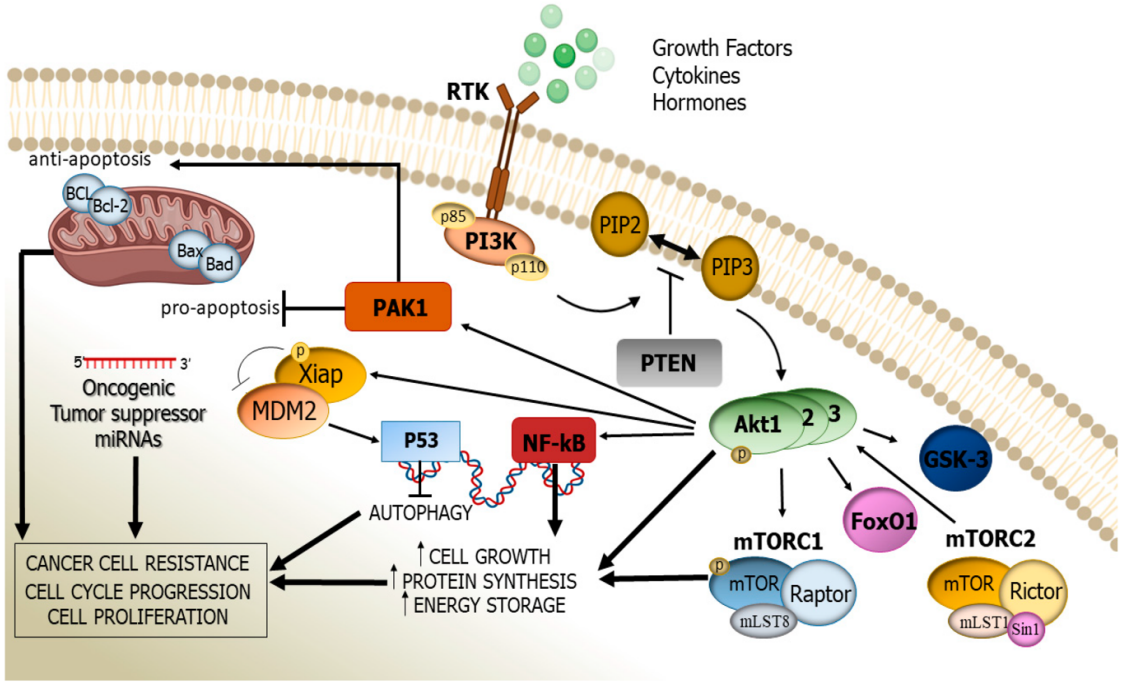

Involvement of PI3K/Akt/mTOR signaling pathways in development of cancers. The auto-phosphorylation of PI3K leads to the activation of AKT trough PIP2 to PIP3 conversion. PI3K/AKT and mTORC1 contribute to tumor growth and energy storage of cancer cells. The upregulation of AKT promotes the phosphorylation of target genes and proteins which promote the inhibition of apoptosis and autophagy. Deregulated miRNAs also contribute to cancer cell proliferation.

Cancers **2021**, *13*(16), 3949; **https://doi.org/10.3390/cancers13163949**

PI3K is generally activated by extracellular signals, such as growth factors, cytokines and hormones. Additionally, PI3K may be directly or indirectly triggered by small Ras-related GTPases.

RAS is one of the major oncogene in human cancers, and PI3K is thought to be its main effector (Rascio et al., 2021).
PI3K/RAS interaction has been shown to be essential for maintaining cancer cell survival and carcinogenesis (Castellano and Downward, 2011).

Fig 25. RAS signaling and PI3K pathway

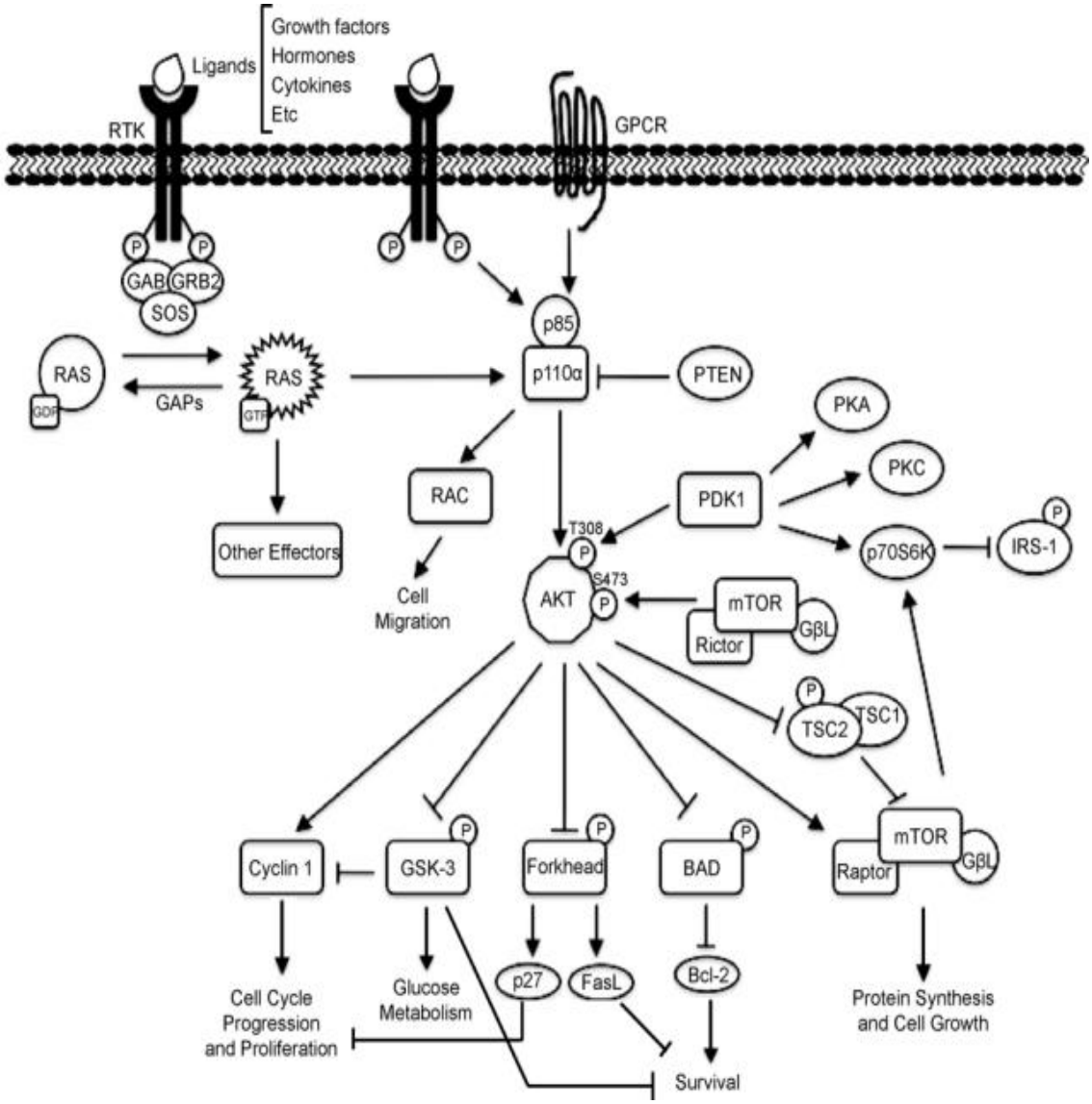

Genes Cancer. 2011 Mar; 2(3): 261–274.
Doi: 10.1177/1947601911408079

8.4 NON-TARGETED EFFECTS OF RADIATION

8.4.1 Bystander and abscopal effects

Early radiobiological studies reported that the major mechanisms of action of ionizing radiation were related to DNA damage (Ravanat et al., 2014)(Nikjoo et al., 2001). While it has been widely accepted that effects of radiotherapy are mediated by direct damage to DNA or through indirect damage through free radicals generated by water radiolysis, this was subsequently challenged by observations that non-irradiated cells either nearby or away from the irradiated site can undergo the same response as irradiated cells.(Seymour and Mothersill, 1997) (Blyth and Sykes, 2011)(Ng and Dai, 2016).

This was further supported by the discovery that irradiated cancer cells can release signals able to influence the outcome of non-irradiated cells. (Levy et al., 2013).

Fig 26. Schematic overview of local and distant effects triggered by tumour irradiation

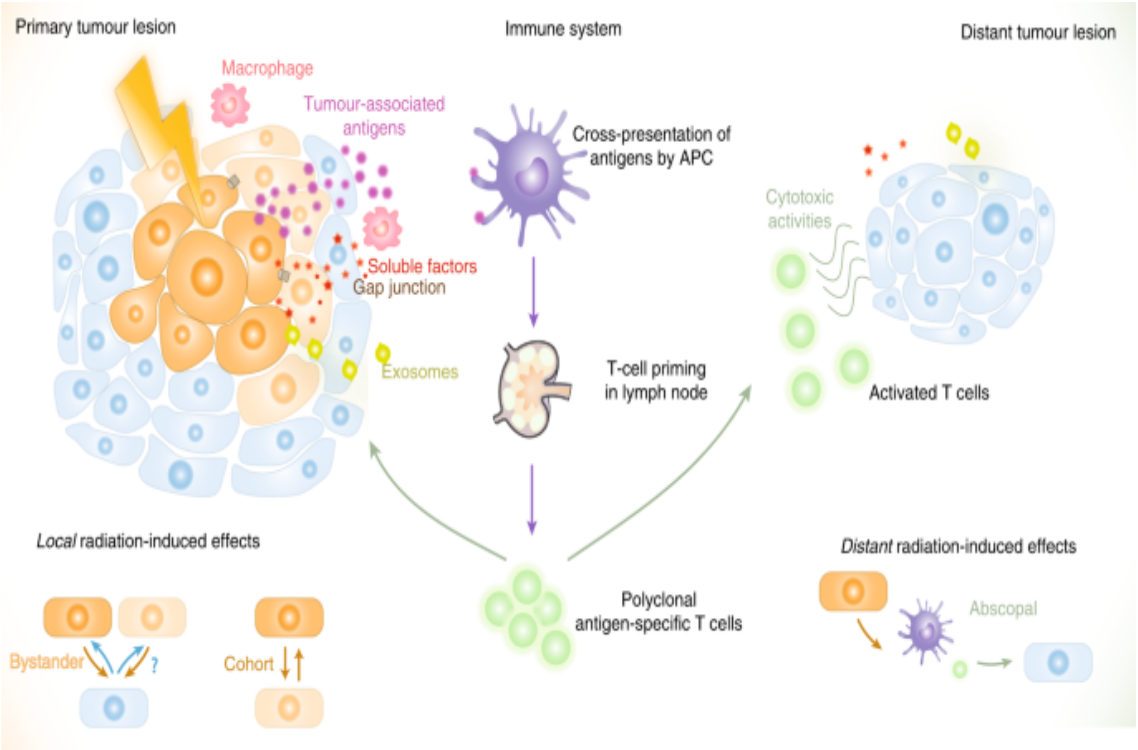

At the heart of the primary lesion that is irradiated (panel on the left), two local effects can be distinguished: first, bystander effects occur between high-dose-targeted cells (dark orange) or low-dose-targeted cells (light orange) and non-irradiated cells (blue); second, cohort effects occur between high-dose-targeted cells and low-dose-targeted cells. Whether/how non-irradiated cells can influence the outcome of irradiated cells (depicted with a question mark) remains to be determined. Irradiation induces immunogenic cell death in cancer cells and the subsequent release of tumour-associated antigens (TAAs) (pink dots), thereby activating the immune system, especially antigen-presenting cells (APC, in purple) and macrophages (in pink). APCs then cross-present TAAs to T cells in draining lymph nodes. As a result, polyclonal antigen-specific T cells are primed to attack tumours located within the irradiated field as well as those in distant locations. This distant radiation-induced effect is termed an abscopal effect (panel on the right). Exosomes (in green) are novel mediators thought to participate in these non-targeted effects locally and at distant sites

Br J Cancer. 2020 Aug 4; 123(3): 339–348.
Published online 2020 Jun 25. doi: 10.1038/s41416-020-0942-3

Three types of non-targeted effects can be distinguished depending on the relationship between the irradiated and non-irradiated cells, as well as the proximity to the original site of treatment. (Blyth and Sykes, 2011)
According to the United Nations Scientific Committee on the Effects of Atomic Radiation (UNSCEAR), the radiation-induced bystander effect is a radiobiological effect that is transmitted from irradiated cells to neighbouring unirradiated cells, leading to biological changes in the recipient cells. (Azzam et al., 2001)(UNSCEAR 2006)

The radiation-induced abscopal effect (from the Latin 'ab scopus', meaning 'away from the target') is a « local radiation-induced systemic effect that extends outside the treated volume, and is able to drive the regression and rejection of non-irradiated, distant tumour lesions ». (Reynders et al., 2015)

When first proposed in 1953, the term 'abscopal' referred to an action at a distance from the irradiated volume but within the same organism.

Further clinical and preclinical work have helped redefine it as a systemic effect of radiation on 'out-of-field' tumor deposits. This effect is mediated by local immune-effector cells and is capable of antitumor activity towards both targeted and distant lesions. (Kaminski et al., 2005).

The bystander refers to the induction of biological effects in cells that are not directly traversed by a charged particle, but are close to those (Hall, 2003). It was first described by Nagasawa et al. in 1992 when his experiment revealed that irradiation of 1% of cells led to chromatid exchange in more than 30% of cells. (Nagasawa and Little, 1992)
It could be reasonably seen as a local communicative effect at the primary site over a very short distance (few millimeters), mediated through the secretion of inflammatory mediators (Prise and O'Sullivan, 2009), signaling through gap junctions or exosomes.

By contrast, the abscopal effect is a long-distance (up to tens of centimetres outside of the irradiated field) and systemic effect at a distant metastatic site that is mediated through immunogenic responses. (Ng and Dai, 2016)(Hall, 2003)(Burdak-Rothkamm and Rothkamm, 2018).

In the context of irradiated/non-irradiated sites within the same organ, it remains difficult to distinguish between a long-range bystander effect and an abscopal effect.

8.4.2 The 'cohort effect'

Although less known, a third type of non-targeted effect "the cohort effect" is defined as the interaction between irradiated cells within an irradiated volume where, under heterogeneous irradiation, high-dose-irradiated cells might affect low-dose-irradiated cells, and vice versa; (McMahon et al., 2013) the cohort effect is limited to an area of millimetres within the target. (Sun et al., 2014).

9 RAS GENE SUPERFAMILY

RAS (Rat Sarcoma virus) gene family represent some of the earliest described oncogenes, whose identification has deeply transformed the understanding of cancer biology.

Somatic gain-of-function mutations in RAS genes were originally identified in the 1960s as a viral component that induced formation of sarcomas in rats (Harvey, 1964)(Kirsten and Mayer, 1967). They were later identified as normal components of the human genome that were capable of transforming normal human cells (Chang et al., 1982)(Ellis et al., 1981).

H-ras, N-ras and K-ras oncogenes are part of the RAS gene superfamily of small GTP-ases (Wennerberg et al., 2005) made up by more than 150 members.

The five main superfamilies are Ras, Rho, Ran, Rab and Arf GTPases (Goitre et al., 2014).

The RAS family itself is divided into 6 subfamilies Ras, Rak, Rap, Rheb, Rad each sharing the common core G domain providing the essential GTP-ase and nucleotide exchange activity.

The RAS oncoprotein family comprised of H-, K-, and N-Ras are frequently activated by mutation in certain tumours such and pancreatic and NSCLC and activated by tyrosine-kinase activity in an even wider range of tumours.

Fig 27. RAS gene super family

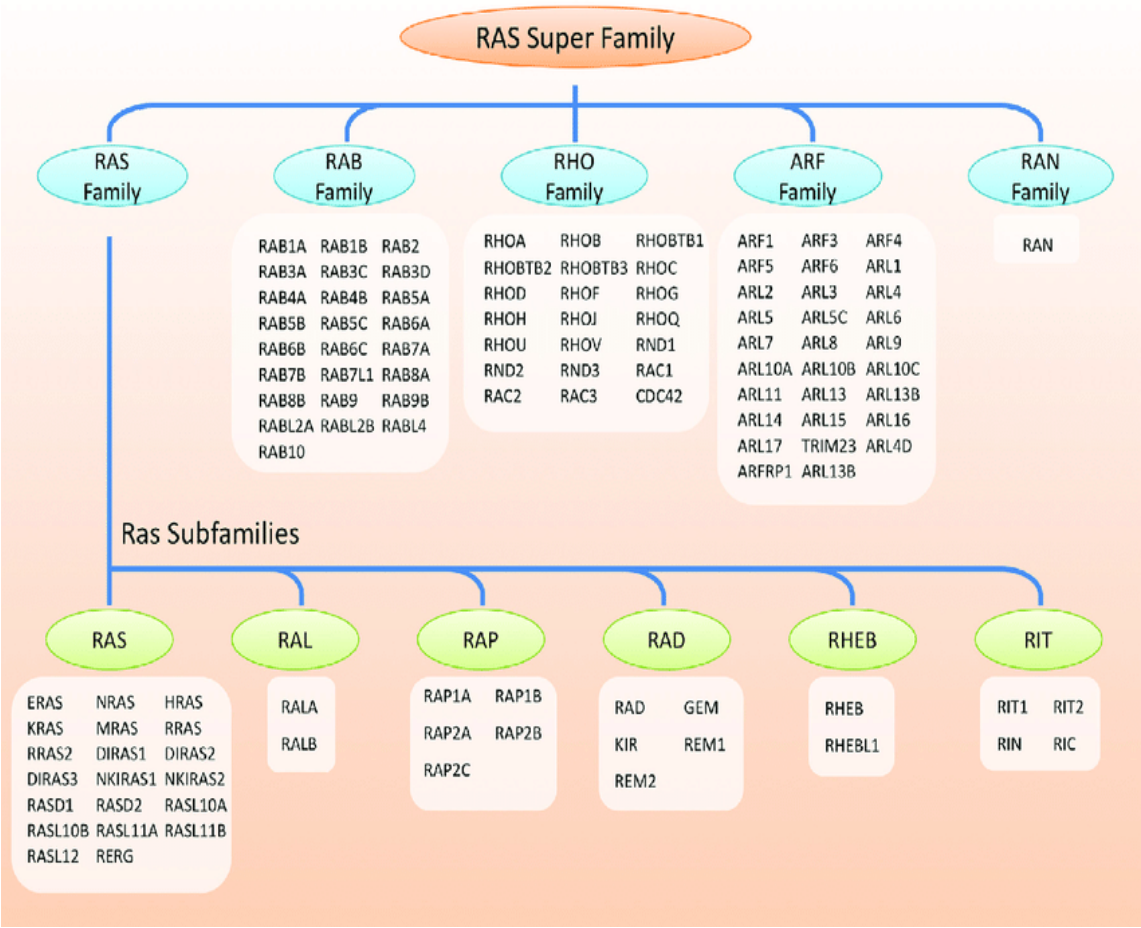

9.1 RAS PROTEINS

Under physiological conditions, RAS proteins function as a binary molecular switch, cycling between an inactive GDP-bound and an active GTP-bound conformation. Activation of RAS is facilitated by guanine nucleotide exchange factors (GEFs) and inactivating GTP hydrolysis is enhanced by GTPase-activating proteins (GAPs) (Mo et al., 2018).

RAS proteins have been shown to be essential components of signaling networks controlling cell proliferation and metabolism, differentiation, migration or survival. (Simanshu et al., 2017).

Fig 28. Conformational Changes in Switch Regions when RAS Transitions from Inactive GDP-Bound State to Active GTP-Bound State

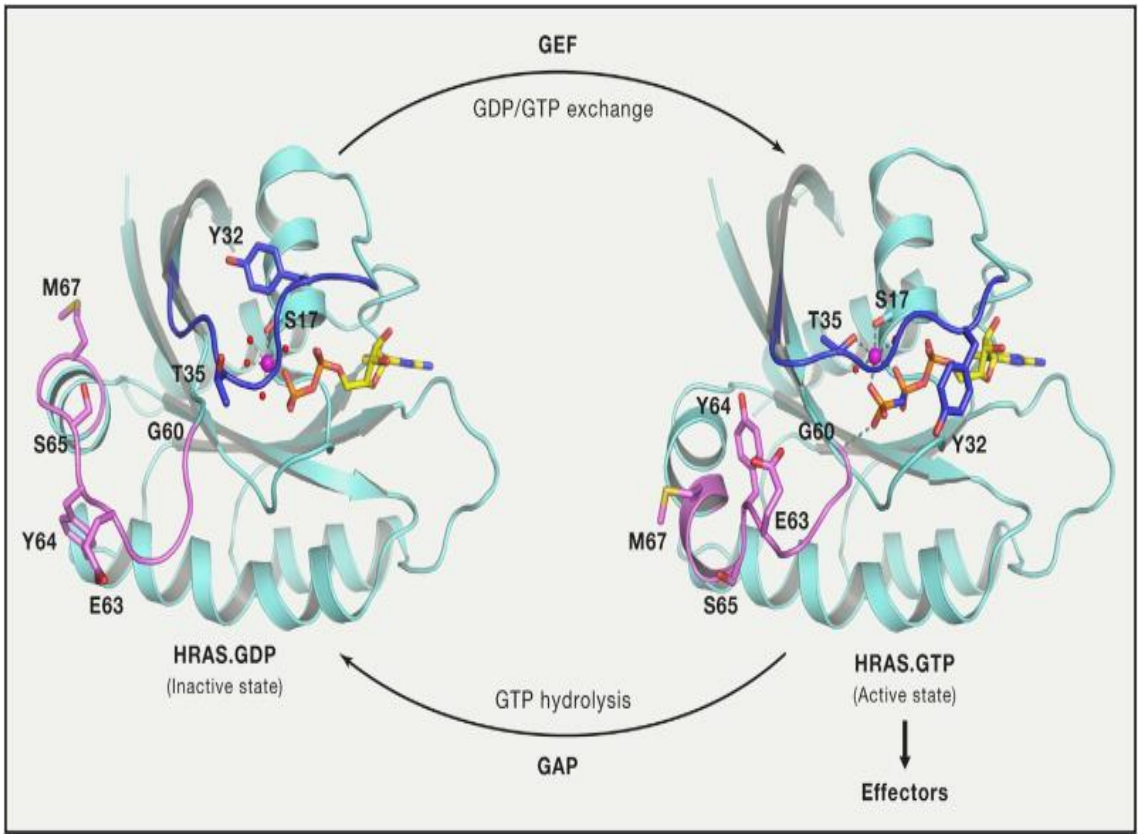

Switch I and switch II regions are colored blue and violet, respectively, and side chain atoms of residues that undergo large conformation changes during transition are shown in stick representation. Interactions formed by γ-phosphate and magnesium ions are shown using dashed lines. HRAS.GDP and HRAS.GppNHp are from PDB: 4Q21 and 5P21, respectively. RAS is activated by GDP/GTP exchange stimulated by GEFs and inactivated by GTP hydrolysis stimulated by GAPs.

Cell. 2017 Jun 29; 170(1): 17–33. doi: 10.1016/j.cell.2017.06.009

KRAS is initially synthesized as an inactive cytosolic pro-peptide before undergoing a series of post-translational modifications at its carboxyl terminus that increase its hydrophobicity allowing its localization to the lipid-rich cell membrane (Ghobrial and Adjei, 2002).
In the GTP-bound state, KRAS binds and activates different downstream effectors in order to activate cell proliferation and survival signaling pathways including mitogen-activated protein kinase (MAPK) and phosphoinositide 3-kinase (PI3K) pathways (Vivanco and Sawyers, 2002).

It has been shown that RAS activation causes a conformational change that allows engagement with more than 20 different proteins from 10 effector families (Hobbs et al., 2016). Activated RAS concentrates effector proteins into plasma membrane signaling non-cluster where they can interact with necessary proteins and lipids to control downstream pathways (Zhou, et al.)

The most extensively studied from an oncological perspective, have been RAF and PI3 kinase families. RAS proteins are tightly regulated by guanine nucleotide exchange factors (GEF) that promote GDP dissociation and GTP binding, and GTPase-activating proteins (GAP) that stimulated the intrinsic GTPase activity of Ras to switch off signaling. Aberrant RAS function is associated with a single mutation typically at codon 12, 13 or 61. (Quinlan and Settleman, 2009).

Upon point mutations, most commonly at codons 12 and 13, KRAS becomes constitutively active and acquires oncogenic properties.

Fig 29. Oncogenic mutations of RAS isoforms

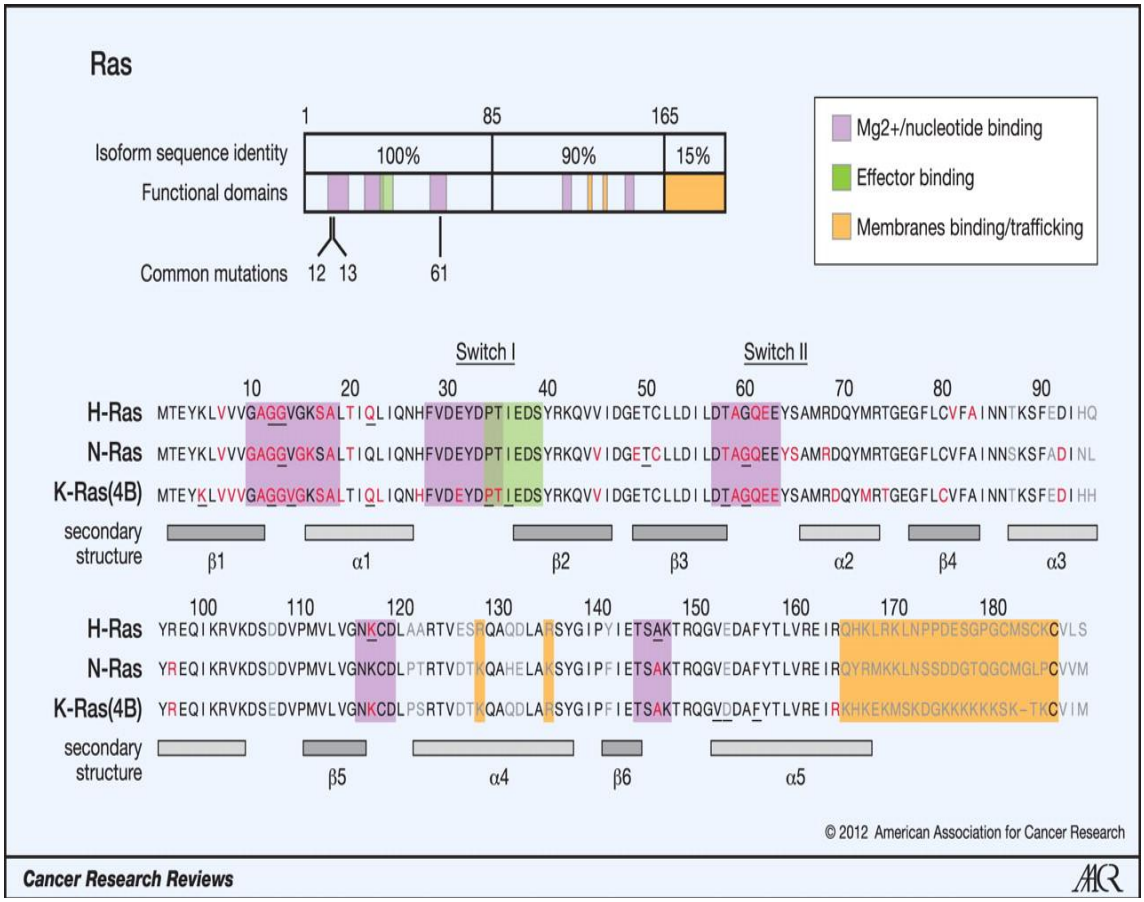

The key oncogenic mutations are in the region that is identical between the 3 isoforms. Forty-four separate point mutations have been identified in Ras isoforms, with 99.2% occurring at codons 12, 13 and 61. Mutations that cluster in and around loops 1, 2 and 4 and are responsible for nucleotide binding and result in enhanced GTP binding. Residues that are mutated in cancer are highlighted in red, those mutated in developmental disorders are underlined, and those that are variable among isoforms are in grey (26,65,66).

Cancer Res. 2012;72(10):2457-2467. doi: 10.1158/0008-5472.CAN-11-2612

While RAS activating mutations are widely observed in cancer, an interesting fact is that different types of cancer seem to be coupled to a mutation of a particular Ras isoform (Boss). Therefore, they are distinctive patterns in the mutation frequencies associated with each RAS gene and cancer type (Prior et al., 2020a).

9.2 RAS ONCOGENE AND ISOFORM FREQUENCY

RAS (Rat sarcoma viral oncogene homolog) is considered the most frequently mutated oncogene with nearly 19% of human cancers harboring a RAS mutation (Soh et al., 2009). Among the 3 main Ras isoforms (KRAS, NRAS and HRAS), KRAS is the most frequently altered gene with mutations occurring in 17 to 25% of all cancers.

Fig 30. RAS isoform and mutations in cancer at a glance

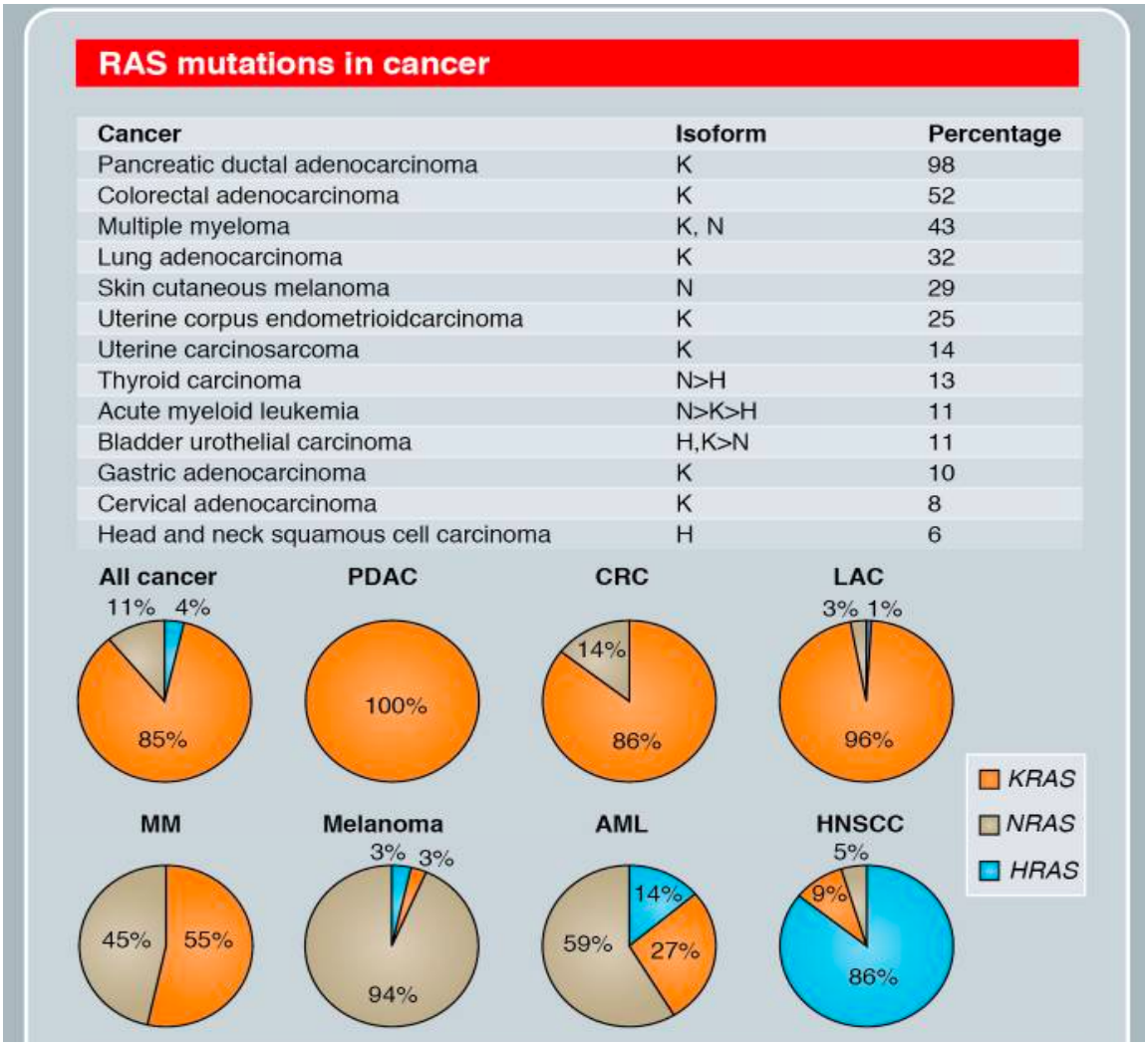

The Company of Biologists Doi:10.1242/jcs.182873

9.2.1 KRAS isoform frequency

The KRAS (Kirsten rat sarcoma viral oncogene) isoform represents 75% of RAS mutant cancers and is therefore considered a crucial oncogene.
According to the catalogue of somatic mutations in cancer (COSMIC) dataset K-Ras is the most frequently mutated isoform present in 22% of all tumors analysed (Forbes et al., 2011).

KRAS isoform mutations occur in approximately 20-30% of non-small-cell lung cancers (NSCLC), 80% of pancreatic adenocarcinomas and more than 30% of colorectal and cholangial cancers. (Skoulidis and Heymach, 2019)

Approximately 40% of CRC patients harbor activating mutations in KRAS with most of them occurring at codons 12, 13 and 61 (Dienstmann et al., 2020). Patients with KRAS-mutant CRC have a poorer prognosis than those with KRAS-wild type CRC, especially in the metastatic setting (Roth et al., 2010) (Zhu et al., 2021). Moreover, the upstream signal regulation of KRAS is interrupted by aberrant activation of the KRAS pathway, resulting in resistance to monoclonal antibodies against epidermal growth receptor (EGFR) (cetuximab, panitumumab) in patients with KRAS-mutant CRC.(Zhu et al., 2021)

1. $KRAS^{G12C}$ isoform

When it comes to $KRAS^{G12C}$ isoform mutations, they are estimated to occur in 13% of NSCLC adenocarcinomas and 3-4% of colorectal cancers (Biernacka et al., 2016)

Colorectal cancer represents a major cause of morbidity and mortality in western countries. Fifty percent of patients will die within five years from diagnosis, usually as a result of metastatic disease.

It is generally accepted that sporadic colorectal cancers frequently arise from preneoplastic lesions through activation of oncogenes (KRAS and BRAF) or inactivation of tumor suppressor genes (APC, p16, p53, DCC) and mismatch repair genes such as MLH1 and MSH2 and to a lower extent PMS2 and hMSH6. (Tanaka et al., 2006). Importantly, approximately a third of colon cancers carry a KRAS mutation.

9.3 RAS EFFECTOR SIGNALING

Fig 31. RAS effector signaling

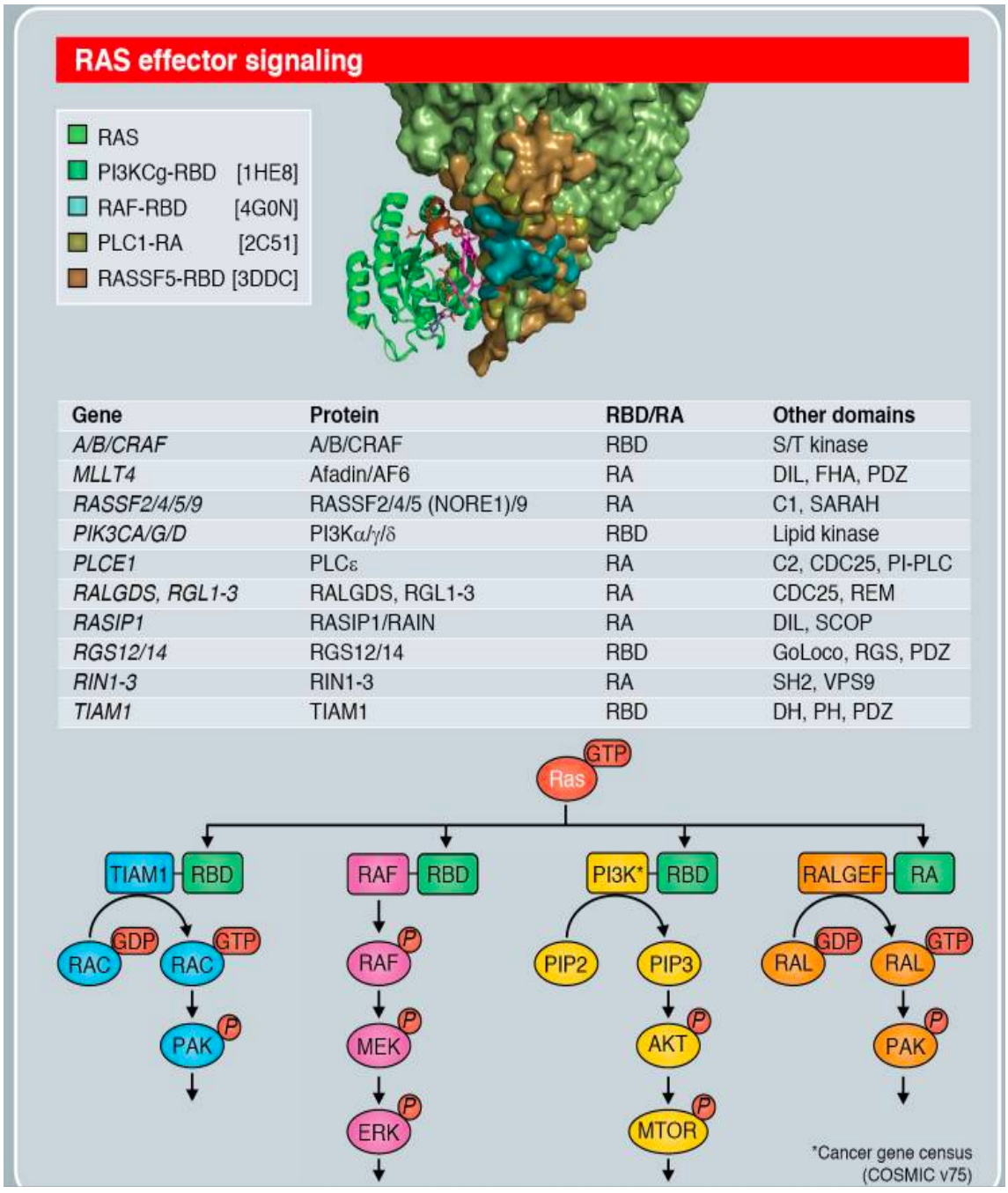

Gene	Protein	RBD/RA	Other domains
A/B/CRAF	A/B/CRAF	RBD	S/T kinase
MLLT4	Afadin/AF6	RA	DIL, FHA, PDZ
RASSF2/4/5/9	RASSF2/4/5 (NORE1)/9	RA	C1, SARAH
PIK3CA/G/D	PI3K$\alpha/\gamma/\delta$	RBD	Lipid kinase
PLCE1	PLCε	RA	C2, CDC25, PI-PLC
RALGDS, RGL1-3	RALGDS, RGL1-3	RA	CDC25, REM
RASIP1	RASIP1/RAIN	RA	DIL, SCOP
RGS12/14	RGS12/14	RBD	GoLoco, RGS, PDZ
RIN1-3	RIN1-3	RA	SH2, VPS9
TIAM1	TIAM1	RBD	DH, PH, PDZ

Once in its active, GTP-bound state, RAS preferentially binds to its downstream effectors resulting in stimulation of their catalytic activity. The main effectors are shown here. RAS-GTP

preferentially binds to RAS-binding-domain (RBD) or RAS-association (RA)-domain-containing effectors. Although the RBD and RA domains do not share primary sequence similarity, they are structurally related and share the topology of the ubiquitin superfold (Kiel et al., 2005)(Wohlgemuth et al., 2005). There are at least 11 distinct RAS effector families, each of which activates a distinct protein signaling cascade (Vigil et al., 2010).

Hobbs, et al. doi:10.1242/jcs.182873

Fig 32. Signaling upstream of RAS

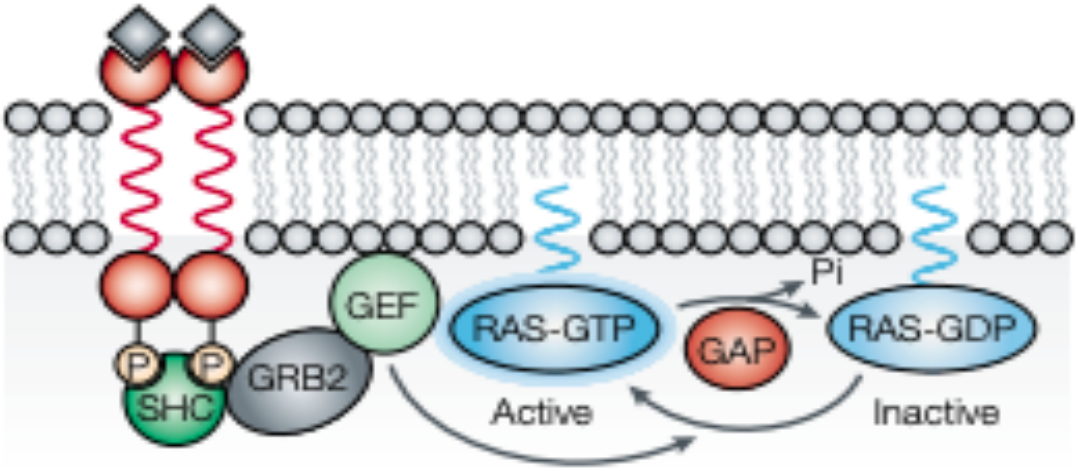

The activation state of RAS is controlled by the cycle of hydrolysis of bound GTP, which is catalyzed by GTPase activating proteins (GAPs), and the replacement of bound GDP with fresh GTP, which is catalyzed by guanine nucleotide exchange factors (GEFs). The best-studied activation mechanism involves the assembly of complexes of activated, auto-phosphorylated growth-factor receptor tyrosine kinases with the GEF SOS through the adaptor protein GRB2, and possibly SHC, resulting in the recruitment of SOS to the plasma membrane, where RAS is located. Several other GEFs exist that have distinct regulatory mechanisms. In addition, a wide range of GAPs have now been identified for RAS, some of which are also subject to regulation. RAS is also activated through GEFs in response to activation of a wide range of G-protein-coupled receptors
Nature Reviews Cancer (Nat Rev Cancer) ISSN 1474-1768 (online) ISSN 1474-175X (print)

Fig 33. RAS pathway genes (simplified version)

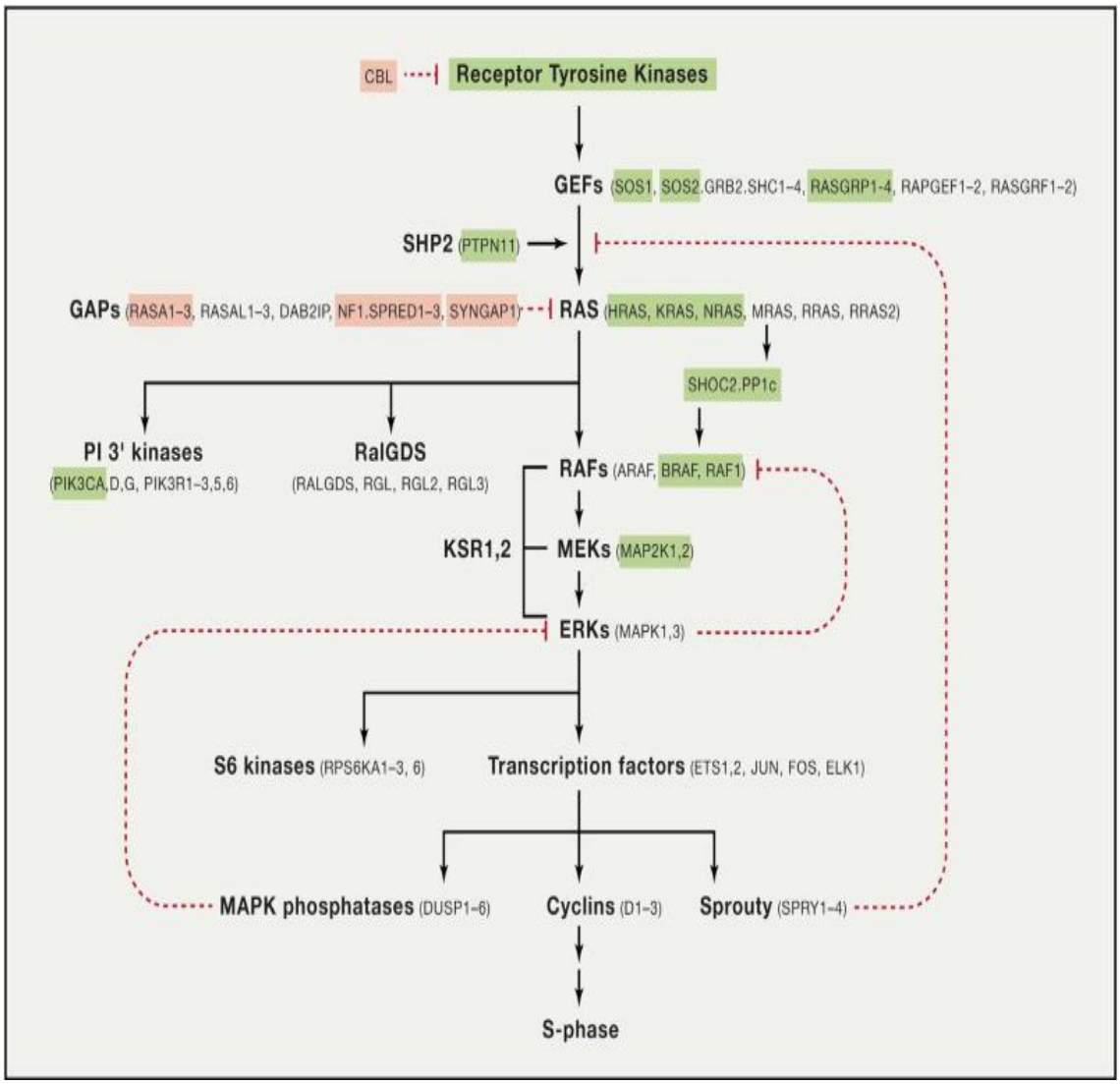

Genes highlighted in pink are frequently deleted in human cancers and RASopathies. Genes in green are frequently activated by mutation. This pathway is a simplified version of the pathways illustrated on http://www.cancer.gov compiled by the RAS initiative and the RAS research community.

Extensive data suggest that the expression of active Ras promotes tumor initiation by activating at least three different effectors based on pre-clinical work using Ras effector binding mutants, dominant-negative and constitutively active proteins downstream of Ras, and pharmacological inhibitors: Raf, PI3-kinase (PI3K) and RaIGEFs (Shields et al., 2000)(Ulkü and Der, 2003).

9.3.1 The RAF-MEK-ERK effector pathway

The first RAS effector pathway to be identified was the RAF-MEK-ERK pathway (Moodie et al., 1993)(Zhang et al., 1993). It is an essential element of mitogenic signaling involving tyrosine kinases receptors , leading to a wide range of cellular responses including cell growth, differentiation, inflammation and apoptosis (Roux and Blenis, 2004).

Fig 34. Ras /Raf/MAPK pathway

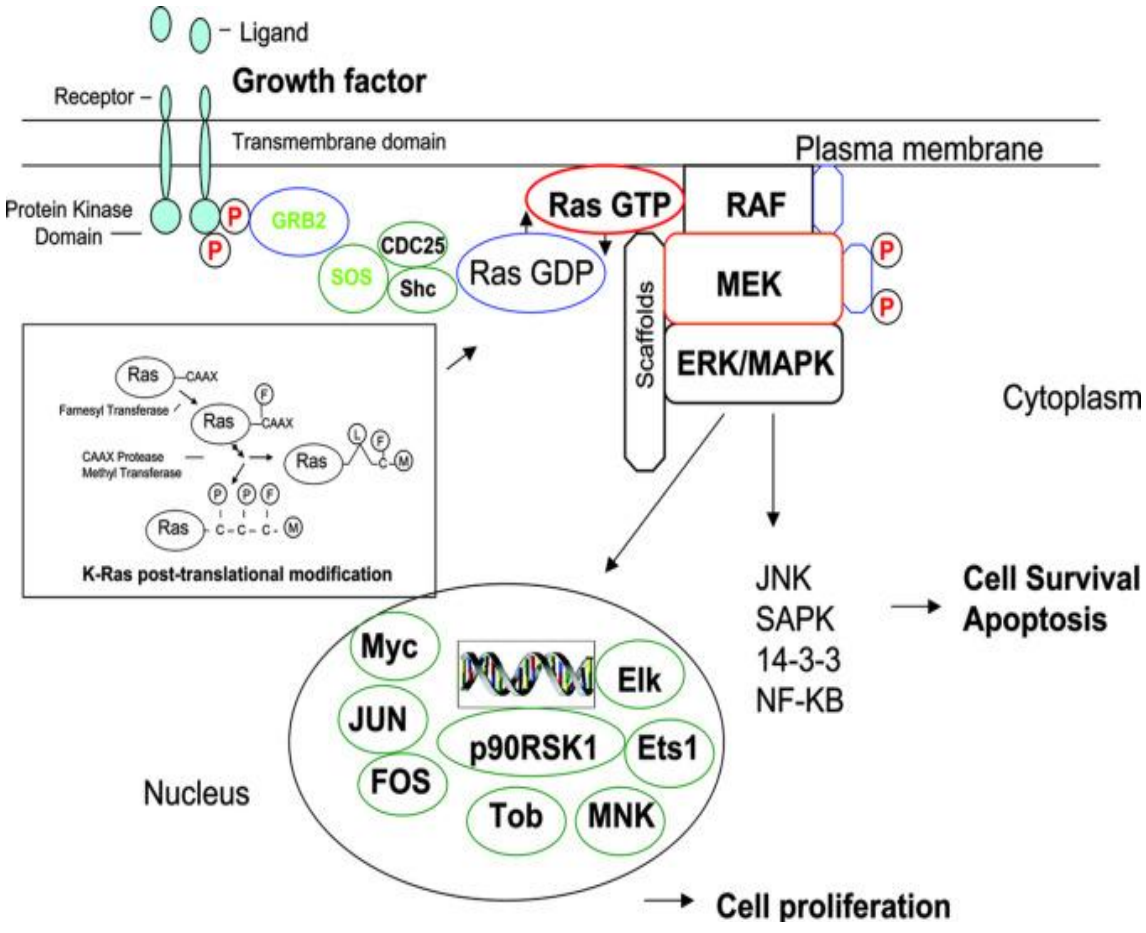

Journal of Thoracic Oncology , Volume 1 Issue 1 Pages 7-9 (January 2006)
DOI: 10.1016/S1556-0864(15)31506-9

Dysregulation of the Ras/Raf/MAPK pathway is a common event as RAS is the most frequently mutated oncogene in human cancer.

Raf is the best characterized Ras effector. It is a member of serine/threonine kinases that includes Raf-1, A-Raf and B-Raf. Raf activation initiates a MAP kinase (MAPK) signal transduction cascade that lead to transformed morphologies, anchorage-independent growth and angiogenesis (Morrison and Cutler, 1997)(Shields et al., 2000). It stimulates a signaling cascade by phosphorylation of MAPK which phosphorylate and activate downstream proteins, such as ERK1 and ERK2. Activation of ERK is critical for a large number of Ras-induced cellular responses.

MAPK, also called MEK in mammalians, is a serine/threonine kinase activated in response to multiple signals including growth factors and cytokines to promote cell survival and apoptosis through a number of mediators such as JNK, SAPK, 14-3-3 and NF-KB (Schlesinger et al., 1998).

MAPK may also regulate both Raf and ERK, providing for cross talk between multiple signaling pathways. It has been shown to directly interact with K-ras in a GTP-dependent way. (Karandikar et al., 2000).

Indeed, Raf and MAPK are not the only downstream targets of K-ras, other downstream effectors include the PI3K cell survival pathway, the small GTP-binding proteins Rac and Rho, and the stress-activated protein kinase pathway (also referred to as the c-jun N-terminal kinase (JNK) pathway) (Schlesinger et al., 1998).

9.3.2 PI3K-AKT-mTOR Pathway

PI3K is one of the main effector pathways of RAS-mediated cell growth, cell cycle entry, cell survival, cytoskeleton reorganization and metabolism (Vivanco and Sawyers, 2002)(Cantley, 2002)
When active, PI3K converts phosphatidylinositol (4,5)-bisphosphate (PIP2) into phosphatidylinositol (3,4,5)-triphosphate (PIP3). PIP3 in turn stimulates Akt/PKB kinase activity resulting in the phosphorylation of other proteins that affect cell growth cell, cycle entry and cell survival (Castellano and Downward, 2011).

Fig 35. PI3K-AKT-mTOR Pathway

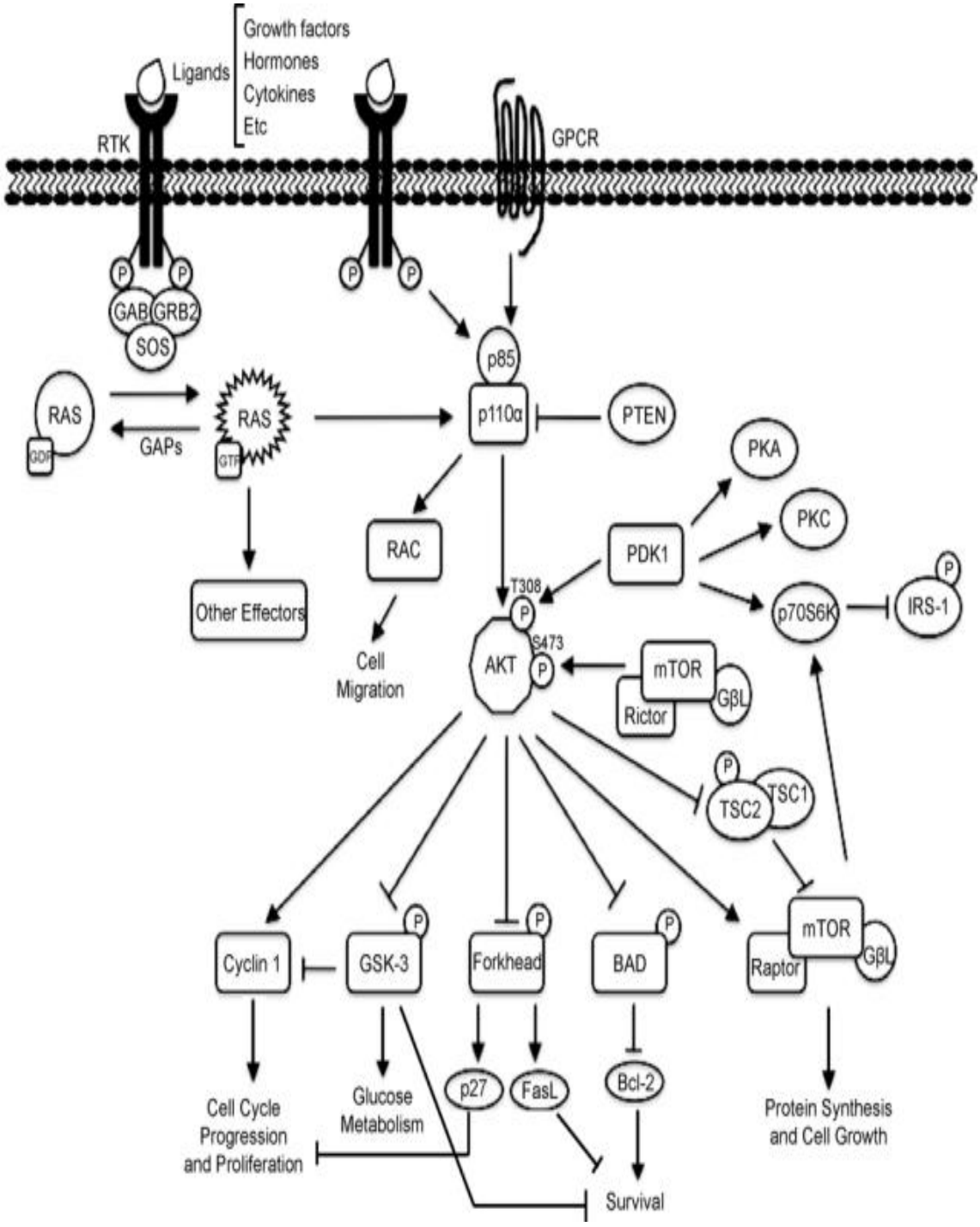

It has been shown that PI3K signaling is needed to maintain transformed growth in RAS mutant cell lines both in vitro and in xenografts in mice.

While, PI3K signaling is essential for RAS-driven tumor maintenance, inhibition of PI3K alone is not sufficient to cause regression of tumors once established.

Ras effector pathways MAPK, RaIGEF and PI3K are required to initiate tumor growth. Conversely, activation of the PI3K/AKT pathway replaced Ras once tumors were established, although other effectors were still activated independently of Ras, presumably by factors provided upon the establishment of a tumor microenvironment (Lim and Counter, 2005).

Lim et al. suggest that once tumorigenesis progresses, the addiction of cancers to their initiating oncogene was reduced to the PI3K/AKT pathway in the case of Ras.

Activation of the phosphatidylinositide-3-kinase (PI3K)/serine/threonine-specific protein kinase (AKT)/mammalian target if rapamycin (mTOR) pathway has been implicated in the growth and progression of various cancers, as well as resistance to therapies (Liao et al., 2012).

9.3.3 New directions in targeting of RAS pathways

When it comes to targeting important growth and survival pathways, a persistent challenge remains how to achieve a sufficient therapeutic window that enables the elimination of tumour cells but not their normal neighbors. Most of the pathways described earlier are used by normal cells as well as by tumour cells, although tumour cells might develop a greater degree of reliance on them. In theory, an ideal cancer therapy would exclusively target transformed abnormal cells, but in practice, this is very difficult.

The development of RTK inhibitors targeting RAS signaling pathways (García-Echeverría, 2009) represents a successful attempt however limited to patients with oncogenic RTK signaling while not benefiting patients with mutant RAS. Other strategies are explored with the aim to inhibit signaling pathways that commonly show increased activity in tumours, even if they are also used by normal cells. Various Raf, MEK, PI3K and mTOR inhibitors have been developed and evaluated in preclinical and for some of them in clinical trial setting (Misaghian et al., 2009)(Choo and Blenis, 2009).
Targeting mTOR has so far been most promising.(Choo and Blenis, 2009).

9.4 HISTORICAL PERSPECTIVES ON KRAS TARGETING THERAPY

Until very recently, KRAS was considered undruggable. Firstly, KRAS protein is a small protein with a relatively smooth surface. Moreover, the KRAS protein doesn't provide enough pockets for small molecular inhibitor binding in addition to the GTP/GDP binding pocket (Papke and Der, 2017). Efforts to target this oncogene directly have faced major difficulties owing to its picomolar affinity for GTP/GDP and the absence of allosteric regulatory sites.

KRAS oncogenic mutations result in functional activation of Ras family proteins by impairing GTP hydrolysis. With diminished regulation by GTPase activity, the nucleotide state of Ras becomes more dependent on relative nucleotide affinity and concentration. (Ostrem et al., 2013a)

KRAS mutated proteins have a reduced capability to hydrolyze GTP or to interact with the GTPase-activating proteins, maintaining the oncogene and the downstream pathways constitutively activated. The lack of specific inhibitors targeting the KRAS hydrophobic pocket and the complexity of downstream pathways have contributed to the challenge of developing effective therapeutic strategies (Hong et al., 2020).

Recent crystallographic studies have revealed the formation of a new pocket, beneath the effector binding switch-II region. Ostrem, et al.(Ostrem et al., 2013) successfully predicted their compounds would disrupt the conformation of the GTP state of Ras and impair interactions with effectors such as Raf and opened the way to drug discovery targeting $KRAS^{G12C}$.

Importantly, indiscriminate inhibition of both wild-type and mutant KRAS may lead to potential toxicity (Ostrem et al., 2013a). Therefore inhibiting KRAS directly is a great challenge for KRAS-mutant tumour treatment.

Fig 36. Approaches for anti-RAS drug discovery

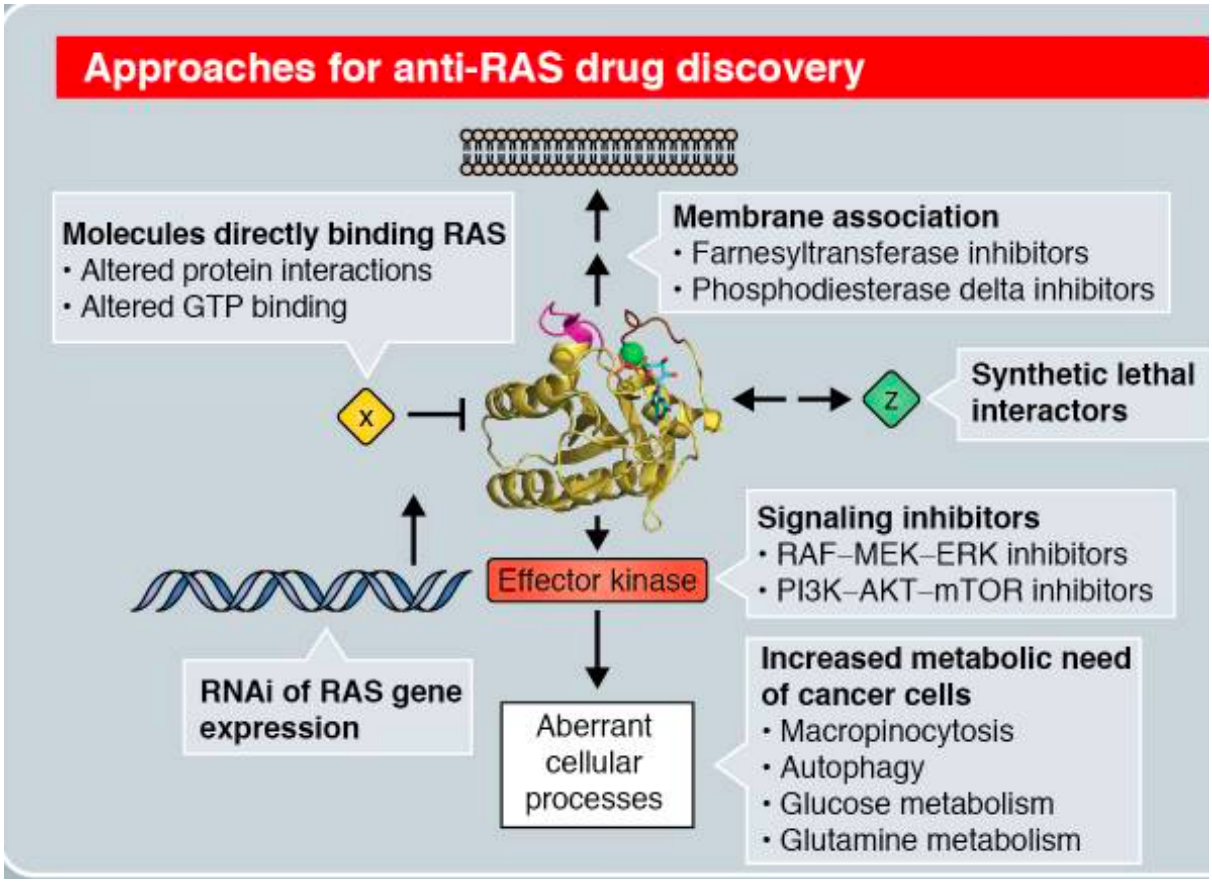

Hobbs, et al. doi:10.1242/jcs.182873

Attempts that indirectly target KRAS including the inhibition of nucleotide exchange, processing, membrane localization and the molecules in signaling pathway have not been very effective clinically partly because multiple positive and negative feedback loops implicated in KRAS signaling network enable easy rebound of the therapeutic (Passiglia et al., 2020)(Nagasaka et al., 2020).

Event tough not a major process, the mutant KRAS cells can activate the cell Warburg metabolism to maintain tumour growth resulting in low inhibitory effect of the indirect targeting of KRAS (Serna-Blasco et al., 2019).

9.4.1 $KRAS^{G12C}$ inhibitors

$KRAS^{G12C}$ arises from a glycine-to-cysteine substitution at codon 12, and the thiol group in the cysteine residue has been an attractive target for covalent inhibitors.

In contrast, wild-type KRAS is not inhibited by this covalent approach due to lack of cysteine in the active site.

Recently, a series of novel $KRAS^{G12C}$ inhibitors were developed including ARS-853 (Patricelli et al., 2016), ARS-1620 (Janes et al., 2018), AMG-510 (Canon et al., 2019a) and MRTX849 (Hallin et al., 2020)(Christensen et al., 2020).

Only two of them, first Sotorasib (AMG 510) and later Adagrasib (MRTX849) earned the breakthrough designation by the US Food and Drug Administration (FDA) to treat metastatic lung cancer patients harboring $KRAS^{G12C}$ mutations who have progressed on at least one systemic therapy. Those inhibitors selectively target $KRAS^{G12C}$ while preserving wild-type or other mutant KRAS to circumvent the toxicity caused by inhibition of all KRAS isoforms.

9.4.1.1 Sotorasib

Sotorasib (AMG510) is a small molecule that specifically and irreversibly inhibits $KRAS^{G12C}$ through a unique interaction with the P2 pocket trapping $KRAS^{G12C}$ in the inactive GDP-bound state similar to other allele-specific inhibitors (Lito et al., 2016a).

Lito et al have described that efficient inhibition of $KRAS^{G12C}$ signaling and cancer cell growth required intact GTPase activity and occurs because drug-bound $KRAS^{G12C}$ is insusceptible to nucleotide exchange factors and thus trapped in its inactive state. This was enabled by the discovery of the new binding pocket as discussed above.

A large part of the success of AMG-510 can be attributed to the discovery of a surface groove created by an alternative orientation of Histidine residue (His95) which could be occupied by aromatic rings enhancing its interactions with the KRASG12 protein(Gentile et al., 2017). As a result, AMG-510 is approximately 10 times more effective than ARS-1620, although they are structurally related and overlap (Canon et al., 2019a).

AMG-510 was the first compound to enter clinical trials showing single-agent efficacy in the phase I/II CodeBreak-100 trial (NCT03600883). The trial enrolled 129 patients with $KRAS^{G12C}$ mutant cancers (59 NSCLC, 42 CRS and 28 other tumors). Among them, NSCLC showed the highest response rate with an objective response rate (ORR) of 33% and and disease control rate (DCR) of 88.1%. The median PFS for all NSCLC patients was 6.3 months. However, the activity in CRC was less impressive with 7.1% had an objective response, 73.8% had disease control and the median PFS for all CRC patients was 4.0 months. No dose-limiting toxicities were reported.

Considering the relatively modest efficacy of AMG-510 as monotherapy in CRC, combination approaches with other therapeutic agents are being explored (NCT04185883) Table

Recently, LUMAKRASTM (Sotorasib) also known as AMG-510 received accelerated FDA approval for the treatment of patients with $KRAS^{G12C}$ mutant locally advanced and metastatic NSCLC who have received at least one prior systemic therapy in this indication (Skoulidis et al., 2015).

9.4.1.2 Adagrasib (MRTX849)

In 2021, Adagrasib (MRTX849) was granted Breakthrough Therapy designation to for the treatment of patients with $KRAS^{G12C}$ mutant NSCLC following prior systemic therapy.

In the preclinical setting, MRTX849 showed remarkable anti-tumor efficacy exclusively in $KRAS^{G12C}$ mutant cell lines resulting in tumor regression in xenograft models (Hallin et al., 2020).

In the same study, anti-tumor efficacy was improved when combined with upstream (EGFR and SHP2) and downstream inhibitors (mTOR and cyclin-dependent kinase 4/6) (CDK4/6)

The phase I/II multiple expansion cohort trial KRYSTAL-1 (NCT03785249) is ongoing with a planned recruitment of 822 patients with $KRAS^{G12C}$ mutant advanced solid tumors.

Results reported from the first disclosure including all patients enrolled in Cohort A, a phase 2 cohort evaluating Adagrasib given 600mg BID in patients with NSCLC previously treated with platinum-based chemotherapy and anti-PD-1/L1 therapy showed that Adagrasib was well tolerated and demonstrates

promising efficacy in pretreated NSCLC patients. The reported ORR was 42.9% and the disease control rate 79.5%. The median duration of response was 8.5 months (95% CI 6.2-13.8), median PFS 6.5 months (95% CI 4.7-8.4) and median OS was 12.6 months (95% CI 9.2-NE) (Spira et al., 2022).

A phase 3 trial evaluating Adagrasib monotherapy versus Docetaxel in previously treated patients with $KRAS^{G12C}$ mutant NSCLC is ongoing (NCT04685135) (Riely et al., 2021).

Table 4. Current $KRAS^{G12C}$ combination therapies

$KRAS^{G12C}$ Inhibitor	**Combination**	**Cancer type**	**Phase**	**NCT number**
AMG-510	Panitumumab and FOLFIRI	Advanced solid tumors	Ib/II	NCT04185883
AMG-510	Trametinib and panitumumab	Advanced solid tumors	Ib/II	NCT04185883
AMG-510	EMVASI (Bevacizumab-awwb) and FOLFIRI or FOLFOX	Advanced solid tumors	Ib/II	NCT04185883
MRTX-849	TN0155	Advanced solid tumors	II	NCT04330664
MRTX-849	Cetuximab	Advanced or metastatic CRC	III	NCT04793958
MRTX849	mFOLFOX6	Advanced or metastatic CRC	III	NCT04793958
MRTX849	FOLFIRI	Advanced or metastatic CRC	III	NCT04793958

Abbreviations : CRC colorectal cancer; FOLFOX 5-fluorouracil, leucovorin, and oxaliplatin, FOLFIRI: 5-fluorouracil, leucovorin, and irinotecan.

9.5 RAS ONCOGENE AND RADIORESISTANCE

The ability of the RAS oncogene to drive radioresistance has been extensively studied since the 1990's.

Pre-clinical results provide compelling evidence that RAS mutation or overexpression of KRAS, NRAS or HRAS can alter radiosensitivity and render tumor cells more resistant to radiation. (FitzGerald et al., 1985a)(Buday and Downward, 2008a) (M. D. Sklar, 1988a). Whether in rodent cells transfected with RAS (McKenna et al., 2003)(Bernhard et al., 1998a) or a series of human derived cell lines bearing endogenous RAS mutations it was shown that inhibition of RAS activation resulted in radio-sensitization whether using lovastatin (A. C. Miller et al., 1993), farnesyl-transferase inhibitor (Bernhard et al., 1998b), transfection of cells expressing activated RAS (Russell et al., 1999a), or expression of antisense vector to RAS (A. Rait et al., 2000), results are concordant with those of cells with endogenous RAS activation (Bernhard, et al. 1998).

9.5.1 Farnesyltransferase inhibitors

The covalent attachment of the farnesyl isoprenoid group to the HRAS, KRAS and NRAS proteins is the first step in the carboxy-terminal post-translational modification of these proteins. This processing results in a stable localization of RAS to the plasma membrane and is essential for the biological activity or RAS. Several strategies have therefore been developed to inhibit the farnesylation of RAS. A large number of FTIs have been identified through high-throughput screening and although they efficiently inhibit farnesylation of HRAS in vitro, this potential has not translated into the expected clinical benefit (Kohl et al., 1995). Some of this might be accounted for by the fact that although HRAS is exclusively modified by FTIs, KRAS and to a lesser extent NRAS can also be modified by gernalygeranlystransferase (GGT). This results in the transfer of RAS to a different isoprenoid group supporting the biological activity of RAS. Attempts to inhibit the function of KRAS and NRAS by using FTIs and GGTIs together has failed because of the very high toxicity that is associated with this combination (Lobell et al., 2001).

It appears likely that the lack of toxicity of FTIs is due to the fact that they fail to inhibit effectively the function of all endogenous RAS proteins, which are known to be essential for normal cell growth.

Despite uncertainty about their mechanism of function, FTIs do have marked effects on the growth and survival of some tumour cell lines *in vitro* and on xenografts in nude mice, although not necessarily those expressing activated RAS. Because FTIs inhibit the growth of some oncogenic KRAS-expressing human tumour cells as xenografts in nude mice, despite the fact that KRAS processing is not blocked, they clearly have potential as anti-tumour drugs, even though the mechanism of action is uncertain. The effects of FTIs in these pre-clinical systems have been reviewed extensively recently (Ohkanda et al., 2002).

Additionally, radiotherapy itself activates RAS-MAPK signaling in KRAS mutant cells and inhibition of MAPK signaling can reduce cell survival after radiotherapy (Williams et al., 2012a).

RAS mutations are often associated with resistance to targeted therapies and poor outcomes in patients with cancer (Nadal et al., 2014a)(Fiala et al., 2016a) (Jones et al., 2017a).

KRAS mutations are associated with radioresistance in colorectal and lung cancer : clinical evidence

Forty years ago, Slebos et al.(R. J. Slebos et al., 1990) identified that the subgroup of patients with KRAS mutated lung adenocarcinoma had a very poor prognosis and disease-free survival despite radical resection and small tumor burden.

In 1988 early in vitro studies suggest that RAS mutations or overexpression of KRAS, NRAS or HRAS induce radioresistance and may therefore be associated with resistance to therapy(M. D. Sklar, 1988b).

Since then, clinical significance of KRAS mutation has been broadly studied but yielded sometimes conflicting results (Schiller et al., 2001)(Mascaux et al., 2005)(Tsao et al., 2007) . This can be partly explained by the heterogeneity of patient population, tumor type, stage or treatments included in the analyses.

More recently, growing clinical evidence supporting the fact that KRAS mutations are associated with radioresistance in colorectal and lung cancer has been emerging.

The "RASCAL" study authors show that KRAS mutations in colorectal cancer are associated with increased risk of relapse and death, with mutation in valine codon 12 conferring an independent increased risk or recurrence and death (Andreyev et al., 2001). Duldulao et al.(Duldulao et al., 2013) have shown that rectal tumors with any KRAS mutation were less likely to have a pCR compared to wild-type KRAS. Similarly, a higher likelihood of pCR after preoperative CRT for locally advanced rectal carcinoma in the absence of mutations has been described (Russo et al., 2014).

Yagishita et al.(Yagishita et al., 2015) have reported a reduced efficacy and shortened survival in patients with KRAS mutated non-squamous stage III NSCLC treated with chemoradiotherapy.

In a phase II study of SBRT in colorectal cancer liver metastases, KRAS mutations were associated with increased risk of failure after radiation (Hong et al., 2020). Additionally, radiotherapy itself activates RAS-MAPK signaling in KRAS mutant cells and inhibition of MAPK signaling can reduce cell survival after radiotherapy (Williams et al., 2012a).

10 PROJECT RATIONALE AND OBJECTIVES

Considering that:

Despite recent clinical advances, resistance to radiation therapy remains a major challenge leading to disease relapse and increased mortality.

As discussed previously, although multifactorial, radioresistance remains largely driven by genomic and molecular alterations.

In view of the reported KRAS-induced radioresistance, and recent development of covalent $KRAS^{G12C}$ inhibitors with promising clinical efficacy in KRAS-mutant tumors, our aim was to explore the radiosensitizing effect of MRTX1257 a novel $KRAS^{G12C}$ inhibitor.

In a first part of this pre-clinical work we have focused on exploring radio-sensitizing properties of MRTX1257 alone and in combination with radiotherapy using in-vitro radiosensitivity assays.
Our second aim consisted in testing tumor growth inhibitory properties of the combination MRTX1257 and radiotherapy using in vivo syngeneic murine models.
Finally, we explore the immunomodulatory effects of the combination on the tumor microenvironment.

11 RESULTS

This paper has been published as a 1st co-author in Journal of Translational Medicine in October 2023. A brief summary is followed by the full version paper and by supplementary material that was not included in the published paper.

11.1 PAPER: KRASG12C INHIBITION USING MRTX1257: A NOVEL RADIO-SENSITIZING PARTNER

Pierre-Antoine Laurent[1,2,3*], Marina Milic[2,3*], Clément Quevrin[2,3], Lydia Meziani[2,3], Winchygn Liu[2,3], Daphné Morel[4], Nicolas Signolle[5], Céline Clémenson[2,3], Antonin Levy[1,2,3], Michele Mondini[2,3], Eric Deutsch[1,2,3]
* Equal contributors

Corresponding author: Eric Deutsch, INSERM U1030, 114 rue Edouard Vaillant; 94805 Villejuif, France; eric.deutsch@gustaveroussy.fr

Affiliations:
Department of Radiation Oncology, Gustave Roussy Cancer Campus, 114 rue Edouard Vaillant; 94805 Villejuif, France
INSERM U1030, Molecular Radiation Therapy and Therapeutic Innovation, Gustave Roussy Cancer Campus, University of Paris-Saclay, Villejuif, France
Labex LERMIT, DHU TORINO, SIRIC SOCRATE
Drug Development Department (DITEP), Gustave Roussy Cancer Campus, Villejuif, France
Experimental and Translational Pathology Platform (PETRA), AMMICa, INSERM US23/UAR3655, Gustave Roussy Cancer Campus, Villejuif, France

Objectives

Following recent successful development of covalent $KRAS^{G12C}$ inhibitors, and the therapeutic challenges associated with KRAS mutant cancers, the focus of this work was to explore the radiosensitizing and immunomodulatory properties of MRTX1257 a potent $KRAS^{G12C}$ covalent inhibitor in combination with radiotherapy.

Results summary

MRTX1257 radio-sensitizes CT26 and LL2 *in vitro* depending on *RAS* mutation profile.

MRTX1257 was able to radio-sensitize CT26 $KRAS^{G12C+/+}$ cells but not CT26 WT cells when used at the concentrations of 20 and 50 nM for 48 hours after irradiation (normalized survival fractions at 4 Gy: 0.06 and 0.04 respectively at 20 nM and 50 nM versus 0.23 in control group; $p<0.0001$). We then explored MRTX1257 in association with RT in two different LL2 cell lines harboring $KRAS^{G12C+/-}$ heterozygous mutation, the LL2 WT and LL2 $NRAS^{-/-}$ line harboring both a heterozygous mutation of *KRAS* and a knock-out (KO) mutation of *NRAS*. MRTX1257 at 20 or 50 nM for 48 hours was not able to influence their radio-sensitivity.

Therefore, these data show MRTX1257 is able to radio-sensitize tumor cells *in vitro* depending on their *RAS* mutational profile.

MRTX1257 increases the efficacy of RT in nude mice bearing CT26 $KRAS^{G12C+/+}$ tumors.

MRTX1257, administered three times at 50 mg/kg increased the efficacy of a single-dose of 6 Gy delivered on CT26 $KRAS^{G12C+/+}$ tumors in nude mice.

Combination treatment showed a better tumor growth and survival however without being able to induce any durable responses. This suggests the involvement of a functional and complete immune compartment in achieving durable responses.

MRTX1257 increases the efficacy of RT in immunocompetent BALB/c mice bearing CT26 $KRAS^{G12C+/+}$ tumors, and is able to induce durable responses in combination with RT.

Mice in the group treated with MRTX1257 alone relapsed quickly after the end of the treatment whereas those in the combination group showed a better survival ($p=0.04$).Twenty percent of mice (2/10) achieved a durable response in the combination group.

To determine if the combination treatment using irradiation and MRTX1257 led to significant anti-tumor immune memory in mice, we rechallenged the mice

showing complete response with s.c.CT26 KRAS$^{G12C+/+}$ or CT26 WT cells in contralateral flank. None of the mice rechallenged this way showed new tumors, in contrast with 100% of naive mice receiving similar s.c. injections. This observation illustrates the potent anti-tumor immune memory provided by the combination treatment against both CT26 KRAS$^{G12C+/+}$ and CT26 WT tumor cells

MRTX1257 increases the anti-proliferative effects of RT in CT26 KRAS$^{G12C+/+}$ tumors but not in CT26 WT tumors

We performed immunohistochemistry (IHC) analyses in both tumor types the day after the last administration of MRTX1257, i.e. D4 after RT.

Although irradiation alone was not able to significantly decrease the expression of Ki67 within CT26 KRAS$^{G12C+/+}$ tumors, the combination of RT with MRTX1257 greatly decreased the density of Ki67^{+} cells within these tumors (p=0.003 versus the control). Moreover, in CT26 KRAS$^{G12C+/+}$ tumors, the combined treatment significantly decreased the density of Ki67^{+} cells compared to irradiation alone (p=0.02), thus confirming the ability of MRTX1257 to increase the efficacy of RT in CT26 KRAS$^{G12C+/+}$ tumors, in line with the tumor growth experiments.

CD8^{+} T cells are not sufficient to explain the efficacy of the association between RT and MRTX1257 in CT26 KRAS$^{G12C+/+}$ tumors

We then performed the staining and the quantification of CD8^{+} cells within both CT26 KRAS$^{G12C+/+}$ and CT26 WT tumors (Fig. 6A).

Compared to the control group, the density of CD8^{+} cells within CT26 KRAS$^{G12C+/+}$ tumors was increased in the group treated using MRTX1257 alone (p=0.05), but not in the combined treatment group (p=0.15) (Fig. 6B and 6C). This shows that the radio-sensitizing effect induced by MRTX1257 in CT26 KRAS$^{G12C+/+}$ tumors cannot be solely attributed to an increase in the infiltration of CD8^{+} T cells within the microenvironment of these tumors, which is consistent with the efficacy of the combined treatment observed in T cell-deficient nude mice.

Regarding CT26 WT tumors, we did not observe any significant difference in the density of CD8^{+} cells within tumors regardless of the treatment (Fig. 6B and 6D).

In CT26 KRAS$^{G12C+/+}$ tumors, MRTX1257 drives the down-regulation of PD-L1 and counteracts its upregulation following RT alone

First, in tumor and stromal cells, identified as CD45 negative cells, we found the expression of PD-L1 was upregulated following RT alone ($p=0.005$) while it was dramatically downregulated in both MRTX1257 alone and combination groups ($p<0.0001$). The same outcomes were observed in myeloid cells, with the upregulation of PD-L1 following RT alone ($p<0.0001$) and its downregulation in groups treated with MRTX1257 alone ($p=0.0003$) or the combined treatment ($p=0.02$).

Then, the proportion of lymphoid cells was increased in groups treated with MRTX1257 alone and the combination compared to the control group. Among the lymphoid subtypes, the proportion of conventional $CD4^+$ T cells, defined as FoxP3 negative $CD4^+$ T cells, was increased in both the groups treated with MRTX1257 alone and with the combined treatment.

However, regarding the proportion of $CD8^+$ T cells, we did not observe any difference between the irradiation alone group and the combination group, while this proportion increased in the MRTX1257 alone group (MRTX1257 alone versus control: $p=0.004$). This is in line with the quantification of $CD8^+$ cells in the IHC experiment above.

RT and the combined treatment were able to polarize macrophages into a pro-inflammatory and anti-tumor phenotype characterized by the upregulation of the activation marker CD80 Moreover, the combination treatment increased the proportion of conventional dendritic cells type 2 (cDC2) and their expression of MHC class II within the tumor immune microenvironment.

Conclusions and Perspectives

To our knowledge, this study is the first to explore the efficacy and immunological properties of the specific association of a KRAS^{G12C} inhibitor with RT in a preclinical animal model of KRAS^{G12C} mutated cancer.

In this work, we first demonstrated the ability of MRTX1257, a potent covalent KRAS^{G12C} inhibitor analogous to MRTX849, to enhance the effect of radiotherapy both *in vitro* and *in vivo*. This effect depended on *RAS* mutational status, dose and timing of administration and was associated with a good safety profile.

Moreover, the use of RT and MRTX1257 led to a significant cure rate in BALB/c mice bearing CT26 $KRAS^{G12C+/+}$ tumors, but not in nude mice, highlighting the role of the tumor immune microenvironment in the radio-sensitizing effect of MRTX1257. This work constitutes a first step towards the implementation of new combinatorial approaches involving RT and MRTX1257 in $KRAS^{G12C}$ mutated cancers, with the aim of providing new therapeutic strategies with a prolonged clinical benefit. The optimal treatment sequencing and selected patient populations warrant further characterization both in the preclinical and clinical settings.

Laurent *et al.*
Journal of Translational Medicine (2023) 21:773
https://doi.org/10.1186/s12967-023-04619-0

Journal of Translational Medicine

RESEARCH

Open Access

KRAS^{G12C} inhibition using MRTX1257: a novel radio-sensitizing partner

Pierre-Antoine Laurent[1,2,3†], Marina Milic[2,3†], Clément Quevrin[2,3], Lydia Meziani[2,3], Winchygn Liu[2,3], Daphné Morel[4], Nicolas Signolle[5], Céline Clémenson[2,3], Antonin Levy[1,2,3], Michele Mondini[2,3] and Eric Deutsch[1,2,3*]

Abstract

Background *KRAS* activating mutations are considered the most frequent oncogenic drivers and are correlated with radio-resistance in multiple cancers including non-small cell lung cancer (NSCLC) and colorectal cancer. Although KRAS was considered undruggable until recently, several KRAS inhibitors have recently reached clinical development. Among them, MRTX849 (Mirati Therapeutics) showed encouraging clinical outcomes for the treatment of selected patients with *KRAS*^{G12C} mutated NSCLC and colorectal cancers. In this work, we explore the ability of MRTX1257, a KRAS^{G12C} inhibitor analogous to MRTX849, to radio-sensitize *KRAS*$^{G12C+/+}$ mutated cell lines and tumors.

Methods Both in vitro and in vivo models of radiotherapy (RT) in association with MRTX1257 were used, with different *RAS* mutational profiles. We assessed in vitro the radio-sensitizing effect of MRTX1257 in CT26 KRAS$^{G12C+/+}$, CT26 WT, LL2 WT and LL2 *NRAS* KO (LL2 NRAS$^{-/-}$) cell lines. In vivo, we used syngeneic models of subcutaneous CT26 KRAS$^{G12C+/+}$ tumors in BALB/c mice and T cell deficient athymic *nu/nu* mice to assess both the radio-sensitizing effect of MRTX1257 and its immunological features.

Results MRTX1257 was able to radio-sensitize CT26 KRAS$^{G12C+/+}$ cells in vitro in a time and dose dependent manner. Moreover, RT in association with MRTX1257 in BALB/c mice bearing CT26 KRAS$^{G12C+/+}$ subcutaneous tumors resulted in an observable cure rate of 20%. However, no durable response was observed with similar treatment in athymic nude mice. The analysis of the immune microenvironment of CT26 KRAS$^{G12C+/+}$ tumors following RT and MRTX1257 showed an increase in the proportion of various cell subtypes including conventional CD4 + T cells, dendritic cells type 2 (cDC2) and inflammatory monocytes. Furthermore, the expression of PD-L1 was dramatically down-regulated within both tumor and myeloid cells, thus illustrating the polarization of the tumor microenvironment towards a pro-inflammatory and anti-tumor phenotype following the combined treatment.

Conclusion This work is the first to demonstrate in vitro as in vivo the radio-sensitizing effect of MRTX1257, a potent KRAS^{G12C} inhibitor compatible with oral administration, in CT26 KRAS^{G12C} mutated cell lines and tumors. This is a first step towards the use of new combinatorial strategies using KRAS inhibitors and RT in KRAS^{G12C} mutated tumors, which are the most represented in NSCLC with 14% of patients harboring this mutational profile.

†Pierre-Antoine Laurent and Marina Milic contributed equally.

*Correspondence:
Eric Deutsch
eric.deutsch@gustaveroussy.fr
Full list of author information is available at the end of the article

Keywords MRTX1257, Radiotherapy, KRAS inhibitors, Tumor, Radio-sensitizing, KRAS G12C, Immune microenvironment

Background

Radiotherapy (RT) plays a central role in cancer treatment. During the course of their treatment, it is estimated that nearly 50% of all cancer patients have indications for radiotherapy either with curative or palliative intent [1, 2].

The presence and type of activated oncogenes within tumor cells influence prognosis and therapeutic response, including RT. *RAS* (Rat sarcoma viral oncogene homolog) is considered the most frequently mutated oncogene with nearly 19% of cancer patients harboring a *RAS* mutation [3]. The *KRAS* (Kirsten rat sarcoma viral oncogene) isoform represents 75% of RAS mutant cancers and is therefore considered a crucial oncogene.

KRAS mutations occur in approximately 20–25% of non-small-cell lung cancers (NSCLC) [4], more than 80% of pancreatic cancers and 30% of colorectal and cholangial cancers [5]. When it comes to $KRAS^{G12C}$ isoform mutations, they are estimated to occur in 14% of NSCLC adenocarcinomas [6] and 5% of colorectal cancers [7].

The ability of the *RAS* oncogene to drive radio-resistance has been extensively studied since the 1990's. *RAS* mutations are long known to provide radiation resistance to tumor cells, as demonstrated first in mouse cell lines transformed with *HRAS*, *NRAS* or *KRAS* mutations [8, 9]. Upstream and downstream pathways from RAS, including EGFR expression, AKT phosphorylation, PI3K and MAPK signaling are also associated with the response to radiation [10, 11].

These results are in line with clinical observations in patients with *RAS* mutated cancers, often showing overall resistance to therapies and thus associated with poor outcomes [12–15]. Therefore, *RAS* mutations appear to be a target of interest, and different strategies of RAS inhibition using transfected rodent cells or human derived cell lines showed promising radio-sensitizing outcomes. These strategies involve farnesyltransferase inhibitors [16], lovastatin [17], prenyltransferase inhibitors [18], the transfection of anti-RAS single chain antibody fragment [19], or the use of an antisense vector [20].

Until recently, *KRAS* mutations were considered undruggable. Efforts to target KRAS directly have faced major difficulties owing to its pico-molar affinity for GTP/GDP and the absence of allosteric regulatory sites. *KRAS* oncogenic mutations result in functional activation of RAS family proteins by impairing GTP hydrolysis [21]. KRAS mutant proteins have a reduced capability to hydrolyze GTP or to interact with the GTPase-activating proteins, maintaining the oncogene and the downstream pathways constitutively activated. The lack of specific inhibitors targeting the KRAS hydrophobic pocket as well as the complexity of downstream pathways have contributed to the challenge of developing effective therapeutic agents.

Two specific $KRAS^{G12C}$ inhibitors, sotorasib (AMG510, Amgen) and adagrasib (MRTX849, Mirati Therapeutics) recently earned the breakthrough designation by the US Food and Drug administration to treat metastatic lung cancer patients harboring $KRAS^{G12C}$ mutations who have progressed on at least one systemic therapy. These small molecules are able to irreversibly inhibit $KRAS^{G12C}$ through a unique interaction with the P2 pocket trapping $KRAS^{G12C}$ in the inactive GDP-bound state similar to other allele-specific inhibitors [22].

Data from the registrational phase 1/2 KRYSTAL-1 trial (NCT03785249) reported results of a phase 2 cohort including 116 patients with metastatic $KRAS^{G12C}$ mutated NSCLC treated with at least one prior systemic therapy before receiving adagrasib [6]. The objective response rate (ORR), progression-free survival (PFS) and median overall survival (OS) were respectively 42.9%, 6.5 months and 12.6 months. Despite these promising results, resistance often occurs in patients, paving the way for further strategies able to improve the long-term efficacy of $KRAS^{G12C}$ inhibitors. Among these strategies, the association of $KRAS^{G12C}$ inhibitors with focal RT is of interest.

RT is standard of care at all non-advanced inoperable NSCLC stages, including $KRAS^{G12C}$ mutant tumors [23]. Therefore, demonstrating the benefit of an association between $KRAS^{G12C}$ inhibitors and RT has the potential to make patients with $KRAS^{G12C}$ mutations benefit from this new therapeutic strategy. Furthermore, *KRAS* is responsible of an immunosuppressive tumor microenvironment within mutated tumors in a PD-L1 dependent manner [24, 25], and the effect of MRTX849 was diminished when CT26 $KRAS^{G12C+/+}$ were grown in T cell deficient nude mice [26]. This illustrates the necessity to consider the infiltrating immune cells in the studies assessing the therapeutic associations using KRAS inhibitors.

In this work, we explore the efficacy of the association between RT and MRTX1257, a selective and covalent $KRAS^{G12C}$ inhibitor analogous to MRTX849, in animal models of cancer. Moreover, we show the different

effects of the association of RT and MRTX1257 in reshaping the tumor immune microenvironment, i.e. the important down-regulation of PD-L1 in tumor and myeloid cells, as well as the increase of the infiltration of conventional $CD4^+$ T cells, inflammatory monocytes and dendritic cells type 2 (cDC2).

Material and methods

Cell culture, chemicals and antibodies

Cell lines CT26 WT and LL2 WT were obtained from ATCC. CT26 harboring homozygous *KRAS*^{G12C} mutation (CT26 KRAS$^{G12C+/+}$) and LL2 KO for *NRAS* (LL2 NRAS$^{-/-}$) were provided by Mirati Therapeutics (USA).

CT26 KRAS$^{G12C+/+}$ and CT26 WT cell lines were maintained in RPMI-1640 (Gibco) supplemented with 10% fetal calf serum and 1% penicillin–streptomycin (Gibco) and cultured at 37 °C with 5% CO2. LL2 WT and LL2 NRAS$^{-/-}$ were maintained in DMEM + GlutaMAX + Pyruvate (Gibco) supplemented with 10% fetal calf serum and 1% penicillin–streptomycin (Gibco) and cultured at 37 °C with 5% CO2.

MRTX1257 was provided by Mirati Therapeutics and reconstituted using cyclodextrin Captisol (Ligand, San Diego, USA) in case of oral administration in mice or dimethylsulfoxide (DMSO) for in vitro experiments.

Clonogenic survival assay

CT26 WT, CT26 KRAS$^{G12C+/+}$, LL2 WT and LL2 NRAS$^{-/-}$ were collected using trypsin–EDTA 0.05% (Gibco) and counted with Cellometer K2 Fluorescent cell counter (NEXCELOM, Massachussetts, USA) by trypan blue viability at least equal to 90%.

For CT26 WT and CT26 KRAS$^{G12C+/+}$ cell lines, cells were seeded in triplicates at 50 to 400 cells/well (CT26 WT) or 100 to 1200 cells/well (CT26 KRAS$^{G12C+/+}$) in 6-well plates during 12 h in 2 mL of culture medium. Three hours before irradiation, the culture medium was changed for the medium containing MRTX1257 at the indicated concentration. Twenty-four or 48 h after irradiation, the medium containing MRTX1257 was changed for drug-free medium.

For LL2 WT and LL2 NRAS$^{-/-}$, 250 to 500 cells were seeded per well in 6-well plates during 3 h in 1 mL of Methocult M3134 (StemCell Technologies) supplemented in culture medium and containing MRTX1257 at the indicated dose. Twenty-four or 48 h after irradiation, a dilution of MRTX1257 by a factor 10 was done by adding 9 mL of drug-free culture medium to the 1 mL of Methocult M3134 in each well.

Plates were irradiated at the indicated dose using an X-RAD 320 irradiator (Precision X-Ray, USA). Seven days after irradiation, colonies equal or higher to 50 cells were counted. The number of colonies counted was normalized by the number of cells per well seeded at the start of the experiment in order to define the survival fraction. The different survival fractions were finally normalized by the survival fraction in the control non-irradiated condition for each concentration of MRTX1257 tested and then plotted in survival curves.

Mouse models

Animal studies were conducted in compliance with all applicable regulations and guidelines of the Ethical approval Committee CCEA 26 at Gustave Roussy.

Seven-week-old BALB/c WT and athymic nude female mice were obtained from Janvier Labs (Le Genest-Saint-Isle, France) and housed in a pathogen-free facility. Mice were subcutaneously inoculated in their right flank with 10^6 CT26 KRAS$^{G12C+/+}$ cells or 5.10^5 CT26 WT cells in 50µL of pH 7.2 phosphate-buffer saline (PBS) solution (Gibco).

Once the tumors reached an average volume of 90–100 mm^3, estimated using the following formula Tumor volume = (length x width x width)/2, with length and width of tumors measured using a digital caliper, mice were randomized into the different treatment groups.

On the day of randomization (= D-1 before RT), as well as on D1 and D3 after RT, mice received an oral administration of MRTX1257 at the dose of 50 mg/kg reconstituted in 5 ml/kg of Captisol vehicle or the same volume of Captisol vehicle alone, according to the treatment group. At D0, mice randomized into RT only and combination groups received a single fraction of 6 Gy to the tumor volume using a Varian Tube NDI 226 (X-ray machine; 200 kV; tube current 15 mA; beam filter: 0.2 mmCu, dose-rate 1.15 Gy/minute). Radiation was only delivered to the tumor mass by using a custom shielding and an appropriate device to immobilize the mouse.

Tumor volumes were measured twice a week using a digital caliper and the previous formula. When tumor volumes reached 1200 mm^3 or when any of critical points including weight loss > 20%, tumor necrosis or suffering appeared, mice were sacrificed.

BALB/c mice showing complete response of CT26 KRAS$^{G12C+/+}$ tumors following irradiation combined with MRTX1257 were rechallenged with s.c. injection of either 10^6 CT26 KRAS$^{G12C+/+}$ cells or 5.10^5 CT26 WT cells in contralateral flank. Tumor growth and survival were evaluated using the same methods than described above, and these data were compared with those of naive BALB/c mice receiving similar s.c. injections.

Immunohistochemistry

The day after the last administration of MRTX1257 (= D4 after RT), animals were sacrificed by cervical dislocation

and subcutaneous tumors were harvested and then fixated using paraformaldehyde (PFA) 4%.

For detection of cleaved CD8, 4 µm sections were processed for heat-induced antigen retrieval (ER2 corresponding EDTA buffer pH9) for 20 min at 100 °C. Slides were incubated with the antibody (clone D4W2Z #98,941, 1: 400, Cell Signaling) for 1 h at room temperature. Then, the slides were incubated with the Rabbit HRP PowerVision Kit (Leica Biosystems, #PV6119). The signal was revealed with diaminobenzidine (DAB).

For Ki67, slides were incubated with a monoclonal rabbit anti-Ki67 antibody (Cell Signaling, 1: 500). The signal was revealed with the Rabbit PowerVision Kit (UltraVision Technologies).

All slides were scanned at 20X using VS120 scanner (Olympus, Japan). Images were processed and staining quantified using QuPath v0.4.0 [27]. Regions of interest were manually delineated. Inside these regions, tissue was automatically detected using a trained classifier. Color deconvolution (Hematoxylin, DAB and residual) was applied to the images. Cells were detected based on their optical density and positivity ($CD8^+$ or $Ki67^+$) was assessed based on the amount of DAB signal in each cell. Results were expressed as a number of stained cells by square millimeter of analyzed tissue.

Flow cytometry

The day after the last administration of MRTX1257 (= D4 after RT), animals were sacrificed by cervical dislocation and subcutaneous tumors were harvested. Tumors were mechanically and then enzymatically dissociated by using the "Tumor Dissociation Kit Mouse" (Miltenyi Biotec, Germany) for 30 min at 37 °C and 1750 rpm. Cell suspensions were then filtered using 70 µm cell strainers (Miltenyi Biotec, Germany), and further used for Fc receptor blockage and then immune-cell staining.

For Fc receptor blockage, cell suspensions were incubated with purified anti-mouse CD16/32 (clone 93; BioLegend) during 10 min at 4 °C. Subsequently, cell populations were stained 20 min at 4 °C using antibodies listed in supplementary table and at dilutions recommended by the manufacturer.

For tumor-infiltrating immune cell staining, anti-CD45 (REA737), anti-Ly6G (REA526), anti-CD11c (REA754; Miltenyi Biotec), anti-CD11b (M1/70; BD Horizon), anti-Ly6C (HK 1.4) and anti-CD64 (X54-5/7.1; BioLegend) were used to identify non-immune cells (CD45-), myeloid cells ($CD45^+$ $CD11b^+$), macrophages ($CD45^+$ $CD11b^+$ $Ly6G^-$ $Ly6C^{-/low}$ $CD64^+$), inflammatory monocytes ($CD45^+$ $CD11b^+$ $Ly6G^-$ $Ly6C^{high}$ $CD64^-$) and conventional dendritic cells type 2 (cDC2: $CD45^+$ $CD11b^+$ $Ly6G^-$ $CD64^-$ $CD11c^+$). Anti-CD45 (REA737; Miltenyi Biotec), anti-CD8 (53–6.7; BD Horizon), anti-CD4 (RM 4–5), anti-CD11b (M1/70) and anti-NKp46 (29A 1.4; BioLegend) were used to identify lymphoid cells ($CD45^+$ $CD11b^-$) $CD4^+$ T cells ($CD45^+$, $CD11b^-$ $CD4^+$), $CD8^+$ T cells ($CD45^+$ $CD11b^-$ $CD8^+$), NK cells ($CD45^+$ $CD11b^-$ $NKp46^+$). Furthermore, after fixation and permeabilization using the « Mouse FoxP3 Buffer Set» (BD Pharmingen), anti-FoxP3 (REA788; Miltenyi Biotec) was used to distinguish between conventional $CD4^+$ T cells ($CD45^+$ $CD11b^-$ $CD4^+$ $FoxP3^-$) and Treg cells ($CD45^+$ $CD11b^-$ $CD4^+$ $FoxP3^+$).

Anti-PD1 (REA802), anti-CD80 (REA983), anti-MHC II (REA813; Miltenyi Biotec) and anti-PD-L1 (MIH5; BD Optibuild) were used. For these markers, mean fluorescence intensities (MFI) for each target population were normalized to an unstained control in each treatment group (DeltaMFI).

Samples were acquired on a LSR Fortessa X20 (BD, Franklin Lakes, NJ) with FACSDiva software, and data were analyzed using FlowJo V10.8.1 software (Tree Star, Ashland, OR).

Statistical analysis

Statistical analysis was performed using GraphPad Prism Software version 8. Differences between groups were analyzed using a one-way ANOVA followed by Dunnett's correction. All values were expressed as means ± standard errors to mean (SEM). All analyses were two-sided and a difference with a P-value < 0.05 was considered statistically significant. Regarding survival data, Kaplan–Meier curves were compared using the log-rank test, with P-values < 0.05 considered statistically significant.

Results

MRTX1257 radio-sensitizes CT26 and LL2 in vitro *depending on RAS mutation profile*

We first assessed in vitro the efficacy of the combination between MRTX1257 at various concentrations and different RT doses in CT26 cell lines harboring different RAS mutation profiles. MRTX1257 was able to radiosensitize CT26 $KRAS^{G12C+/+}$ cells when used at the concentrations of 20 and 50 nM for 48 h after irradiation (normalized survival fractions at 4 Gy: 0.06 and 0.04 respectively at 20 nM and 50 nM versus 0.23 in control group; $p < 0.0001$) (Fig. 1A).

Regarding CT26 WT cells, which are reported in literature as harboring homozygous $KRAS^{G12D}$ mutation [28, 29], MRTX1257 at 20 nM or 50 nM for 48 h did not increase their radio-sensitivity at the tested RT doses, i.e. from 2 to 6 Gy (Fig. 1B). To explore the absence of efficacy of MRTX1257 in this cell line, we performed a dose-escalation assay by using increasing concentrations of MRTX1257 in vitro. The results showed a half maximal inhibitory concentration (IC50) between 2 and 10 µM,

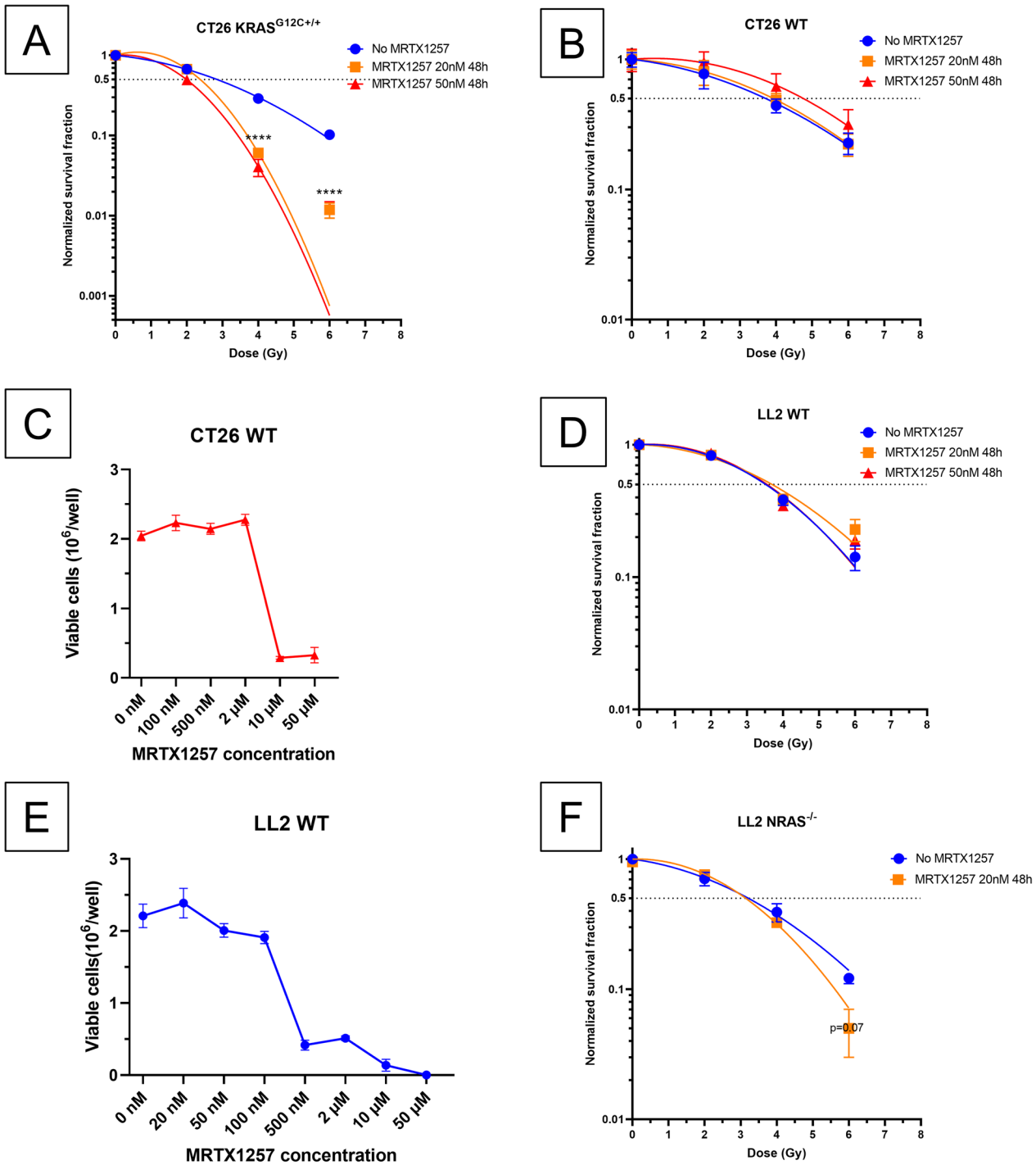

Fig. 1 MRTX1257 radio-sensitizes in vitro CT26 and LL2 tumor cell lines according to their KRAS mutational status. Clonogenic survival assays were performed after treatment using RT and MRTX1257 at various doses in different cell lines harboring different KRAS mutational profiles. Normalized survival fractions are represented in mean ± standard-error to mean (SEM), with n = 3 to 6 replicates per condition. Survival curves are extrapolations according to the linear quadratic model. ****: $p < 0.0001$ (one-way ANOVA). Survival curves for (**A**) CT26 KRAS$^{G12C+/+}$; **B** CT26 WT; **C** LL2 NRAS$^{-/-}$; **D** LL2 WT. **E, F** Dose–response curves for CT26 WT and LL2 WT cell lines exposed to various concentrations of KRAS.^{G12C} inhibitor MRTX1257

far beyond the 20 to 50 nM used in CT26 KRAS$^{G12C+/+}$ (Fig. 1C).

We then explored MRTX1257 in association with RT in two different LL2 cell lines. Regarding LL2 WT cells, we decided to sequence the gene *Kras* and found this cell line harbors *KRAS*$^{G12C\pm}$ heterozygous mutation (data not shown). MRTX1257 at 20 or 50 nM for 48 h did not influence the radio-sensitivity of this cell line (Fig. 1D), which suggests that a heterozygous G12C mutation of *KRAS* is not sufficient to allow a proper efficacy of the combination treatment. As in CT26 WT cell line, we performed a dose-escalation assay in LL2 WT cell line and found an IC50 between 100 and 500 nM (Fig. 1E), which is inferior to the IC50 in CT26 WT cell line and may be explained by the presence of a single *KRAS*^{G12C} mutation.

LL2 NRAS$^{-/-}$ cells harbor both a heterozygous mutation of *KRAS* and a knock-out (KO) mutation of *NRAS*. Although we observed a trend in radio-sensitizing these cells using MRTX1257 at 20 nM for 48 h, this effect was not statistically significant ($p=0.07$) (Fig. 1F). This suggests that, even when silencing *NRAS*, a heterozygous KRAS^{G12C} mutation is not sufficient to provide a strong radio-sensitizing effect of MRTX1257 comparable to the one observed in KRAS$^{G12C+/+}$ cells.

Of note, the use of MRTX1257 at the concentrations of 5 and 10 nM during 24 h did not provide any radio-sensitizing effect in both CT26 KRAS$^{G12C+/+}$ and LL2 NRAS$^{-/-}$ tumor cells (Additional file 1: Figure S1A, B

Overall, these data show MRTX1257 is able to radio-sensitize tumor cells in vitro depending on their *RAS* mutational profile. Moreover, the impact of *KRAS*^{G12C} mutational status on this effect was predominant, since *NRAS* mutational status had a moderate, non-significant impact on it in addition to *KRAS* status.

MRTX1257 increases the efficacy of RT in nude mice bearing CT26 KRAS$^{G12C+/+}$ tumors

After the demonstration of in vitro radio-sensitization of CT26 KRAS$^{G12C+/+}$ using MRTX1257, we aimed to explore a similar setting of combinatorial approach in athymic nude mice bearing CT26 KRAS$^{G12C+/+}$ tumors. This allowed us to assess the in vivo efficacy of the combination of MRTX1257 and RT in a lymphoid compartment-depleted setting, serving as an extension of the previous in vitro experiment.

MRTX1257, administered three times at 50 mg/kg (Fig. 2A) increased the efficacy of a single-dose of 6 Gy delivered on CT26 KRAS$^{G12C+/+}$ tumors in nude mice. Regarding the tumor growth curve (Fig. 2B) as well as the average tumor volume in each group at D10 after radiotherapy (Fig. 2C), the differences are significant in all treatment groups compared to control group ($p<0.0001$). Moreover, the group treated with combination treatment shows better outcomes compared to both the groups treated with irradiation alone ($p=0.005$) and with MRTX1257 alone ($p=0.03$).

This translated in a better survival in the group treated with combination ($p<0.0001$ versus the control group and MRTX1257 alone group, $p=0.006$ versus the irradiation alone group) (Fig. 2D and 2E). However, despite these interesting results, none of the conditions tested was able to induce a durable response in nude mice, since all mice finally relapsed. This observation may be due to the putative involvement of a functional and complete immune compartment in achieving durable responses following RT and MRTX1257.

MRTX1257 increases the efficacy of RT in immunocompetent BALB/c mice bearing CT26 KRAS$^{G12C+/+}$ tumors, and is able to induce durable responses in combination with RT

We then decided to explore the efficacy of the combination of MRTX1257 and RT in immunocompetent BALB/c mice bearing CT26 KRAS$^{G12C+/+}$ tumors.

As in nude mice, MRTX1257 administered 3 times at 50 mg/kg (Fig. 3A) increased the efficacy of RT delivered at a single dose of 6 Gy. Indeed, the tumor growth rate decreased in all treated groups compared with the control untreated group with a maximum of efficacy reached in the combination group (irradiation alone: $p=0.004$; MRTX1257 alone: $p=0.0005$; irradiation + MRTX1257: $p<0.0001$) (Fig. 3B). Moreover, the difference in average tumor volume at D10 between the irradiation alone group and the combination group, even if not meeting the statistical significance threshold, was notable ($p=0.07$, Fig. 3C). Furthermore, as illustrated in the individual growth profiles (Fig. 3D) and in the survival curves (Fig. 3E), mice in the group treated with MRTX1257 alone relapsed quickly after the end of the treatment whereas those in the combination group showed a better survival ($p=0.04$), with 2 mice out of 10 achieving durable responses. To determine if the combination treatment using irradiation and MRTX1257 led to significant anti-tumor immune memory in mice, we rechallenged the mice showing complete response with s.c. injection of CT26 KRAS$^{G12C+/+}$ or CT26 WT cells in contralateral flank. None of the rechallenged mice developed new tumors, in contrast with 100% of naive mice receiving similar s.c. injections, suggesting a potent anti-tumor immune memory provided by the combination treatment against both CT26 KRAS$^{G12C+/+}$ and CT26 WT tumor cells (Fig. 3F).

Of note, no significant toxicities were observed in mice when treating with MRTX1257 and RT in these conditions.

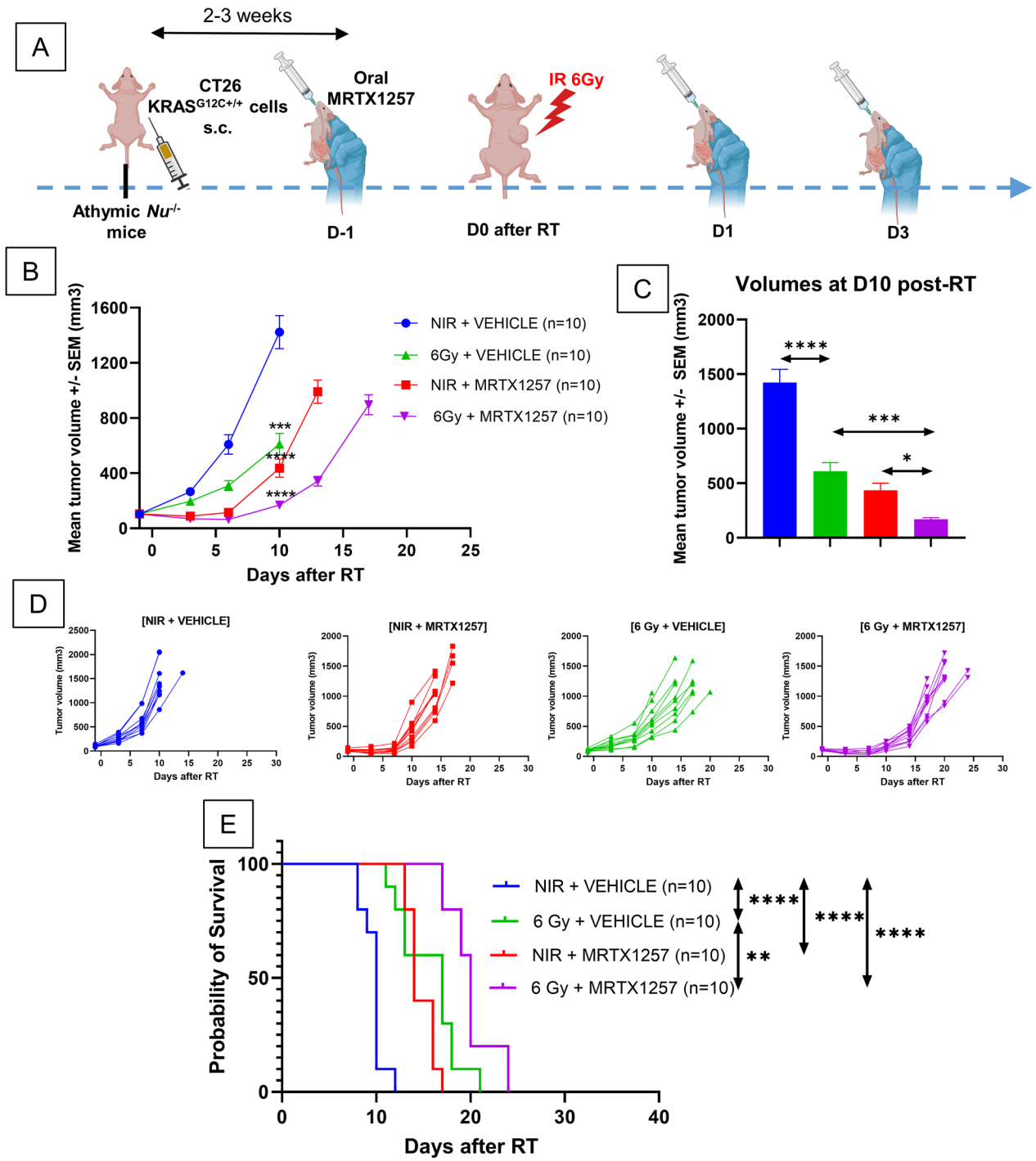

Fig. 2 MRTX1257 increases the efficacy of RT in nude mice bearing CT26 KRAS$^{G12C+/+}$ however without achieving durable responses **A** Athymic nude mice were subcutaneously inoculated with CT26 KRAS$^{G12C+/+}$ cells. Once the tumors reached an average volume of 90–100 mm^3, mice received via oral administration 50 mg/kg of MRTX1257 or vehicle. The day after, mice received a single fraction of 6 Gy on the tumor mass. MRTX1257 at the dose of 50 mg/kg or vehicle were then administered at D1 and D3 after RT. The experiment was repeated twice. **B** Tumor growth (mean ± SEM) ***: $p < 0.001$; ****: $p < 0.0001$ (two-way ANOVA). **C** Mean tumor volumes in each group 10 days after RT are represented. *: $p < 0.05$; ***: $p < 0.001$; ****: $p < 0.0001$ (one-way ANOVA). **D** Individual growth profiles of CT26 KRAS.$^{G12C+/+}$ tumors are represented for each condition. **E** Survival Kaplan–Meier curves were compared between each group using the log-rank test. **: $p < 0.01$; ****: $p < 0.0001$

As a reminder, we did not observe any durable response in nude mice and, as illustrated in their individual growth profiles (Fig. 2D), all nude mice experienced fast and homogeneous relapses. This suggests that the presence of a functional lymphoid compartment has an impact on the efficacy of the combination of RT and MRTX1257.

We then explored whether the combination of irradiation and MRTX1257 was able to generate systemic anti-tumor immune response leading to the abscopal response of a lesion outside of the irradiation field. To this end, we administered this combination in BALB/c mice bearing 2 s.c. CT26 KRAS$^{G12C+/+}$ tumors of which only one received irradiation (Additional file 1: Fig. S2A). In primary (irradiated) tumors, in a comparable manner than in the one-tumor experiments described above, MRTX1257 increased the anti-tumor efficacy of RT ([RT + MRTX1257] VS RT alone: $p = 0.003$). Moreover, at late timepoint (D13 after RT), the combined treatment showed an interesting anti-tumor superiority compared to MRTX1257 alone, although not reaching the significance criteria due to the low number of mice included in each group ($p = 0.10$) (Additional file 1: Figure S2B). In secondary (unirradiated) tumors, the addition of RT to the primary tumor failed to improve the efficacy of MRTX1257, thus suggesting the absence of abscopal effect in this setting (Additional file 1: Figure S2C). These findings translated into the absence of significant benefit of survival in mice treated with primary tumor irradiation and MRTX1257 compared to those treated with MRTX1257 only (Additional file 1: Figure S2D).

MRTX1257 does not show any significant efficacy in CT26 WT derived tumors

To determine if the efficacy of the combination between RT and MRTX1257 relies upon the presence of *KRAS^{G12C}* mutation in CT26 tumors, we performed a similar tumor growth experiment in BALB/c mice bearing CT26 WT tumors (Fig. 4A).

A significant decrease in tumor growth rate was observed in both groups treated using RT compared to the control group ($p = 0.0006$ for groups treated with RT alone and RT + MRTX1257) (Fig. 4B and C). However, we did not observe any positive effect on tumor growth rate attributable to the administration of MRTX1257 alone or in combination with RT in mice bearing CT26 WT tumors.

Regarding the survival outcomes, survival was improved only in groups treated with RT compared to their non-irradiated counterparts [(6 Gy + VEHICLE) versus (NIR + VEHICLE): $p = 0.001$; (6 Gy + MRTX1257) versus (NIR + MRTX1257): $p = 0.0009$]. Interestingly, we were able to cure 4 mice out of 11 in the combination group, which is higher than in CT26 KRAS$^{G12C+/+}$ tumors. However, we were also able to cure 2 mice out of 11 in the irradiation alone group, with similar associated tumor growth profiles (Fig. 4D) and non-statistically different survival (Fig. 4E). Taken together, these data suggest a higher level of radio-sensitivity of CT26 WT tumors compared to CT26 KRAS$^{G12C+/+}$.

MRTX1257 increases the anti-proliferative effects of RT in CT26 KRAS$^{G12C+/+}$ tumors but not in CT26 WT tumors

To assess the anti-proliferative effect of the association between RT and MRTX1257 in CT26 KRAS$^{G12C+/+}$ and CT26 WT tumors, we performed immunohistochemistry (IHC) analyses in both tumor types the day after the last administration of MRTX1257, i.e. D4 after RT (Fig. 5A).

Although irradiation alone was not able to significantly decrease the expression of Ki67 within CT26 KRAS$^{G12C+/+}$ tumors, the combination of RT with MRTX1257 greatly decreased the density of Ki67^{+} cells within these tumors ($p = 0.003$ versus the control) (Fig. 5B, C). Moreover, in CT26 KRAS$^{G12C+/+}$ tumors, the combined treatment significantly decreased the density of Ki67^{+} cells compared to irradiation alone ($p = 0.02$), thus confirming the ability of MRTX1257 to increase the efficacy of RT in CT26 KRAS$^{G12C+/+}$ tumors, in line with the tumor growth experiments.

In CT26 WT tumors, unlike in CT26 KRAS$^{G12C+/+}$ tumors, the expression of Ki67 decreased only in

(See figure on next page.)

Fig. 3 MRTX1257 increases the efficacy of RT in immunocompetent BALB/c mice bearing CT26 KRAS$^{G12C+/+}$ tumors and achieved durable responses in association with RT. **A** BALB/c mice were subcutaneously inoculated with CT26 KRAS$^{G12C+/+}$ cells. Once the tumors reached an average volume of 90–100 mm^3, mice received via oral administration 50 mg/kg of MRTX1257 or vehicle. The day after, mice received a single fraction of 6 Gy on the tumor mass. MRTX1257 at the dose of 50 mg/kg or vehicle were then administered at D1 and D3 after RT. The experiment was repeated twice. **B** Tumor growth (mean ± SEM). **: $p < 0.01$; ***: $p < 0.001$; ****: $p < 0.0001$ (two-way ANOVA). (**C**) Mean tumor volumes in each group 10 days after RT are represented. **: $p < 0.01$; ***: $p < 0.001$; ****: $p < 0.0001$ (one-way ANOVA). **D** Individual growth profiles of CT26 KRAS G12C$^{+/+}$ tumors are represented for each condition. The number of mice achieving durable response with no tumor being assessed at the end of the experiment is indicated below each panel. **E** Survival Kaplan–Meier curves were compared between each group using the log-rank test. *: $p < 0.05$; **: $p < 0.01$; ****: $p < 0.0001$. **F** Immunocompetent BALB/c mice bearing CT26 KRAS$^{G12C+/+}$ tumors and cured by the combination of RT and MRTX1257 were subsequently rechallenged with either 1.10^6 CT26 KRAS$^{G12C+/+}$ (top) or 5.10^5 CT26 WT cells (bottom) subcutaneously injected in their contralateral flank. Their survivals were then compared with those of naive mice receiving similar injections

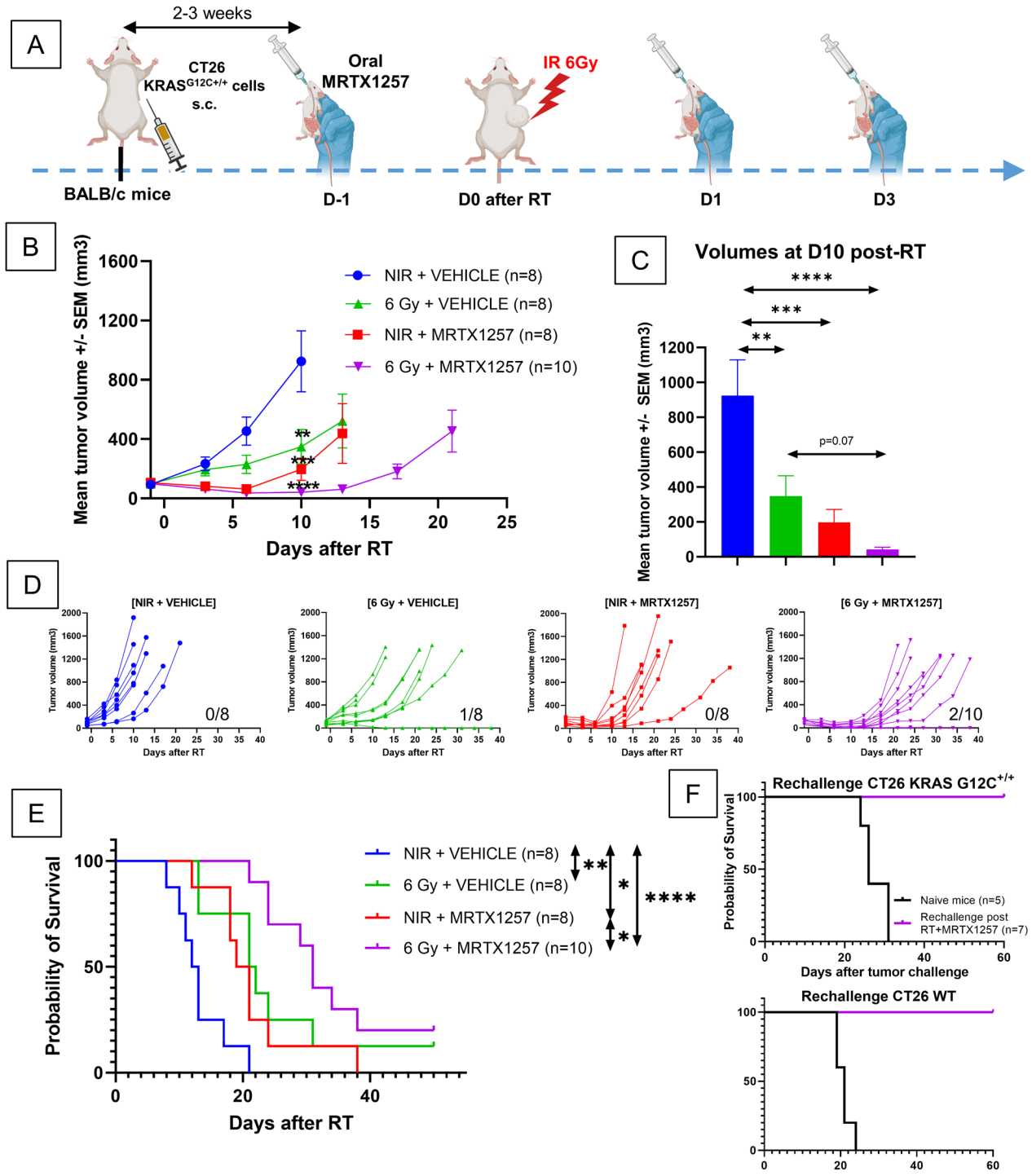

Fig. 3 (See legend on previous page.)

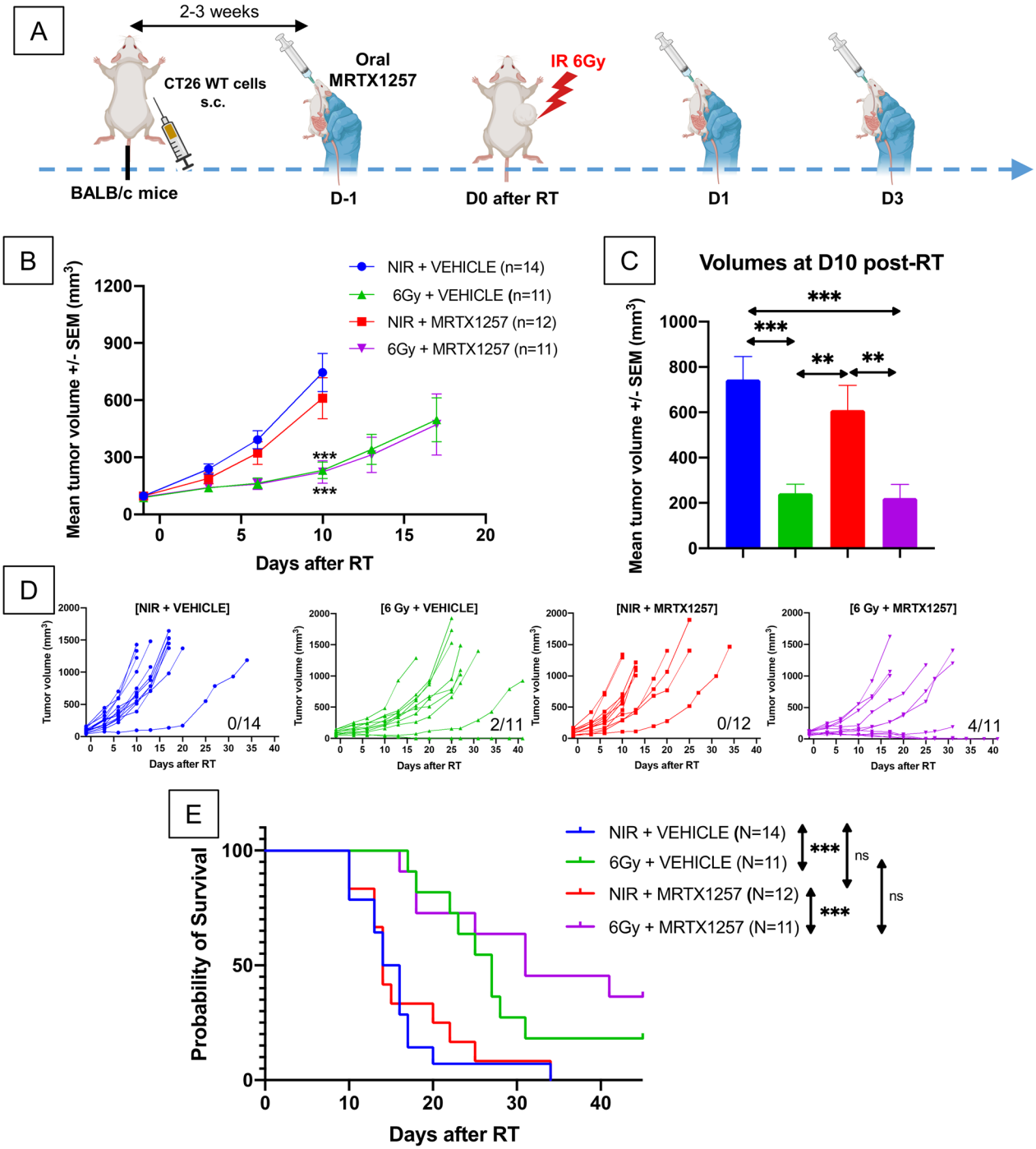

Fig. 4 MRTX1257 does not have any significant effect alone or in combination with RT in immunocompetent BALB/c mice bearing CT26 WT tumors. **A** BALB/c mice were subcutaneously inoculated with CT26 WT cells. Once the tumors reached an average volume of 90–100 mm^3, mice received via oral administration 50 mg/kg of MRTX1257 or vehicle. The day after, mice received a single fraction of 6 Gy on the tumor mass. MRTX1257 at the dose of 50 mg/kg or vehicle were then administered at D1 and D3 after RT. The experiment was repeated three times. **B** Tumor growth (mean ± SEM). ***: $p < 0.001$ (two-way ANOVA). **C** Mean tumor volumes in each group 10 days after RT are represented. **: $p < 0.01$; ***: $p < 0.001$ (one-way ANOVA). **D** Individual growth profiles of CT26 KRAS G12C.$^{+/+}$ tumors are represented for each condition. The number of mice achieving durable response with no tumor being assessed at the end of the experiment is indicated below each panel. **E** Survival Kaplan–Meier curves were compared between each group using the log-rank test. ***: $p < 0.001$

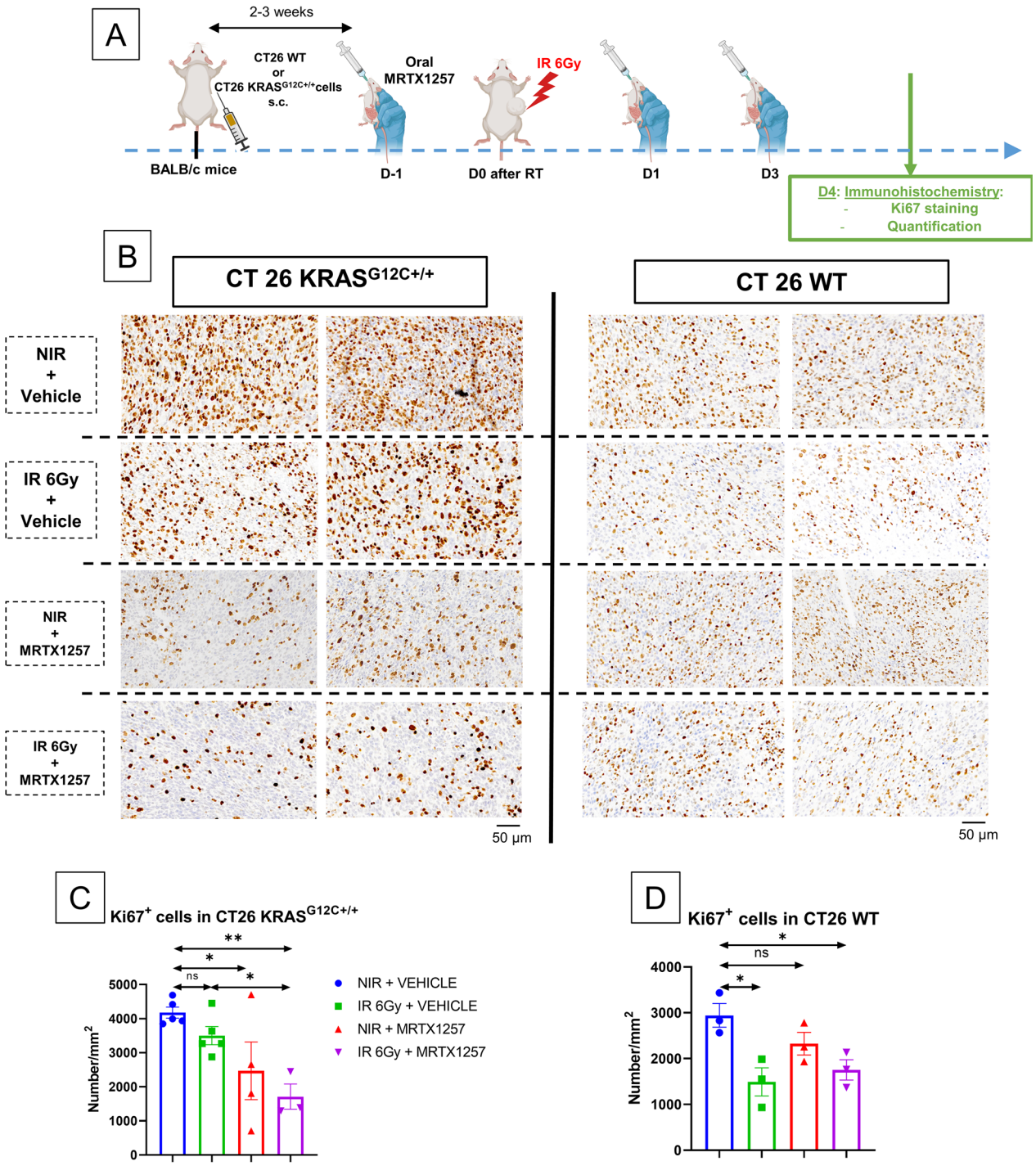

Fig. 5 MRTX1257 increases the anti-proliferative effect of RT in CT26 KRAS$^{G12C+/+}$ tumors but not in CT26 WT tumors. **A** BALB/c mice were subcutaneously inoculated with CT26 WT cells or CT26 KRAS$^{G12C+/+}$ cells. Once the tumors reached an average volume of 90–100 mm^3, mice received via oral administration 50 mg/kg of MRTX1257 or vehicle. The day after, mice received a single fraction of 6 Gy on the tumor mass. MRTX1257 at the dose of 50 mg/kg or vehicle were then administered at D1 and D3 after RT. At D4 after RT, mice were sacrificed, tumors were harvested and then fixated using paraformaldehyde (PFA) 4%. Immunohistochemistry for Ki67 and then the quantification of Ki67$^+$ cells were performed. **B** Photographs at magnification 13X of 4 µm-thick CT26 KRAS$^{G12C+/+}$ (left) or CT26 WT (right) tumor slices stained with anti-Ki67 antibody. Two representative photographs, each of them from a different tumor, are represented for each condition. **C** Quantification of Ki67$^+$ cells per mm^2 in CT26 KRAS G12C$^{+/+}$ tumor slices. Each point is representative of a single tumor. Mean ± standard-errors to mean (SEM). N = 3–5 tumors/group. *: $p < 0.05$; **: $p < 0.01$ (one-way ANOVA). **D** Quantification of Ki67$^+$ cells per mm.^{2} in CT26 WT tumor slices. Each point is representative of a single tumor. Mean ± standard-errors to mean (SEM). n = 3 tumors/group. *: $p < 0.05$ (one-way ANOVA)

irradiated tumors, with or without the adjunction of MRTX1257 ($p=0.02$ and $p=0.03$ respectively for irradiation alone versus the control and combination versus the control) (Fig. 5B, D). This is in line with the tumor growth experiments showing the absence of efficacy of MRTX1257 in CT26 WT tumors.

CD8$^+$ T cells are not sufficient to explain the efficacy of the association between RT and MRTX1257 in CT26 KRAS$^{G12C+/+}$ tumors

We then performed the staining and the quantification of CD8$^+$ cells within both CT26 KRAS G12C$^{+/+}$ and CT26 WT tumors (Fig. 6A).

Compared to the control group, the density of CD8$^+$ cells within CT26 KRAS$^{G12C+/+}$ tumors was increased in the group treated using MRTX1257 alone ($p=0.05$), but not in the combined treatment group ($p=0.12$) (Fig. 6B, C). This result shows that the radio-sensitizing effect induced by MRTX1257 in CT26 KRAS$^{G12C+/+}$ tumors cannot be solely attributed to an increase in the infiltration of CD8$^+$ T cells within the microenvironment of these tumors, which is consistent with the efficacy of the combined treatment also observed in T cell-deficient nude mice.

Regarding CT26 WT tumors, we did not observe any significant difference in the density of CD8$^+$ cells within tumors regardless of the treatment (Fig. 6B, D).

In CT26 KRAS$^{G12C+/+}$ tumors, MRTX1257 drives the down-regulation of PD-L1 and counteracts its upregulation following RT alone

The tumor growth experiments exposed earlier in this article showed that, after treatment, nude mice bearing CT26 KRAS$^{G12C+/+}$ relapsed faster than immunocompetent BALB/c mice. Thus, we did not observe any durable response in nude mice treated with the combination. Therefore, we hypothesized MRTX1257 could reshape the immune microenvironment of CT26 KRAS$^{G12C+/+}$ tumors into a pro-inflammatory and anti-tumor phenotype that contributes to the radio-sensitizing effect observed in these tumors. We hence used flow cytometry to explore the microenvironment of CT26 KRAS$^{G12C+/+}$ tumors harvested from BALB/c mice (Fig. 7A).

First, in tumor and stromal cells, identified as CD45 negative cells, we found the expression of PD-L1 was upregulated following RT alone ($p=0.005$) while it was dramatically downregulated in both MRTX1257 alone and combination groups ($p<0.0001$) (Fig. 7B). The same outcomes were observed in myeloid cells, with the upregulation of PD-L1 following RT alone ($p<0.0001$) and its downregulation in groups treated with MRTX1257 alone ($p=0.0003$) or the combined treatment ($p=0.02$) (Fig. 7D).

Then, the proportion of lymphoid cells was increased in groups treated with MRTX1257 alone and the combination compared to the control group. Among the lymphoid subtypes, the proportion of conventional CD4$^+$ T cells, defined as FoxP3 negative CD4$^+$ T cells, was increased in both the groups treated with MRTX1257 alone and with the combined treatment. (Fig. 7C).

However, regarding the proportion of CD8$^+$ T cells, we did not observe any difference between the irradiation alone group and the combination group, while this proportion increased in the MRTX1257 alone group (MRTX1257 alone versus control: $p=0.004$). This is in line with the quantification of CD8$^+$ cells in the IHC experiment above. In contrast, we observed a non-significant trend in the increase of NK cells following the combination treatment compared to the untreated control condition ($p=0.14$) (Fig. 7C).

The analysis of the myeloid compartment also revealed the microenvironment of CT26 KRAS$^{G12C+/+}$ tumors was reshaped depending on the treatment condition. Indeed, the combination treatment increased the proportion of conventional dendritic cells type 2 (cDC2) and their expression of MHC class II within the tumor immune microenvironment (Fig. 7E). Moreover, the combined treatment increased the proportion of inflammatory monocytes within the tumor microenvironment ($p=0.008$) while it decreased the proportion of macrophages ($p=0.02$). However, RT and the combined treatment were able to polarize macrophages into a

(See figure on next page.)

Fig. 6 An increase in tumor-infiltrating CD8$^+$ T cells is not sufficient to explain the radio-sensitizing effect of MRTX1257. **A** BALB/c mice were subcutaneously inoculated with CT26 WT cells or CT26 KRAS G12C$^{+/+}$ cells. Once the tumors reached an average volume of 90–100 mm^3, mice received via oral administration 50 mg/kg of MRTX1257 or vehicle. The day after, mice received a single fraction of 6 Gy on the tumor mass. MRTX1257 at the dose of 50 mg/kg or vehicle were then administered at D1 and D3 after RT. At D4 after RT, mice were sacrificed, tumors were harvested and then fixated using paraformaldehyde (PFA) 4%. Immunohistochemistry analyses for CD8 and then the quantification of CD8$^+$ cells were performed. **B** Photographs at magnification 1.5X of 4 µm-thick CT26 KRAS$^{G12C+/+}$ (left) or CT26 WT (right) tumor slices stained with anti-CD8 antibody. **C** Quantification of CD8$^+$ cells per mm^2 in CT26 KRAS$^{G12C+/+}$ tumor slices. Each point is representative of a single tumor. Mean ± standard-errors to mean (SEM). n = 3–5 tumors/group. *: $p<0.05$ (one-way ANOVA). **D** Quantification of CD8$^+$ cells per mm^2 in CT26 WT tumor slices. Each point is representative of a single tumor. Mean ± standard-errors to mean (SEM). n = 3 tumors/group. Ns: non-significant (one-way ANOVA)

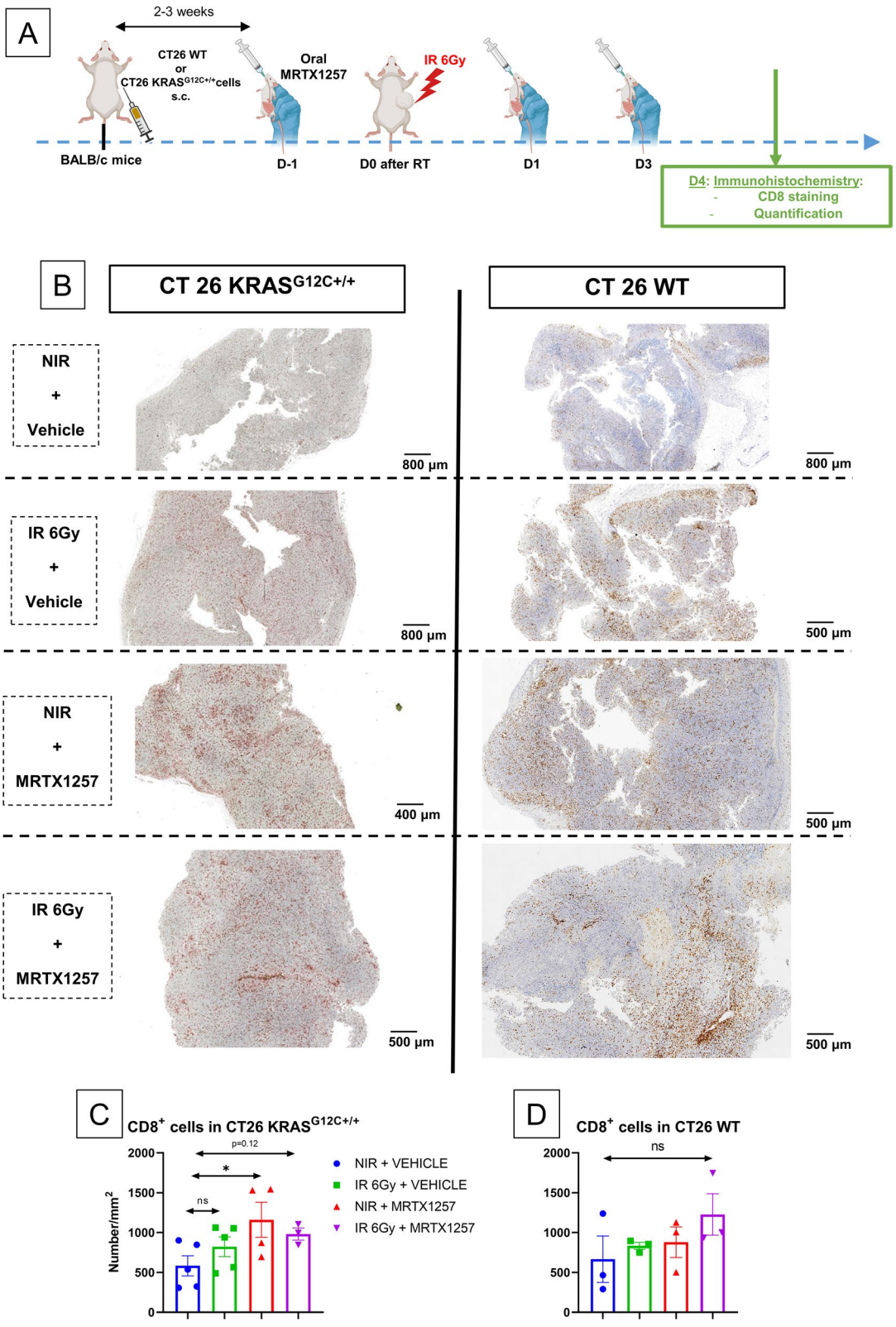

Fig. 6 (See legend on previous page.)

pro-inflammatory and anti-tumor phenotype characterized by the upregulation of the activation marker CD80 (Fig. 7F, G).

Taken together, these results highlight the different impacts of RT and MRTX1257 on the lymphoid and the myeloid compartments within CT26 KRAS$^{G12C+/+}$ tumors, with therefore the combinatorial approach taking benefit of the positive effects of both treatments. They also highlight an important decrease in the expression of PD-L1 within tumor cells and myeloid cells following MRTX1257 alone and RT + MRTX1257, which is likely to reshape the tumor immune microenvironment into a pro-inflammatory, anti-tumor phenotype, contributing to the efficacy of the combination.

Discussion

To our knowledge, this study is the first to explore the efficacy and immunological properties of the specific association of a KRAS^{G12C} inhibitor with RT in a preclinical animal model of KRAS^{G12C} mutated cancer. The recent work by Zheng et al. mainly focused on a triple association of RT, MEK inhibitor and KRAS inhibitor (AMG510), with therefore the difficulty to identify which features are attributable to each of these 3 treatments [30]. Moreover, we chose to perform flow cytometry directly in single-cell suspensions from CT26 *KRAS* mutated tumors, which is more reliable than a flow cytometry analysis of the spleen. In their study, RT in association with AMG510 was able to decrease the tumor growth of LLC tumors. This is in line with our results and confirms in vivo the radio-sensitizing effect of a potent KRAS inhibitor in preclinical setting, and therefore the interest to move towards the implementation of combinatorial strategies involving RT and KRAS inhibitors in KRAS-mutated cancers.

Furthermore, our results demonstrate the concomitant administration of MRTX1257 in multiple doses provides optimal efficacy and durable responses in CT26 KRAS$^{G12C+/+}$ tumors in combination with RT. As a preliminary experiment (data not shown), we administered MRTX1257 in a single dose of 75 mg/kg in BALB/c mice bearing CT26 KRAS$^{G12C+/+}$ tumors the day before RT. This resulted in the absence of efficacy of MRTX1257, and the only positive effects observed were due to RT, similarly to what we observed in CT26 WT tumors. Therefore, we next decided to administer MRTX1257 in 3 doses of 50 mg/kg at different time points both before and after RT. This resulted in an increase in the efficacy of RT due to MRTX1257 leading to the achievement of durable responses in immunocompetent mice and the generation of a potent anti-tumor immune memory against both CT26 KRAS$^{G12C+/+}$ and CT26 WT cells. Such cross-reactive immune memory may result from the high clonal proximity between these two cell lines. Of note, in our study, we did not achieve any complete remission using MRTX1257 alone.

Moreover, MRTX1257 did not provide any effect in CT26 WT cell lines nor tumors, demonstrating the absence of off-target effect and therefore the safety of MRTX1257, which is a crucial issue in the particular setting of a combination with RT. This is in line with the absence of toxicity observed in mice treated with 3 administrations of 50 mg/kg of MRTX1257 alone or with RT.

Regarding the radio-sensitizing effect of MRTX1257 in CT26 KRAS$^{G12C+/+}$ tumors, sensitizing *KRAS* mutant cells to radiation using KRAS inhibitors is a well-known strategy and various agents have been used in such a goal, of which prenyltransferase inhibitors [18], farnesyltransferase inhibitors [16], or antisense vectors [20]. However, these studies did not explore the immunological aspects of the association of RT and KRAS inhibitors in KRAS mutant tumors. In our study, the achievement of cures in 20% of the immunocompetent mice treated with the

(See figure on next page.)

Fig. 7 RT and MRTX1257 reshape the tumor immune microenvironment in CT26 KRAS$^{G12C+/+}$ tumors. Flow cytometry analyses were performed in single-suspensions derived from CT26 KRAS$^{G12C+/+}$ tumors. Results are represented in mean ± standard-error to mean (SEM). Each point represents a single tumor in both the untreated control group (NIR + VEHICLE) and the group treated with RT alone (IR 6 Gy + VEHICLE). Each point represents 2 different tumors pooled in a single sample in both the group treated with MRTX1257 alone (NIR + MRTX1257) and the group treated with combined RT and MRTX1257 (IR 6 Gy + MRTX1257). n = 3/group. Except for dendritic cells, the proportions of the different immune cell subtypes are expressed in percentage in viable cells whereas the expression of PD-L1, major histocompatibility complex II (MHC II), and CD80 are expressed in the difference in mean fluorescence intensity compared to an unstained control within each condition (Delta MFI). NS: non-significant; *: $p < 0.05$; **: $p < 0.01$; ***: $p < 0.001$; ****: $p < 0.0001$ (one-way ANOVA) **A** BALB/c mice were subcutaneously inoculated with CT26 KRAS$^{G12C+/+}$ cells. Once the tumors reached an average volume of 90–100 mm^3, mice received via oral administration 50 mg/kg of MRTX1257 or vehicle. The day after, mice received a single fraction of 6 Gy on the tumor mass. MRTX1257 at the dose of 50 mg/kg or vehicle were then administered at D1 and D3 after RT. At D4 after RT, mice were sacrificed, tumors were harvested and were used to perform flow cytometry. **B** Expression of PD-L1 in tumor and stromal CD45$^-$ cells. Mean ± SEM (left panel) and histogram overlay (right panel). **C** Proportion of lymphoid cells, conventional CD4 + T cells, CD8 + T cells and Tregs. **D** Proportion of myeloid cells and expression of PD-L1 within myeloid cells. **E** Proportion of dendritic cells type 2 (cDC2) in percentage of myeloid cells and expression of MHC II within cDC2. **F** Proportion of inflammatory monocytes and expression of MHC II within inflammatory monocytes. **G** Proportion of macrophages and expression of CD80 within macrophages

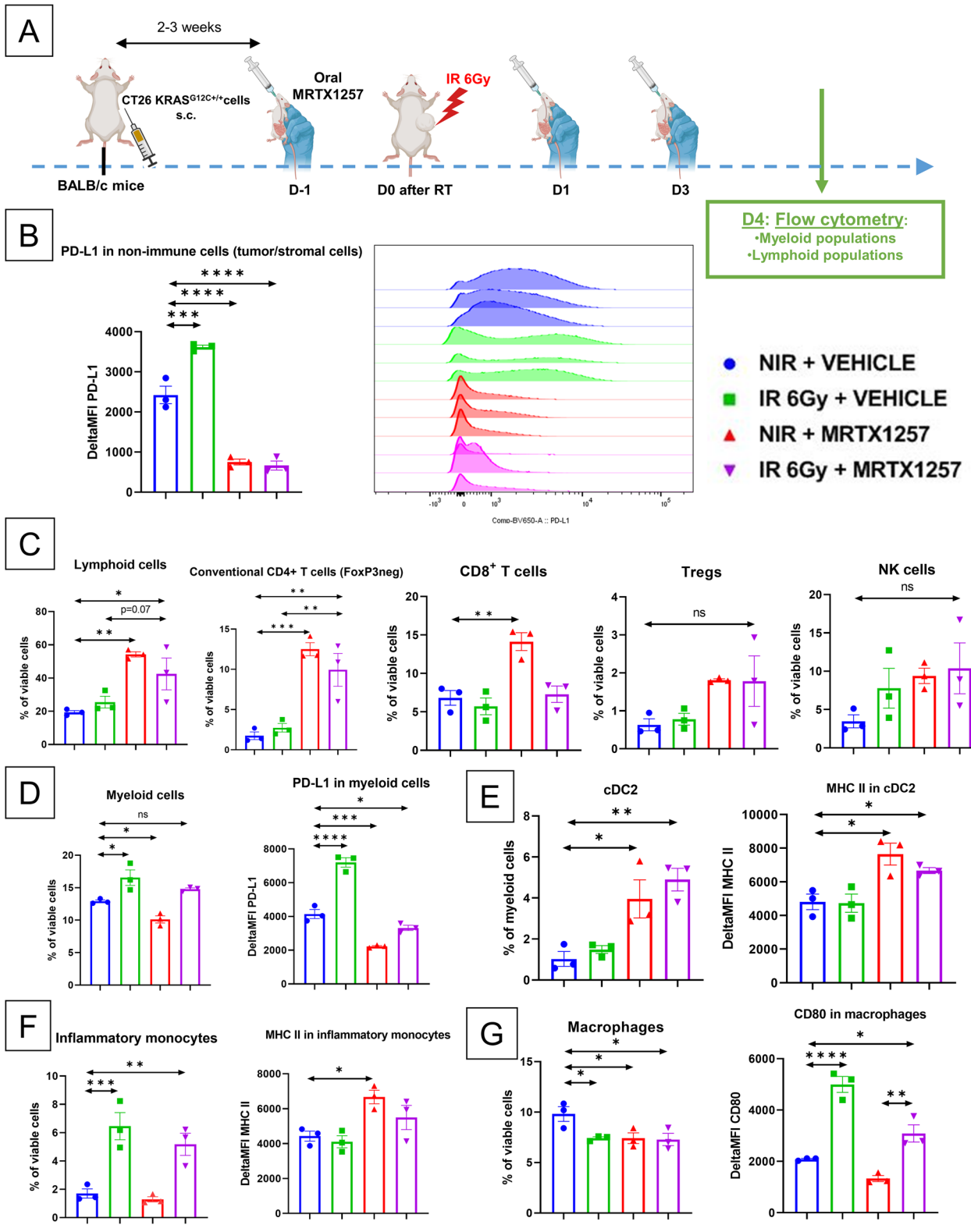

Fig. 7 (See legend on previous page.)

combination, in contrast with the fast relapses observed in nude mice, suggest the involvement of the immune compartment in the efficacy of the combined treatment. However, MRTX1257, alone or in combination with RT, significantly delayed tumor growth also in nude mice. Therefore, T cells, although crucial in the anti-tumor immune response, cannot be considered as the key pillar of the immunological outcomes observed following the combination. This deduction is in line with our results of IHC and flow cytometry not showing any significant increase in the infiltration of $CD8^+$ T cells following the combined treatment.

In addition to $CD8^+$ T cells, the proportion of NK cells within CT26 $KRAS^{G12C+/+}$ tumors only showed a slight and non-significant increase following the combination of RT and MRTX1257. Overall, these results are in favor of the participation of non-lymphoid cell subtypes in the efficacy of the combined treatment. In line with such a hypothesis, our flow cytometry experiments in CT26 $KRAS^{G12C+/+}$ tumors showed meaningful changes within the non-lymphoid compartment, including the downregulation of PD-L1 in myeloid cells as in tumor and stromal cells. The other meaningful changes observed in myeloid cells following the combination were an increase in the proportion of inflammatory monocytes and conventional dendritic cells type 2, as well as the upregulation of the activation marker CD80 within macrophages which is in favor of a more pro-inflammatory phenotype of these cells following RT alone or RT with MRTX1257.

The down-regulation of PD-L1 is a major positive effect of MRTX1257, and may be crucial for the efficacy of the combination as it counterbalances the upregulation of PD-L1 following RT, demonstrated in our study as in many other models [31, 32]. Moreover, the specific downregulation of PD-L1 in myeloid cells in the groups treated using MRTX1257 may be of major importance. Indeed, Strauss et al. demonstrated the specific ablation of PD-1 in myeloid cells more effectively decreased tumor growth compared to T cell-specific PD-1 ablation, notably by preventing the accumulation of myeloid-derived suppressor cells (MDSC) [33]. Therefore, this downregulation may contribute to the efficacy of RT + MRTX1257 in nude mice, but is not sufficient to induce long-term responses among them.

Overall, our immunological outcomes are in phase with most of those presented in the work by Briere et al. on MRTX849 used alone in preclinical models of $KRAS^{G12C}$ mutated cancers, including an increase in the proportion of $CD4^+$ T cells, $CD4^+$ helper T cells and $CD8^+$ T cells [26]. Moreover, our results are also congruent with the outcomes highlighted by Canon et al. with AMG510, including an increased infiltration of T cells and dendritic cells [34]. However, we are not able to compare the immunological outcomes for the association of RT with MRTX1257, since none of these studies associated KRAS inhibition with RT. It is notable that, in our immune profiling of CT26 $KRAS^{G12C+/+}$ tumors, the lymphoid compartment appeared to be enhanced in the conditions treated with MRTX1257 whereas the myeloid compartment appeared to be enhanced following RT. A key feature of the combination of RT and MRTX1257 may be to leverage the enhancement of both of these immune cell compartments, a condition achievable only in immunocompetent mice. Therefore, one of the challenges for the future of combinations of RT with KRAS inhibitors will consist in identifying the individual impact of each immune subtype apart from the others and therefore benchmark the best strategies of combinations treatments in solid tumors harboring $KRAS^{G12C}$ mutation.

Finally, recent data support a heterogeneity in the innate cancer cell radio-sensitivity itself, independent of cell cycle and microenvironment [35]. Taken together with a varying degree of dependence of cancer cells on the presence of $KRAS^{G12C}$ mutations for growth and survival, as well as the heterogeneity of intratumoral *KRAS* mutation expression, our data highlight the importance of combination strategies in overcoming treatment resistance. This hypothesis is confirmed by the potent immune memory generated in mice bearing CT26 $KRAS^{G12C+/+}$ tumors which have been cured following RT combined with MRTX1257. Indeed, this immune memory rejected both CT26 $KRAS^{G12C+/+}$ and CT26 WT tumors subsequently implanted. In this complex setting, where monotherapies draw the limits of durable response achievement and most oncogene driven cancers relapse, while immune checkpoints benefit only a small patient group, defining new rational combinations is paramount.

Conclusion

In this work, we first demonstrated the ability of MRTX1257, a potent covalent $KRAS^{G12C}$ inhibitor analogous to MRTX849, to enhance the effect of radiotherapy both in vitro and in vivo. This effect depended on *RAS* mutational status, dose and timing of administration and was associated with a good safety profile. Moreover, the use of RT and MRTX1257 led to a significant cure rate in BALB/c mice bearing CT26 $KRAS^{G12C+/+}$ tumors, but not in nude mice, highlighting the role of the tumor immune microenvironment in the radio-sensitizing effect of MRTX1257. This work constitutes a first step towards the implementation of new combinatorial approaches involving RT and MRTX1257 in KRAS G12C mutated cancers, with the aim of providing new therapeutic strategies with a prolonged clinical benefit. The optimal

treatment sequencing and selected patient populations warrant further characterization both in the preclinical and clinical settings.

Abbreviations

AKT	Serine/threonine-protein kinase
ANOVA	Analysis of variance
cDC2	Conventional dendritic cell type 2
CT26	Colon tumor 26 cell line
EGFR	Epithelial growth factor receptor
FoxP3	Forkhead box P3
GDP	Guanosine diphosphate
GTP	Guanosine triphosphate
LL2	Lewis Lung carcinoma cell line
MAPK	Microtubule associated protein kinase
MHC II	Major histocompatibility complex II
NSCLC	Non-small cell lung cancer
ORR	Objective response rate
OS	Overall survival
PD-L1	Programmed cell-death ligand 1
PFA	Paraformaldehyde
PFS	Progression-free survival
PI3K	Phosphatidylinositol 3-kinase
RAS	Rat sarcoma viral oncogene homolog
RT	Radiotherapy
SEM	Standard error to the mean
Tregs	T regulator lymphocytes
WT	Wild-type

Supplementary Information

The online version contains supplementary material available at https://doi.org/10.1186/s12967-023-04619-0.

Additional file 1: Table S1. List of the antibodies used and their respective dilutions in flow cytometry experiments. **Figure S1.** (complementary to Fig. 1): MRTX1257 at the concentration of 5 nM or 10 nM for 24 h does not sensitize CT26 KRAS$^{G12C+/+}$ or LL2 NRAS$^{-/-}$ tumor cells to radiation. Clonogenic survival assays were performed in CT26 KRAS$^{G12C+/+}$ or LL2 NRAS$^{-/-}$ tumor cells exposed to various concentrations of MRTX1257 for 24 h. Normalized survival fractions are represented in mean ± standard-error to mean (SEM), with n = 3 to 6 replicates per condition. Survival curves are extrapolations according to the linear quadratic model. Survival curves for **A** CT26 KRAS$^{G12C+/+}$ cell line and **B** LL2 NRAS$^{-/-}$ cell line. **Figure S2.** A single-fraction irradiation of 6 Gy does not increase the efficacy of MRTX1257 in a distant unirradiated tumor. The combination of RT delivered to a single-tumor and oral administration of MRTX1257 was experimented in BALB/c mice bearing bilateral s.c. CT26 KRAS$^{G12C+/+}$ tumors according to the supplementary material and methods. **A** Schematic view of the experimental setting. A single fraction of 6 Gy was delivered to the right (primary) tumor (primary) whereas the left (secondary) tumor remained unirradiated. **B** Primary tumor volumes in each condition at the different timepoints (left), and specifically at D6 and D13 after RT (right). All the volumes are represented in mean ± standard-error to mean (SEM) (mm^3). *: $p < 0.05$; **: $p < 0.01$; ****: $p < 0.0001$ (one-way ANOVA). **C** Secondary tumor volumes in each condition at the different timepoints (left), and specifically at D6 and D13 after RT (right). All the volumes are represented in mean ± standard-error to mean (SEM) (mm^3). *: $p < 0.05$; **: $p < 0.01$; ****: $p < 0.0001$ (one-way ANOVA). **D** Survival Kaplan–Meier curves were compared between each group using the log-rank test. The sacrifice of mice was determined by the conditions described in the supplementary material and methods. ns: non-significant; **: $p < 0.01$.

Acknowledgements

The authors want to thank Mirati Therapeutics for their support. Thanks are also expressed to Patrick Gonin and Karine Ser-Le Roux from the Preclinic Evaluation Platform (PFEP, Gustave Roussy), and Philippe Rameau, Yann Lecluse and Cyril Catelain from the Imaging and Cytometry Platform (PFIC, Gustave Roussy) for their technical support. Finally, the authors want to thank Olivia Bawa and Hélène Rocheteau (PETRA, AMMICa, INSERM US23/UAR3655, Gustave Roussy) for immunohistochemistry analysis.

Author contributions

PAL and MM performed the experiments and wrote the manuscript. CQ and WL performed the experiments. NS provided technical support and reviewed the manuscript. LM, DM, CC and AL reviewed the manuscript. MM provided scientific support and reviewed the manuscript. ED supervise the study and reviewed the manuscript.

Funding

PAL received a grant from Fondation Philantropia/Lombard Odier outside the submitted work. E.D reports grants and personal fees from Roche Genentech, grants from Servier, grants from AstraZeneca, grants and personal fees from Merck-Serono, grants from BMS, and grants from MSD, all of them outside the submitted work.

Availability of data and materials

The datasets supporting the conclusions of this article are included within this article and its additional file. For any further data requests, please contact the corresponding author.

Declarations

Ethics approval and consent to participate

All animal studies were conducted in compliance with all applicable regulations and guidelines of the Ethical approval Committee CCEA 26 at Gustave Roussy.

Consent for publication

Not applicable.

Competing interests

The authors declare that they have no competing interests.

Author details

[1]Department of Radiation Oncology, Gustave Roussy Cancer Campus, 114 rue Edouard Vaillant, 94805 Villejuif, France. [2]INSERM U1030, Molecular Radiation Therapy and Therapeutic Innovation, Gustave Roussy Cancer Campus, University of Paris-Saclay, 114 rue Edouard Vaillant, 94805 Villejuif, France. [3]SIRIC SOCRATE, Gustave Roussy, Villejuif, France. [4]Drug Development Department (DITEP), Gustave Roussy Cancer Campus, Villejuif, France. [5]Experimental and Translational Pathology Platform (PETRA), AMMICa, INSERM US23/UAR3655, Gustave Roussy Cancer Campus, Villejuif, France.

Received: 11 March 2023 Accepted: 11 October 2023
Published online: 31 October 2023

References

1. Barton MB, Jacob S, Shafiq J, Wong K, Thompson SR, Hanna TP, et al. Estimating the demand for radiotherapy from the evidence: a review of changes from 2003 to 2012. Radiother Oncol. 2014;112(1):140–4.
2. Hanna TP, Shafiq J, Delaney GP, Vinod SK, Thompson SR, Barton MB. The population benefit of evidence-based radiotherapy: 5-year local control and overall survival benefits. Radiother Oncol. 2018;126(2):191–7.
3. Prior IA, Hood FE, Hartley JL. The frequency of ras mutations in cancer. Can Res. 2020;80(14):2969–74.
4. Liu P, Wang Y, Li X. Targeting the untargetable KRAS in cancer therapy. Acta Pharmaceutica Sinica B. 2019;9(5):871–9.
5. Buday L, Downward J. Many faces of ras activation. Biochim Biophys Acta. 2008;1786(2):178–87.
6. Jänne PA, Riely GJ, Gadgeel SM, Heist RS, Ou SHI, Pacheco JM, et al. Adagrasib in non–small-cell lung cancer harboring a *KRAS* ^{G12C} mutation. N Engl J Med. 2022;387(2):120–31.

7. Yaeger R, Weiss J, Pelster MS, Spira AI, Barve M, Ou SHI, et al. Adagrasib with or without cetuximab in colorectal cancer with mutated *KRAS* G12C. N Engl J Med. 2023;388(1):44–54.
8. FitzGerald TJ, Daugherty C, Kase K, Rothstein LA, McKenna M, Greenberger JS. Activated human N-ras oncogene enhances x-irradiation repair of mammalian cells in vitro less effectively at low dose rate: Implications for increased therapeutic ratio of low dose rate irradiation. Am J Clin Oncol. 1985;8(6):517–22.
9. Sklar MD. The *ras* oncogenes increase the intrinsic resistance of nih 3T3 cells to ionizing radiation. Science. 1988;239(4840):645–7.
10. Gillies McKenna W, Muschel RJ, Gupta AK, Hahn SM, Bernhard EJ. The RAS signal transduction pathway and its role in radiation sensitivity. Oncogene. 2003;22(37):5866–75.
11. Williams TM, Flecha AR, Keller P, Ram A, Karnak D, Galbán S, et al. Cotargeting MAPK and PI3K Signaling with concurrent radiotherapy as a strategy for the treatment of pancreatic cancer. Mol Cancer Ther. 2012;11(5):1193–202.
12. Nadal E, Chen G, Prensner JR, Shiratsuchi H, Sam C, Zhao L, et al. KRAS-G12C Mutation is associated with poor outcome in surgically resected lung adenocarcinoma. J Thorac Oncol. 2014;9(10):1513–22.
13. Fiala O, Buchler T, Mohelnikova-Duchonova B, Melichar B, Matejka VM, Holubec L, et al. G12V and G12A KRAS mutations are associated with poor outcome in patients with metastatic colorectal cancer treated with bevacizumab. Tumor Biol. 2016;37(5):6823–30.
14. Jones RP, Sutton PA, Evans JP, Clifford R, McAvoy A, Lewis J, et al. Specific mutations in KRAS codon 12 are associated with worse overall survival in patients with advanced and recurrent colorectal cancer. Br J Cancer. 2017;116(7):923–9.
15. Slebos RJC, Kibbelaar RE, Dalesio O, Kooistra A, Stam J, Meijer CJLM, et al. K- *ras* Oncogene activation as a prognostic marker in adenocarcinoma of the lung. N Engl J Med. 1990;323(9):561–5.
16. Bernhard EJ, Kao G, Cox AD, Sebti SM, Hamilton AD, Muschel RJ, et al. The farnesyltransferase inhibitor FTI-277 radiosensitizes H-ras-transformed rat embryo fibroblasts. Cancer Res. 1996;56(8):1727–30.
17. Miller AC, Kariko K, Myers CE, Clark EP, Samid D. Increased radioresistance of ejras-transformed human osteosarcoma cells and its modulation by lovastatin, an inhibitor of p21ras isoprenylation. Int J Cancer. 1993;53(2):302–7.
18. Bernhard EJ, McKenna WG, Hamilton AD, Sebti SM, Qian Y, Wu JM, et al. Inhibiting Ras prenylation increases the radiosensitivity of human tumor cell lines with activating mutations of ras oncogenes. Cancer Res. 1998;58(8):1754–61.
19. Russell JS, Lang FF, Huet T, Janicot M, Chada S, Wilson DR, et al. Radiosensitization of human tumor cell lines induced by the adenovirus-mediated expression of an anti-Ras single-chain antibody fragment. Cancer Res. 1999;59(20):5239–44.
20. Rait A, Pirollo K, Will DW, Peyman A, Rait V, Uhlmann E, et al. 3'-End conjugates of minimally phosphorothioate-protected oligonucleotides with 1-*O*-hexadecylglycerol: synthesis and anti- *ras* activity in radiation-resistant cells. Bioconjugate Chem. 2000;11(2):153–60.
21. Ostrem JM, Peters U, Sos ML, Wells JA, Shokat KM. K-Ras(G12C) inhibitors allosterically control GTP affinity and effector interactions. Nature. 2013;503(7477):548–51.
22. Lito P, Solomon M, Li LS, Hansen R, Rosen N. Allele-specific inhibitors inactivate mutant KRAS G12C by a trapping mechanism. Science. 2016;351(6273):604–8.
23. Daly ME, Singh N, Ismaila N, Antonoff MB, Arenberg DA, Bradley J, et al. Management of stage III non-small-cell lung cancer: ASCO guideline. J Clin Oncol. 2022;40(12):1356–84.
24. Kortlever RM, Sodir NM, Wilson CH, Burkhart DL, Pellegrinet L, Brown Swigart L, et al. Myc cooperates with ras by programming inflammation and immune suppression. Cell. 2017;171(6):1301-1315.e14.
25. Liao W, Overman MJ, Boutin AT, Shang X, Zhao D, Dey P, et al. KRAS-IRF2 axis drives immune suppression and immune therapy resistance in colorectal cancer. Cancer Cell. 2019;35(4):559-572.e7.
26. Briere DM, Li S, Calinisan A, Sudhakar N, Aranda R, Hargis L, et al. The KRASG12C Inhibitor MRTX849 reconditions the tumor immune microenvironment and sensitizes tumors to checkpoint inhibitor therapy. Mol Cancer Ther. 2021;20(6):975–85.
27. Bankhead P, Loughrey MB, Fernández JA, Dombrowski Y, McArt DG, Dunne PD, et al. QuPath: open source software for digital pathology image analysis. Sci Rep. 2017;7(1):16878.
28. Sakamoto K, Lin B, Nunomura K, Izawa T, Nakagawa S. The K-Ras(G12D)-inhibitory peptide KS-58 suppresses growth of murine CT26 colorectal cancer cell-derived tumors. Sci Rep. 2022;12(1):8121.
29. Castle JC, Loewer M, Boegel S, de Graaf J, Bender C, Tadmor AD, et al. Immunomic, genomic and transcriptomic characterization of CT26 colorectal carcinoma. BMC Genomics. 2014;15(1):190.
30. Zheng Y, Liu Y, Zhang F, Su C, Chen X, Zhang M, et al. Radiation combined with KRAS-MEK inhibitors enhances anticancer immunity in KRAS-mutated tumor models. Transl Res. 2023;252:79–90.
31. Sato H, Niimi A, Yasuhara T, Permata TBM, Hagiwara Y, Isono M, et al. DNA double-strand break repair pathway regulates PD-L1 expression in cancer cells. Nat Commun. 2017;8(1):1751.
32. Dovedi SJ, Adlard AL, Lipowska-Bhalla G, McKenna C, Jones S, Cheadle EJ, et al. Acquired resistance to fractionated radiotherapy can be overcome by concurrent PD-L1 blockade. Can Res. 2014;74(19):5458–68.
33. Strauss L, Mahmoud MAA, Weaver JD, Tijaro-Ovalle NM, Christofides A, Wang Q, et al. Targeted deletion of PD-1 in myeloid cells induces antitumor immunity. Sci Immunol. 2020;5(43):eaay1863.
34. Canon J, Rex K, Saiki AY, Mohr C, Cooke K, Bagal D, et al. The clinical KRAS(G12C) inhibitor AMG 510 drives anti-tumour immunity. Nature. 2019;575(7781):217–23.
35. Allam A, Taghian A, Gioioso D, Duffy M, Suit HD. Intratumoral heterogeneity of malignant gliomas measured in vitro. Int J Radiat Oncol Biol Phys. 1993;27(2):303–8.

Publisher's Note

11.2 SUPPLEMENTARY MATERIAL AND METHODS

Dose-response curves on WT cells:

Two hundred thousand CTT26 WT or LL2 WT cells were seeded in 6-well plates with 2 mL of their respective culture media containing MRTX1257 at various concentrations ranging from 0 nM to 50 µM. At 48 hours of culturing, the medium containing MRTX1257 was changed and washed for a drug-free one. The day after, i.e. at 72h of culturing, cells were harvested separately in each well by using tryspin-EDTA 0.05% (Gicbo) and counted using an automated cell counter Cellometer K2 (Nexcellom Bioscience, MA) after trypan blue staining. The viable cells were thus counted and plotted in dose-response curves.

Two-tumors experiment

Immunocompetent female BALB/c mice were subcutaneously inoculated with 1.2 10^6 CT26 $KRAS^{G12C+/+}$ in their right flank and 8.10^5 CT26 $KRAS^{G12C+/+}$cells in their left flank, in 50µL of pH 7.2 phosphate-buffer saline (PBS) solution (Gibco).
Once the tumors reached an average of 100-110 mm^3 for right tumors (primary tumors) and 60-70 mm^3 for the corresponding left tumors (secondary tumors), estimated using the formula exposed in the methods section, mice were randomized into the different treatment groups.
On the day of randomization (= D-1 before RT), as well as on D1 and D3 after RT, mice received an oral administration of MRTX1257 at the dose of 50 mg/kg reconstituted in 5 ml/kg of Captisol vehicle or the same volume of Captisol vehicle alone, according to the treatment group. At D0, mice randomized into RT only and combination groups received a single fraction of 6 Gy to the primary tumor volume using a Varian Tube NDI 226 (X-ray machine; 200 kV; tube current 15mA; beam filter: 0.2 mmCu, dose-rate 1.15 Gy/minute). Radiation was only delivered to the primary tumor by using a custom shielding and an appropriate device to immobilize the mouse.
Tumor volumes were measured 3 times a week using a digital caliper and the formula described in the methods section. When any of the tumors reached 1200 mm^3 or when any of critical points including weight loss > 20%, tumor necrosis or suffering appeared, mice were sacrificed.

Supplementary Table: List of the antibodies used and their respective dilutions in flow cytometry experiments.

Supplementary Figure 1 (complementary to Figure 1): MRTX1257 at the concentration of 5 nM or 10 nM for 24 hours does not sensitize CT26 KRAS$^{G12C+/+}$ or LL2 NRAS$^{-/-}$ tumor cells to radiation.
Clonogenic survival assays were performed in CT26 KRAS$^{G12C+/+}$ or LL2 NRAS$^{-/-}$ tumor cells exposed to various concentrations of MRTX1257 for 24 hours. Normalized survival fractions are represented in mean +/- standard-error to mean (SEM), with n=3 to 6 replicates per condition. Survival curves are extrapolations according to the linear quadratic model. Survival curves for (**A**) CT26 KRAS$^{G12C+/+}$ cell line and (**B**) LL2 NRAS$^{-/-}$ cell line.

Supplementary Figure 2: A single-fraction irradiation of 6 Gy does not increase the efficacy of MRTX1257 in a distant unirradiated tumor.
The combination of RT delivered to a single-tumor and oral administration of MRTX1257 was experimented in BALB/c mice bearing bilateral s.c. CT26 KRAS$^{G12C+/+}$ tumors according to the supplementary material and methods. (**A**) Schematic view of the experimental setting. A single fraction of 6 Gy was delivered to the right (primary) tumor (primary) whereas the left (secondary) tumor remained unirradiated. (**B**) Primary tumor volumes in each condition at the different timepoints (left), and specifically at D6 and D13 after RT (right). All the volumes are represented in mean +/- standard-error to mean (SEM) (mm^3). *: $p<0.05$; **: $p<0.01$; ****: $p<0.0001$ (one-way ANOVA). (**C**) Secondary tumor volumes in each condition at the different timepoints (left), and specifically at D6 and D13 after RT (right). All the volumes are represented in mean +/- standard-error to mean (SEM) (mm^3). *: $p<0.05$; **: $p<0.01$; ****: $p<0.0001$ (one-way ANOVA). (**D**) Survival Kaplan-Meier curves were compared between each group using the log-rank test. The sacrifice of mice was determined by the conditions described in the supplementary material and methods. ns: non-significant; **: $p<0.01$.

SUPPLEMENTARY TABLE

Antibody (fluorochrome)	Clone	Manufacturer	Dilution
CD 16/32 Fc Block	93	BioLegend	1:50
CD45 (APC Vio770)	REA 737	Miltenyi Biotec	1:50
CD11b (BUV395)	M1/70	BD Biosciences	1:100
CD11b (BV605)	M1/70	BioLegend	1:100
PD1 (PerCp Vio700)	REA 802	Miltenyi Biotec	1:50
PD-L1 (BV650)	MIH5	BD Biosciences	1:100
CD4 (BV510)	RM 4-5	BioLegend	1:400
CD8 (BUV737)	53-6.7	BD Horizon	1:400
NKp46 (BV421)	29A 1.4	BioLegend	1:100
CD64 (BV605)	X 54-5/7.1	BioLegend	1:50
Ly6G (PerCp Vio700)	REA 526	Miltenyi Biotec	1:50
CD11c (PE Vio770)	REA 754	Miltenyi Biotec	1:50
H-2Ld/H-2Db (BV650)	28-14-8	BD Optibuild	1:100
Ly6c (AlexaFluor700)	HK1.4	BioLegend	1:50
MHC II (VioGreen)	REA 813	Miltenyi Biotec	1:50
FoxP3 (PE)	REA 788	Miltenyi Biotec	1:50
CD80 (PE Vio615)	REA 983	Miltenyi	1:50

SUPPLEMENTARY FIGURE 1

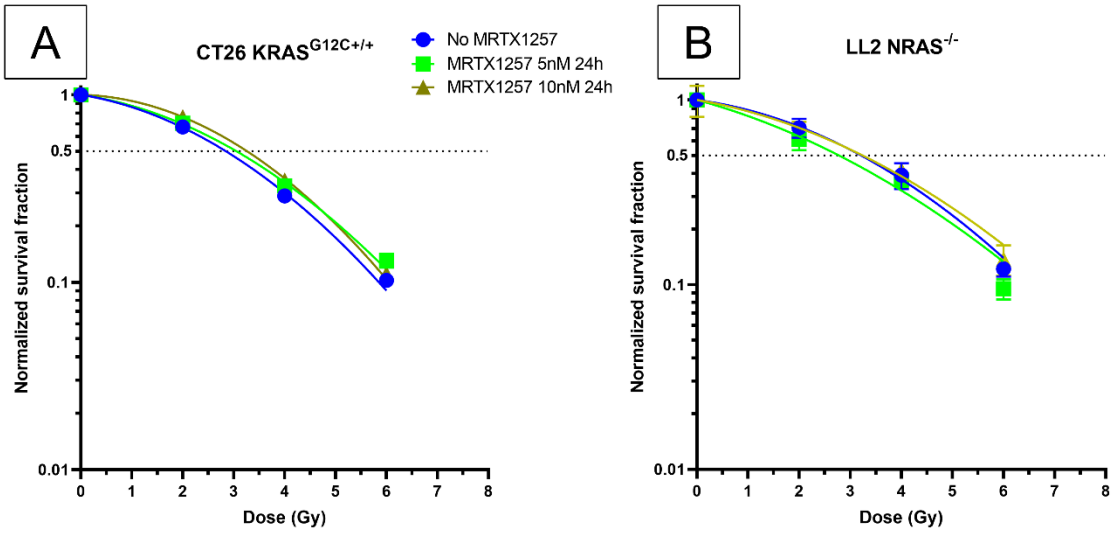

SUPPLEMENTARY FIGURE 2

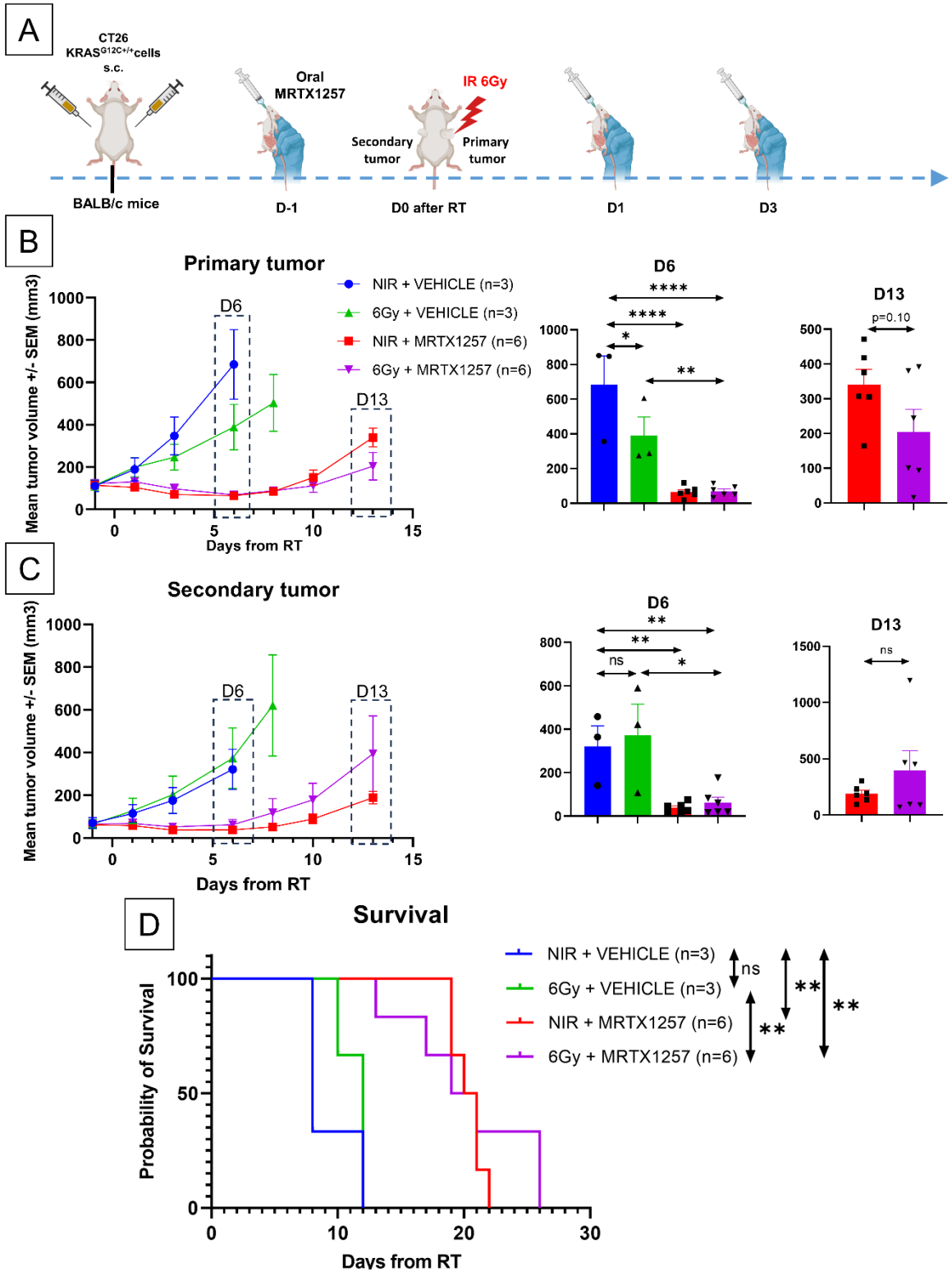

Durable responses. To determine if the combination treatment using irradiation and MRTX1257 led to significant anti-tumor immune memory in mice, we rechallenged the mice showing complete response with s.c. injection of 10^6 CT26 $KRAS^{G12C+/+}$ or 5.10^5 CT26 WT cells in contralateral flank. None of the mice rechallenged this way showed new tumors, in contrast with 100% of naive mice receiving similar s.c. injections. This observation illustrates the potent anti-tumor immune memory provided by the combination treatment against both CT26 $KRAS^{G12C+/+}$ and CT26 WT tumor cells (Fig. 3E).

Of note, no significant toxicities were observed in mice when treating with MRTX1257 and RT in these conditions.

As a reminder, we did not observe any durable response in nude mice and, as illustrated in their individual growth profiles (Fig. 2E to 2H), all nude mice experienced fast and homogeneous relapses. This suggests the presence of a functional lymphoid compartment has an impact on the efficacy of the combination of RT and MRTX1257.

12 DISCUSSION AND PERSPECTIVES

Therapeutic resistance to RT and chemo-immunotherapy remains a considerable challenge in $KRAS^{G12C}$ mutant cancers. Therefore understanding underlying mechanisms is crucial.

Recent successful development of covalent $KRAS^{G12C}$ inhibitors with encouraging pre-clinical and clinical efficacy has opened a new therapeutic combinations era.

Monotherapy with $KRAS^{G12C}$ inhibitors Adagrasib or Sotorasib has demonstrated tolerability and antitumor activity in heavily pretreated patients.

Adagrasib (MRTX 849) is being tested in an ongoing phase1/2 trial (Krystal-1°across multiple tumor types harboring $KRAS^{G12C}$ mutations including CRC (NCT03785249), it has currently showed an objective 45% response rate (ORR) among patients with NSCLC and 17% among those with colorectal cancer.

Evaluation of Adagrasib in combination with Cetuximab in $KRAS^{G12C}$ mutant metastatic CRC is ongoing in a phase 1/2 trial with a median PFS of 6.9 months (95% CI, 5.4 to 8.1) vs. 5.6 months (95% CI, 4.1 to 8.3) in the Adagrasib monotherapy group as of June 2022 (Yaeger, et al).

Sotorasib in $KRAS^{G12C}$ mutant advanced or metastatic NSCLC in the CodeBreak 100 trial (NCT03600883).

A first phase 3 randomized controlled trial CodeBreak 200 comparing the efficacy of Sotorasib vs. standard of care Docetaxel chemotherapy in previously treated advanced $KRAS^{G12C}$ -mutant NSCLC has shown an increase in the PFS for the Sotorasib arm 5.6 months vs 4.5 months. (p=0017).

However, despite encouraging results, treatment resistance is emerging either due to short-term signaling adaptation or long-term selection of minor variants One can reasoanably anticipate that acquired resistance to the $KRAS^{G12C}$ inhibitors will represent an inevitable challenge going forward.

Awad et al. looked at the acquired mechanisms of resistance in 38 patients treated with Adagrasib monotherapy. Putative mechanism of resistance to Adagrasib were identified in 45% of patients with nearly one in five had multiple concomitant alterations. In their study, acquired bypass mechanisms of

resistance were complex,including *MET* amplification; activating mutations in *NRAS*, *BRAF*, *MAP2K1*, and *RET*; oncogenic fusions involving *ALK*, *RET*, *BRAF*, *RAF1*, and *FGFR3*; and loss-of-function mutations in *NF1* and *PTEN*.

Preclinical studies have suggested several mechanisms of upfront resistance including reactivation of ERK- dependent signaling to bypass $KRAS^{G12C}$ blockade (Hallin, et al). Subsequently, adaptive RAS pathway feedback reactivation has emerged as a key mechanism of primary resistance to $KRAS^{G12C}$ inhibition. (Solanski, et al.) (Ryan, et al.)

Upstream feedback reactivation of the RAS/MAPK pathway signaling through wild-type NRAS and HRAS, as opposed to a shift in $KRAS^{G12C}$ to its active GTP-bound state can drive adaptive resistance to $KRAS^{G12C}$ inhibitors in a $KRAS^{G12C}$ independent manner as shown by Ryan et al. Data published by Tanaka et al. also suggest polyclonal RAS-MAPK reactivation as a central resistance mechanism to Adagrasib.

To further complexify the picture, multiple receptor tyrosine kinases (RTKs) can drive feedback reactivation potentially requiring targeting of convergent signaling nodes.

As discussed earlier, diverse genomic and histologic mechanisms impart resistance to covalent $KRAS^{G12C}$ inhibitors, and new therapeutic strategies are required to delay and overcome this drug resistance in patients with cancer. Therefore, combination strategies are needed and are very likely to yield additional therapeutic benefit.

A profound inhibition of the pathways downstream of KRAS is required for a durable suppression of cell proliferation and tumor regression which can be achieved through combined inhibition of MEK, mTOR and IGF1R.

However, attempts to combine MEK inhibition with Trametinib and mTOR inhibition with Everolimus in clinic have led to unacceptable adverse effects (Tolcher, et al).

In the preclinical setting, addition of mTOR and IGF1R inhibitor greatly increased the impact of ARS-1620 on $KRAS^{G12C}$ mutant cancer cell lines in vitro and in vivo.When ARS-1620 was combined with Linsitinib and Everolimus in the pre-clinical setting, no cell growth was observed for up to 17 days suggesting that such a combination might also delay or prevent the appearance of

resistance mechanisms that emerge when inhibiting PI3K/AKT or MEK/ERK pathways with single targeted agents (Molina-Arcas et al).

Due to a variety of mechanisms of resistance, shutting down growth signaling pathway reactivation by cross-talk and negative feedback is very likely to be superseded by the evolution of treatment resistance du to tumor heterogeneity complexifying the picture further.

The integration of different therapeutic approaches is likely to be needed.

In an attempt to address the need for novel therapeutic approaches and radioresistance of KRAS mutant cancer, our work is the first to our knowledge to explore radiosensitizing and immunomodulatory properties of the specific association of a covalent $KRAS^{G12C}$ inhibitor with RT in a preclinical animal model of $KRAS^{G12C}$ mutated cancer.

The recent work by Zheng et al. mainly focused on a triple association of RT, MEK inhibitor and KRAS inhibitor (AMG510), with therefore the difficulty to identify which features are attributable to each of these 3 treatments.

In vitro radio-sensitizing properties

The first objective of this thesis work consisted in exploring in vitro radiosensitizing properties of MRTX1257 and its combination with RT before moving to pre-clinical in vivo modeling.

Regarding CT26 WT cells, which are reported in the literature as harboring homozygous $KRAS^{G12D}$ mutation, MRTX1257 at 20nM or 50nM for 48 hours did not increase their radio-sensitivity at the tested RT doses, i.e. from 2 to 6 Gy To explore the absence of efficacy of MRTX1257 in this cell line, we performed a dose-escalation assay by using increasing concentrations of MRTX1257 *in vitro*. The results showed a half maximal inhibitory concentration (IC50) between 2 and 10 µM, far beyond the 20 to 50 nM used in CT26 $KRAS^{G12C+/+}$. Such a dose would be lethal in mice, therefore we decided not to explore it further in association with RT.

We then explored MRTX1257 in association with RT in two different LL2 cell lines. We started with the LL2 WT celle line where we carried out KRAS gene sequencing confirming this cell line harbors $KRAS^{G12C+/-}$ heterozygous mutation. MRTX1257 at 20 or 50 nM for 48 hours did not influence the radio-sensitivity of

this cell line which suggests that a heterozygous G12C mutation of *KRAS* is not sufficient to allow a proper efficacy of the combination treatment.

As in CT26 WT cell line, a dose-escalation assay performed in LL2 WT cell line found an IC50 between 100nM and 500nM which is inferior to the IC50 in CT26 WT cell line and may be explained by the presence of a single $KRAS^{G12C}$ mutation.

We subsequently tested LL2 $NRAS^{-/-}$ cells harboring both a heterozygous mutation of *KRAS* and a knock-out (KO) mutation of *NRAS*. Although we observed a trend in radio-sensitizing these cells using MRTX1257 at 20 nM for 48 hours, this effect was not statistically significant (p=0.07). These results suggests that, even when silencing *NRAS*, a single $KRAS^{G12C}$ mutation is not sufficient to provide a strong radio-sensitizing effect of MRTX1257 comparable to the one observed in $KRAS^{G12C+/+}$ cells.

Halin et al. evaluated cell viability across a panel of 17 $KRAS^{G12C}$ mutant cell lines and 3 non-$KRAS^{G12C}$ mutant cancer cell lines. The IC50 values ranged between 10 and 973 nM in the 2D format showing a differential degree of sensitivity to treatment within the $KRAS^{G12C}$ mutant lines. All three non-$KRAS^{G12C}$ cell lines demonstrated IC50 values great er than 1 µM which is in line with our values seen in the CT26 WT model (between 2 and 10 µM).

Taken together, our data show that MRTX1257 is able to radio-sensitize tumor cells *in vitro* depending on their *RAS* mutational profile. Moreover, the impact of $KRAS^{G12C}$ mutational status on this effect was predominant, since *NRAS* mutational status had a moderate, non-significant impact on it in addition to *KRAS* status.

Characterization of vivo efficacy

We used the CT26 $KRAS^{G12C}$ and CT26 WT colon cancer cell lines in a syngeneic immunocompetent BALB/c mouse model choosing a single 6 Gy non-ablative dose of radiation to determine the therapeutic efficacy of the combination RT+MRTX1257.

Our dosing regimen consisted of only 3 oral administrations starting 24h pre-RT, 24h and 48h post-irradiation in line with the radiosensitizing effect being explored. As a matter of fact, pharmacodynamic studies published by Halin, et al. show an extended pharmacodynamic effect of MRTX849 consistent with

irreversible $KRAS^{G12C}$ inhibition and prolonged half-life of the $KRAS^{G12C}$ protein (24-48h). After a single dose of 30mg/kg the modified fraction of $KRAS^{G12C}$ was 74% at 6 hours and remained very close to that level in the first 24h, gradually decreasing to 47% by 72 hours. Their studies also point out a dose-dependent increase in covalent modification of $KRAS^{G12C}$ by MRTX849 highlighting that the majority of targetable KRAS was covalently modified over a repeated administration schedule at dose levels at or exceeding 30mg/kg.

The choice of our dosing regimen consisting of three treatments starting 24h before RT, 24h and 48h post-RT reflecting consideration of the pharmacodynamic data and the aim to provide sufficient KRAS inhibition cover in the first days post RT, period after which main immunomodulatory effects are expected to start manifesting.

In vivo efficacy in the CT26 $KRAS^{G12C}$ immune competent model

Mice treated with MRTX1257 alone relapsed quickly after the end of treatment with no durable remissions achieved, while $KRAS^{G12C}$ inhibition combined with radiation therapy induced significant tumor growth retardation and durable tumor regressions in 20% of cases. As expected, this also translated into overall survival benefit ($p<0.05$).

Our results are in line with those of Briere et al. where MRTX849 used at double dose of 100mg/kg daily through study day 25 caused tumor growth retardation while its combination with a PD-1 antibody administered every 3 days for 3 doses (days 1, 4 and 7) caused tumor regression in mice bearing subcutaneous CT26 $KRAS^{G12C}$ tumors.

Survival was statistically significant in the combination-treated cohort compared with all others ($p<0.05$).

Effect of KRASG12C inhibition in the CT26 WT model

MRTX1257 did not provide any effect in CT26 WT cell lines nor tumors, demonstrating the absence of off-target effect and therefore the safety of MRTX1257, which is a crucial issue in the particular setting of a combination with RT. This is in line with the absence of toxicity observed in mice treated with 3 administrations of 50 mg/kg of MRTX1257 alone or with RT.

Effect of $KRAS^{G12C}$ inhibition in the LL2 mouse syngeneic lung cancer cell line harboring $KRAS^{G12C}$ and $NRAS^{Q61H}$ mutations

Although an antitumor efficacy was observed, no durable responses were achieved in line with Briere et al. results, where tumors treated with MRTX1257 at 50mg/kg for a total of 4 or 8 days decreased in volume over time of administration. Those results are corroborated by our in vitro data showing that MRTX1257 was able to radio-sensitize tumor cells depending on their *RAS* mutational profile. As such, the impact of *KRAS*^{G12C} mutational status on this effect was predominant, since *NRAS* mutational status had a moderate, non-significant impact on it in addition to *KRAS* status.

Nude mice

Generation of anti-tumor immune memory

We then explored the existence of anti-tumor immune memory in our immunocompetent BALB/c mice bearing CT26 KRAS$^{G12C+/+}$ tumors treated with RT and MRTX1257. To do so, we rechallenged the mice showing complete response with s.c. injection of CT26 KRAS$^{G12C+/+}$ or CT26 WT cells in the contralateral flank. None of the mice rechallenged this way showed new tumors, in contrast with 100% of naive mice receiving similar s.c. injections. This observation illustrates the potent anti-tumor immune memory provided by the combination treatment against both CT26 KRAS$^{G12C+/+}$ and CT26 WT tumor cells (Fig. 3E). Such cross-reactive immune memory may result from the high clonal proximity between these two cell lines.

Generation of systemic antitumoral response

To further characterize the antitumoral immune response, we sought to determine if the combination was able to generate a systemic anti-tumor immune response leading to the abscopal response of a lesion outside of the irradiation field. Therefore, we administered MRTX1257+/- RT combination in BALB/c mice bearing 2 s.c. CT26 KRAS^{G12C} tumors of which only one received irradiation (Supplementary Fig. 1A). However, as expected both treatments MRTX1257 alone or in combination with RT showed interesting growth delay of both primary/irradiated (Supplementary Fig. 1B) and secondary/unirradiated tumors (Supplementary Fig. 1C).. However, the addition of irradiation to MRTX1257 provided no additional benefit in survival (Supplementary Fig. 1D)

These results suggest that the combination of single-fraction 6 Gy irradiation and MRTX1257 despite generating significant anti-tumor immune memory is not able to enhance the effect of MRTX1257 in a distant lesion outside of the

irradiation field through the abscopal effect. From this point of view, a deeper understanding of the impact the fractionation regimen, as well as the concurrent use of immune checkpoint blockades to increase systemic anti-tumor immunity are most likley necessary.

Exploring immunological aspects of the RT and KRAS^{G12C} inhibition with MRTX1257

Sensitizing to radiation KRAS mutant cells has been a well know strategy and agents such as prenyltransferase inhibitors, farnesyltransferase inhibitors, or antisense vectors have been used in such a goal.

However, these studies did not explore the immunological aspects of the association of RT and KRAS inhibitors in KRAS mutant tumors.

In our study, the achievement of cures in 20% of the immunocompetent mice treated with the combination, in contrast with the fast relapses observed in nude mice, suggest the involvement of the immune compartment in the efficacy of the combined treatment.

However, MRTX1257, alone or in combination with RT, despite not being able to achieve durable cures, significantly delayed tumor growth also in nude mice. Therefore, T cells, although crucial in the anti-tumor immune response, cannot be considered as the key pillar of the immunological outcomes observed following the combination. This deduction is in line with our results of IHC and flow cytometry not showing any significant increase in the infiltration of $CD8^+$ T cells following the combined treatment.

In line with the participation of non-lymphoid cell subtypes to the anti-tumor immune response following the combination treatment, the analysis of NK cells showed only a slight and non-significant increase in their proportion following the combination treatment compared to the untreated control condition.

Moreover, our flow cytometry experiments in CT26 KRAS$^{G12C+/+}$ tumors showed meaningful changes within the non-lymphoid compartment, including the downregulation of PD-L1 in myeloid cells as in tumor and stromal cells. The other meaningful changes observed in myeloid cells following the combination were an increase in the proportion of inflammatory monocytes and conventional dendritic cells type 2, as well as the upregulation of the activation marker CD80 within macrophages which is in favor of a more pro-inflammatory phenotype of these cells following RT alone or RT with MRTX1257.

The down-regulation of PD-L1 is a major positive effect of MRTX1257, and may be crucial for the efficacy of the combination as it counterbalances the upregulation of PD-L1 following RT, demonstrated in our study as in many other models (Sato, et al.) (Dovedi, et al.).

PD-L1 expression is upregulated in many cancers in response to exogenous cellular stress. Mutiple studies have shown that IR synergistically promotes antitumor immunity when applied in combination with immune checkpoint inhibitors.

Sato et al, show that expression of PD-L1 in cancer cells is upregulated in response to DSBs via STAT and IRF1. Importantly, PD-L1 expression in cancer cells was found to be transiently upregulated following RT including for several days after irradiation, PD1/PD-L1 blockade during this upregulation achieved with an anti-PD-1 antibody was able to rescue T cell activity and delay tumor growth (Wu, et al.)(Dovedi, et al.).

Moreover, the specific downregulation of PD-L1 in myeloid cells in the groups treated using MRTX1257 may be of major importance. Indeed, Strauss et al. demonstrated the specific ablation of PD-1 in myeloid cells more effectively decreased tumor growth compared to T cell-specific PD-1 ablation, notably by preventing the accumulation of myeloid-derived suppressor cells (MDSC). Therefore, this downregulation may contribute to the efficacy of RT+MRTX1257 in nude mice, but is not sufficient to induce long-term responses among them.

Overall, our immunological outcomes are in phase with most of those presented in the work by Briere et al. on MRTX849 used alone in preclinical models of $KRAS^{G12C}$ mutated cancers, including an increase in the proportion of $CD4^+$ T cells, $CD4^+$ helper T cells and $CD8^+$ T cells. Moreover, our results are also congruent with the outcomes highlighted by Canon et al. with AMG510, including an increased infiltration of T cells and dendritic cells. However, we are not able to compare the immunological outcomes for the association of RT with MRTX1257, since none of these studies associated KRAS inhibition with RT. It is notable that, in our immune profiling of CT26 $KRAS^{G12C+/+}$ tumors, the lymphoid compartment appeared to be enhanced in the conditions treated with MRTX1257 whereas the myeloid compartment appeared to be enhanced following RT. A key feature of the combination of RT and MRTX1257 may be to leverage the enhancement of both of these immune cell compartments, a condition achievable only in immunocompetent mice. Therefore, one of the challenges for the future of combinations of RT with KRAS inhibitors will consist in identifying the individual impact of each immune subtype apart from the

others and therefore benchmark the best strategies of combinations treatments in solid tumors harboring *KRAS*^{G12C} mutation.

Finally, recent data support a heterogeneity in the innate cancer cell radio-sensitivity itself, independent of cell cycle and microenvironment (Allam, et al.). Taken together with a varying degree of dependence of cancer cells on the presence of *KRAS*^{G12C} mutations for growth and survival, as well as the heterogeneity of intratumoral *KRAS* mutation expression, our data highlight the importance of combination strategies in overcoming treatment resistance. This hypothesis is confirmed by the potent immune memory generated in mice bearing CT26 KRAS$^{G12C+/+}$ tumors which have been cured following RT combined with MRTX1257. Indeed, this immune memory rejected both CT26 KRAS$^{G12C+/+}$ and CT26 WT tumors subsequently implanted. In this complex setting, where monotherapies draw the limits of durable response achievement and most oncogene driven cancers relapse, while immune checkpoints benefit only a small patient group, defining new rational combinations is paramount.

13 CONCLUSION

In this work, we first demonstrated the ability of MRTX1257, a potent covalent KRAS^{G12C} inhibitor analogous to MRTX849, to enhance the effect of radiotherapy both *in vitro* and *in vivo*.

This effect depended on *RAS* mutational status, dose and timing of administration and was associated with a good safety profile. Moreover, the use of RT and MRTX1257 led to a significant cure rate in BALB/c mice bearing CT26 KRAS$^{G12C+/+}$ tumors, but not in nude mice, highlighting the role of the tumor immune microenvironment in the radio-sensitizing effect of MRTX1257. This work constitutes a first step towards the implementation of new combinatorial approaches involving RT and MRTX1257 in KRAS G12C mutated cancers, with the aim of providing new therapeutic strategies with a prolonged clinical benefit. The optimal treatment sequencing and selected patient populations warrant further characterization both in the preclinical and clinical settings.

14 ANNEX

How to improve SBRT outcomes in NSCLC: from pre-clinical modeling to successful clinical translation.

***Marina Milic**, Michele Mondini, Eric Deutsch*

Published as a first author in Cancers, March 2022

Objectives

Despite major research and clinical efforts, lung cancer remains the leading cause of cancer-related death. While the delivery of conformal radiotherapy and image guidance of stereotactic body radiotherapy (SBRT) have revolutionized the treatment of early-stage non-small-cell lung cancer (NSCLC), additional research is needed to elucidate underlying mechanisms of resistance and identify novel therapeutic combinations. Clinical progress relies on the successful translation of preclinical work, which so far has not always yielded expected results. Improved clinical modelling involves characterizing the preclinical models and selecting appropriate experimental designs that faithfully mimic precise clinical scenarios. We review the current role of SBRT and the scope of pre-clinical armamentarium at our disposal to improve successful clinical translation of pre-clinical research in the radiation oncology of NSCLC.

Results

More than ever, one dose or schedule does not fit all clinical scenarios, but neither does it synergize with all immunomodulatory agents. Preclinical models represent an essential tool in the process of harvesting this fundamental understanding and translating it to patient-derived benefits. Clinical benefits derived from recent progress can only be achieved by appropriate and reliable preclinical research mimicking clinical scenarios in almost every aspect: immune status, dose and fraction, radiotherapy delivery modality and planning and tumor microenvironment. Better immunocompetent mouse models of lung cancer are urgently needed to allow faithful study of the tumor–immune interactions and therapeutic modalities relying on those very interactions such as SBRT and immunotherapy. For this reason, orthotropic implantation sites should be systematically used in the currently available immunocompetent syngeneic models.

cancers

MDPI

Review

How to Improve SBRT Outcomes in NSCLC: From Pre-Clinical Modeling to Successful Clinical Translation

Marina Milic [1], Michele Mondini [1,*,†] and Eric Deutsch [1,2,*,†]

[1] Gustave Roussy, Université Paris-Saclay, INSERM U1030, F-94805 Villejuif, France; marina.milic@gustaveroussy.fr
[2] Gustave Roussy, Département d'Oncologie-Radiothérapie, F-94805 Villejuif, France
* Correspondence: michele.mondini@gustaveroussy.fr (M.M.); eric.deutsch@gustaveroussy.fr (E.D.)
† Share senior authorship.

Simple Summary: Despite major research and clinical efforts, lung cancer remains the leading cause of cancer-related death. Stereotactic body radiotherapy (SBRT) has emerged as a major treatment modality for lung cancer in the last decade. Additional research is needed to elucidate underlying mechanisms of resistance and to develop improved therapeutic strategies. Clinical progress relies on accurate preclinical modelling of human disease in order to yield clinically meaningful results; however, successful translation of pre-clinical research is still lagging behind. In this review, we summarize the major clinical developments of radiation therapy for non-small-cell lung cancer (NSCLC), and we discuss the pre-clinical research models at our disposal, highlighting ongoing translational challenges and future perspectives.

Abstract: Despite major research and clinical efforts, lung cancer remains the leading cause of cancer-related death. While the delivery of conformal radiotherapy and image guidance of stereotactic body radiotherapy (SBRT) have revolutionized the treatment of early-stage non-small-cell lung cancer (NSCLC), additional research is needed to elucidate underlying mechanisms of resistance and identify novel therapeutic combinations. Clinical progress relies on the successful translation of pre-clinical work, which so far has not always yielded expected results. Improved clinical modelling involves characterizing the preclinical models and selecting appropriate experimental designs that faithfully mimic precise clinical scenarios. Here, we review the current role of SBRT and the scope of pre-clinical armamentarium at our disposal to improve successful clinical translation of pre-clinical research in the radiation oncology of NSCLC.

Keywords: non-small-cell lung cancer; radiotherapy; SBRT; pre-clinical models

Citation: Milic, M.; Mondini, M.; Deutsch, E. How to Improve SBRT Outcomes in NSCLC: From Pre-Clinical Modeling to Successful Clinical Translation. *Cancers* **2022**, *14*, 1705. https://doi.org/10.3390/cancers14071705

Academic Editor: David Wong

Received: 3 February 2022
Accepted: 22 March 2022
Published: 27 March 2022

1. Introduction

Despite major research and clinical efforts, lung cancer remains the leading cause of cancer-related death. While the delivery of conformal radiotherapy and image guidance of stereotactic body radiotherapy (SBRT) have revolutionized the treatment of early-stage non-small-cell lung cancer (NSCLC), additional research is needed to elucidate underlying mechanisms of resistance and identify novel therapeutic combinations. Clinical progress relies on the successful translation of pre-clinical work, which so far has not always yielded expected results. Improved clinical modelling involves understanding our models and selecting appropriate experimental designs that faithfully mimic precise clinical scenarios. Here, we review the current role of SBRT and the scope of pre-clinical armamentarium at our disposal to improve the successful clinical translation of pre-clinical research in the radiation oncology of NSCLC.

2. Place of SBRT in the Treatment of NSCLC

The fundamental difference between SBRT and conventional radiotherapy is that SBRT allows the delivery of ablative doses in 1 to 5 fractions with high conformal techniques. A typical SBRT course of stage I disease delivers 54 Gy in three fractions over 1 week.

2.1. Early-Stage NSCLC

SBRT has established itself as the standard of care in peripheral stage I disease in those patients who are not medically fit for surgery. The high tolerability rate and the outpatient nature of treatment make it a highly appealing treatment option without compromising local tumor control rates, which exceed 90%.

Whether SBRT should be offered as an alternative to surgery to those patients who are medically fit remains a matter of debate [1] as most data originate from retrospective or non-randomized studies. Findings from the single-arm phase 2 NRG Oncology RTOG0618 Trial [2] involving operable early-stage patients suggest a favorable 96% local control rate and treatment-related morbidity, supporting the need for further phase 3 randomized trials. That said, carrying out phase 3 trials has proven challenging. A pooled analysis by Chang et al. [3] of two phase 3 STARS (NCT00840749) and ROSEL (NCT00687986) trials that were closed prematurely due to poor accrual showed a 3-year overall survival of 95% vs. 79% favoring SBRT. Additionally, a better quality of life was reported [4] in the SBRT arm.

However, high-quality level 1 evidence is still scarce and recent randomized trials comparing SBRT vs. surgery including SABRTooth (NCT02629458) have failed to bring such evidence, partly due to barriers to recruitment and intrinsic patient preferences. Nonetheless, several phase 3 or randomized trials are on the way, including JoLT-Ca/STABLE-MATES (NCT02468024), VALOR (NCT02984761) and POSTILV (NCT03833154).

2.2. Oligometastatic Disease

Patients with oligometastatic disease [5,6], meaning a limited number of metastases in a limited number of organs (typically less than five in 1 to 3 organs), represent an increasingly important subset that can benefit from the addition of SBRT to systemic treatment [7]. They represent a subset of patients in which we can aim to achieve long-term survival or even cure. SBRT has been increasingly integrated into the treatment schemes of selected oligometastatic patients as an alternative to surgery. Data from multiple early-phase studies have shown that SBRT is a technically feasible, low-toxicity and highly effective local therapy (70–90% local control) for patients with metastasis in the lung, liver, spine, brain or multiple sites. Local control using SBRT was achieved across tumor types including colorectal [8], breast [9], NSCLC [10] and other rather radioresistant types such as sarcoma, renal cell and melanoma [11].

In NSCLC, most trials investigating systemic treatments do not stratify patients by the number of lesions, leading to a wide range of PFS and OS [12]. It is only recently that trials have started looking into the benefits of SBRT in NSCLC patients. In a prospective phase 2 study, De Ruysscher et al. [13] enrolled metastatic NSCLC patients with <5 synchronous lesions treated with SBRT showing a median overall survival (OS) of 13.5 months and a median PFS of 12.1 months. Only two patients (5%) had local recurrence. The treatment was well tolerated, highlighting a favorable subgroup of NSCLC with synchronous oligometastasis who might benefit from radical treatment. Similarly, Salama et al. [14] included patients with five or less NSCLC lesions administering a dose of 50 Gy in five fractions. Median OS and PFS were 22.7 and 7.6 months. A worse PFS was observed in patients who had more than two sites treated with SBRT, adenocarcinoma histology or progression after systemic therapy. These data are to be taken with caution due to the single-arm nature of studies and the scarcity of randomized level 1 evidence data. Palma et al. rightly argue that non-randomized data suggest that ablative treatment is feasible

and able to achieve local control in patients with liver, lung, spine or brain metastasis and even at multiple organ sites. When used in patients with CRC hepatic metastasectomy, SABR led to a nearly 50% 5-year survival but was as low as 15% in the less favorable risk factors patient group [15]. Ablative treatment of adrenal metastasis led to a 25% 5-year survival in NSCLC patients [16], while treatment of hepatic metastasis in breast cancer patients resulted in a 22% 5-year survival [17].

Additionally, some of the studies included multiple tumor histologies with different curability rates and behaviors. Even though the survival data reported are encouraging and sometimes better than anticipated, one should also ask the question of selection bias based on favorable inclusion criteria [18] and support urgent prospective randomized trials.

3. From Bench to Bedside: Pre-Clinical Models and Their Challenges

As discussed above, the field of radiation oncology has rapidly evolved in terms of both the understanding of radiobiology and technical advances including image-guided, intensity-modulated and stereotactic radiotherapy. We should rightly ask ourselves the question: have all those advances translated into clinical benefit? If not, why? Indeed, the harvesting and successful translation of discoveries relies on the development of advanced preclinical models that reflect clinical scenarios both in terms of radiation exposure conditions and biological responses [19,20].

While SBRT has begun to revolutionize the clinical management of patients, much remains to be investigated in the preclinical setting in order to reveal its full potential. Recent evidence highlights a different underlying radiobiology of high dose per fraction to that of conventionally fractionated radiotherapy [21–23]. Therefore, there is an urgent need for appropriate preclinical models that are able to accurately mimic the clinical use of SBRT and provide reliable and translational information on radiobiology, efficacy, combinations and toxicities.

The current poor performance of many investigational treatments suggests that the preclinical models used so far to investigate the efficacy of SBRT lack clinical predictive power. One of the explanations is the lack of preclinical models that truly recapitulate human disease heterogeneity and complexity. The scientific community has attempted to address this issue with the development of increasingly complex models [24], some of which are reviewed below. It has become clear over the last decades that a significant mismatch exists between data generated in preclinical in vitro and in vivo models and successful clinical translation (Johnson et al.). The failure of preclinical models to recapitulate patients' tumor heterogeneity and complexity is the most cited reason.

4. In Vitro Models

4.1. Cell Lines

Even though cell culture has immensely contributed to expanding our knowledge of cancer biology, the translation of in vitro data into clinical practice has been inconsistent. Many different reasons have been put forward to account for this inconsistency. First, cell lines are difficult to derive from patients' tumors and, when expanded, develop outside their natural tumor microenvironment in an artificial normoxic environment that is rich in glucose and growth-factors, which selects for a nearly clonal subpopulation of rapidly-growing cells, neutralizing the initial cell heterogeneity [25]. In a primary xenograft model of small-cell lung cancer (SCLC), Daniel et al. [26] compared gene expression within the xenograft model, identifying a group of tumor-specific genes expressed in primary SCLC and xenografts that was lost during the transition to tissue culture and that was not regained when the tumors were re-established as secondary xenografts. It can be reasonably argued that such genetic divergence may be a common feature of many cancer cell culture systems and their primary tumors, highlighting the functional limitations of such models in preclinical development. As discussed above, solid evidence indicates that the genetic

divergence between a primary tumor and the derived cell line is greater than that of a direct xenograft [27].

Determining cancer cell radiosensitivity using clonogenic assays has been the gold standard approach over last few decades, and it was shown to be relevant to the tumor response to irradiation [28]. One of the first links between oncogenes and radioresistance was established with the KRAS oncogene more than two decades ago. RAS activation was shown to increase clonogenic survival and decrease tumor growth delay following irradiation [29–31]. However, it is only recently that the association of genetic profiles such as EGFR mutational status in NSCLC on clonogenic survival parameters has been described [32,33]. Similarly, cell lines have been used to investigate the role of p53 in sensitivity to radiation. It has been generally admitted that p53 is required for radiation-induced apoptosis. Hu et al. [34] showed that H460 wild-type cells were more radiosensitive than their p53 null (H460crp53) counterparts but that this differential response was due to increased senescence rather than apoptosis. Considering that radiosensitivity is influenced by other concomitant genetic alterations, preclinical models integrating the inherent genetic profile complexity are needed.

4.2. Ex Vivo Tumor Models

First described in 1993 by Benali et al. [35], lung organoids have been subsequently established to model cystic fibrosis or bronchiolitis and, more recently, COVID-19 (SARS-CoV-2) infection. Different types of organoids exist, including tissue-derived, embryonic stem-cell-derived and induced pluripotent stem-cell-derived organoids. The successful three-dimensional culture of patient-derived NSCLC organoids was reported in 2013 by Endo et al. [36], with an 80% success rate being achieved using matrigel. However, it was not before 2019 that a protocol for long-term expansion was described by Sachs et al. [37] One of the challenges inherent to the long-term expansion of NSCLC organoids is the overgrowth by normal airway tissue over primary NSCLC as tumor cells lack a selective advantage in the organoid model, leading potentially to the loss of certain NSCLC subtypes. This has also been reported in colorectal and prostate cancers [38]. Organoids have been proposed to be a better in vitro model than 2D cell lines due to higher rates of preservation of histologic and molecular characteristics of their parental tumors.

Patient-derived organoids have contributed to successful drug screenings, showing concordance with matched patient tumors [39,40]. Until now, only a few reports of primary NSCLC organoids for drug screening have been published. Sachs et al. showed differential responses of NSCLC organoids to conventional chemotherapy agents including cisplatin and paclitaxel and reproduced tyrosine kinase inhibitors (TKI) sensitivity in ERBB2-mutant organoids. Recently, Li et al. [41] demonstrated the feasibility of a high-throughput drug response screening using 24 drugs with a consistent drug-response profile to parental NSCLC.

Organoid technology offers new opportunities to study tumor immunobiology and is rapidly adapting to cancer modelling [42]. Organoid cultures using native or reconstituted tumor micro environment (TME) components have the potential to provide valuable information on the role of the TME immune components in cancer development and progression. Tumor organoids recapitulating the immune TME or immune-organoids offer promising future applications including the testing of immunotherapy agents as well as personalized cancer immunotherapy [43].

Despite those novel approaches, a direct clinical application for personalized treatment is still awaited. Some of the challenges that will have to be faced include the availability of sufficient tissue in patients' samples and establishing sufficiently fast-growing organoids in order to inform treatment decisions on time.

4.3. In Vivo Models

There is no doubt that animal models represent invaluable experimental tools and have played a key role over decades in the advances made in radiation biology. One of the first example is the use of the ram testicular model by Regaud and Nogier in 1911 [44] to investigate the ability of fractionation to spare normal tissue. In the oncology discovery race, the mouse model has established itself as the gold standard tool to study tumor response and novel drug–radiation combinations.

4.3.1. Traditional Xenograft Models

Xenotransplantation is the process of transplanting living cells or tissues to another species. Traditional xenograft mouse models involving transplantation of human immortalized cell lines engrafted into immunocompromised mice have been the cornerstone of research. Human cancer cells can be injected subcutaneously, orthotopically or systemically by intravenous injection. They involve the use of athymic nude mice or severe-compromised immunodeficient (SCID) mice. Several cell lines are currently used to model the lung adenocarcinoma response to treatment, including A549, H1975, HCC406 and HCC827, with A549 carrying the highest engraftment rate. The NCI-H226 line is commonly used to model squamous-cell carcinoma and carries a variable engraftment rate. The vast majority of those models use subcutaneous implantation sites (Table 1), representing a major drawback, as discussed later in this paper.

Table 1. Preclinical models of NSCLC.

Reference	Cell Line	Histology	Implantation Site	Animal Model
Raben et al. [45], McLemore et al. [46]	A549	Adenocarcinoma	s.c. endo bronchial	BALB/cAnNCrlBR athymic (nu+/+) BALB/c or NMRI-nu/nu
Akhtar et al. [47], Chen et al. [48], Wang et al. [49]	H1299	Carcinoma	s.c	Athymic nude mice BALB/c nude
Steiner et al. [50], McLemore et al. [46], Carter et al. [51], Yamori et al. [52]	NCI-H460	Large cell carcinoma	s.c. endo bronchial	athymic nude (Ncr nu/nu
Steiner et al. [50]	H1975	Adenocarcinoma	s.c.	Athymic nude (nu/nu) NMRI-nu/nu mice
Yamori et al. [52]	NCI-H226	Squamous cell carcinoma	s.c.	BALB/c nude SCID/SCID mice
Akhtar et al. [47], Wang et al. [53]	HCC827	Adenocarcinoma	s.c. orthotopic	Athymic nu/nu BALB/cA nude mice
Lam et al. [54]	HCC4006	Adenocarcinoma	s.c.	Nude BALB/cAnN-nu
Zimonjic et al. [55], Steiner et al. [50], Lam et al. [54],	NCI-H358	Broncho alveolar carcinoma	s.c. orthotopic	Athymic nu/nu mice BALB/c nude Athymic nude

Onn et al. [56]				
Doki et al. [57], Mordant et al. [58]	LLC	Lewis Lung carcinoma	Orthotopic	C57BL/6 mice
Yamori et al. [52]	NCI-H23	Adenocarcinoma	s.c.	BALB/c nude mice
Williams et al. [25]	TL-1	Squamous cell carcinoma	s.c.	CB-17 scid/scid mice
Takahoshi et al. [59]	NCI-H441 and H440	Adenocarcinoma	Orthotopic	Athymic nude

s.c.: subcutaneous.

Traditional xenograft models harbor several limitations, including a significant loss of heterogeneity of human cancers. As tumor cell lines are often grown in vitro for many years, they are likely to develop genotypic and phenotypic alterations [60] and, more importantly, such models fail to reproduce human TME. It is now widely accepted that, at least in part, the efficacy of radiotherapy relies on the host immune response. Four decades ago, Stone et al. [61] demonstrated that the tumor response to irradiation was impaired in the absence of a normal T-cell repertoire. They used a syngeneic mouse model, showing a drastic difference in radio-sensitivity where T-cell-deficient mice required over 60 Gy to achieve a comparable tumor control to immunocompetent mice who received 30 Gy.

Since then, extensive evidence has accumulated regarding the involvement of the immune system in the response to RT [62]. These observations highlight the importance of the use of immunocompetent animal models to study the antitumoral effect of radiotherapy.

The widespread use of immune-deficient animals, together with the other factors enlisted above, have resulted in the low success of clinical translation, approaching a failure rate of 85% in early-stage clinical trials [63]. Wong et al. [64] estimated the probability of success of each clinical phase across multiple indications, concluding that 13.8% of all drug development programs lead to approval. However, this figure was only 3.4% for oncology drugs, which was even lower than previously estimated [65].

4.3.2. Patient-Derived Xenograft Models

In an attempt to improve preclinical models and clinical translation rates, patient-derived xenograft models (PDX) have been developed. PDX models allow the transplantation of fresh patient tumor samples or cell suspensions but this comes with a cost: needing increasingly immuno-deficient hosts to prevent rejection. Many different mouse strains were developed over time in an attempt to increase the low take rate associated with human tissue transplantation as opposed to immortalized cell lines. They have widened the horizons of possible preclinical models and rendered previously difficult engraftments possible. Early generations of genetically determined immuno-deficient mice harbor a single mutation and confer modest immune dysfunction. They include nude [66], severe combined immunodeficient (SCID) [67], non-obese diabetic/SCID (NOD/SCID) [68] or RAG-1 null [69] or RAG-2 null [70] mice. A step further was the development of mice carrying a deletion or truncation of the common gamma chain/Il2rg [71], who completely lack NK activity, for example, with new complex immunodeficient models emerging constantly. However, careful attention should be paid to the choice of experimental irradiation models: when it comes to their relevance in radiation oncology, one should bear in mind that some immunodeficient models are inherently radiosensitive due to impaired double strand breaks (DSB) repair capacities. Rübe et al. [72] showed distinct

yH2AX-foci kinetics in various immunodeficient mouse strains characterized by different genetically defined DSB repair capacities. In addition, using SCID mice that lack functional lymphocytes and have heightened sensitivity to ionizing irradiation [73] with a LD50/30 of 3 Gy might not be the preferred experimental tool in view of the key role of lymphocytes in the immune response to radiation. Importantly, the vast majority of xenograft models use the subcutaneous site of injection and studies involving orthotopic implantation are rare.

One of the advantages of PDX models is that they retain the characteristics of the primary patient tumors, including the histological characteristics and architectures, gene expression profiles, and molecular and tumor heterogeneity [74], and are to date one of the most reliable in vivo human cancer models displaying the most concordant drug response profile to human cancer. A good illustration is a recent study by Crystal et al. [75] demonstrating the utility of establishing in vivo PDX NSCLC models directly from patients' biopsy specimens for identifying new drug combinations in a model of acquired drug resistance. On the other hand, in PDX models, the tumor stroma, including the vasculature, is that of the host (mouse), and therefore does not reflect the human tumor situation. This makes it difficult to faithfully evaluate tumor and stroma interactions that are key to response radiation therapy but also to combinations with drugs. Additionally, a "murine drift" was described in severely immunocompromised mice, where human tumors became more mouse-like with repeat passaging [27].

4.3.3. Syngeneic Immunocompetent Mouse Models

Syngeneic models involve the injection of murine tumor cell lines that are grown and expanded in vitro into immunocompetent animals. This presents the major advantage of preserving an intact murine immune system, making them the only available choice to test immunomodulatory drugs in vivo. Nevertheless, they also present major drawbacks, such as the lack of mutational and microenvironmental heterogeneity, as seen in human cancers: the cell lines used a lack of mutational patterns that recapitulated human intrapatient genomic heterogeneity and were implanted into a limited number of inbred mouse strains that lacked inter-patient heterogeneity. Additionally, the vast majority of syngeneic models are injected subcutaneously, failing to reproduce the complex architecture associated with de novo tumor growth and the natural development of the tumor microenvironment.

Only two C57BL/6-derived murine lung cancer cell lines are currently commercially available. One of them is the Lewis Lung Carcinoma (LLC) established in 1951 from the lung of a C57BL/6 mouse bearing a tumor established from the implantation of primary Lewis Lung Carcinoma [76]. The second is the CMT64 cell line (and its derivative CMT167 line sub cloned for metastatic potential) derived from a spontaneous lung tumor [77]. Recently, some GEMM-derived cell lines have emerged, such as KRASG12D p53−/−, forming lung tumors after intravenous injection, but also giving rise to a metastatic model. In 2020, Nolan et al. [78] were able to develop six new lines capable of forming orthotopic tumors in 75% of recipient C57BL/6 host lungs. While those lines will need further validation, such initiatives are very much needed.

4.3.4. Orthotopic Mouse Models

While subcutaneous injection is easy to perform, it does not allow the simulation of the natural history of cancer dissemination as no lymphatic or hematogenous metastatic extension is occurring. More importantly, it is associated with a low translation rate, as evidenced by the high rate of negative clinical trials [79].

Orthotopic implantation involves the engraftment of tumor cells into the relevant organ of tumor origin or metastatic site, preserving microenvironmental interactions and offering appropriate microvasculature and angiogenesis for tumor growth. The tumor microenvironment is crucial in tumor development and response to treatment [80] and recent evidence suggests that it varies with the anatomical site of implantation. Devaud et

al. [81] observed that despite injecting matched cancer cells, the same tumors implanted in different anatomical sites varied in their response to immunotherapy and differed in their microenvironment. In addition, the surrounding normal tissue at the site of implantation plays a key role in shaping the TME composition, and by extension, the response to treatment. Growing evidence suggests that the TME itself is involved in the initiation and progression of primary lung carcinoma [82,83]. Another important characteristic not to be overlooked is hypoxia, a key feature of solid tumors significantly affecting the sensitivity to radiation therapy and, as a result, clinical outcomes including tumor progression, likelihood to metastasize and overall survival [84,85]. Preclinical modelling ought to take into account that different animal models can yield different hypoxic profiles [86] and influence treatment outcomes. Graves et al. studied hypoxia in A549 human lung adenocarcinoma orthotopic and subcutaneous models, showing the presence of hypoxia in the heterotopic model, while hypoxia was minimal in orthotopic models [87].

All these data suggest that the site of implantation matters and careful attention should be paid when considering which model is best suited to replicate individual human scenarios and assess responses to individual treatment modalities. Another challenge in orthotopic lung models is the development of solitary nodules with no regional or metastatic dissemination simulating the clinical features of human lung cancer and clinically relevant treatment modalities including SBRT.

The traditional implantation route for orthotopic models is surgical transpleural or percutaneous, allowing the induction of localized tumors with multiple nodules such as the model developed by our group [58,88]. Recently, Nakajima et al. [89] established an orthotopic lung cancer model by means of a non-surgical transbronchial approach in nude mice using human NSCLC lines, establishing a clinically relevant model human xenograft model bearing a solitary nodule.

To allow the generation of more reliable preclinical data, the use of such orthotopic models should be expanded in the forthcoming years.

4.3.5. Genetically Engineered Mouse Models (GEMMs)

GEMM models have been developed using gene targeting by inserting targeted donor constructs into embryonic stem cells of mice. These embryonic stem cells, containing the desired gene mutation, are then injected into recipient mice blastocysts and implanted into pregnant females [90]. This complex process was recently facilitated by the development of genome-editing tools such as the CRISPR/Cas9 systems, allowing the insertion of targeted mutations into the mouse germ line [91] and the study of gene function in vivo.

GEMMs models develop de novo spontaneous tumors due to the oncogene activation or somatic inactivation of tumor suppressor genes in a natural immune-proficient microenvironment. Tumors developing in GEMMs accurately mimic histological and molecular features of human cancers but also reasonably preserve genetic heterogeneity. In this way, they are superior models to cancer cell inoculation models, which can also be metastatic in nature from the start. They are a useful model to study tumor responses to radiotherapy in specifically defined genomic backgrounds that are seen in human tumors. Recently, successful models of AIJ-SPC-TP53-273H transgenic mice allowed the exploration of the oncogenic potential of TP53 gene in the spontaneous development of lung adenocarcinoma [92]. Importantly, cancer development in these mice had a latency period and was associated with other genetic alterations that are similar to human adenocarcinoma. Equally, they allow the study of radiation-induced carcinogenesis and normal tissues. GEMMs have been successfully used in assessing radio-sensitizers and, more recently, immune checkpoint inhibitors in a KRAS-mutant NSCLC model [93].

However, as with all models, GEM models have limitations. Several mutations are often introduced simultaneously, not mimicking the sequential acquisition of mutations in the multistep oncogenesis of human cancers, which can have a significant impact on tumor evolution and modelling. For example, in a GEM model with simultaneous activa-

tion of K-Ras and inactivation of p53, the tumor would undergo lower evolutionary pressure and present less genetic complexity than if sequential events were happening. While this can be overcome by using different recombination systems, we should bear in mind that GEM-derived tumors are not human tumors. They are developed within months, whereas human tumors may take years or sometimes decades and carry less genetic aberrations and complexity. Another challenge lies in the ability of GEMs to model metastasis [94]. However, more importantly, GEMs often develop multiple spontaneous tumors at different sites, limiting the applicability to SBRT where a precise delineated radiation is applied to the target lesion. Another drawback is that developing GEMMs models requires significant time, money and expertise.

Nonetheless, GEMMs represent valuable tools in cancer research. They have the advantage of offering preserved microenvironmental, genetic and histological features and, therefore, can be predictive of human tumor response. In pre-clinical radiation research, they are an interesting tool, allowing the preservation of an immunocompetent host and the study of tumor–stroma interactions. The main pros and cons of preclinical models discussed are summarized in Table 2 below.

Table 2. Summary of advantages and limitations of the main preclinical models used in cancer research.

Models	Advantages	Limitations
Cell line models (2D)	Easy and widely available wide range of tumor models	Fail to reproduce tumor heterogeneity Do not reflect original tumor biology
Organoids	Simple Mass production Co-culture possible	Difficult long-term culture Low throughput
Patient-derived tumor xenograft models (PDX)	Reproduce heterogeneity of human disease	Immune-deficient hosts Vasculature and stroma of murine origin Low implantation rate
Humanized patient-derived xenografts	Robust human immune system engraftment Resemblance of tumors to human donor	Requires autologous immune reconstitution Residual mouse innate immunity Cost and infrastructure
Syngeneic mouse models	Immunocompetent host Evaluation of targeted therapies and toxicity Good concordance in drug response Ease of manipulation Rapid growth and reproducible	Lack of native tumor microenvironment Lack of heterogeneity Few host strains Limited number of transplantable cell lines
Genetically Engineered Mouse Models (GEMMs)	Study of the role of specific mutations in cancer development and progression Native microenvironment Variety of genetic backgrounds possible	Slow tumor development Simultaneous study of a limited number of genes Tumor and TME of murine origin Frequent multiple simultaneous tumors Breeding challenges

5. Discussion and Future Perspectives

5.1. Drug Combinations with SBRT

The immunomodulatory effects of SBRT have revealed a promising potential world of synergy with immune-modulatory agents, starting with immune checkpoint inhibitors in the treatment of NSCLC.

5.1.1. Immune-Checkpoint Inhibitors

Mounting evidence suggests that radiotherapy combined with PD-1/PD-L1 inhibitors can improve immunosuppression and restore CTL responses, leading to tumor growth suppression and improved survival. Radio-immunotherapy combinations are offering new perspectives from early stage to oligo and metastatic disease spectrums.

Current clinical practice in advanced NSCLC is largely based on results from the phase 3 PACIFIC trial [95], which demonstrated the benefit of consolidation therapy with the PD-L1 inhibitor Durvalumab in patients who did not have disease progression after two or more cycles of chemo-radiotherapy. Patients treated in the Durvalumab arm had a median PFS (Progression-Free Survival) of 16.8 months vs. 5.6 months and an overall response rate (ORR) of 28.4% vs. 16.0% in the placebo arm. Similarly, an ongoing phase 2 Hooiser Cancer Research Study, LUN14-179 [96](NCT02343952), looking at the benefit of consolidation pembrolizumab following concurrent chemo-radiotherapy in patients with unresectable stage III NSCLC has shown promising results, with a mPFS of 18.7 months. It is becoming increasingly clear that SBRT has the features of a key partner in adjuvant immunotherapy. SBRT has the advantage of sparing radiation-induced lymphopenia as compared to conventionally fractionated radiation, a key consideration considering the increasing importance of the immune system in antitumoral response and in combination with immune-checkpoints [97,98]. Currently, more than 100 trials combining SBRT and anti-PD-1/ PD-L1 are ongoing despite limited knowledge on how dose and fractionation schedules or timings affect antitumor responses. The majority of available data are currently from retrospective or small-size cohorts, meaning that the optimal sequencing and time window for combination treatment are still to be determined, as discussed later.

5.1.2. SMAC Mimetics

SMAC (second mitochondria-derived activator of caspase) is a pro-apoptotic mitochondrial protein that is an endogenous inhibitor of a family of cellular proteins called the Inhibitor of Apoptosis Proteins (IAPs). SMAC mimetics (SMs) are promising new agents that are progressing from bench to bedside. They induce cancer cell death predominantly via a cIAP-dependent mechanism regulated by death receptor ligands [99] acting as sensitizers and reducing the threshold for cell death induced by chemo or radiotherapy. Eight new molecules have been tested in clinical trials and proven to be well tolerated and, importantly, non-toxic towards healthy tissue. However, their clinical efficacy as monotherapies is limited. Recent data indicate that tumors must be able to produce and respond to tumor necrosis factor alpha (TNFα) in order for SMs to exert their anti-tumor effect. Tumors that do not fulfil the previous TNFα criteria are inherently resistant to SM treatment [100].

Radiation therapy is a promising candidate for combination treatment with SMs in order to overcome TNF-mediated resistance. In a pre-clinical model of HNSCC, Eytan et al. [101] were able to cure mice using the SM Birinapant and radiotherapy and observed an increase in endogenous TNFα in the tumors. Similar findings supporting a radio-sensitizing role of SMs were observed in different models including NSCLC and Esophageal Squamous Carcinoma (ESCC) using the SM Debio 1143. Encouraging pre-clinical data has been taken forward in HNSCC clinical trials with Birinapant (NCT03803774) and Debio 1143 (NCT02022098). Tao et al. [102] reported increased specific adaptive immunity after treatment with Debio 1143 and ablative radiotherapy (30 Gy) in a LLC-OVA syngeneic

model of NSCLC, highlighting a new treatment strategy to increase the immunogenicity of radiation therapy.

5.1.3. Other Immuno-Stimulatory Agents

Similarly, recent preclinical evidence addressing other immuno-stimulatory agents such as TLR (Toll Like Receptors) agonists (TLR2,3,7 and 9) and cytokines (e.g., GM-CSF and FLT-3 ligand) have resulted in some promising preclinical data; however, successful clinical translation has failed to date, partly due to toxicity. TLR agonists are important mediators of inflammatory pathways in the gut, playing a major role in mediating immune responses towards a wide variety of pathogen-derived ligands linking adaptive and innate immunity. Younes et al. [103] showed that immunosuppressive properties of radiation therapy such as recruitment of CD11b+ myeloid cell population can be at least partly overcome by a TLR9 agonist, as those cells express Toll-like-receptors (TLRs). Other immunotherapeutic modalities including cytokines and their inducers, vaccines or adoptive cell transfer (NK cells, DCs, T cells) have been described to augment RT-induced tumor killing.

Intra-tumoral delivery of dendritic cells (DCs) in combination with RT has led to a CD8+ T cell increase in the TILs in a localized prostate cancer model [104] and in tumor-specific immune responses in soft tissue sarcoma [105].

Another explored strategy is the reprogramming of the TME and, more precisely, of Tumor-Associated Macrophages (TAMs). Successful pre-clinical attempts to block M2 polarization by inhibiting STAT3 and STAT6 transcription factors have been reported. Resveratrol was used to block M2 polarization (by decreasing STAT3 activity) and inhibit tumor growth in a mouse xenograft model of lung cancer [106]. However, none of the inhibitors were taken further to clinical studies. Very recently, Lan et al. [107] reported promising data on the simultaneous targeting of TGFβ and PD-L1 with the bispecific antibody Bintrafusp alpha in combination with radiotherapy. The combination resulted in a TME reprogramming and reconstitution of tumor immune-surveillance in poorly immunogenic syngeneic mouse models with very encouraging preclinical results. Additionally, the associated TGFβ sequestration has the potential to result in reduced overlapping toxicities of combination immune-checkpoint inhibition and RT treatment and spare normal tissue toxicity.

5.2. Challenges

Despite encouraging combination treatment data, multiple challenges remain.

5.2.1. Dose and Fractionation

One of the challenges is the optimal dose and fractionation of SBRT, as there is currently no international consensus for use in clinical practice. Different regimens have been tested in clinical trials including 30–34 Gy × 1, 15–20 Gy × 3, 12 Gy × 4 and 10–12 Gy × 5 in different settings, making it difficult to favor one single regimen over another.

Demaria et al. [108] proposed a classification of SBRT regimens into three categories, immunogenic ablative (34 Gy × 1, 18 Gy × 3, 10 Gy × 5), immunomodulatory sub-ablative (8 Gy × 3, 6 Gy × 5) and TME modulatory (0.5 Gy × 4), based on their dominant effects on the crosstalk between the tumor and the immune system. In this way, RT can be viewed as an immunomodulatory tool that can be dispensed or delivered at different doses and fractions according to the nature of the desired immunomodulatory effect to be elicited.

Designing successful combination treatments with radiotherapy requires understanding precisely how dose and fractionation do matter and accepting that one size dose or regimen do not fit all scenarios. Different fractionation regimens result in distinct immune-modulatory effects, which still remain to be fully deciphered [108]. Considering the dual effects of RT on the host immune system, the RT schedule should be tailored and optimized based on the synergistic effect expected and the immunomodulatory agent

used. While aiming at determining one or a range of optimal doses for each type of modulatory agent seeking synergy with RT may seem daunting, it is a necessary task. Similarly, even though synergistic effects with RT have been reported with different agents and tumor models, the mechanisms involved are likely to be different.

Understanding the underlying biology of different doses and fraction regimens of RT is key and can be achieved with adequately designed preclinical research followed by prospective validation in clinical trials.

5.2.2. Sequence of Treatments

Combination treatment can be delivered concurrently to or sequentially to radiation therapy, and once again, the optimal sequence remains to be determined. Considering that different immunomodulatory agents target different pathways and result in different immune changes, careful attention should be paid to the sequencing of treatment in order to elicit the greatest synergistic effect. Preclinical and early clinical data examining both approaches suggest that both sequential and concurrent sequencing are safe and feasible. It is worth nothing that, so far, the optimal sequencing seems to be dependent on the tumor type and the immunotherapy agent being used. Young et al. [109] showed that hypofractionated radiotherapy with anti-CTLA4 worked most effectively when given before irradiation, but anti-OX40 was more effective when administered 1 day after radiation. Another preclinical study by Dovedi et al. [110] showed that PDL-1 inhibition was effective only when given concurrently or at the end of radiation and not one week later.

Several clinical trials that are testing the concurrent approach are ongoing. Pembrolizumab with concurrent SBRT (50 Gy in four fractions) to lung and liver lesions was deemed safe in patients with metastatic NSCLC in a randomized phase I/II trial. [111]. Another single arm I/II trial testing concurrent Ipilimumab commenced with SABR is ongoing [112]. While multiple early-phase data suggest the combination is efficacious and safe, confirmatory large-scale data are eagerly awaited.

Currently the sequential or early sequential approach as seen in the PACIFIC trial is preferred in the treatment of NSCLC [95]. A secondary analysis of the PACIFIC trial points to a better PFS in patients who started Durvalumab within 14 days of chemoradiation completion as opposed to after 14 days. On the other hand, a retrospective analysis of 758 patients who received immunotherapy and radiotherapy within 30 days of each other showed a better overall survival when ICIs were started at least one month before RT [113].

It appears evident that more extensive data on the optimal treatment sequencing are needed, taking into account the types of immunotherapy agents used in selected tumor types. This will enable confirmation of the safety and efficacy of the combination in large cohorts of patients.

5.2.3. How do We Predict Response?

Predicting the likelihood of individual patients to respond to a radio-immunomodulatory combination is certainly a challenge for the next decade. While some types of biomarkers have been shown to have a predictive value of response to RT, such as components of the DDR machinery [34], genetic [114–116], epigenetic signatures [117] and microenvironmental biomarkers [118,119], they have had little impact on the individualized RT treatment delivery, with a few exceptions.

Predictive markers of response to immune-checkpoint blockers have emerged and some are already informing individual decision making in clinical practice, such as PD-L1 expression or the tumor mutational load [120], or DNA mismatch repair (MMR) status [121]. However, markers able to predict the potential synergistic effects of radio-immunotherapy combinations are still in the candidate roles. Expression of the soluble NKG2D (NK-cell-activatory receptor) ligand was described as a potential predictive biomarker candidate. NKG2D was shown to stabilize immunological synapsis between CD8+ CTL and their targets and support adaptive immunity [122]. Radiotherapy promotes exposure

of NKG2D ligands on malignant cells, exposing them to NK-cell-dependent lysis or improved recognition by CTLs [123]. In their study, Ruocco et al. [123] showed that the NKG2D ligand is required for synergy between RT and anti-CTLA-4 in 4T1 tumors in vivo.

Another promising approach is the quantification of radiotherapy's ability to induce a Type 1 interferon response in individual tumors. This could be achieved by measuring levels of TREX1, which has been shown to counteract RT's ability to drive the secretion of Type 1 IFN by degrading cytosolic dsDNA [124] in ex vivo PDX irradiation models. That would potentially enable dose selection that synergizes with immune checkpoint inhibitors. Recent developments in functional imaging and large scale data analyses using computer algorithms have seen the advent of radiomics [125]. Radiomics allows the extraction of quantitative imaging biomarkers named "radiomic signatures" that most statistically significantly relate to a measured outcome or a tumor biology parameter. A recent review found 43 CT-image based studies, evaluating prognostic or predictive roles of radiomic signatures in NSCLC, that reported at least one positive association between the CT radiomic signature and either outcome or tumor biology [126]. However, the particular radiomic signature derived varies among studies, making a direct comparison difficult. Despite some methodological challenges that need to be addressed before large multicenter studies, imaging biomarkers carry a considerable potential for successful translation.

5.2.4. SBRT-Related Treatment Toxicity

The therapeutic index [127] represents the ratio between the probability of tumor control and that of normal tissue damage or toxicity. SBRT is associated with a steep-dose gradient outside the target volume, thus minimizing the dose to organs at risk and the probability of normal tissue complications. Moreover, advancements in imaging and SBRT delivery including IGRT and IMRT allow a remarkably precise delivery of high dose radiation per fraction to intra-thoracic targets with a good tolerability profile. Nevertheless, toxicities are still reported, ranging from mild fatigue and transient esophagitis to pneumonitis, hemorrhage, chest wall pain, rib fracture or brachial plexopathy [128,129]. Normal tissue toxicity can manifest itself days to years after irradiation, mainly in the heart and lung tissues in patients whose thoracic tumors are irradiated. The most common toxicities include acute pneumonitis, chronic lung fibrosis [130] or radiation-induced heart dysfunction (RIHD) [53,131,132]. Another important manifestation of radiation toxicity is endothelial/vascular injury leading to a loss of endothelial barrier function, resulting in tissue injury [133]. When organs at risk are exposed to sufficiently high doses, the endothelial damage and its associated vascular changes can lead to chronic lesions in those organs [134]. Initial reports suggested an increased risk of toxicity when treating centrally located lung tumors with SBRT, including an 8% risk of death with the 60 Gy in 3 fraction dose [135]. As a result, efforts to sub-classify central lesions and adapt treatment with protracted courses of radiation (5 to 10 fractions) have been made, indicating that SBRT may be safe [136]. However, the results highlight the need for careful attention when selecting patients with ultracentral tumors. An example of the risk-adapted dose fractionation in early-stage NSCLC is 8 × 7 Gy for centrally located tumors [137] and 3 × 18–20 Gy for peripheral lesions. Ultra-central tumors that GTV (Gross Tumor Volume) or PTV (Planned Tumor Volume) directly abuts or overlaps the trachea or proximal bronchial tree still represent a treatment challenge [138], but prospective data from ongoing SUNSET (NCT03306680) and future trials may provide further guidance.

Combination treatment regimens including SBRT and immune-checkpoint inhibitors raise the question of potential additive toxicities and adverse impact on normal tissues [139]. To date, there are few reports describing the toxicity of the combination but prospective data are slowly emerging. Several phase I and II trials investigating the immune-checkpoint inhibitors Pembrolizumab (NCT02608385) Pembrolizumab, Atezolizumab (NCT02400814) and Durvalumab (NCT02904954) in combination with SBRT are on the

way. Thus, the importance of accurate preclinical modelling of radiation is key for identifying and preventing normal tissue toxicities. Currently, small animal image-guided conformal irradiators are commercially available and are able to deliver irradiation with a precision close to that used in clinical practice. They also deliver a lower mean dose to surrounding tissues and their use should become standard in studies modelling irradiation in the preclinical setting.

6. Conclusions

The field of radiation oncology has significantly evolved with the advent of SBRT, leading to clinical benefits in the management of NSCLC patients. At the same time, an increasing amount of preclinical and clinical data continues to emerge regarding the combination of radiotherapy and immunomodulatory agents. While the rationale for such combinations is strong and promising, several key factors still need to be fully addressed, such as dose and fractionation, sequencing, selection of the best-suited immunomodulatory agent, toxicities of the combination on healthy tissues and biomarkers to predict responses (Figure 1).

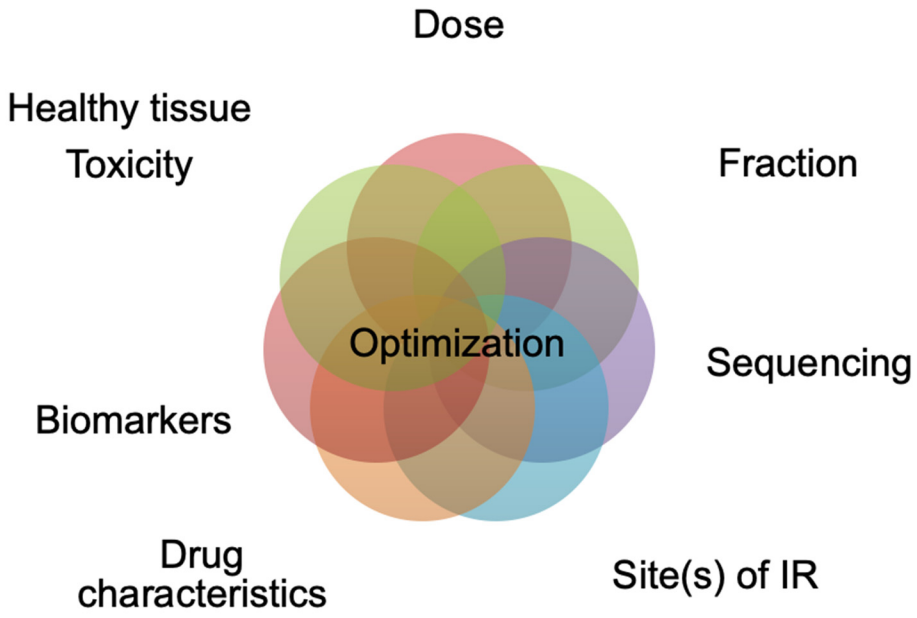

Figure 1. Ongoing challenges of radiotherapy–drug combinations.

We are starting to acknowledge unique immune-modulatory properties of different dose-fraction regimens and the subsequent need for individually tested combination approaches tailored to the desired synergistic effect. More than ever, one dose or schedule does not fit all clinical scenarios, but neither does it synergize with all immunomodulatory agents. Preclinical models represent an essential tool in the process of harvesting this fundamental understanding and translating it to patient-derived benefits. Clinical benefits derived from recent progress can only be achieved by appropriate and reliable preclinical research mimicking clinical scenarios in almost every aspect: immune status, dose and fraction, radiotherapy delivery modality and planning and tumor microenvironment. Better immunocompetent mouse models of lung cancer are urgently needed to allow faithful study of the tumor–immune interactions and therapeutic modalities relying on those very interactions such as SBRT and immunotherapy. For this reason, orthotropic implantation sites should be systematically used in the currently available immunocompetent syngeneic models. In addition, considering that the majority of preclinical studies looking at

synergy between radiotherapy and immunotherapy have been performed in syngeneic ectopic models, GEMMs represent a valuable tool in this setting despite their cited limitations. A further optimization, not achieved yet, would be represented by the development of state-of-the-art humanized PDX models using immunocompetent mice to mimic tumor- and organ-specific microenvironments, especially using orthotropic implantations.

Due to considerable tumor and micro-environmental heterogeneity, multi-target multi-agent therapeutic strategies are currently being explored and are likely to yield promising results in the near future. One such example is the combination of anti-PD1 and anti-angiogenic agents aiming to alleviate immunosuppression with radiotherapy [140]. Similarly, dual immune-checkpoint blockade including established (anti-PD-1 and anti-CTLA-4) but also new combinations such as Relatlimab (anti LAG-3), as demonstrated in the RELATIVITY-047 (NCT03470922) study on the reinvigoration of T-cell activity, are awaited to be explored in combination with radiation therapy.

While multi-agent multi-modality strategies seem promising, we are a long way from their routine clinical use as a frontline treatment. Not only does the safety profile remain largely unexplored, but as discussed earlier, patient selection, biomarkers, optimal dose and sequencing are all to be addressed. The complexity of any multi-modal combination treatment can be broken down by understanding the immunomodulatory properties of each individual treatment component and how to achieve a balance to make them thrive together. Finally, personalization of radiotherapy is likely to be the cornerstone of the next decade's progress. Delivering the same dose and fraction to each unique patient and tumor with unique biology and radiation sensitivity is likely to be a distant memory. This cannot be achieved without the development of preclinical models integrating biological and immunological tumor parameters in the dose-fraction equation in order to maximize therapeutic effects.

Author Contributions: Conceptualization, M.M. (Michele Mondini) and E.D.; writing—original draft preparation, M.M. (Marina Milic); writing—review and editing, M.M. (Michele Mondini) and E.D. All authors have read and agreed to the published version of the manuscript.

Funding: The authors received financial support from INSERM, SIRIC SOCRATE, Canceropole IdF, Fondation ARC pour la recherche sur le cancer (Projet Fondation ARC and ARC SIGN'IT), Institut National du Cancer (INCa 2018-1-PL BIO-06-1) and Fondation pour la Recherche Médicale (FRM DIC20161236437).

Conflicts of Interest: E.D. and M.M. (Michele Mondini) declare grants from Roche Genentech, Servier, AstraZeneca, Merck Serono, Bristol-Myers Squibb, Boehringer Ingelheim, Eli Lilly and MSD, outside the submitted work. E.D. declares personal fees from Roche Genentech, AstraZeneca, MSD, AMGEN, Accuray and Boehringer Ingelheim outside the submitted work. E.D. declares shared patents with NH-Theraguix and Clevexel.

References

1. Tandberg, D.J.; Tong, B.C.; Ackerson, B.G.; Kelsey, C.R. Surgery versus Stereotactic Body Radiation Therapy for Stage I Non-Small Cell Lung Cancer: A Comprehensive Review. *Cancer* **2018**, *124*, 667–678. https://doi.org/10.1002/cncr.31196.
2. Timmerman, R.; Paulus, R.; Galvin, J.; Michalski, J.; Straube, W.; Bradley, J.; Fakiris, A.; Bezjak, A.; Videtic, G.; Johnstone, D.; et al. Stereotactic Body Radiation Therapy for Inoperable Early Stage Lung Cancer. *JAMA* **2010**, *303*, 1070–1076. https://doi.org/10.1001/jama.2010.261.
3. Chang, J.Y.; Senan, S.; Paul, M.A.; Mehran, R.J.; Louie, A.V.; Balter, P.; Groen, H.J.M.; McRae, S.E.; Widder, J.; Feng, L.; et al. Stereotactic Ablative Radiotherapy versus Lobectomy for Operable Stage I Non-Small-Cell Lung Cancer: A Pooled Analysis of Two Randomised Trials. *Lancet Oncol.* **2015**, *16*, 630–637. https://doi.org/10.1016/S1470-2045(15)70168-3.
4. Lagerwaard, F.J.; Haasbeek, C.J.A.; Smit, E.F.; Slotman, B.J.; Senan, S. Outcomes of Risk-Adapted Fractionated Stereotactic Radiotherapy for Stage I Non-Small-Cell Lung Cancer. *Int. J. Radiat. Oncol. Biol. Phys.* **2008**, *70*, 685–692. https://doi.org/10.1016/j.ijrobp.2007.10.053.
5. Hellman, S.; Weichselbaum, R.R. Oligometastases. *J. Clin. Oncol. Off. J. Am. Soc. Clin. Oncol.* **1995**, *13*, 8–10. https://doi.org/10.1200/JCO.1995.13.1.8.
6. Guckenberger, M.; Lievens, Y.; Bouma, A.B.; Collette, L.; Dekker, A.; deSouza, N.M.; Dingemans, A.-M.C.; Fournier, B.; Hurkmans, C.; Lecouvet, F.E.; et al. Characterisation and Classification of Oligometastatic Disease: A European Society for

Radiotherapy and Oncology and European Organisation for Research and Treatment of Cancer Consensus Recommendation. *Lancet Oncol.* **2020**, *21*, e18–e28. https://doi.org/10.1016/S1470-2045(19)30718-1.
7. Gomez, D.R.; Tang, C.; Zhang, J.; Blumenschein, G.R.; Hernandez, M.; Lee, J.J.; Ye, R.; Palma, D.A.; Louie, A.V.; Camidge, D.R.; et al. Local Consolidative Therapy Vs. Maintenance Therapy or Observation for Patients With Oligometastatic Non-Small-Cell Lung Cancer: Long-Term Results of a Multi-Institutional, Phase II, Randomized Study. *J. Clin. Oncol. Off. J. Am. Soc. Clin. Oncol.* **2019**, *37*, 1558–1565. https://doi.org/10.1200/JCO.19.00201.
8. Hoyer, M.; Roed, H.; Traberg Hansen, A.; Ohlhuis, L.; Petersen, J.; Nellemann, H.; Kiil Berthelsen, A.; Grau, C.; Aage Engelholm, S.; Von der Maase, H. Phase II Study on Stereotactic Body Radiotherapy of Colorectal Metastases. *Acta Oncol. Stockh. Swed.* **2006**, *45*, 823–830. https://doi.org/10.1080/02841860600904854.
9. Milano, M.T.; Zhang, H.; Metcalfe, S.K.; Muhs, A.G.; Okunieff, P. Oligometastatic Breast Cancer Treated with Curative-Intent Stereotactic Body Radiation Therapy. *Breast Cancer Res. Treat.* **2009**, *115*, 601–608. https://doi.org/10.1007/s10549-008-0157-4.
10. Hasselle, M.D.; Haraf, D.J.; Rusthoven, K.E.; Golden, D.W.; Salgia, R.; Villaflor, V.M.; Shah, N.; Hoffman, P.C.; Chmura, S.J.; Connell, P.P.; et al. Hypofractionated Image-Guided Radiation Therapy for Patients with Limited Volume Metastatic Non-Small Cell Lung Cancer. *J. Thorac. Oncol. Off. Publ. Int. Assoc. Study Lung Cancer* **2012**, *7*, 376–381. https://doi.org/10.1097/JTO.0b013e31824166a5.
11. Stinauer, M.A.; Kavanagh, B.D.; Schefter, T.E.; Gonzalez, R.; Flaig, T.; Lewis, K.; Robinson, W.; Chidel, M.; Glode, M.; Raben, D. Stereotactic Body Radiation Therapy for Melanoma and Renal Cell Carcinoma: Impact of Single Fraction Equivalent Dose on Local Control. *Radiat. Oncol. Lond. Engl.* **2011**, *6*, 34. https://doi.org/10.1186/1748-717X-6-34.
12. Guerrero, E.; Ahmed, M. The Role of Stereotactic Ablative Radiotherapy (SBRT) in the Management of Oligometastatic Non Small Cell Lung Cancer. *Lung Cancer Amst. Neth.* **2016**, *92*, 22–28. https://doi.org/10.1016/j.lungcan.2015.11.015.
13. De Ruysscher, D.; Wanders, R.; van Baardwijk, A.; Dingemans, A.-M.C.; Reymen, B.; Houben, R.; Bootsma, G.; Pitz, C.; van Eijsden, L.; Geraedts, W.; et al. Radical Treatment of Non-Small-Cell Lung Cancer Patients with Synchronous Oligometastases: Long-Term Results of a Prospective Phase II Trial (Nct01282450). *J. Thorac. Oncol. Off. Publ. Int. Assoc. Study Lung Cancer* **2012**, *7*, 1547–1555. https://doi.org/10.1097/JTO.0b013e318262caf6.
14. Salama, J.K.; Hasselle, M.D.; Chmura, S.J.; Malik, R.; Mehta, N.; Yenice, K.M.; Villaflor, V.M.; Stadler, W.M.; Hoffman, P.C.; Cohen, E.E.W.; et al. Stereotactic Body Radiotherapy for Multisite Extracranial Oligometastases: Final Report of a Dose Escalation Trial in Patients with 1 to 5 Sites of Metastatic Disease. *Cancer* **2012**, *118*, 2962–2970. https://doi.org/10.1002/cncr.26611.
15. Nordlinger, B.; Guiguet, M.; Vaillant, J.C.; Balladur, P.; Boudjema, K.; Bachellier, P.; Jaeck, D. Surgical Resection of Colorectal Carcinoma Metastases to the Liver. A Prognostic Scoring System to Improve Case Selection, Based on 1568 Patients. Association Française de Chirurgie. *Cancer* **1996**, *77*, 1254–1262.
16. Tanvetyanon, T.; Robinson, L.A.; Schell, M.J.; Strong, V.E.; Kapoor, R.; Coit, D.G.; Bepler, G. Outcomes of Adrenalectomy for Isolated Synchronous versus Metachronous Adrenal Metastases in Non-Small-Cell Lung Cancer: A Systematic Review and Pooled Analysis. *J. Clin. Oncol. Off. J. Am. Soc. Clin. Oncol.* **2008**, *26*, 1142–1147. https://doi.org/10.1200/JCO.2007.14.2091.
17. Selzner, M.; Morse, M.A.; Vredenburgh, J.J.; Meyers, W.C.; Clavien, P.A. Liver Metastases from Breast Cancer: Long-Term Survival after Curative Resection. *Surgery* **2000**, *127*, 383–389. https://doi.org/10.1067/msy.2000.103883.
18. Palma, D.A.; Salama, J.K.; Lo, S.S.; Senan, S.; Treasure, T.; Govindan, R.; Weichselbaum, R. The Oligometastatic State—Separating Truth from Wishful Thinking. *Nat. Rev. Clin. Oncol.* **2014**, *11*, 549–557. https://doi.org/10.1038/nrclinonc.2014.96.
19. Dilworth, J.T.; Krueger, S.A.; Wilson, G.D.; Marples, B. Preclinical Models for Translational Research Should Maintain Pace with Modern Clinical Practice. *Int. J. Radiat. Oncol. Biol. Phys.* **2014**, *88*, 540–544. https://doi.org/10.1016/j.ijrobp.2013.11.209.
20. Sharma, R.A.; Plummer, R.; Stock, J.K.; Greenhalgh, T.A.; Ataman, O.; Kelly, S.; Clay, R.; Adams, R.A.; Baird, R.D.; Billingham, L.; et al. Clinical Development of New Drug-Radiotherapy Combinations. *Nat. Rev. Clin. Oncol.* **2016**, *13*, 627–642. https://doi.org/10.1038/nrclinonc.2016.79.
21. Park, H.J.; Griffin, R.J.; Hui, S.; Levitt, S.H.; Song, C.W. Radiation-Induced Vascular Damage in Tumors: Implications of Vascular Damage in Ablative Hypofractionated Radiotherapy (SBRT and SRS). *Radiat. Res.* **2012**, *177*, 311–327. https://doi.org/10.1667/rr2773.1.
22. Song, C.; Hong, B.-J.; Bok, S.; Lee, C.-J.; Kim, Y.-E.; Jeon, S.-R.; Wu, H.-G.; Lee, Y.-S.; Cheon, G.J.; Paeng, J.C.; et al. Real-Time Tumor Oxygenation Changes after Single High-Dose Radiation Therapy in Orthotopic and Subcutaneous Lung Cancer in Mice: Clinical Implication for Stereotactic Ablative Radiation Therapy Schedule Optimization. *Int. J. Radiat. Oncol. Biol. Phys.* **2016**, *95*, 1022–1031. https://doi.org/10.1016/j.ijrobp.2016.01.064.
23. Macià, I.; Garau, M. Radiobiology of Stereotactic Body Radiation Therapy (SBRT). *Rep. Pract. Oncol. Radiother. J. Gt. Cancer Cent. Poznan Pol. Soc. Radiat. Oncol.* **2017**, *22*, 86–95. https://doi.org/10.1016/j.rpor.2017.02.010.
24. Hidalgo, M.; Amant, F.; Biankin, A.V.; Budinská, E.; Byrne, A.T.; Caldas, C.; Clarke, R.B.; de Jong, S.; Jonkers, J.; Mælandsmo, G.M.; et al. Patient-Derived Xenograft Models: An Emerging Platform for Translational Cancer Research. *Cancer Discov.* **2014**, *4*, 998–1013. https://doi.org/10.1158/2159-8290.CD-14-0001.
25. Williams, S.A.; Anderson, W.C.; Santaguida, M.T.; Dylla, S.J. Patient-Derived Xenografts, the Cancer Stem Cell Paradigm, and Cancer Pathobiology in the 21st Century. *Lab. Investig.* **2013**, *93*, 970–982. https://doi.org/10.1038/labinvest.2013.92.
26. Daniel, V.C.; Marchionni, L.; Hierman, J.S.; Rhodes, J.T.; Devereux, W.L.; Rudin, C.M.; Yung, R.; Parmigiani, G.; Dorsch, M.; Peacock, C.D.; et al. A Primary Xenograft Model of Small-Cell Lung Cancer Reveals Irreversible Changes in Gene Expression Imposed by Culture In Vitro. *Cancer Res.* **2009**, *69*, 3364–3373. https://doi.org/10.1158/0008-5472.CAN-08-4210.

27. Tentler, J.J.; Tan, A.C.; Weekes, C.D.; Jimeno, A.; Leong, S.; Pitts, T.M.; Arcaroli, J.J.; Messersmith, W.A.; Eckhardt, S.G. Patient-Derived Tumour Xenografts as Models for Oncology Drug Development. *Nat. Rev. Clin. Oncol.* **2012**, *9*, 338–350. https://doi.org/10.1038/nrclinonc.2012.61.
28. Fertil, B.; Malaise, E.-P. Inherent Cellular Radiosensitivity as a Basic Concept for Human Tumor Radiotherapy. *Int. J. Radiat. Oncol.* **1981**, *7*, 621–629. https://doi.org/10.1016/0360-3016(81)90377-1.
29. Bernhard, E.J.; Stanbridge, E.J.; Gupta, S.; Gupta, A.K.; Soto, D.; Bakanauskas, V.J.; Cerniglia, G.J.; Muschel, R.J.; McKenna, W.G. Direct Evidence for the Contribution of Activated N-Ras and K-Ras Oncogenes to Increased Intrinsic Radiation Resistance in Human Tumor Cell Lines. *Cancer Res.* **2000**, *60*, 6597–6600.
30. Grana, T.M.; Rusyn, E.V.; Zhou, H.; Sartor, C.I.; Cox, A.D. Ras Mediates Radioresistance through Both Phosphatidylinositol 3-Kinase-Dependent and Raf-Dependent but Mitogen-Activated Protein Kinase/Extracellular Signal-Regulated Kinase Kinase-Independent Signaling Pathways. *Cancer Res.* **2002**, *62*, 4142–4150.
31. Cengel, K.A.; Voong, K.R.; Chandrasekaran, S.; Maggiorella, L.; Brunner, T.B.; Stanbridge, E.; Kao, G.D.; McKenna, W.G.; Bernhard, E.J. Oncogenic K-Ras Signals through Epidermal Growth Factor Receptor and Wild-Type H-Ras to Promote Radiation Survival in Pancreatic and Colorectal Carcinoma Cells. *Neoplasia* **2007**, *9*, 341–348. https://doi.org/10.1593/neo.06823.
32. Anakura, M.; Nachankar, A.; Kobayashi, D.; Amornwichet, N.; Hirota, Y.; Shibata, A.; Oike, T.; Nakano, T. Radiosensitivity Differences between EGFR Mutant and Wild-Type Lung Cancer Cells Are Larger at Lower Doses. *Int. J. Mol. Sci.* **2019**, *20*, 3635. https://doi.org/10.3390/ijms20153635.
33. Amornwichet, N.; Oike, T.; Shibata, A.; Nirodi, C.S.; Ogiwara, H.; Makino, H.; Kimura, Y.; Hirota, Y.; Isono, M.; Yoshida, Y.; et al. The EGFR Mutation Status Affects the Relative Biological Effectiveness of Carbon-Ion Beams in Non-Small Cell Lung Carcinoma Cells. *Sci. Rep.* **2015**, *5*, 11305. https://doi.org/10.1038/srep11305.
34. Hu, H.; Nahas, S.; Gatti, R.A. Assaying Radiosensitivity of Ataxia-Telangiectasia. In *ATM Kinase*; Humana Press: New York, NY, USA, 2017; Volume 1599, pp. 1–11. https://doi.org/10.1007/978-1-4939-6955-5_1.
35. Benali, R.; Tournier, J.M.; Chevillard, M.; Zahm, J.M.; Klossek, J.M.; Hinnrasky, J.; Gaillard, D.; Maquart, F.X.; Puchelle, E. Tubule Formation by Human Surface Respiratory Epithelial Cells Cultured in a Three-Dimensional Collagen Lattice. *Am. J. Physiol.* **1993**, *264*, L183–L192. https://doi.org/10.1152/ajplung.1993.264.2.L183.
36. Endo, H.; Okami, J.; Okuyama, H.; Kumagai, T.; Uchida, J.; Kondo, J.; Takehara, T.; Nishizawa, Y.; Imamura, F.; Higashiyama, M.; et al. Spheroid Culture of Primary Lung Cancer Cells with Neuregulin 1/HER3 Pathway Activation. *J. Thorac. Oncol. Off. Publ. Int. Assoc. Study Lung Cancer* **2013**, *8*, 131–139. https://doi.org/10.1097/JTO.0b013e3182779ccf.
37. Sachs, N.; Papaspyropoulos, A.; Zomer-van Ommen, D.D.; Heo, I.; Böttinger, L.; Klay, D.; Weeber, F.; Huelsz-Prince, G.; Iakobachvili, N.; Amatngalim, G.D.; et al. Long-Term Expanding Human Airway Organoids for Disease Modeling. *EMBO J.* **2019**, *38*, e100300. https://doi.org/10.15252/embj.2018100300.
38. van de Wetering, M.; Francies, H.E.; Francis, J.M.; Bounova, G.; Iorio, F.; Pronk, A.; van Houdt, W.; van Gorp, J.; Taylor-Weiner, A.; Kester, L.; et al. Prospective Derivation of a Living Organoid Biobank of Colorectal Cancer Patients. *Cell* **2015**, *161*, 933–945. https://doi.org/10.1016/j.cell.2015.03.053.
39. Yan, H.H.N.; Siu, H.C.; Law, S.; Ho, S.L.; Yue, S.S.K.; Tsui, W.Y.; Chan, D.; Chan, A.S.; Ma, S.; Lam, K.O.; et al. A Comprehensive Human Gastric Cancer Organoid Biobank Captures Tumor Subtype Heterogeneity and Enables Therapeutic Screening. *Cell Stem Cell* **2018**, *23*, 882–897.e11. https://doi.org/10.1016/j.stem.2018.09.016.
40. Sachs, N.; de Ligt, J.; Kopper, O.; Gogola, E.; Bounova, G.; Weeber, F.; Balgobind, A.V.; Wind, K.; Gracanin, A.; Begthel, H.; et al. A Living Biobank of Breast Cancer Organoids Captures Disease Heterogeneity. *Cell* **2018**, *172*, 373–386.e10. https://doi.org/10.1016/j.cell.2017.11.010.
41. Li, Z.; Qian, Y.; Li, W.; Liu, L.; Yu, L.; Liu, X.; Wu, G.; Wang, Y.; Luo, W.; Fang, F.; et al. Human Lung Adenocarcinoma-Derived Organoid Models for Drug Screening. *iScience* **2020**, *23*, 101411. https://doi.org/10.1016/j.isci.2020.101411.
42. Drost, J.; Clevers, H. Organoids in Cancer Research. *Nat. Rev. Cancer* **2018**, *18*, 407–418. https://doi.org/10.1038/s41568-018-0007-6.
43. Yuki, K.; Cheng, N.; Nakano, M.; Kuo, C.J. Organoid Models of Tumor Immunology. *Trends Immunol.* **2020**, *41*, 652–664. https://doi.org/10.1016/j.it.2020.06.010.
44. Regaud, C.; Nogier, T. Sterilization Rontgenienne Totale et Definitive, sans Radiodermite, Des Testicules Du Belier Adulte: Conditions de Sa Realisation. *Compt. Rend. Soc. Biol* **1911**, *70*, 202–203.
45. Raben, D.; Bianco, C.; Damiano, V.; Bianco, R.; Melisi, D.; Mignogna, C.; D'Armiento, F.P.; Cionini, L.; Bianco, A.R.; Tortora, G.; et al. Antitumor Activity of ZD6126, a Novel Vascular-Targeting Agent, Is Enhanced When Combined with ZD1839, an Epidermal Growth Factor Receptor Tyrosine Kinase Inhibitor, and Potentiates the Effects of Radiation in a Human Non-Small Cell Lung Cancer Xenograft Model. *Mol. Cancer Ther.* **2004**, *3*, 977–983.
46. McLemore, T.L.; Eggleston, J.C.; Shoemaker, R.H.; Abbott, B.J.; Bohlman, M.E.; Liu, M.C.; Fine, D.L.; Mayo, J.G.; Boyd, M.R. Comparison of Intrapulmonary, Percutaneous Intrathoracic, and Subcutaneous Models for the Propagation of Human Pulmonary and Nonpulmonary Cancer Cell Lines in Athymic Nude Mice. *Cancer Res.* **1988**, *48*, 2880–2886.
47. Akhtar, S.; Meeran, S.M.; Katiyar, N.; Katiyar, S.K. Grape Seed Proanthocyanidins Inhibit the Growth of Human Non-Small Cell Lung Cancer Xenografts by Targeting Insulin-Like Growth Factor Binding Protein-3, Tumor Cell Proliferation, and Angiogenic Factors. *Clin. Cancer Res.* **2009**, *15*, 821–831. https://doi.org/10.1158/1078-0432.CCR-08-1901.
48. Chen, Y.; Tang, Y.; Tang, Y.; Yang, Z.; Ding, G. Serine Protease from Nereis Virens Inhibits H1299 Lung Cancer Cell Proliferation via the PI3K/AKT/MTOR Pathway. *Mar. Drugs* **2019**, *17*, 366. https://doi.org/10.3390/md17060366.

49. Wang, H.; Li, M.; Rinehart, J.J.; Zhang, R. Pretreatment with Dexamethasone Increases Antitumor Activity of Carboplatin and Gemcitabine in Mice Bearing Human Cancer Xenografts: In Vivo Activity, Pharmacokinetics, and Clinical Implications for Cancer Chemotherapy. *Clin. Cancer Res. Off. J. Am. Assoc. Cancer Res.* **2004**, *10*, 1633–1644. https://doi.org/10.1158/1078-0432.ccr-0829-3.
50. Steiner, P.; Joynes, C.; Bassi, R.; Wang, S.; Tonra, J.R.; Hadari, Y.R.; Hicklin, D.J. Tumor Growth Inhibition with Cetuximab and Chemotherapy in Non–Small Cell Lung Cancer Xenografts Expressing Wild-Type and Mutated Epidermal Growth Factor Receptor. *Clin. Cancer Res.* **2007**, *13*, 1540–1551. https://doi.org/10.1158/1078-0432.CCR-06-1887.
51. Carter, C.A.; Chen, C.; Brink, C.; Vincent, P.; Maxuitenko, Y.Y.; Gilbert, K.S.; Waud, W.R.; Zhang, X. Sorafenib Is Efficacious and Tolerated in Combination with Cytotoxic or Cytostatic Agents in Preclinical Models of Human Non-Small Cell Lung Carcinoma. *Cancer Chemother. Pharmacol.* **2006**, *59*, 183–195. https://doi.org/10.1007/s00280-006-0257-y.
52. Yamori, T.; Sato, S.; Chikazawa, H.; Kadota, T. Anti-Tumor Efficacy of Paclitaxel against Human Lung Cancer Xenografts. *Jpn. J. Cancer Res.* **1997**, *88*, 1205–1210. https://doi.org/10.1111/j.1349-7006.1997.tb00350.x.
53. Wang, J.-L.; Lan, Y.-W.; Tsai, Y.-T.; Chen, Y.-C.; Staniczek, T.; Tsou, Y.-A.; Yen, C.-C.; Chen, C.-M. Additive Antiproliferative and Antiangiogenic Effects of Metformin and Pemetrexed in a Non-Small-Cell Lung Cancer Xenograft Model. *Front. Cell Dev. Biol.* **2021**, *9*, 688062. https://doi.org/10.3389/fcell.2021.688062.
54. Lam, S.K.; Li, Y.; Xu, S.; Cheng, P.; Ho, J. Inhibition of Ornithine Decarboxylase 1 Facilitates Pegylated Arginase Treatment in Lung Adenocarcinoma Xenograft Models. *Oncol. Rep.* **2018**, *40*, 1994–2004. https://doi.org/10.3892/or.2018.6598.
55. Zimonjic, D.B.; Chan, L.N.; Tripathi, V.; Lu, J.; Kwon, O.; Popescu, N.C.; Lowy, D.R.; Tamanoi, F. In Vitro and in Vivo Effects of Geranylgeranyltransferase I Inhibitor P61A6 on Non-Small Cell Lung Cancer Cells. *BMC Cancer* **2013**, *13*, 198. https://doi.org/10.1186/1471-2407-13-198.
56. Onn, A.; Isobe, T.; Itasaka, S.; Wu, W.; O'Reilly, M.S.; Ki Hong, W.; Fidler, I.J.; Herbst, R.S. Development of an Orthotopic Model to Study the Biology and Therapy of Primary Human Lung Cancer in Nude Mice. *Clin. Cancer Res. Off. J. Am. Assoc. Cancer Res.* **2003**, *9*, 5532–5539.
57. Doki, Y.; Murakami, K.; Yamaura, T.; Sugiyama, S.; Misaki, T.; Saiki, I. Mediastinal Lymph Node Metastasis Model by Orthotopic Intrapulmonary Implantation of Lewis Lung Carcinoma Cells in Mice. *Br. J. Cancer* **1999**, *79*, 1121–1126. https://doi.org/10.1038/sj.bjc.6690178.
58. Mordant, P.; Loriot, Y.; Lahon, B.; Castier, Y.; Lesèche, G.; Soria, J.-C.; Vozenin, M.-C.; Decraene, C.; Deutsch, E. Bioluminescent Orthotopic Mouse Models of Human Localized Non-Small Cell Lung Cancer: Feasibility and Identification of Circulating Tumour Cells. *PLoS ONE* **2011**, *6*, e26073. https://doi.org/10.1371/journal.pone.0026073.
59. Takahashi, O.; Komaki, R.; Smith, P.D.; Jürgensmeier, J.M.; Ryan, A.; Bekele, B.N.; Wistuba, I.I.; Jacoby, J.J.; Korshunova, M.V.; Biernacka, A.; et al. Combined MEK and VEGFR Inhibition in Orthotopic Human Lung Cancer Models Results in Enhanced Inhibition of Tumor Angiogenesis, Growth, and Metastasis. *Clin. Cancer Res. Off. J. Am. Assoc. Cancer Res.* **2012**, *18*, 1641–1654. https://doi.org/10.1158/1078-0432.CCR-11-2324.
60. Wenger, S.L.; Senft, J.R.; Sargent, L.M.; Bamezai, R.; Bairwa, N.; Grant, S.G. Comparison of Established Cell Lines at Different Passages by Karyotype and Comparative Genomic Hybridization. *Biosci. Rep.* **2004**, *24*, 631–639. https://doi.org/10.1007/s10540-005-2797-5.
61. Stone, H.B.; Peters, L.J.; Milas, L. Effect of Host Immune Capability on Radiocurability and Subsequent Transplantability of a Murine Fibrosarcoma. *J. Natl. Cancer Inst.* **1979**, *63*, 1229–1235.
62. Mondini, M.; Levy, A.; Meziani, L.; Milliat, F.; Deutsch, E. Radiotherapy–Immunotherapy Combinations—Perspectives and Challenges. *Mol. Oncol.* **2020**, *14*, 1529–1537. https://doi.org/10.1002/1878-0261.12658.
63. Ledford, H. Translational Research: 4 Ways to Fix the Clinical Trial. *Nature* **2011**, *477*, 526–528. https://doi.org/10.1038/477526a.
64. Wong, C.H.; Siah, K.W.; Lo, A.W. Estimation of Clinical Trial Success Rates and Related Parameters. *Biostatistics* **2019**, *20*, 273–286. https://doi.org/10.1093/biostatistics/kxx069.
65. Hay, M.; Thomas, D.W.; Craighead, J.L.; Economides, C.; Rosenthal, J. Clinical Development Success Rates for Investigational Drugs. *Nat. Biotechnol.* **2014**, *32*, 40–51. https://doi.org/10.1038/nbt.2786.
66. Flanagan, S.P. "Nude", a New Hairless Gene with Pleiotropic Effects in the Mouse. *Genet. Res.* **1966**, *8*, 295–309. https://doi.org/10.1017/s0016672300010168.
67. Bosma, G.C.; Custer, R.P.; Bosma, M.J. A Severe Combined Immunodeficiency Mutation in the Mouse. *Nature* **1983**, *301*, 527–530. https://doi.org/10.1038/301527a0.
68. Ishikawa, F.; Yasukawa, M.; Lyons, B.; Yoshida, S.; Miyamoto, T.; Yoshimoto, G.; Watanabe, T.; Akashi, K.; Shultz, L.D.; Harada, M. Development of Functional Human Blood and Immune Systems in NOD/SCID/IL2 Receptor γ Chain^{null} Mice. *Blood* **2005**, *106*, 1565–1573. https://doi.org/10.1182/blood-2005-02-0516.
69. Mombaerts, P.; Iacomini, J.; Johnson, R.S.; Herrup, K.; Tonegawa, S.; Papaioannou, V.E. RAG-1-Deficient Mice Have No Mature B and T Lymphocytes. *Cell* **1992**, *68*, 869–877. https://doi.org/10.1016/0092-8674(92)90030-g.
70. Shinkai, Y.; Rathbun, G.; Lam, K.P.; Oltz, E.M.; Stewart, V.; Mendelsohn, M.; Charron, J.; Datta, M.; Young, F.; Stall, A.M. RAG-2-Deficient Mice Lack Mature Lymphocytes Owing to Inability to Initiate V(D)J Rearrangement. *Cell* **1992**, *68*, 855–867. https://doi.org/10.1016/0092-8674(92)90029-c.
71. Cao, X.; Shores, E.W.; Hu-Li, J.; Anver, M.R.; Kelsall, B.L.; Russell, S.M.; Drago, J.; Noguchi, M.; Grinberg, A.; Bloom, E.T. Defective Lymphoid Development in Mice Lacking Expression of the Common Cytokine Receptor Gamma Chain. *Immunity* **1995**, *2*, 223–238. https://doi.org/10.1016/1074-7613(95)90047-0.

72. Rübe, C.E.; Fricke, A.; Wendorf, J.; Stützel, A.; Kühne, M.; Ong, M.F.; Lipp, P.; Rübe, C. Accumulation of DNA Double-Strand Breaks in Normal Tissues after Fractionated Irradiation. *Int. J. Radiat. Oncol. Biol. Phys.* **2010**, *76*, 1206–1213. https://doi.org/10.1016/j.ijrobp.2009.10.009.
73. Budach, W.; Hartford, A.; Gioioso, D.; Freeman, J.; Taghian, A.; Suit, H.D. Tumors Arising in SCID Mice Share Enhanced Radiation Sensitivity of SCID Normal Tissues. *Cancer Res.* **1992**, *52*, 6292–6296.
74. Cassidy, J.W.; Caldas, C.; Bruna, A. Maintaining Tumor Heterogeneity in Patient-Derived Tumor Xenografts. *Cancer Res.* **2015**, *75*, 2963–2968. https://doi.org/10.1158/0008-5472.CAN-15-0727.
75. Crystal, A.S.; Shaw, A.T.; Sequist, L.V.; Friboulet, L.; Niederst, M.J.; Lockerman, E.L.; Frias, R.L.; Gainor, J.F.; Amzallag, A.; Greninger, P.; et al. Patient-Derived Models of Acquired Resistance Can Identify Effective Drug Combinations for Cancer. *Science* **2014**, *346*, 1480–1486. https://doi.org/10.1126/science.1254721.
76. Bertram, J.S.; Janik, P. Establishment of a Cloned Line of Lewis Lung Carcinoma Cells Adapted to Cell Culture. *Cancer Lett.* **1980**, *11*, 63–73. https://doi.org/10.1016/0304-3835(80)90130-5.
77. Layton, M.G.; Franks, L.M. Heterogeneity in a Spontaneous Mouse Lung Carcinoma: Selection and Characterisation of Stable Metastatic Variants. *Br. J. Cancer* **1984**, *49*, 415–421. https://doi.org/10.1038/bjc.1984.67.
78. Nolan, K.; Verzosa, G.; Cleaver, T.; Tippimanchai, D.; DePledge, L.N.; Wang, X.-J.; Young, C.; Le, A.; Doebele, R.; Li, H.; et al. Development of Syngeneic Murine Cell Lines for Use in Immunocompetent Orthotopic Lung Cancer Models. *Cancer Cell Int.* **2020**, *20*, 417. https://doi.org/10.1186/s12935-020-01503-5.
79. Sausville, E.A.; Burger, A.M. Contributions of Human Tumor Xenografts to Anticancer Drug Development. *Cancer Res.* **2006**, *66*, 3351–3354. https://doi.org/10.1158/0008-5472.CAN-05-3627.
80. Nakasone, E.S.; Askautrud, H.A.; Kees, T.; Park, J.-H.; Plaks, V.; Ewald, A.J.; Fein, M.; Rasch, M.G.; Tan, Y.-X.; Qiu, J.; et al. Imaging Tumor-Stroma Interactions during Chemotherapy Reveals Contributions of the Microenvironment to Resistance. *Cancer Cell* **2012**, *21*, 488–503. https://doi.org/10.1016/j.ccr.2012.02.017.
81. Devaud, C.; Westwood, J.A.; John, L.B.; Flynn, J.K.; Paquet-Fifield, S.; Duong, C.P.M.; Yong, C.S.M.; Pegram, H.J.; Stacker, S.A.; Achen, M.G.; et al. Tissues in Different Anatomical Sites Can Sculpt and Vary the Tumor Microenvironment to Affect Responses to Therapy. *Mol. Ther. J. Am. Soc. Gene Ther.* **2014**, *22*, 18–27. https://doi.org/10.1038/mt.2013.219.
82. Quail, D.F.; Joyce, J.A. Microenvironmental Regulation of Tumor Progression and Metastasis. *Nat. Med.* **2013**, *19*, 1423–1437. https://doi.org/10.1038/nm.3394.
83. Hanahan, D.; Coussens, L.M. Accessories to the Crime: Functions of Cells Recruited to the Tumor Microenvironment. *Cancer Cell* **2012**, *21*, 309–322. https://doi.org/10.1016/j.ccr.2012.02.022.
84. Gray, L.H.; Conger, A.D.; Ebert, M.; Hornsey, S.; Scott, O.C.A. The Concentration of Oxygen Dissolved in Tissues at the Time of Irradiation as a Factor in Radiotherapy. *Br. J. Radiol.* **1953**, *26*, 638–648. https://doi.org/10.1259/0007-1285-26-312-638.
85. Tatum, J.L. Hypoxia: Importance in Tumor Biology, Noninvasive Measurement by Imaging, and Value of Its Measurement in the Management of Cancer Therapy. *Int. J. Radiat. Biol.* **2006**, *82*, 699–757. https://doi.org/10.1080/09553000601002324.
86. Maity, A.; Koumenis, C. Location, Location, Location-Makes All the Difference for Hypoxia in Lung Tumors: Fig. 1. *Clin. Cancer Res.* **2010**, *16*, 4685–4687. https://doi.org/10.1158/1078-0432.CCR-10-2004.
87. Graves, E.E.; Vilalta, M.; Cecic, I.K.; Erler, J.T.; Tran, P.T.; Felsher, D.; Sayles, L.; Sweet-Cordero, A.; Le, Q.-T.; Giaccia, A.J. Hypoxia in Models of Lung Cancer: Implications for Targeted Therapeutics. *Clin. Cancer Res. Off. J. Am. Assoc. Cancer Res.* **2010**, *16*, 4843–4852. https://doi.org/10.1158/1078-0432.CCR-10-1206.
88. Tran Chau, V.; Liu, W.; Gerbé de Thoré, M.; Meziani, L.; Mondini, M.; O'Connor, M.J.; Deutsch, E.; Clémenson, C. Differential Therapeutic Effects of PARP and ATR Inhibition Combined with Radiotherapy in the Treatment of Subcutaneous versus Orthotopic Lung Tumour Models. *Br. J. Cancer* **2020**, *123*, 762–771. https://doi.org/10.1038/s41416-020-0931-6.
89. Nakajima, T.; Anayama, T.; Matsuda, Y.; Hwang, D.M.; McVeigh, P.Z.; Wilson, B.C.; Zheng, G.; Keshavjee, S.; Yasufuku, K. Orthotopic Lung Cancer Murine Model by Nonoperative Transbronchial Approach. *Ann. Thorac. Surg.* **2014**, *97*, 1771–1775. https://doi.org/10.1016/j.athoracsur.2014.01.048.
90. Capecchi, M.R. Gene Targeting in Mice: Functional Analysis of the Mammalian Genome for the Twenty-First Century. *Nat. Rev. Genet.* **2005**, *6*, 507–512. https://doi.org/10.1038/nrg1619.
91. Dow, L.E. Modeling Disease In Vivo with CRISPR/Cas9. *Trends Mol. Med.* **2015**, *21*, 609–621. https://doi.org/10.1016/j.molmed.2015.07.006.
92. Ramelow, J.; Brooks, C.D.; Gao, L.; Almiman, A.A.; Williams, T.M.; Villalona-Calero, M.A.; Duan, W. The Oncogenic Potential of a Mutant TP53 Gene Explored in Two Spontaneous Lung Cancer Mice Models. *BMC Cancer* **2020**, *20*, 738. https://doi.org/10.1186/s12885-020-07212-6.
93. Herter-Sprie, G.S.; Koyama, S.; Korideck, H.; Hai, J.; Deng, J.; Li, Y.Y.; Buczkowski, K.A.; Grant, A.K.; Ullas, S.; Rhee, K.; et al. Synergy of Radiotherapy and PD-1 Blockade in Kras-Mutant Lung Cancer. *JCI Insight* **2016**, *1*, e87415. https://doi.org/10.1172/jci.insight.87415.
94. Rampetsreiter, P.; Casanova, E.; Eferl, R. Genetically Modified Mouse Models of Cancer Invasion and Metastasis. *Drug Discov. Today Dis. Models* **2011**, *8*, 67–74. https://doi.org/10.1016/j.ddmod.2011.05.003.
95. Antonia, S.J.; Villegas, A.; Daniel, D.; Vicente, D.; Murakami, S.; Hui, R.; Kurata, T.; Chiappori, A.; Lee, K.H.; de Wit, M.; et al. Overall Survival with Durvalumab after Chemoradiotherapy in Stage III NSCLC. *N. Engl. J. Med.* **2018**, *379*, 2342–2350. https://doi.org/10.1056/NEJMoa1809697.

96. Durm, G.A.; Jabbour, S.K.; Althouse, S.K.; Liu, Z.; Sadiq, A.A.; Zon, R.T.; Jalal, S.I.; Kloecker, G.H.; Williamson, M.J.; Reckamp, K.L.; et al. A Phase 2 Trial of Consolidation Pembrolizumab Following Concurrent Chemoradiation for Patients with Unresectable Stage III Non–Small Cell Lung Cancer: Hoosier Cancer Research Network LUN 14-179. *Cancer* **2020**, *126*, 4353–4361. https://doi.org/10.1002/cncr.33083.
97. McLaughlin, M.F.; Alam, M.; Smith, L.; Ryckman, J.; Lin, C.; Baine, M.J. Stereotactic Body Radiation Therapy Mitigates Radiation Induced Lymphopenia in Early Stage Non-Small Cell Lung Cancer. *PLoS ONE* **2020**, *15*, e0241505. https://doi.org/10.1371/journal.pone.0241505.
98. Chen, D.; Patel, R.R.; Verma, V.; Ramapriyan, R.; Barsoumian, H.B.; Cortez, M.A.; Welsh, J.W. Interaction between Lymphopenia, Radiotherapy Technique, Dosimetry, and Survival Outcomes in Lung Cancer Patients Receiving Combined Immunotherapy and Radiotherapy. *Radiother. Oncol.* **2020**, *150*, 114–120. https://doi.org/10.1016/j.radonc.2020.05.051.
99. Zhao, X.-Y.; Wang, X.-Y.; Wei, Q.-Y.; Xu, Y.-M.; Lau, A.T.Y. Potency and Selectivity of SMAC/DIABLO Mimetics in Solid Tumor Therapy. *Cells* **2020**, *9*, 1012. https://doi.org/10.3390/cells9041012.
100. Morrish, E.; Brumatti, G.; Silke, J. Future Therapeutic Directions for Smac-Mimetics. *Cells* **2020**, *9*, 406. https://doi.org/10.3390/cells9020406.
101. Eytan, D.F.; Snow, G.E.; Carlson, S.; Derakhshan, A.; Saleh, A.; Schiltz, S.; Cheng, H.; Mohan, S.; Cornelius, S.; Coupar, J.; et al. SMAC Mimetic Birinapant plus Radiation Eradicates Human Head and Neck Cancers with Genomic Amplifications of Cell Death Genes FADD and BIRC2. *Cancer Res.* **2016**, *76*, 5442–5454. https://doi.org/10.1158/0008-5472.CAN-15-3317.
102. Tao, Z.; McCall, N.S.; Wiedemann, N.; Vuagniaux, G.; Yuan, Z.; Lu, B. SMAC Mimetic Debio 1143 and Ablative Radiation Therapy Synergize to Enhance Antitumor Immunity against Lung Cancer. *Clin. Cancer Res. Off. J. Am. Assoc. Cancer Res.* **2019**, *25*, 1113–1124. https://doi.org/10.1158/1078-0432.CCR-17-3852.
103. Younes, A.I.; Barsoumian, H.B.; Sezen, D.; Verma, V.; Patel, R.; Wasley, M.; Hu, Y.; Dunn, J.D.; He, K.; Chen, D.; et al. Addition of TLR9 Agonist Immunotherapy to Radiation Improves Systemic Antitumor Activity. *Transl. Oncol.* **2021**, *14*, 100983. https://doi.org/10.1016/j.tranon.2020.100983.
104. Finkelstein, S.E.; Iclozan, C.; Bui, M.M.; Cotter, M.J.; Ramakrishnan, R.; Ahmed, J.; Noyes, D.R.; Cheong, D.; Gonzalez, R.J.; Heysek, R.V.; et al. Combination of External Beam Radiotherapy (EBRT) with Intratumoral Injection of Dendritic Cells as Neo-Adjuvant Treatment of High-Risk Soft Tissue Sarcoma Patients. *Int. J. Radiat. Oncol. Biol. Phys.* **2012**, *82*, 924–932. https://doi.org/10.1016/j.ijrobp.2010.12.068.
105. Finkelstein, S.E.; Rodriguez, F.; Dunn, M.; Farmello, M.-J.; Smilee, R.; Janssen, W.; Kang, L.; Chuang, T.; Seigne, J.; Pow-Sang, J.; et al. Serial Assessment of Lymphocytes and Apoptosis in the Prostate during Coordinated Intraprostatic Dendritic Cell Injection and Radiotherapy. *Immunotherapy* **2012**, *4*, 373–382. https://doi.org/10.2217/imt.12.24.
106. Sun, L.; Chen, B.; Jiang, R.; Li, J.; Wang, B. Resveratrol Inhibits Lung Cancer Growth by Suppressing M2-like Polarization of Tumor Associated Macrophages. *Cell. Immunol.* **2017**, *311*, 86–93. https://doi.org/10.1016/j.cellimm.2016.11.002.
107. Lan, Y.; Moustafa, M.; Knoll, M.; Xu, C.; Furkel, J.; Lazorchak, A.; Yeung, T.-L.; Hasheminasab, S.-M.; Jenkins, M.H.; Meister, S.; et al. Simultaneous Targeting of TGF-β/PD-L1 Synergizes with Radiotherapy by Reprogramming the Tumor Microenvironment to Overcome Immune Evasion. *Cancer Cell* **2021**, *39*, 1388–1403.e10. https://doi.org/10.1016/j.ccell.2021.08.008.
108. Demaria, S.; Guha, C.; Schoenfeld, J.; Morris, Z.; Monjazeb, A.; Sikora, A.; Crittenden, M.; Shiao, S.; Khleif, S.; Gupta, S.; et al. Radiation Dose and Fraction in Immunotherapy: One-Size Regimen Does Not Fit All Settings, so How Does One Choose? *J. Immunother. Cancer* **2021**, *9*, e002038. https://doi.org/10.1136/jitc-2020-002038.
109. Young, K.H.; Baird, J.R.; Savage, T.; Cottam, B.; Friedman, D.; Bambina, S.; Messenheimer, D.J.; Fox, B.; Newell, P.; Bahjat, K.S.; et al. Optimizing Timing of Immunotherapy Improves Control of Tumors by Hypofractionated Radiation Therapy. *PLoS ONE* **2016**, *11*, e0157164. https://doi.org/10.1371/journal.pone.0157164.
110. Dovedi, S.J.; Adlard, A.L.; Lipowska-Bhalla, G.; McKenna, C.; Jones, S.; Cheadle, E.J.; Stratford, I.J.; Poon, E.; Morrow, M.; Stewart, R.; et al. Acquired Resistance to Fractionated Radiotherapy Can Be Overcome by Concurrent PD-L1 Blockade. *Cancer Res.* **2014**, *74*, 5458–5468. https://doi.org/10.1158/0008-5472.CAN-14-1258.
111. Welsh, J.W.; Heymach, J.V.; Guo, C.; Menon, H.; Klein, K.; Cushman, T.R.; Verma, V.; Hess, K.R.; Shroff, G.; Tang, C.; et al. Phase 1/2 Trial of Pembrolizumab and Concurrent Chemoradiation Therapy for Limited-Stage SCLC. *J. Thorac. Oncol. Off. Publ. Int. Assoc. Study Lung Cancer* **2020**, *15*, 1919–1927. https://doi.org/10.1016/j.jtho.2020.08.022.
112. Formenti, S.C.; Rudqvist, N.-P.; Golden, E.; Cooper, B.; Wennerberg, E.; Lhuillier, C.; Vanpouille-Box, C.; Friedman, K.; Ferrari de Andrade, L.; Wucherpfennig, K.W.; et al. Radiotherapy Induces Responses of Lung Cancer to CTLA-4 Blockade. *Nat. Med.* **2018**, *24*, 1845–1851. https://doi.org/10.1038/s41591-018-0232-2.
113. Samstein, R.; Rimner, A.; Barker, C.A.; Yamada, Y. Combined Immune Checkpoint Blockade and Radiation Therapy: Timing and Dose Fractionation Associated with Greatest Survival Duration Among Over 750 Treated Patients. *Int. J. Radiat. Oncol.* **2017**, *99*, S129–S130. https://doi.org/10.1016/j.ijrobp.2017.06.303.
114. Meng, J.; Li, P.; Zhang, Q.; Yang, Z.; Fu, S. A Radiosensitivity Gene Signature in Predicting Glioma Prognostic via EMT Pathway. *Oncotarget* **2014**, *5*, 4683–4693. https://doi.org/10.18632/oncotarget.2088.
115. Weichselbaum, R.R.; Ishwaran, H.; Yoon, T.; Nuyten, D.S.A.; Baker, S.W.; Khodarev, N.; Su, A.W.; Shaikh, A.Y.; Roach, P.; Kreike, B.; et al. An Interferon-Related Gene Signature for DNA Damage Resistance Is a Predictive Marker for Chemotherapy and Radiation for Breast Cancer. *Proc. Natl. Acad. Sci. USA* **2008**, *105*, 18490–18495. https://doi.org/10.1073/pnas.0809242105.

116. Scott, J.G.; Berglund, A.; Schell, M.J.; Mihaylov, I.; Fulp, W.J.; Yue, B.; Welsh, E.; Caudell, J.J.; Ahmed, K.; Strom, T.S.; et al. A Genome-Based Model for Adjusting Radiotherapy Dose (GARD): A Retrospective, Cohort-Based Study. *Lancet Oncol.* **2017**, *18*, 202–211. https://doi.org/10.1016/S1470-2045(16)30648-9.
117. He, J.; Feng, X.; Hua, J.; Wei, L.; Lu, Z.; Wei, W.; Cai, H.; Wang, B.; Shi, W.; Ding, N.; et al. MiR-300 Regulates Cellular Radiosensitivity through Targeting P53 and Apaf1 in Human Lung Cancer Cells. *Cell Cycle Georget. Tex* **2017**, *16*, 1943–1953. https://doi.org/10.1080/15384101.2017.1367070.
118. Hill, R.P.; Bristow, R.G.; Fyles, A.; Koritzinsky, M.; Milosevic, M.; Wouters, B.G. Hypoxia and Predicting Radiation Response. *Semin. Radiat. Oncol.* **2015**, *25*, 260–272. https://doi.org/10.1016/j.semradonc.2015.05.004.
119. Fridman, W.H.; Zitvogel, L.; Sautès-Fridman, C.; Kroemer, G. The Immune Contexture in Cancer Prognosis and Treatment. *Nat. Rev. Clin. Oncol.* **2017**, *14*, 717–734. https://doi.org/10.1038/nrclinonc.2017.101.
120. Schumacher, T.N.; Schreiber, R.D. Neoantigens in Cancer Immunotherapy. *Science* **2015**, *348*, 69–74. https://doi.org/10.1126/science.aaa4971.
121. Le, D.T.; Durham, J.N.; Smith, K.N.; Wang, H.; Bartlett, B.R.; Aulakh, L.K.; Lu, S.; Kemberling, H.; Wilt, C.; Luber, B.S.; et al. Mismatch Repair Deficiency Predicts Response of Solid Tumors to PD-1 Blockade. *Science* **2017**, *357*, 409–413. https://doi.org/10.1126/science.aan6733.
122. López-Soto, A.; Gonzalez, S.; Smyth, M.J.; Galluzzi, L. Control of Metastasis by NK Cells. *Cancer Cell* **2017**, *32*, 135–154. https://doi.org/10.1016/j.ccell.2017.06.009.
123. Ruocco, M.G.; Pilones, K.A.; Kawashima, N.; Cammer, M.; Huang, J.; Babb, J.S.; Liu, M.; Formenti, S.C.; Dustin, M.L.; Demaria, S. Suppressing T Cell Motility Induced by Anti-CTLA-4 Monotherapy Improves Antitumor Effects. *J. Clin. Investig.* **2012**, *122*, 3718–3730. https://doi.org/10.1172/JCI61931.
124. Vanpouille-Box, C.; Alard, A.; Aryankalayil, M.J.; Sarfraz, Y.; Diamond, J.M.; Schneider, R.J.; Inghirami, G.; Coleman, C.N.; Formenti, S.C.; Demaria, S. DNA Exonuclease Trex1 Regulates Radiotherapy-Induced Tumour Immunogenicity. *Nat. Commun.* **2017**, *8*, 15618. https://doi.org/10.1038/ncomms15618.
125. Sun, R.; Limkin, E.J.; Vakalopoulou, M.; Dercle, L.; Champiat, S.; Han, S.R.; Verlingue, L.; Brandao, D.; Lancia, A.; Ammari, S.; et al. A Radiomics Approach to Assess Tumour-Infiltrating CD8 Cells and Response to Anti-PD-1 or Anti-PD-L1 Immunotherapy: An Imaging Biomarker, Retrospective Multicohort Study. *Lancet Oncol.* **2018**, *19*, 1180–1191. https://doi.org/10.1016/S1470-2045(18)30413-3.
126. Fornacon-Wood, I.; Faivre-Finn, C.; O'Connor, J.P.B.; Price, G.J. Radiomics as a Personalized Medicine Tool in Lung Cancer: Separating the Hope from the Hype. *Lung Cancer Amst. Neth.* **2020**, *146*, 197–208. https://doi.org/10.1016/j.lungcan.2020.05.028.
127. Beasley, M.; Driver, D.; Dobbs, H.J. Complications of Radiotherapy: Improving the Therapeutic Index. *Cancer Imaging Off. Publ. Int. Cancer Imaging Soc.* **2005**, *5*, 78–84. https://doi.org/10.1102/1470-7330.2005.0012.
128. Kang, K.H.; Okoye, C.C.; Patel, R.B.; Siva, S.; Biswas, T.; Ellis, R.J.; Yao, M.; Machtay, M.; Lo, S.S. Complications from Stereotactic Body Radiotherapy for Lung Cancer. *Cancers* **2015**, *7*, 981–1004. https://doi.org/10.3390/cancers7020820.
129. De Rose, F.; Franceschini, D.; Reggiori, G.; Stravato, A.; Navarria, P.; Ascolese, A.M.; Tomatis, S.; Mancosu, P.; Scorsetti, M. Organs at Risk in Lung SBRT. *Phys. Medica PM Int. J. Devoted Appl. Phys. Med. Biol. Off. J. Ital. Assoc. Biomed. Phys. AIFB* **2017**, *44*, 131–138. https://doi.org/10.1016/j.ejmp.2017.04.010.
130. Jain, V.; Berman, A.T. Radiation Pneumonitis: Old Problem, New Tricks. *Cancers* **2018**, *10*, 222. https://doi.org/10.3390/cancers10070222.
131. Curigliano, G.; Cardinale, D.; Dent, S.; Criscitiello, C.; Aseyev, O.; Lenihan, D.; Cipolla, C.M. Cardiotoxicity of Anticancer Treatments: Epidemiology, Detection, and Management. *CA Cancer J. Clin.* **2016**, *66*, 309–325. https://doi.org/10.3322/caac.21341.
132. Tapio, S. Pathology and Biology of Radiation-Induced Cardiac Disease. *J. Radiat. Res.* **2016**, *57*, 439–448. https://doi.org/10.1093/jrr/rrw064.
133. Wijerathne, H.; Langston, J.C.; Yang, Q.; Sun, S.; Miyamoto, C.; Kilpatrick, L.E.; Kiani, M.F. Mechanisms of Radiation-Induced Endothelium Damage: Emerging Models and Technologies. *Radiother. Oncol.* **2021**, *158*, 21–32. https://doi.org/10.1016/j.radonc.2021.02.007.
134. Satyamitra, M.M.; DiCarlo, A.L.; Taliaferro, L. Understanding the Pathophysiology and Challenges of Development of Medical Countermeasures for Radiation-Induced Vascular/Endothelial Cell Injuries: Report of a NIAID Workshop, August 20, 2015. *Radiat. Res.* **2016**, *186*, 99–111. https://doi.org/10.1667/RR14436.1.
135. Timmerman, R.; McGarry, R.; Yiannoutsos, C.; Papiez, L.; Tudor, K.; DeLuca, J.; Ewing, M.; Abdulrahman, R.; DesRosiers, C.; Williams, M.; et al. Excessive Toxicity When Treating Central Tumors in a Phase II Study of Stereotactic Body Radiation Therapy for Medically Inoperable Early-Stage Lung Cancer. *J. Clin. Oncol. Off. J. Am. Soc. Clin. Oncol.* **2006**, *24*, 4833–4839. https://doi.org/10.1200/JCO.2006.07.5937.
136. Chang, J.Y.; Li, Q.-Q.; Xu, Q.-Y.; Allen, P.K.; Rebueno, N.; Gomez, D.R.; Balter, P.; Komaki, R.; Mehran, R.; Swisher, S.G.; et al. Stereotactic Ablative Radiation Therapy for Centrally Located Early Stage or Isolated Parenchymal Recurrences of Non-Small Cell Lung Cancer: How to Fly in a "No Fly Zone". *Int. J. Radiat. Oncol. Biol. Phys.* **2014**, *88*, 1120–1128. https://doi.org/10.1016/j.ijrobp.2014.01.022.
137. Lindberg, K.; Grozman, V.; Karlsson, K.; Lindberg, S.; Lax, I.; Wersäll, P.; Persson, G.F.; Josipovic, M.; Khalil, A.A.; Moeller, D.S.; et al. The HILUS-Trial—A Prospective Nordic Multicenter Phase 2 Study of Ultracentral Lung Tumors Treated With Stereotactic Body Radiotherapy. *J. Thorac. Oncol.* **2021**, *16*, 1200–1210. https://doi.org/10.1016/j.jtho.2021.03.019.

138. Tekatli, H.; Haasbeek, N.; Dahele, M.; De Haan, P.; Verbakel, W.; Bongers, E.; Hashemi, S.; Nossent, E.; Spoelstra, F.; de Langen, A.J.; et al. Outcomes of Hypofractionated High-Dose Radiotherapy in Poor-Risk Patients with "Ultracentral" Non-Small Cell Lung Cancer. *J. Thorac. Oncol. Off. Publ. Int. Assoc. Study Lung Cancer* **2016**, *11*, 1081–1089. https://doi.org/10.1016/j.jtho.2016.03.008.
139. Shaverdian, N.; Lisberg, A.E.; Bornazyan, K.; Veruttipong, D.; Goldman, J.W.; Formenti, S.C.; Garon, E.B.; Lee, P. Previous Radiotherapy and the Clinical Activity and Toxicity of Pembrolizumab in the Treatment of Non-Small-Cell Lung Cancer: A Secondary Analysis of the KEYNOTE-001 Phase 1 Trial. *Lancet Oncol.* **2017**, *18*, 895–903. https://doi.org/10.1016/S1470-2045(17)30380-7.
140. Zhu, L.; Yu, X.; Wang, L.; Liu, J.; Qu, Z.; Zhang, H.; Li, L.; Chen, J.; Zhou, Q. Angiogenesis and Immune Checkpoint Dual Blockade in Combination with Radiotherapy for Treatment of Solid Cancers: Opportunities and Challenges. *Oncogenesis* **2021**, *10*, 47. https://doi.org/10.1038/s41389-021-00335-w.

15 REFERENCES

Abraha, I., Aristei, C., Palumbo, I., Lupattelli, M., Trastulli, S., Cirocchi, R., De Florio, R., Valentini, V., 2018. Preoperative radiotherapy and curative surgery for the management of localised rectal carcinoma. Cochrane Database Syst Rev 10, CD002102. https://doi.org/10.1002/14651858.CD002102.pub3

Allam, A., Taghian, A., Gioioso, D., Duffy, M., Suit, H.D., 1993. Intratumoral heterogeneity of malignant gliomas measured in vitro. International Journal of Radiation Oncology*Biology*Physics 27, 303–308. https://doi.org/10.1016/0360-3016(93)90241-M

Andreyev, H.J., Norman, A.R., Cunningham, D., Oates, J., Dix, B.R., Iacopetta, B.J., Young, J., Walsh, T., Ward, R., Hawkins, N., Beranek, M., Jandik, P., Benamouzig, R., Jullian, E., Laurent-Puig, P., Olschwang, S., Muller, O., Hoffmann, I., Rabes, H.M., Zietz, C., Troungos, C., Valavanis, C., Yuen, S.T., Ho, J.W., Croke, C.T., O'Donoghue, D.P., Giaretti, W., Rapallo, A., Russo, A., Bazan, V., Tanaka, M., Omura, K., Azuma, T., Ohkusa, T., Fujimori, T., Ono, Y., Pauly, M., Faber, C., Glaesener, R., de Goeij, A.F., Arends, J.W., Andersen, S.N., Lövig, T., Breivik, J., Gaudernack, G., Clausen, O.P., De Angelis, P.D., Meling, G.I., Rognum, T.O., Smith, R., Goh, H.S., Font, A., Rosell, R., Sun, X.F., Zhang, H., Benhattar, J., Losi, L., Lee, J.Q., Wang, S.T., Clarke, P.A., Bell, S., Quirke, P., Bubb, V.J., Piris, J., Cruickshank, N.R., Morton, D., Fox, J.C., Al-Mulla, F., Lees, N., Hall, C.N., Snary, D., Wilkinson, K., Dillon, D., Costa, J., Pricolo, V.E., Finkelstein, S.D., Thebo, J.S., Senagore, A.J., Halter, S.A., Wadler, S., Malik, S., Krtolica, K., Urosevic, N., 2001. Kirsten ras mutations in patients with colorectal cancer: the "RASCAL II" study. Br J Cancer 85, 692–696. https://doi.org/10.1054/bjoc.2001.1964

Aparicio, T., Baer, R., Gautier, J., 2014. DNA double-strand break repair pathway choice and cancer. DNA Repair (Amst) 19, 169–175. https://doi.org/10.1016/j.dnarep.2014.03.014

Aupérin, A., Le Péchoux, C., Rolland, E., Curran, W.J., Furuse, K., Fournel, P., Belderbos, J., Clamon, G., Ulutin, H.C., Paulus, R., Yamanaka, T., Bozonnat, M.-C., Uitterhoeve, A., Wang, X., Stewart, L., Arriagada, R., Burdett, S., Pignon, J.-P., 2010. Meta-analysis of concomitant versus sequential radiochemotherapy in locally advanced non-small-cell lung cancer. J Clin Oncol 28, 2181–2190. https://doi.org/10.1200/JCO.2009.26.2543

Azzam, E.I., de Toledo, S.M., Little, J.B., 2001. Direct evidence for the participation of gap junction-mediated intercellular communication in the transmission of damage signals from alpha -particle irradiated to nonirradiated cells. Proc Natl Acad Sci U S A 98, 473–478. https://doi.org/10.1073/pnas.98.2.473

Bankhead, P., Loughrey, M.B., Fernández, J.A., Dombrowski, Y., McArt, D.G., Dunne, P.D., McQuaid, S., Gray, R.T., Murray, L.J., Coleman, H.G., James, J.A., Salto-Tellez, M., Hamilton, P.W., 2017. QuPath: Open source software for digital

pathology image analysis. Sci Rep 7, 16878. https://doi.org/10.1038/s41598-017-17204-5
Barnett, G.C., West, C.M.L., Dunning, A.M., Elliott, R.M., Coles, C.E., Pharoah, P.D.P., Burnet, N.G., 2009. Normal tissue reactions to radiotherapy: towards tailoring treatment dose by genotype. Nat Rev Cancer 9, 134–142. https://doi.org/10.1038/nrc2587
Barney, J.D., Churchill, E.J., 1939. Adenocarcinoma of the Kidney with Metastasis to the Lung: Cured by Nephrectomy and Lobectomy. Journal of Urology 42, 269–276. https://doi.org/10.1016/S0022-5347(17)71516-9
Barnum, K.J., O'Connell, M.J., 2014. Cell Cycle Regulation by Checkpoints, in: Noguchi, E., Gadaleta, M.C. (Eds.), Cell Cycle Control, Methods in Molecular Biology. Springer New York, New York, NY, pp. 29–40. https://doi.org/10.1007/978-1-4939-0888-2_2
Barton, M.B., Jacob, S., Shafiq, J., Wong, K., Thompson, S.R., Hanna, T.P., Delaney, G.P., 2014a. Estimating the demand for radiotherapy from the evidence: A review of changes from 2003 to 2012. Radiotherapy and Oncology 112, 140–144. https://doi.org/10.1016/j.radonc.2014.03.024
Barton, M.B., Jacob, S., Shafiq, J., Wong, K., Thompson, S.R., Hanna, T.P., Delaney, G.P., 2014b. Estimating the demand for radiotherapy from the evidence: A review of changes from 2003 to 2012. Radiotherapy and Oncology 112, 140–144. https://doi.org/10.1016/j.radonc.2014.03.024
Becherel, O.J., Jakob, B., Cherry, A.L., Gueven, N., Fusser, M., Kijas, A.W., Peng, C., Katyal, S., McKinnon, P.J., Chen, J., Epe, B., Smerdon, S.J., Taucher-Scholz, G., Lavin, M.F., 2010. CK2 phosphorylation-dependent interaction between aprataxin and MDC1 in the DNA damage response. Nucleic Acids Research 38, 1489–1503. https://doi.org/10.1093/nar/gkp1149
Benedict, S.H., Yenice, K.M., Followill, D., Galvin, J.M., Hinson, W., Kavanagh, B., Keall, P., Lovelock, M., Meeks, S., Papiez, L., Purdie, T., Sadagopan, R., Schell, M.C., Salter, B., Schlesinger, D.J., Shiu, A.S., Solberg, T., Song, D.Y., Stieber, V., Timmerman, R., Tomé, W.A., Verellen, D., Wang, L., Yin, F., 2010. Stereotactic body radiation therapy: The report of AAPM Task Group 101. Medical Physics 37, 4078–4101. https://doi.org/10.1118/1.3438081
Bernhard, E.J., Kao, G., Cox, A.D., Sebti, S.M., Hamilton, A.D., Muschel, R.J., McKenna, W.G., 1996. The farnesyltransferase inhibitor FTI-277 radiosensitizes H-ras-transformed rat embryo fibroblasts. Cancer Res 56, 1727–1730.
Bernhard, E.J., McKenna, W.G., Hamilton, A.D., Sebti, S.M., Qian, Y., Wu, J.M., Muschel, R.J., 1998a. Inhibiting Ras prenylation increases the radiosensitivity of human tumor cell lines with activating mutations of ras oncogenes. Cancer Res 58, 1754–1761.
Bernhard, E.J., McKenna, W.G., Hamilton, A.D., Sebti, S.M., Qian, Y., Wu, J.M., Muschel, R.J., 1998b. Inhibiting Ras prenylation increases the radiosensitivity of human tumor cell lines with activating mutations of ras oncogenes. Cancer Res 58, 1754–1761.
Bernhard, E.J., McKenna, W.G., Hamilton, A.D., Sebti, S.M., Qian, Y., Wu, J.M., Muschel, R.J., 1998c. Inhibiting Ras prenylation increases the radiosensitivity of

human tumor cell lines with activating mutations of ras oncogenes. Cancer Res 58, 1754–1761.
Bertout, J.A., Patel, S.A., Simon, M.C., 2008. The impact of O2 availability on human cancer. Nat Rev Cancer 8, 967–975. https://doi.org/10.1038/nrc2540
Biade, S., Stobbe, C.C., Chapman, J.D., 1997. The intrinsic radiosensitivity of some human tumor cells throughout their cell cycles. Radiat Res 147, 416–421.
Biernacka, A., Tsongalis, P.D., Peterson, J.D., de Abreu, F.B., Black, C.C., Gutmann, E.J., Liu, X., Tafe, L.J., Amos, C.I., Tsongalis, G.J., 2016. The potential utility of re-mining results of somatic mutation testing: KRAS status in lung adenocarcinoma. Cancer Genet 209, 195–198. https://doi.org/10.1016/j.cancergen.2016.03.001
Blyth, B.J., Sykes, P.J., 2011. Radiation-induced bystander effects: what are they, and how relevant are they to human radiation exposures? Radiat Res 176, 139–157. https://doi.org/10.1667/rr2548.1
Boustani, Grapin, Laurent, Apetoh, Mirjolet, 2019. The 6th R of Radiobiology: Reactivation of Anti-Tumor Immune Response. Cancers 11, 860. https://doi.org/10.3390/cancers11060860
Briere, D.M., Li, S., Calinisan, A., Sudhakar, N., Aranda, R., Hargis, L., Peng, D.H., Deng, J., Engstrom, L.D., Hallin, J., Gatto, S., Fernandez-Banet, J., Pavlicek, A., Wong, K.-K., Christensen, J.G., Olson, P., 2021. The KRASG12C Inhibitor MRTX849 Reconditions the Tumor Immune Microenvironment and Sensitizes Tumors to Checkpoint Inhibitor Therapy. Molecular Cancer Therapeutics 20, 975–985. https://doi.org/10.1158/1535-7163.MCT-20-0462
Brown, S., Banfill, K., Aznar, M.C., Whitehurst, P., Faivre Finn, C., 2019. The evolving role of radiotherapy in non-small cell lung cancer. Br J Radiol 92, 20190524. https://doi.org/10.1259/bjr.20190524
Buday, L., Downward, J., 2008a. Many faces of Ras activation. Biochim Biophys Acta 1786, 178–187. https://doi.org/10.1016/j.bbcan.2008.05.001
Buday, L., Downward, J., 2008b. Many faces of Ras activation. Biochimica et Biophysica Acta (BBA) - Reviews on Cancer 1786, 178–187. https://doi.org/10.1016/j.bbcan.2008.05.001
Budke, B., Logan, H.L., Kalin, J.H., Zelivianskaia, A.S., Cameron McGuire, W., Miller, L.L., Stark, J.M., Kozikowski, A.P., Bishop, D.K., Connell, P.P., 2012. RI-1: a chemical inhibitor of RAD51 that disrupts homologous recombination in human cells. Nucleic Acids Res 40, 7347–7357. https://doi.org/10.1093/nar/gks353
Burdak-Rothkamm, S., Rothkamm, K., 2018. Radiation-induced bystander and systemic effects serve as a unifying model system for genotoxic stress responses. Mutat Res Rev Mutat Res 778, 13–22. https://doi.org/10.1016/j.mrrev.2018.08.001
Cairns, R., Papandreou, I., Denko, N., 2006. Overcoming physiologic barriers to cancer treatment by molecularly targeting the tumor microenvironment. Mol Cancer Res 4, 61–70. https://doi.org/10.1158/1541-7786.MCR-06-0002
Cammà, C., Giunta, M., Fiorica, F., Pagliaro, L., Craxì, A., Cottone, M., 2000. Preoperative Radiotherapy for Resectable Rectal Cancer: A Meta-analysis. JAMA 284, 1008. https://doi.org/10.1001/jama.284.8.1008
Canon, J., Rex, K., Saiki, A.Y., Mohr, C., Cooke, K., Bagal, D., Gaida, K., Holt, T., Knutson, C.G., Koppada, N., Lanman, B.A., Werner, J., Rapaport, A.S., San

Miguel, T., Ortiz, R., Osgood, T., Sun, J.-R., Zhu, X., McCarter, J.D., Volak, L.P., Houk, B.E., Fakih, M.G., O'Neil, B.H., Price, T.J., Falchook, G.S., Desai, J., Kuo, J., Govindan, R., Hong, D.S., Ouyang, W., Henary, H., Arvedson, T., Cee, V.J., Lipford, J.R., 2019a. The clinical KRAS(G12C) inhibitor AMG 510 drives anti-tumour immunity. Nature 575, 217–223. https://doi.org/10.1038/s41586-019-1694-1

Canon, J., Rex, K., Saiki, A.Y., Mohr, C., Cooke, K., Bagal, D., Gaida, K., Holt, T., Knutson, C.G., Koppada, N., Lanman, B.A., Werner, J., Rapaport, A.S., San Miguel, T., Ortiz, R., Osgood, T., Sun, J.-R., Zhu, X., McCarter, J.D., Volak, L.P., Houk, B.E., Fakih, M.G., O'Neil, B.H., Price, T.J., Falchook, G.S., Desai, J., Kuo, J., Govindan, R., Hong, D.S., Ouyang, W., Henary, H., Arvedson, T., Cee, V.J., Lipford, J.R., 2019b. The clinical KRAS(G12C) inhibitor AMG 510 drives anti-tumour immunity. Nature 575, 217–223. https://doi.org/10.1038/s41586-019-1694-1

Cantley, L.C., 2002. The phosphoinositide 3-kinase pathway. Science 296, 1655–1657. https://doi.org/10.1126/science.296.5573.1655

Castellano, E., Downward, J., 2011. RAS Interaction with PI3K: More Than Just Another Effector Pathway. Genes Cancer 2, 261–274. https://doi.org/10.1177/1947601911408079

Castle, J.C., Loewer, M., Boegel, S., de Graaf, J., Bender, C., Tadmor, A.D., Boisguerin, V., Bukur, T., Sorn, P., Paret, C., Diken, M., Kreiter, S., Türeci, Ö., Sahin, U., 2014. Immunomic, genomic and transcriptomic characterization of CT26 colorectal carcinoma. BMC Genomics 15, 190. https://doi.org/10.1186/1471-2164-15-190

Cengel, K.A., Voong, K.R., Chandrasekaran, S., Maggiorella, L., Brunner, T.B., Stanbridge, E., Kao, G.D., McKenna, W.G., Bernhard, E.J., 2007. Oncogenic K-Ras signals through epidermal growth factor receptor and wild-type H-Ras to promote radiation survival in pancreatic and colorectal carcinoma cells. Neoplasia 9, 341–348. https://doi.org/10.1593/neo.06823

Chang, E.H., Gonda, M.A., Ellis, R.W., Scolnick, E.M., Lowy, D.R., 1982. Human genome contains four genes homologous to transforming genes of Harvey and Kirsten murine sarcoma viruses. Proc. Natl. Acad. Sci. U.S.A. 79, 4848–4852. https://doi.org/10.1073/pnas.79.16.4848

Chen, Y.-H., Wei, M.-F., Wang, C.-W., Lee, H.-W., Pan, S.-L., Gao, M., Kuo, S.-H., Cheng, A.-L., Teng, C.-M., 2015. Dual Phosphoinositide 3-kinase/mammalian target of rapamycin inhibitor is an effective radiosensitizer for colorectal cancer. Cancer Letters 357, 582–590. https://doi.org/10.1016/j.canlet.2014.12.015

Chen, Z., Cao, K., Xia, Y., Li, Y., Hou, Y., Wang, L., Li, L., Chang, L., Li, W., 2019. Cellular senescence in ionizing radiation (Review). Oncol Rep. https://doi.org/10.3892/or.2019.7209

Chew, M.T., Jones, B., Hill, M., Bradley, D.A., 2021. Radiation, a two-edged sword: From untoward effects to fractionated radiotherapy. Radiation Physics and Chemistry 178, 108994. https://doi.org/10.1016/j.radphyschem.2020.108994

Chhabra, S.N., Booth, B.W., 2021. Asymmetric cell division of mammary stem cells. Cell Div 16, 5. https://doi.org/10.1186/s13008-021-00073-w

Choo, A., Blenis, J., 2009. Not all substrates are treated equally: implications for mTOR, rapamycin-resistance and cancer therapy. Cell Cycle, 8, 567-572. https://doi.org/10.4161/cc.8.4.7659
Chow, H.-M., Cheng, A., Song, X., Swerdel, M.R., Hart, R.P., Herrup, K., 2019. ATM is activated by ATP depletion and modulates mitochondrial function through NRF1. Journal of Cell Biology 218, 909–928. https://doi.org/10.1083/jcb.201806197
Christensen, J.G., Olson, P., Briere, T., Wiel, C., Bergo, M.O., 2020. Targeting Krasg12c -mutant cancer with a mutation-specific inhibitor. J Intern Med 288, 183–191. https://doi.org/10.1111/joim.13057
Cilla, S., Caravatta, L., Picardi, V., Sabatino, D., Macchia, G., Digesù, C., Deodato, F., Massaccesi, M., De Spirito, M., Piermattei, A., Morganti, A.G., 2012. Volumetric Modulated Arc Therapy with Simultaneous Integrated Boost for Locally Advanced Rectal Cancer. Clinical Oncology 24, 261–268. https://doi.org/10.1016/j.clon.2011.07.001
Cremona, C.A., Behrens, A., 2014. ATM signalling and cancer. Oncogene 33, 3351–3360. https://doi.org/10.1038/onc.2013.275
Crokart, N., Jordan, B.F., Baudelet, C., Ansiaux, R., Sonveaux, P., Grégoire, V., Beghein, N., DeWever, J., Bouzin, C., Feron, O., Gallez, B., 2005. Early reoxygenation in tumors after irradiation: determining factors and consequences for radiotherapy regimens using daily multiple fractions. Int J Radiat Oncol Biol Phys 63, 901–910. https://doi.org/10.1016/j.ijrobp.2005.02.038
Cuddihy, A.R., O'Connell, M.J., 2003. Cell-cycle responses to DNA damage in G2. Int Rev Cytol 222, 99–140. https://doi.org/10.1016/s0074-7696(02)22013-6
Daly, M.E., Singh, N., Ismaila, N., Antonoff, M.B., Arenberg, D.A., Bradley, J., David, E., Detterbeck, F., Früh, M., Gubens, M.A., Moore, A.C., Padda, S.K., Patel, J.D., Phillips, T., Qin, A., Robinson, C., Simone, C.B., 2022. Management of Stage III Non-Small-Cell Lung Cancer: ASCO Guideline. J Clin Oncol 40, 1356–1384. https://doi.org/10.1200/JCO.21.02528
Deckbar, D., Jeggo, P.A., Löbrich, M., 2011. Understanding the limitations of radiation-induced cell cycle checkpoints. Critical Reviews in Biochemistry and Molecular Biology 46, 271–283. https://doi.org/10.3109/10409238.2011.575764
Demaria, S., Bhardwaj, N., McBride, W.H., Formenti, S.C., 2005. Combining radiotherapy and immunotherapy: a revived partnership. Int J Radiat Oncol Biol Phys 63, 655–666. https://doi.org/10.1016/j.ijrobp.2005.06.032
Derbyshire, D.J., 2002. Crystal structure of human 53BP1 BRCT domains bound to p53 tumour suppressor. The EMBO Journal 21, 3863–3872. https://doi.org/10.1093/emboj/cdf383
Dienstmann, R., Connor, K., Byrne, A.T., COLOSSUS Consortium, 2020. Precision Therapy in RAS Mutant Colorectal Cancer. Gastroenterology 158, 806–811. https://doi.org/10.1053/j.gastro.2019.12.051
Diez, P., Hanna, G.G., Aitken, K.L., Van As, N., Carver, A., Colaco, R.J., Conibear, J., Dunne, E.M., Eaton, D.J., Franks, K.N., Good, J.S., Harrow, S., Hatfield, P., Hawkins, M.A., Jain, S., McDonald, F., Patel, R., Rackley, T., Sanghera, P., Tree, A., Murray, L., 2022. UK 2022 Consensus on Normal Tissue Dose-Volume

Constraints for Oligometastatic, Primary Lung and Hepatocellular Carcinoma Stereotactic Ablative Radiotherapy. Clinical Oncology 34, 288–300. https://doi.org/10.1016/j.clon.2022.02.010

Diwanji, T.P., Mohindra, P., Vyfhuis, M., Snider, J.W., Kalavagunta, C., Mossahebi, S., Yu, J., Feigenberg, S., Badiyan, S.N., 2017. Advances in radiotherapy techniques and delivery for non-small cell lung cancer: benefits of intensity-modulated radiation therapy, proton therapy, and stereotactic body radiation therapy. Transl Lung Cancer Res 6, 131–147. https://doi.org/10.21037/tlcr.2017.04.04

Dovedi, S.J., Adlard, A.L., Lipowska-Bhalla, G., McKenna, C., Jones, S., Cheadle, E.J., Stratford, I.J., Poon, E., Morrow, M., Stewart, R., Jones, H., Wilkinson, R.W., Honeychurch, J., Illidge, T.M., 2014. Acquired Resistance to Fractionated Radiotherapy Can Be Overcome by Concurrent PD-L1 Blockade. Cancer Research 74, 5458–5468. https://doi.org/10.1158/0008-5472.CAN-14-1258

Drané, P., Brault, M.-E., Cui, G., Meghani, K., Chaubey, S., Detappe, A., Parnandi, N., He, Y., Zheng, X.-F., Botuyan, M.V., Kalousi, A., Yewdell, W.T., Münch, C., Harper, J.W., Chaudhuri, J., Soutoglou, E., Mer, G., Chowdhury, D., 2017. TIRR regulates 53BP1 by masking its histone methyl-lysine binding function. Nature 543, 211–216. https://doi.org/10.1038/nature21358

Duldulao, M.P., Lee, W., Nelson, R.A., Li, W., Chen, Z., Kim, J., Garcia-Aguilar, J., 2013. Mutations in specific codons of the KRAS oncogene are associated with variable resistance to neoadjuvant chemoradiation therapy in patients with rectal adenocarcinoma. Ann Surg Oncol 20, 2166–2171. https://doi.org/10.1245/s10434-013-2910-0

Ellis, R.W., Defeo, D., Shih, T.Y., Gonda, M.A., Young, H.A., Tsuchida, N., Lowy, D.R., Scolnick, E.M., 1981. The p21 src genes of Harvey and Kirsten sarcoma viruses originate from divergent members of a family of normal vertebrate genes. Nature 292, 506–511. https://doi.org/10.1038/292506a0

Estrada-Bernal, A., Chatterjee, M., Haque, S.J., Yang, L., Morgan, M.A., Kotian, S., Morrell, D., Chakravarti, A., Williams, T.M., 2015. MEK inhibitor GSK1120212-mediated radiosensitization of pancreatic cancer cells involves inhibition of DNA double-strand break repair pathways. Cell Cycle 14, 3713–3724. https://doi.org/10.1080/15384101.2015.1104437

Evans, S.M., Koch, C.J., 2003. Prognostic significance of tumor oxygenation in humans. Cancer Lett 195, 1–16. https://doi.org/10.1016/s0304-3835(03)00012-0

Fabbro, M., Savage, K., Hobson, K., Deans, A.J., Powell, S.N., McArthur, G.A., Khanna, K.K., 2004. BRCA1-BARD1 Complexes Are Required for p53Ser-15 Phosphorylation and a G1/S Arrest following Ionizing Radiation-induced DNA Damage. Journal of Biological Chemistry 279, 31251–31258. https://doi.org/10.1074/jbc.M405372200

Fiala, O., Buchler, T., Mohelnikova-Duchonova, B., Melichar, B., Matejka, V.M., Holubec, L., Kulhankova, J., Bortlicek, Z., Bartouskova, M., Liska, V., Topolcan, O., Sedivcova, M., Finek, J., 2016a. G12V and G12A KRAS mutations are associated with poor outcome in patients with metastatic colorectal cancer treated with bevacizumab. Tumor Biol. 37, 6823–6830. https://doi.org/10.1007/s13277-015-4523-7

Fiala, O., Buchler, T., Mohelnikova-Duchonova, B., Melichar, B., Matejka, V.M., Holubec, L., Kulhankova, J., Bortlicek, Z., Bartouskova, M., Liska, V., Topolcan, O., Sedivcova, M., Finek, J., 2016b. G12V and G12A KRAS mutations are associated with poor outcome in patients with metastatic colorectal cancer treated with bevacizumab. Tumor Biol. 37, 6823–6830. https://doi.org/10.1007/s13277-015-4523-7

Finkielstein, C.V., Chen, L.G., Maller, J.L., 2002. A role for G1/S cyclin-dependent protein kinases in the apoptotic response to ionizing radiation. J Biol Chem 277, 38476–38485. https://doi.org/10.1074/jbc.M206184200

FitzGerald, T.J., Daugherty, C., Kase, K., Rothstein, L.A., McKenna, M., Greenberger, J.S., 1985a. Activated human N-ras oncogene enhances x-irradiation repair of mammalian cells in vitro less effectively at low dose rate. Implications for increased therapeutic ratio of low dose rate irradiation. Am J Clin Oncol 8, 517–522. https://doi.org/10.1097/00000421-198512000-00012

FitzGerald, T.J., Daugherty, C., Kase, K., Rothstein, L.A., McKenna, M., Greenberger, J.S., 1985b. Activated human N-ras oncogene enhances x-irradiation repair of mammalian cells in vitro less effectively at low dose rate: Implications for increased therapeutic ratio of low dose rate irradiation. American Journal of Clinical Oncology 8, 517–522. https://doi.org/10.1097/00000421-198512000-00012

Flynn, R.L., Zou, L., 2011. ATR: a master conductor of cellular responses to DNA replication stress. Trends Biochem Sci 36, 133–140. https://doi.org/10.1016/j.tibs.2010.09.005

Fokas, E., Prevo, R., Pollard, J.R., Reaper, P.M., Charlton, P.A., Cornelissen, B., Vallis, K.A., Hammond, E.M., Olcina, M.M., Gillies McKenna, W., Muschel, R.J., Brunner, T.B., 2012. Targeting ATR in vivo using the novel inhibitor VE-822 results in selective sensitization of pancreatic tumors to radiation. Cell Death Dis 3, e441. https://doi.org/10.1038/cddis.2012.181

Folkesson, J., Birgisson, H., Pahlman, L., Cedermark, B., Glimelius, B., Gunnarsson, U., 2005. Swedish Rectal Cancer Trial: long lasting benefits from radiotherapy on survival and local recurrence rate. J Clin Oncol 23, 5644–5650. https://doi.org/10.1200/JCO.2005.08.144

Forbes, S.A., Bindal, N., Bamford, S., Cole, C., Kok, C.Y., Beare, D., Jia, M., Shepherd, R., Leung, K., Menzies, A., Teague, J.W., Campbell, P.J., Stratton, M.R., Futreal, P.A., 2011. COSMIC: mining complete cancer genomes in the Catalogue of Somatic Mutations in Cancer. Nucleic Acids Res 39, D945-950. https://doi.org/10.1093/nar/gkq929

Formenti, S.C., Symmans, W.F., Volm, M., Skinner, K., Cohen, D., Spicer, D., Danenberg, P.V., 1999. Concurrent paclitaxel and radiation therapy for breast cancer. Semin Radiat Oncol 9, 34–42.

Fowler, J.F. 1989. The linear-quadratic formula and progress in fractionated radiotherapy. The British Journal of Radiology 62,679-694 https://doi.org/10.1259/0007-1285-62-740-679

Frank, A.O., Feldkamp, M.D., Kennedy, J.P., Waterson, A.G., Pelz, N.F., Patrone, J.D., Vangamudi, B., Camper, D.V., Rossanese, O.W., Chazin, W.J., Fesik, S.W.,

2013. Discovery of a potent inhibitor of replication protein a protein-protein interactions using a fragment-linking approach. J Med Chem 56, 9242–9250. https://doi.org/10.1021/jm401333u
Friedberg, E.C., 2019. Fixing your damaged and incorrect genes.
García-Echeverría, C., 2009. Protein and lipid kinase inhibitors as targeted anticancer agents of the Ras/Raf/MEK and PI3K/PKB pathways. Purinergic Signal 5, 117–125. https://doi.org/10.1007/s11302-008-9111-5
Gentile, D.R., Rathinaswamy, M.K., Jenkins, M.L., Moss, S.M., Siempelkamp, B.D., Renslo, A.R., Burke, J.E., Shokat, K.M., 2017. Ras Binder Induces a Modified Switch-II Pocket in GTP and GDP States. Cell Chem Biol 24, 1455-1466.e14. https://doi.org/10.1016/j.chembiol.2017.08.025
Ghobrial, I.M., Adjei, A.A., 2002. Inhibitors of the ras oncogene as therapeutic targets. Hematol Oncol Clin North Am 16, 1065–1088. https://doi.org/10.1016/s0889-8588(02)00050-3
Gilad, O., Nabet, B.Y., Ragland, R.L., Schoppy, D.W., Smith, K.D., Durham, A.C., Brown, E.J., 2010. Combining ATR suppression with oncogenic Ras synergistically increases genomic instability, causing synthetic lethality or tumorigenesis in a dosage-dependent manner. Cancer Res 70, 9693–9702. https://doi.org/10.1158/0008-5472.CAN-10-2286
Gillies McKenna, W., Muschel, R.J., Gupta, A.K., Hahn, S.M., Bernhard, E.J., 2003. The RAS signal transduction pathway and its role in radiation sensitivity. Oncogene 22, 5866–5875. https://doi.org/10.1038/sj.onc.1206699
Girinsky, T., Lubin, R., Pignon, J.P., Chavaudra, N., Gazeau, J., Dubray, B., Cosset, J.M., Socie, G., Fertil, B., 1993. Predictive value of in vitro radiosensitivity parameters in head and neck cancers and cervical carcinomas: Preliminary correlations with local control and overall survival. International Journal of Radiation Oncology*Biology*Physics 25, 3–7. https://doi.org/10.1016/0360-3016(93)90137-K
Glanzer, J.G., Liu, S., Wang, L., Mosel, A., Peng, A., Oakley, G.G., 2014. RPA inhibition increases replication stress and suppresses tumor growth. Cancer Res 74, 5165–5172. https://doi.org/10.1158/0008-5472.CAN-14-0306
Goitre, L., Trapani, E., Trabalzini, L., Retta, S.F., 2014. The Ras superfamily of small GTPases: the unlocked secrets. Methods Mol Biol 1120, 1–18. https://doi.org/10.1007/978-1-62703-791-4_1
Goldstein, M., Kastan, M.B., 2015. The DNA damage response: implications for tumor responses to radiation and chemotherapy. Annu Rev Med 66, 129–143. https://doi.org/10.1146/annurev-med-081313-121208
Gomez, D.R., Tang, C., Zhang, J., Blumenschein, G.R., Hernandez, M., Lee, J.J., Ye, R., Palma, D.A., Louie, A.V., Camidge, D.R., Doebele, R.C., Skoulidis, F., Gaspar, L.E., Welsh, J.W., Gibbons, D.L., Karam, J.A., Kavanagh, B.D., Tsao, A.S., Sepesi, B., Swisher, S.G., Heymach, J.V., 2019. Local Consolidative Therapy Vs. Maintenance Therapy or Observation for Patients With Oligometastatic Non-Small-Cell Lung Cancer: Long-Term Results of a Multi-Institutional, Phase II, Randomized Study. J Clin Oncol 37, 1558–1565. https://doi.org/10.1200/JCO.19.00201

Goodhead, D.T., 1994. Initial events in the cellular effects of ionizing radiations: clustered damage in DNA. Int J Radiat Biol 65, 7–17. https://doi.org/10.1080/09553009414550021

Grana, T.M., Rusyn, E.V., Zhou, H., Sartor, C.I., Cox, A.D., 2002. Ras mediates radioresistance through both phosphatidylinositol 3-kinase-dependent and Raf-dependent but mitogen-activated protein kinase/extracellular signal-regulated kinase kinase-independent signaling pathways. Cancer Res 62, 4142–4150.

Grimm, J., LaCouture, T., Croce, R., Yeo, I., Zhu, Y., Xue, J., 2011. Dose tolerance limits and dose volume histogram evaluation for stereotactic body radiotherapy. J Applied Clin Med Phys 12, 267–292. https://doi.org/10.1120/jacmp.v12i2.3368

Guckenberger, M., Andratschke, N., Alheit, H., Holy, R., Moustakis, C., Nestle, U., Sauer, O., Deutschen Gesellschaft für Radioonkologie (DEGRO), 2014. Definition of stereotactic body radiotherapy: principles and practice for the treatment of stage I non-small cell lung cancer. Strahlenther Onkol 190, 26–33. https://doi.org/10.1007/s00066-013-0450-y

Gupta, A.K., Bakanauskas, V.J., Cerniglia, G.J., Cheng, Y., Bernhard, E.J., Muschel, R.J., McKenna, W.G., 2001. The Ras radiation resistance pathway. Cancer Res 61, 4278–4282.

Hall, E.J., 2003. The bystander effect. Health Phys 85, 31–35. https://doi.org/10.1097/00004032-200307000-00008

Hall E., and Giacca, A.J. , 2006. Radiobiology for the Radiologist, 6th Edition. Lippincott Williams and Wilkins, Philadelphia.

Hallin, J., Engstrom, L.D., Hargis, L., Calinisan, A., Aranda, R., Briere, D.M., Sudhakar, N., Bowcut, V., Baer, B.R., Ballard, J.A., Burkard, M.R., Fell, J.B., Fischer, J.P., Vigers, G.P., Xue, Y., Gatto, S., Fernandez-Banet, J., Pavlicek, A., Velastagui, K., Chao, R.C., Barton, J., Pierobon, M., Baldelli, E., Patricoin, E.F., Cassidy, D.P., Marx, M.A., Rybkin, I.I., Johnson, M.L., Ou, S.-H.I., Lito, P., Papadopoulos, K.P., Jänne, P.A., Olson, P., Christensen, J.G., 2020. The KRASG12C Inhibitor MRTX849 Provides Insight toward Therapeutic Susceptibility of KRAS-Mutant Cancers in Mouse Models and Patients. Cancer Discovery 10, 54–71. https://doi.org/10.1158/2159-8290.CD-19-1167

Hanna, G.G., Murray, L., Patel, R., Jain, S., Aitken, K.L., Franks, K.N., Van As, N., Tree, A., Hatfield, P., Harrow, S., McDonald, F., Ahmed, M., Saran, F.H., Webster, G.J., Khoo, V., Landau, D., Eaton, D.J., Hawkins, M.A., 2018. UK Consensus on Normal Tissue Dose Constraints for Stereotactic Radiotherapy. Clinical Oncology 30, 5–14. https://doi.org/10.1016/j.clon.2017.09.007

Hanna, T.P., Shafiq, J., Delaney, G.P., Vinod, S.K., Thompson, S.R., Barton, M.B., 2018a. The population benefit of evidence-based radiotherapy: 5-Year local control and overall survival benefits. Radiotherapy and Oncology 126, 191–197. https://doi.org/10.1016/j.radonc.2017.11.004

Hanna, T.P., Shafiq, J., Delaney, G.P., Vinod, S.K., Thompson, S.R., Barton, M.B., 2018b. The population benefit of evidence-based radiotherapy: 5-Year local control and overall survival benefits. Radiotherapy and Oncology 126, 191–197. https://doi.org/10.1016/j.radonc.2017.11.004

Harada, H., Itasaka, S., Kizaka-Kondoh, S., Shibuya, K., Morinibu, A., Shinomiya, K., Hiraoka, M., 2009. The Akt/mTOR pathway assures the synthesis of HIF-1alpha protein in a glucose- and reoxygenation-dependent manner in irradiated tumors. J Biol Chem 284, 5332–5342. https://doi.org/10.1074/jbc.M806653200
Harris, S.L., Levine, A.J., 2005. The p53 pathway: positive and negative feedback loops. Oncogene 24, 2899–2908. https://doi.org/10.1038/sj.onc.1208615
Harting, C., Peschke, P., Borkenstein, K., Karger, C.P., 2007. Single-cell-based computer simulation of the oxygen-dependent tumour response to irradiation. Phys. Med. Biol. 52, 4775–4789. https://doi.org/10.1088/0031-9155/52/16/005
Harvey, J.J., 1964. An Unidentified Virus which causes the Rapid Production of Tumours in Mice. Nature 204, 1104–1105. https://doi.org/10.1038/2041104b0
Hau, P.M., Tsao, S.W., 2017. Epstein-Barr Virus Hijacks DNA Damage Response Transducers to Orchestrate Its Life Cycle. Viruses 9, 341. https://doi.org/10.3390/v9110341
Havaki, S., Kotsinas, A., Chronopoulos, E., Kletsas, D., Georgakilas, A., Gorgoulis, V.G., 2015. The role of oxidative DNA damage in radiation induced bystander effect. Cancer Letters 356, 43–51. https://doi.org/10.1016/j.canlet.2014.01.023
Hennequin, C., Giocanti, N., Favaudon, V., 1996. Interaction of ionizing radiation with paclitaxel (Taxol) and docetaxel (Taxotere) in HeLa and SQ20B cells. Cancer Res 56, 1842–1850.
Herzenberg, Leonard A., Parks, D., Sahaf, B., Perez, O., Roederer, M., Herzenberg, Leonore A., 2002. The history and future of the fluorescence activated cell sorter and flow cytometry: a view from Stanford. Clin Chem 48, 1819–1827.
Hiraike, H., Wada-Hiraike, O., Nakagawa, S., Koyama, S., Miyamoto, Y., Sone, K., Tanikawa, M., Tsuruga, T., Nagasaka, K., Matsumoto, Y., Oda, K., Shoji, K., Fukuhara, H., Saji, S., Nakagawa, K., Kato, S., Yano, T., Taketani, Y., 2010. Identification of DBC1 as a transcriptional repressor for BRCA1. Br J Cancer 102, 1061–1067. https://doi.org/10.1038/sj.bjc.6605577
Hobbs, G.A., Der, C.J., Rossman, K.L., 2016. RAS isoforms and mutations in cancer at a glance. J Cell Sci 129, 1287–1292. https://doi.org/10.1242/jcs.182873
Hong, D.S., Fakih, M.G., Strickler, J.H., Desai, J., Durm, G.A., Shapiro, G.I., Falchook, G.S., Price, T.J., Sacher, A., Denlinger, C.S., Bang, Y.-J., Dy, G.K., Krauss, J.C., Kuboki, Y., Kuo, J.C., Coveler, A.L., Park, K., Kim, T.W., Barlesi, F., Munster, P.N., Ramalingam, S.S., Burns, T.F., Meric-Bernstam, F., Henary, H., Ngang, J., Ngarmchamnanrith, G., Kim, J., Houk, B.E., Canon, J., Lipford, J.R., Friberg, G., Lito, P., Govindan, R., Li, B.T., 2020. KRAS ^{G12C} Inhibition with Sotorasib in Advanced Solid Tumors. N Engl J Med 383, 1207–1217. https://doi.org/10.1056/NEJMoa1917239
Horn, H.F., Vousden, K.H., 2007. Coping with stress: multiple ways to activate p53. Oncogene 26, 1306–1316. https://doi.org/10.1038/sj.onc.1210263
Huang, F., Mazin, A.V., 2014. A small molecule inhibitor of human RAD51 potentiates breast cancer cell killing by therapeutic agents in mouse xenografts. PLoS One 9, e100993. https://doi.org/10.1371/journal.pone.0100993
Huang, R.-X., Zhou, P.-K., 2020. DNA damage response signaling pathways and targets for radiotherapy sensitization in cancer. Sig Transduct Target Ther 5, 60. https://doi.org/10.1038/s41392-020-0150-x

Iliakis, G., Mladenov, E., Mladenova, V., 2019. Necessities in the Processing of DNA Double Strand Breaks and Their Effects on Genomic Instability and Cancer. Cancers (Basel) 11, 1671. https://doi.org/10.3390/cancers11111671

Jackson, S.P., Bartek, J., 2009. The DNA-damage response in human biology and disease. Nature 461, 1071–1078. https://doi.org/10.1038/nature08467

Janes, M.R., Zhang, J., Li, L.-S., Hansen, R., Peters, U., Guo, X., Chen, Y., Babbar, A., Firdaus, S.J., Darjania, L., Feng, J., Chen, J.H., Li, Shuangwei, Li, Shisheng, Long, Y.O., Thach, C., Liu, Yuan, Zarieh, A., Ely, T., Kucharski, J.M., Kessler, L.V., Wu, T., Yu, K., Wang, Y., Yao, Y., Deng, X., Zarrinkar, P.P., Brehmer, D., Dhanak, D., Lorenzi, M.V., Hu-Lowe, D., Patricelli, M.P., Ren, P., Liu, Yi, 2018. Targeting KRAS Mutant Cancers with a Covalent G12C-Specific Inhibitor. Cell 172, 578-589.e17. https://doi.org/10.1016/j.cell.2018.01.006

Jänne, P.A., Riely, G.J., Gadgeel, S.M., Heist, R.S., Ou, S.-H.I., Pacheco, J.M., Johnson, M.L., Sabari, J.K., Leventakos, K., Yau, E., Bazhenova, L., Negrao, M.V., Pennell, N.A., Zhang, J., Anderes, K., Der-Torossian, H., Kheoh, T., Velastegui, K., Yan, X., Christensen, J.G., Chao, R.C., Spira, A.I., 2022. Adagrasib in Non–Small-Cell Lung Cancer Harboring a *KRAS* ^{G12C} Mutation. N Engl J Med 387, 120–131. https://doi.org/10.1056/NEJMoa2204619

Jin, M., Xiao, A., Zhu, L., Zhang, Z., Huang, H., Jiang, L., 2019. The diversity and commonalities of the radiation-resistance mechanisms of Deinococcus and its up-to-date applications. AMB Express 9, 138. https://doi.org/10.1186/s13568-019-0862-x

Jones, B., Dale, R.,Deehan, C., Hopkins, K.I., Morgan D.A., 2018. The evolution of practical radiobiological modelling. BJR 20180097. https://doi.org/10.1259/bjr.20180097

Jones, B., Dale, R.; 2001. The role of biologically effective dose (BED) in clinical oncology. Clin Oncol 2001,71-81. https://doi.org/10.1053/clon.2001.9221

Jones, R.P., Sutton, P.A., Evans, J.P., Clifford, R., McAvoy, A., Lewis, J., Rousseau, A., Mountford, R., McWhirter, D., Malik, H.Z., 2017a. Specific mutations in KRAS codon 12 are associated with worse overall survival in patients with advanced and recurrent colorectal cancer. Br J Cancer 116, 923–929. https://doi.org/10.1038/bjc.2017.37

Jones, R.P., Sutton, P.A., Evans, J.P., Clifford, R., McAvoy, A., Lewis, J., Rousseau, A., Mountford, R., McWhirter, D., Malik, H.Z., 2017b. Specific mutations in KRAS codon 12 are associated with worse overall survival in patients with advanced and recurrent colorectal cancer. Br J Cancer 116, 923–929. https://doi.org/10.1038/bjc.2017.37

Kabakov, A.E., Yakimova, A.O., 2021. Hypoxia induced cancer cell responses driving radioresistance of hypoxic tumors: approaches to targeting and radiosensitizing. Cancers 13, 1102. https://doi.org/10.3390/cancers13051102

Kaminski, J.M., Shinohara, E., Summers, J.B., Niermann, K.J., Morimoto, A., Brousal, J., 2005. The controversial abscopal effect. Cancer Treat Rev 31, 159–172. https://doi.org/10.1016/j.ctrv.2005.03.004

Kano, Y., Akutsu, M., Tsunoda, S., Furuta, M., Yazawa, Y., Ando, J., 1998. Schedule-dependent synergism and antagonism between paclitaxel and methotrexate in human carcinoma cell lines. Oncol Res 10, 347–354.

Karandikar, M., Xu, S., Cobb, M.H., 2000. MEKK1 binds raf-1 and the ERK2 cascade components. J Biol Chem 275, 40120–40127. https://doi.org/10.1074/jbc.M005926200
Karlin, J.D., Tokarz, M., Beckta, J., Farhan, A., Pike, K., Barlaam, B., MacFaul, P., Patel, B., Thomason, A., Tudge, E., Wilson, J., Lau, A., Cadogan, E., Durant, S., Valerie, K., 2014. A Novel ATM Kinase Inhibitor Effectively Radiosensitizes Glioblastoma in Mice. International Journal of Radiation Oncology*Biology*Physics 90, S35. https://doi.org/10.1016/j.ijrobp.2014.05.148
Kastan, M.B., Bartek, J., 2004. Cell-cycle checkpoints and cancer. Nature 432, 316–323. https://doi.org/10.1038/nature03097
Kempf, H., Bleicher, M., Meyer-Hermann, M., 2015. Spatio-Temporal Dynamics of Hypoxia during Radiotherapy. PLoS ONE 10, e0133357. https://doi.org/10.1371/journal.pone.0133357
Khalil, D.N., Smith, E.L., Brentjens, R.J., Wolchok, J.D., 2016. The future of cancer treatment: immunomodulation, CARs and combination immunotherapy. Nat Rev Clin Oncol 13, 394. https://doi.org/10.1038/nrclinonc.2016.65
Khoronenkova, S.V., Dianov, G.L., 2015. ATM prevents DSB formation by coordinating SSB repair and cell cycle progression. Proc. Natl. Acad. Sci. U.S.A. 112, 3997–4002. https://doi.org/10.1073/pnas.1416031112
Kiel, C., Wohlgemuth, S., Rousseau, F., Schymkowitz, J., Ferkinghoff-Borg, J., Wittinghofer, F., Serrano, L., 2005. Recognizing and Defining True Ras Binding Domains II: In Silico Prediction Based on Homology Modelling and Energy Calculations. Journal of Molecular Biology 348, 759–775. https://doi.org/10.1016/j.jmb.2005.02.046
Kim, W., Youn, H., Kang, C., Youn, B., 2015. Inflammation-induced radioresistance is mediated by ROS-dependent inactivation of protein phosphatase 1 in non-small cell lung cancer cells. Apoptosis 20, 1242–1252. https://doi.org/10.1007/s10495-015-1141-1
Kirsten, W.H., Mayer, L.A., 1967. Morphologic responses to a murine erythroblastosis virus. J Natl Cancer Inst 39, 311–335.
Knijnenburg, T.A., Wang, L., Zimmermann, M.T., Chambwe, N., Gao, G.F., Cherniack, A.D., Fan, H., Shen, H., Way, G.P., Greene, C.S., Liu, Y., Akbani, R., Feng, B., Donehower, L.A., Miller, C., Shen, Y., Karimi, M., Chen, H., Kim, P., Jia, P., Shinbrot, E., Zhang, S., Liu, Jianfang, Hu, H., Bailey, M.H., Yau, C., Wolf, D., Zhao, Z., Weinstein, J.N., Li, L., Ding, L., Mills, G.B., Laird, P.W., Wheeler, D.A., Shmulevich, I., Monnat, R.J., Xiao, Y., Wang, C., Caesar-Johnson, S.J., Demchok, J.A., Felau, I., Kasapi, M., Ferguson, M.L., Hutter, C.M., Sofia, H.J., Tarnuzzer, R., Wang, Z., Yang, L., Zenklusen, J.C., Zhang, J. (Julia), Chudamani, S., Liu, Jia, Lolla, L., Naresh, R., Pihl, T., Sun, Q., Wan, Y., Wu, Y., Cho, J., DeFreitas, T., Frazer, S., Gehlenborg, N., Getz, G., Heiman, D.I., Kim, J., Lawrence, M.S., Lin, P., Meier, S., Noble, M.S., Saksena, G., Voet, D., Zhang, Hailei, Bernard, B., Chambwe, N., Dhankani, V., Knijnenburg, T., Kramer, R., Leinonen, K., Liu, Y., Miller, M., Reynolds, S., Shmulevich, I., Thorsson, V., Zhang, W., Akbani, R., Broom, B.M., Hegde, A.M., Ju, Z., Kanchi, R.S., Korkut, A., Li, J., Liang, H., Ling, S., Liu, W., Lu, Y., Mills, G.B., Ng, K.-S., Rao, A.,

Ryan, M., Wang, Jing, Weinstein, J.N., Zhang, J., Abeshouse, A., Armenia, J., Chakravarty, D., Chatila, W.K., De Bruijn, I., Gao, J., Gross, B.E., Heins, Z.J., Kundra, R., La, K., Ladanyi, M., Luna, A., Nissan, M.G., Ochoa, A., Phillips, S.M., Reznik, E., Sanchez-Vega, F., Sander, C., Schultz, N., Sheridan, R., Sumer, S.O., Sun, Y., Taylor, B.S., Wang, Jioajiao, Zhang, Hongxin, Anur, P., Peto, M., Spellman, P., Benz, C., Stuart, J.M., Wong, C.K., Yau, C., Hayes, D.N., Parker, J.S., Wilkerson, M.D., Ally, A., Balasundaram, M., Bowlby, R., Brooks, D., Carlsen, R., Chuah, E., Dhalla, N., Holt, R., Jones, S.J.M., Kasaian, K., Lee, D., Ma, Y., Marra, M.A., Mayo, M., Moore, R.A., Mungall, A.J., Mungall, K., Robertson, A.G., Sadeghi, S., Schein, J.E., Sipahimalani, P., Tam, A., Thiessen, N., Tse, K., Wong, T., Berger, A.C., Beroukhim, R., Cherniack, A.D., Cibulskis, C., Gabriel, S.B., Gao, G.F., Ha, G., Meyerson, M., Schumacher, S.E., Shih, J., Kucherlapati, M.H., Kucherlapati, R.S., Baylin, S., Cope, L., Danilova, L., Bootwalla, M.S., Lai, P.H., Maglinte, D.T., Van Den Berg, D.J., Weisenberger, D.J., Auman, J.T., Balu, S., Bodenheimer, T., Fan, C., Hoadley, K.A., Hoyle, A.P., Jefferys, S.R., Jones, C.D., Meng, S., Mieczkowski, P.A., Mose, L.E., Perou, A.H., Perou, C.M., Roach, J., Shi, Y., Simons, J.V., Skelly, T., Soloway, M.G., Tan, D., Veluvolu, U., Fan, H., Hinoue, T., Laird, P.W., Shen, H., Zhou, W., Bellair, M., Chang, K., Covington, K., Creighton, C.J., Dinh, H., Doddapaneni, H., Donehower, L.A., Drummond, J., Gibbs, R.A., Glenn, R., Hale, W., Han, Y., Hu, J., Korchina, V., Lee, S., Lewis, L., Li, W., Liu, X., Morgan, M., Morton, D., Muzny, D., Santibanez, J., Sheth, M., Shinbrot, E., Wang, L., Wang, M., Wheeler, D.A., Xi, L., Zhao, F., Hess, J., Appelbaum, E.L., Bailey, M., Cordes, M.G., Ding, L., Fronick, C.C., Fulton, L.A., Fulton, R.S., Kandoth, C., Mardis, E.R., McLellan, M.D., Miller, C.A., Schmidt, H.K., Wilson, R.K., Crain, D., Curley, E., Gardner, J., Lau, K., Mallery, D., Morris, S., Paulauskis, J., Penny, R., Shelton, C., Shelton, T., Sherman, M., Thompson, E., Yena, P., Bowen, J., Gastier-Foster, J.M., Gerken, M., Leraas, K.M., Lichtenberg, T.M., Ramirez, N.C., Wise, L., Zmuda, E., Corcoran, N., Costello, T., Hovens, C., Carvalho, A.L., De Carvalho, A.C., Fregnani, J.H., Longatto-Filho, A., Reis, R.M., Scapulatempo-Neto, C., Silveira, H.C.S., Vidal, D.O., Burnette, A., Eschbacher, J., Hermes, B., Noss, A., Singh, R., Anderson, M.L., Castro, P.D., Ittmann, M., Huntsman, D., Kohl, B., Le, X., Thorp, R., Andry, C., Duffy, E.R., Lyadov, V., Paklina, O., Setdikova, G., Shabunin, A., Tavobilov, M., McPherson, C., Warnick, R., Berkowitz, R., Cramer, D., Feltmate, C., Horowitz, N., Kibel, A., Muto, M., Raut, C.P., Malykh, A., Barnholtz-Sloan, J.S., Barrett, W., Devine, K., Fulop, J., Ostrom, Q.T., Shimmel, K., Wolinsky, Y., Sloan, A.E., De Rose, A., Giuliante, F., Goodman, M., Karlan, B.Y., Hagedorn, C.H., Eckman, J., Harr, J., Myers, J., Tucker, K., Zach, L.A., Deyarmin, B., Hu, H., Kvecher, L., Larson, C., Mural, R.J., Somiari, S., Vicha, A., Zelinka, T., Bennett, J., Iacocca, M., Rabeno, B., Swanson, P., Latour, M., Lacombe, L., Têtu, B., Bergeron, A., McGraw, M., Staugaitis, S.M., Chabot, J., Hibshoosh, H., Sepulveda, A., Su, T., Wang, T., Potapova, O., Voronina, O., Desjardins, L., Mariani, O., Roman-Roman, S., Sastre, X., Stern, M.-H., Cheng, F., Signoretti, S., Berchuck, A., Bigner, D., Lipp, E., Marks, J., McCall, S., McLendon, R., Secord, A., Sharp, A., Behera, M., Brat, D.J., Chen, A., Delman, K., Force, S., Khuri, F., Magliocca, K., Maithel, S.,

Olson, J.J., Owonikoko, T., Pickens, A., Ramalingam, S., Shin, D.M., Sica, G., Van Meir, E.G., Zhang, Hongzheng, Eijckenboom, W., Gillis, A., Korpershoek, E., Looijenga, L., Oosterhuis, W., Stoop, H., Van Kessel, K.E., Zwarthoff, E.C., Calatozzolo, C., Cuppini, L., Cuzzubbo, S., DiMeco, F., Finocchiaro, G., Mattei, L., Perin, A., Pollo, B., Chen, C., Houck, J., Lohavanichbutr, P., Hartmann, A., Stoehr, C., Stoehr, R., Taubert, H., Wach, S., Wullich, B., Kycler, W., Murawa, D., Wiznerowicz, M., Chung, K., Edenfield, W.J., Martin, J., Baudin, E., Bubley, G., Bueno, R., De Rienzo, A., Richards, W.G., Kalkanis, S., Mikkelsen, T., Noushmehr, H., Scarpace, L., Girard, N., Aymerich, M., Campo, E., Giné, E., Guillermo, A.L., Van Bang, N., Hanh, P.T., Phu, B.D., Tang, Y., Colman, H., Evason, K., Dottino, P.R., Martignetti, J.A., Gabra, H., Juhl, H., Akeredolu, T., Stepa, S., Hoon, D., Ahn, K., Kang, K.J., Beuschlein, F., Breggia, A., Birrer, M., Bell, D., Borad, M., Bryce, A.H., Castle, E., Chandan, V., Cheville, J., Copland, J.A., Farnell, M., Flotte, T., Giama, N., Ho, T., Kendrick, M., Kocher, J.-P., Kopp, K., Moser, C., Nagorney, D., O'Brien, D., O'Neill, B.P., Patel, T., Petersen, G., Que, F., Rivera, M., Roberts, L., Smallridge, R., Smyrk, T., Stanton, M., Thompson, R.H., Torbenson, M., Yang, J.D., Zhang, L., Brimo, F., Ajani, J.A., Gonzalez, A.M.A., Behrens, C., Bondaruk, J., Broaddus, R., Czerniak, B., Esmaeli, B., Fujimoto, J., Gershenwald, J., Guo, C., Lazar, A.J., Logothetis, C., Meric-Bernstam, F., Moran, C., Ramondetta, L., Rice, D., Sood, A., Tamboli, P., Thompson, T., Troncoso, P., Tsao, A., Wistuba, I., Carter, C., Haydu, L., Hersey, P., Jakrot, V., Kakavand, H., Kefford, R., Lee, K., Long, G., Mann, G., Quinn, M., Saw, R., Scolyer, R., Shannon, K., Spillane, A., Stretch, J., Synott, M., Thompson, J., Wilmott, J., Al-Ahmadie, H., Chan, T.A., Ghossein, R., Gopalan, A., Levine, D.A., Reuter, V., Singer, S., Singh, B., Tien, N.V., Broudy, T., Mirsaidi, C., Nair, P., Drwiega, P., Miller, J., Smith, J., Zaren, H., Park, J.-W., Hung, N.P., Kebebew, E., Linehan, W.M., Metwalli, A.R., Pacak, K., Pinto, P.A., Schiffman, M., Schmidt, L.S., Vocke, C.D., Wentzensen, N., Worrell, R., Yang, H., Moncrieff, M., Goparaju, C., Melamed, J., Pass, H., Botnariuc, N., Caraman, I., Cernat, M., Chemencedji, I., Clipca, A., Doruc, S., Gorincioi, G., Mura, S., Pirtac, M., Stancul, I., Tcaciuc, D., Albert, M., Alexopoulou, I., Arnaout, A., Bartlett, J., Engel, J., Gilbert, S., Parfitt, J., Sekhon, H., Thomas, G., Rassl, D.M., Rintoul, R.C., Bifulco, C., Tamakawa, R., Urba, W., Hayward, N., Timmers, H., Antenucci, A., Facciolo, F., Grazi, G., Marino, M., Merola, R., De Krijger, R., Gimenez-Roqueplo, A.-P., Piché, A., Chevalier, S., McKercher, G., Birsoy, K., Barnett, G., Brewer, C., Farver, C., Naska, T., Pennell, N.A., Raymond, D., Schilero, C., Smolenski, K., Williams, F., Morrison, C., Borgia, J.A., Liptay, M.J., Pool, M., Seder, C.W., Junker, K., Omberg, L., Dinkin, M., Manikhas, G., Alvaro, D., Bragazzi, M.C., Cardinale, V., Carpino, G., Gaudio, E., Chesla, D., Cottingham, S., Dubina, M., Moiseenko, F., Dhanasekaran, R., Becker, K.-F., Janssen, K.-P., Slotta-Huspenina, J., Abdel-Rahman, M.H., Aziz, D., Bell, S., Cebulla, C.M., Davis, A., Duell, R., Elder, J.B., Hilty, J., Kumar, B., Lang, J., Lehman, N.L., Mandt, R., Nguyen, P., Pilarski, R., Rai, K., Schoenfield, L., Senecal, K., Wakely, P., Hansen, P., Lechan, R., Powers, J., Tischler, A., Grizzle, W.E., Sexton, K.C., Kastl, A., Henderson, J., Porten, S., Waldmann, J., Fassnacht, M., Asa, S.L., Schadendorf, D., Couce, M., Graefen, M., Huland, H.,

Sauter, G., Schlomm, T., Simon, R., Tennstedt, P., Olabode, O., Nelson, M., Bathe, O., Carroll, P.R., Chan, J.M., Disaia, P., Glenn, P., Kelley, R.K., Landen, C.N., Phillips, J., Prados, M., Simko, J., Smith-McCune, K., VandenBerg, S., Roggin, K., Fehrenbach, A., Kendler, A., Sifri, S., Steele, R., Jimeno, A., Carey, F., Forgie, I., Mannelli, M., Carney, M., Hernandez, B., Campos, B., Herold-Mende, C., Jungk, C., Unterberg, A., Von Deimling, A., Bossler, A., Galbraith, J., Jacobus, L., Knudson, M., Knutson, T., Ma, D., Milhem, M., Sigmund, R., Godwin, A.K., Madan, R., Rosenthal, H.G., Adebamowo, C., Adebamowo, S.N., Boussioutas, A., Beer, D., Giordano, T., Mes-Masson, A.-M., Saad, F., Bocklage, T., Landrum, L., Mannel, R., Moore, K., Moxley, K., Postier, R., Walker, J., Zuna, R., Feldman, M., Valdivieso, F., Dhir, R., Luketich, J., Pinero, E.M.M., Quintero-Aguilo, M., Carlotti, C.G., Dos Santos, J.S., Kemp, R., Sankarankuty, A., Tirapelli, D., Catto, J., Agnew, K., Swisher, E., Creaney, J., Robinson, B., Shelley, C.S., Godwin, E.M., Kendall, S., Shipman, C., Bradford, C., Carey, T., Haddad, A., Moyer, J., Peterson, L., Prince, M., Rozek, L., Wolf, G., Bowman, R., Fong, K.M., Yang, I., Korst, R., Rathmell, W.K., Fantacone-Campbell, J.L., Hooke, J.A., Kovatich, A.J., Shriver, C.D., DiPersio, J., Drake, B., Govindan, R., Heath, S., Ley, T., Van Tine, B., Westervelt, P., Rubin, M.A., Lee, J.I., Aredes, N.D., Mariamidze, A., 2018. Genomic and Molecular Landscape of DNA Damage Repair Deficiency across The Cancer Genome Atlas. Cell Reports 23, 239-254.e6. https://doi.org/10.1016/j.celrep.2018.03.076

Knott, G.J., Doudna, J.A., 2018. CRISPR-Cas guides the future of genetic engineering. Science 361, 866–869. https://doi.org/10.1126/science.aat5011

Kobayashi, J., Tauchi, H., Sakamoto, S., Nakamura, A., Morishima, K., Matsuura, S., Kobayashi, T., Tamai, K., Tanimoto, K., Komatsu, K., 2002. NBS1 Localizes to γ-H2AX Foci through Interaction with the FHA/BRCT Domain. Current Biology 12, 1846–1851. https://doi.org/10.1016/S0960-9822(02)01259-9

Kohl, N.E., Omer, C.A., Conner, M.W., Anthony, N.J., Davide, J.P., deSolms, S.J., Giuliani, E.A., Gomez, R.P., Graham, S.L., Hamilton, K., 1995. Inhibition of farnesyltransferase induces regression of mammary and salivary carcinomas in ras transgenic mice. Nat Med 1, 792–797. https://doi.org/10.1038/nm0895-792

Kortlever, R.M., Sodir, N.M., Wilson, C.H., Burkhart, D.L., Pellegrinet, L., Brown Swigart, L., Littlewood, T.D., Evan, G.I., 2017. Myc Cooperates with Ras by Programming Inflammation and Immune Suppression. Cell 171, 1301-1315.e14. https://doi.org/10.1016/j.cell.2017.11.013

Kouranti, I., Peyroche, A., 2012. Protein degradation in DNA damage response. Semin Cell Dev Biol 23, 538–545. https://doi.org/10.1016/j.semcdb.2012.02.004

Kroemer, G., Galluzzi, L., Kepp, O., Zitvogel, L., 2013. Immunogenic cell death in cancer therapy. Annu Rev Immunol 31, 51–72. https://doi.org/10.1146/annurev-immunol-032712-100008

Kuo, L.J., Yang, L.-X., 2008. Gamma-H2AX - a novel biomarker for DNA double-strand breaks. In Vivo 22, 305–309.

Lapenna, S., Giordano, A., 2009. Cell cycle kinases as therapeutic targets for cancer. Nat Rev Drug Discov 8, 547–566. https://doi.org/10.1038/nrd2907

Lederman, M., 1981. The early history of radiotherapy: 1895-1939. Int J Radiat Oncol Biol Phys 7, 639–648. https://doi.org/10.1016/0360-3016(81)90379-5

Lee, K.Y., Im, J.-S., Shibata, E., Park, J., Handa, N., Kowalczykowski, S.C., Dutta, A., 2015. MCM8-9 complex promotes resection of double-strand break ends by MRE11-RAD50-NBS1 complex. Nat Commun 6, 7744. https://doi.org/10.1038/ncomms8744

Levy, A., Chargari, C., Cheminant, M., Simon, N., Bourgier, C., Deutsch, E., 2013. Radiation therapy and immunotherapy: implications for a combined cancer treatment. Crit Rev Oncol Hematol 85, 278–287. https://doi.org/10.1016/j.critrevonc.2012.09.001

Li, Z., Pearlman, A.H., Hsieh, P., 2016. DNA mismatch repair and the DNA damage response. DNA Repair 38, 94–101. https://doi.org/10.1016/j.dnarep.2015.11.019

Liao, W., Overman, M.J., Boutin, A.T., Shang, X., Zhao, D., Dey, P., Li, Jiexi, Wang, G., Lan, Z., Li, Jun, Tang, M., Jiang, S., Ma, X., Chen, P., Katkhuda, R., Korphaisarn, K., Chakravarti, D., Chang, A., Spring, D.J., Chang, Q., Zhang, J., Maru, D.M., Maeda, D.Y., Zebala, J.A., Kopetz, S., Wang, Y.A., DePinho, R.A., 2019. KRAS-IRF2 Axis Drives Immune Suppression and Immune Therapy Resistance in Colorectal Cancer. Cancer Cell 35, 559-572.e7. https://doi.org/10.1016/j.ccell.2019.02.008

Liao, X., Morikawa, T., Lochhead, P., Imamura, Y., Kuchiba, A., Yamauchi, M., Nosho, K., Qian, Z.R., Nishihara, R., Meyerhardt, J.A., Fuchs, C.S., Ogino, S., 2012. Prognostic role of PIK3CA mutation in colorectal cancer: cohort study and literature review. Clin Cancer Res 18, 2257–2268. https://doi.org/10.1158/1078-0432.CCR-11-2410

Lim, K.-H., Counter, C.M., 2005. Reduction in the requirement of oncogenic Ras signaling to activation of PI3K/AKT pathway during tumor maintenance. Cancer Cell 8, 381–392. https://doi.org/10.1016/j.ccr.2005.10.014

Lito, P., Solomon, M., Li, L.-S., Hansen, R., Rosen, N., 2016a. Allele-specific inhibitors inactivate mutant KRAS G12C by a trapping mechanism. Science 351, 604–608. https://doi.org/10.1126/science.aad6204

Lito, P., Solomon, M., Li, L.-S., Hansen, R., Rosen, N., 2016b. Allele-specific inhibitors inactivate mutant KRAS G12C by a trapping mechanism. Science 351, 604–608. https://doi.org/10.1126/science.aad6204

Liu, Q., Guntuku, S., Cui, X.S. 2000. Chk1 is an essential kinase that is regulated by ATR and required for the G2/M DNA damage checkpoint. Genes and Development, 14, 1448-1459. https://doi.org/10.1101/gad.14.12.1448

Liu, P., Wang, Y., Li, X., 2019. Targeting the untargetable KRAS in cancer therapy. Acta Pharmaceutica Sinica B 9, 871–879. https://doi.org/10.1016/j.apsb.2019.03.002

Liu, Y., Yang, M., Luo, J., Zhou, H., 2020. Radiotherapy targeting cancer stem cells "awakens" them to induce tumour relapse and metastasis in oral cancer. Int J Oral Sci 12, 19. https://doi.org/10.1038/s41368-020-00087-0

Lobell, R.B., Omer, C.A., Abrams, M.T., Bhimnathwala, H.G., Brucker, M.J., Buser, C.A., Davide, J.P., deSolms, S.J., Dinsmore, C.J., Ellis-Hutchings, M.S., Kral, A.M., Liu, D., Lumma, W.C., Machotka, S.V., Rands, E., Williams, T.M., Graham, S.L., Hartman, G.D., Oliff, A.I., Heimbrook, D.C., Kohl, N.E., 2001. Evaluation of

farnesyl:protein transferase and geranylgeranyl:protein transferase inhibitor combinations in preclinical models. Cancer Res 61, 8758–8768.
Lodovichi, S., Bellè, F., Cervelli, T., Lorenzoni, A., Maresca, L., Cozzani, C., Caligo, M.A., Galli, A., 2020. Effect of BRCA1 missense variants on gene reversion in DNA double-strand break repair mutants and cell cycle-arrested cells of Saccharomyces cerevisiae. Mutagenesis 35, 189–195. https://doi.org/10.1093/mutage/gez043
Mac Manus, M.P., Matthews, J.P., Wada, M., Wirth, A., Worotniuk, V., Ball, D.L., 2006. Unexpected long-term survival after low-dose palliative radiotherapy for non-small cell lung cancer. Cancer 106, 1110–1116. https://doi.org/10.1002/cncr.21704
Machtay, M., Paulus, R., Moughan, J., Komaki, R., Bradley, J.E., Choy, H., Albain, K., Movsas, B., Sause, W.T., Curran, W.J., 2012. Defining local-regional control and its importance in locally advanced non-small cell lung carcinoma. J Thorac Oncol 7, 716–722. https://doi.org/10.1097/JTO.0b013e3182429682
Mak, S., Till, J.E., 1963. THE EFFECTS OF X-RAYS ON THE PROGRESS OF L-CELLS THROUGH THE CELL CYCLE. Radiat Res 20, 600–618.
Matsumura, S., Demaria, S., 2010. Up-regulation of the pro-inflammatory chemokine CXCL16 is a common response of tumor cells to ionizing radiation. Radiation Research 173, 418-425. https://doi.org/10.1667/RR1860.1
Mascaux, C., Iannino, N., Martin, B., Paesmans, M., Berghmans, T., Dusart, M., Haller, A., Lothaire, P., Meert, A.-P., Noel, S., Lafitte, J.-J., Sculier, J.-P., 2005. The role of RAS oncogene in survival of patients with lung cancer: a systematic review of the literature with meta-analysis. Br J Cancer 92, 131–139. https://doi.org/10.1038/sj.bjc.6602258
McKenna, W.G., Muschel, R.J., Gupta, A.K., Hahn, S.M., Bernhard, E.J., 2003. The RAS signal transduction pathway and its role in radiation sensitivity. Oncogene 22, 5866–5875. https://doi.org/10.1038/sj.onc.1206699
McMahon, S.J., Butterworth, K.T., Trainor, C., McGarry, C.K., O'Sullivan, J.M., Schettino, G., Hounsell, A.R., Prise, K.M., 2013. A kinetic-based model of radiation-induced intercellular signalling. PLoS One 8, e54526. https://doi.org/10.1371/journal.pone.0054526
Miller, A. C., Kariko, K., Myers, C.E., Clark, E.P., Samid, D., 1993. Increased radioresistance of EJras-transformed human osteosarcoma cells and its modulation by lovastatin, an inhibitor of p21ras isoprenylation. Int J Cancer 53, 302–307. https://doi.org/10.1002/ijc.2910530222
Miller, Alexandra C., Kariko, K., Myers, C.E., Clark, E.P., Samid, D., 1993. Increased radioresistance of ejras-transformed human osteosarcoma cells and its modulation by lovastatin, an inhibitor of p21ras isoprenylation. Int. J. Cancer 53, 302–307. https://doi.org/10.1002/ijc.2910530222
Misaghian, N., Ligresti, G., Steelman, L.S., Bertrand, F.E., Basecke, J. 2009. Targeting stem cell: the Holy Grail of leukemia therapy. Leukemia, 23, 25-42. https://doi.org/10.1038/leu.2008.246
Mladenov, E., Magin, S., Soni, A., Iliakis, G., 2013. DNA double-strand break repair as determinant of cellular radiosensitivity to killing and target in radiation therapy. Front Oncol 3, 113. https://doi.org/10.3389/fonc.2013.00113

Mo, S.P., Coulson, J.M., Prior, I.A., 2018. RAS variant signalling. Biochem Soc Trans 46, 1325–1332. https://doi.org/10.1042/BST20180173
Mohni, K.N., Kavanaugh, G.M., Cortez, D., 2014. ATR pathway inhibition is synthetically lethal in cancer cells with ERCC1 deficiency. Cancer Res 74, 2835–2845. https://doi.org/10.1158/0008-5472.CAN-13-3229
Moodie, S.A., Willumsen, B.M., Weber, M.J., Wolfman, A., 1993. Complexes of Ras.GTP with Raf-1 and mitogen-activated protein kinase kinase. Science 260, 1658–1661. https://doi.org/10.1126/science.8503013
Morrison, D.K., Cutler, R.E., 1997. The complexity of Raf-1 regulation. Curr Opin Cell Biol 9, 174–179. https://doi.org/10.1016/s0955-0674(97)80060-9
Nadal, E., Chen, G., Prensner, J.R., Shiratsuchi, H., Sam, C., Zhao, L., Kalemkerian, G.P., Brenner, D., Lin, J., Reddy, R.M., Chang, A.C., Capellà, G., Cardenal, F., Beer, D.G., Ramnath, N., 2014a. KRAS-G12C Mutation Is Associated with Poor Outcome in Surgically Resected Lung Adenocarcinoma. Journal of Thoracic Oncology 9, 1513–1522. https://doi.org/10.1097/JTO.0000000000000305
Nadal, E., Chen, G., Prensner, J.R., Shiratsuchi, H., Sam, C., Zhao, L., Kalemkerian, G.P., Brenner, D., Lin, J., Reddy, R.M., Chang, A.C., Capellà, G., Cardenal, F., Beer, D.G., Ramnath, N., 2014b. KRAS-G12C Mutation Is Associated with Poor Outcome in Surgically Resected Lung Adenocarcinoma. Journal of Thoracic Oncology 9, 1513–1522. https://doi.org/10.1097/JTO.0000000000000305
Nagasaka, M., Li, Y., Sukari, A., Ou, S.-H.I., Al-Hallak, M.N., Azmi, A.S., 2020. KRAS G12C Game of Thrones, which direct KRAS inhibitor will claim the iron throne? Cancer Treat Rev 84, 101974. https://doi.org/10.1016/j.ctrv.2020.101974
Nagasawa, H., Little, J.B., 1992. Induction of sister chromatid exchanges by extremely low doses of alpha particles. Cancer Research 52, 6394-6396.
Najafi, M., Farhood, B., Mortezaee, K., Kharazinejad, E., Majidpoor, J., Ahadi, R., 2020. Hypoxia in solid tumors: a key promoter of cancer stem cell (CSC) resistance. J Cancer Res Clin Oncol 146, 19–31. https://doi.org/10.1007/s00432-019-03080-1
Nakanishi, M., Shimada, M., Niida, H., 2006. Genetic instability in cancer cells by impaired cell cycle checkpoints. Cancer Sci 97, 984–989. https://doi.org/10.1111/j.1349-7006.2006.00289.x
NCNN Practice Guidelines in Oncology-Non-small cell lung cancer. Version 5.2022, 2022.
Neher, T.M., Bodenmiller, D., Fitch, R.W., Jalal, S.I., Turchi, J.J., 2011. Novel irreversible small molecule inhibitors of replication protein A display single-agent activity and synergize with cisplatin. Mol Cancer Ther 10, 1796–1806. https://doi.org/10.1158/1535-7163.MCT-11-0303
Ng, J., Dai, T., 2016. Radiation therapy and the abscopal effect: a concept comes of age. Ann Transl Med 4, 118. https://doi.org/10.21037/atm.2016.01.32
Nguyen, H.Q., To, N.H., Zadigue, P., Kerbrat, S., De La Taille, A., Le Gouvello, S., Belkacemi, Y., 2018. Ionizing radiation-induced cellular senescence promotes tissue fibrosis after radiotherapy. A review. Critical Reviews in Oncology/Hematology 129, 13–26. https://doi.org/10.1016/j.critrevonc.2018.06.012

Nikitaki, Z., Nikolov, V., Mavragani, I.V., Mladenov, E., Mangelis, A., Laskaratou, D.A., Fragkoulis, G.I., Hellweg, C.E., Martin, O.A., Emfietzoglou, D., Hatzi, V.I., Terzoudi, G.I., Iliakis, G., Georgakilas, A.G., 2016. Measurement of complex DNA damage induction and repair in human cellular systems after exposure to ionizing radiations of varying linear energy transfer (LET). Free Radic Res 50, S64–S78. https://doi.org/10.1080/10715762.2016.1232484

Nikjoo, H., O'Neill, P., Wilson, W.E., Goodhead, D.T., 2001. Computational approach for determining the spectrum of DNA damage induced by ionizing radiation. Radiat Res 156, 577–583. https://doi.org/10.1667/0033-7587(2001)156[0577:cafdts]2.0.co;2

Ohkanda, J., Knowles, D.B., Blaskovich, M.A., Sebti, S.M., Hamilton, A.D., 2002. Inhibitors of protein farnesyltransferase as novel anticancer agents. Curr Top Med Chem 2, 303–323. https://doi.org/10.2174/1568026023394281

Olivares-Urbano, M.A., Griñán-Lisón, C., Marchal, J.A., Núñez, M.I., 2020. CSC Radioresistance: A Therapeutic Challenge to Improve Radiotherapy Effectiveness in Cancer. Cells 9, 1651. https://doi.org/10.3390/cells9071651

Olive, P.L., 1998. The Role of DNA Single- and Double-Strand Breaks in Cell Killing by Ionizing Radiation. Radiation Research 150, S42. https://doi.org/10.2307/3579807

Ost, P., Reynders, D., Decaestecker, K., Fonteyne, V., Lumen, N., De Bruycker, A., Lambert, B., Delrue, L., Bultijnck, R., Claeys, T., Goetghebeur, E., Villeirs, G., De Man, K., Ameye, F., Billiet, I., Joniau, S., Vanhaverbeke, F., De Meerleer, G., 2018. Surveillance or Metastasis-Directed Therapy for Oligometastatic Prostate Cancer Recurrence: A Prospective, Randomized, Multicenter Phase II Trial. JCO 36, 446–453. https://doi.org/10.1200/JCO.2017.75.4853

Ostrem, J.M., Peters, U., Sos, M.L., Wells, J.A., Shokat, K.M., 2013a. K-Ras(G12C) inhibitors allosterically control GTP affinity and effector interactions. Nature 503, 548–551. https://doi.org/10.1038/nature12796

Ostrem, J.M., Peters, U., Sos, M.L., Wells, J.A., Shokat, K.M., 2013b. K-Ras(G12C) inhibitors allosterically control GTP affinity and effector interactions. Nature 503, 548–551. https://doi.org/10.1038/nature12796

Palma, D.A., Olson, R., Harrow, S., Gaede, S., Louie, A.V., Haasbeek, C., Mulroy, L., Lock, M., Rodrigues, G.B., Yaremko, B.P., Schellenberg, D., Ahmad, B., Senthi, S., Swaminath, A., Kopek, N., Liu, M., Moore, K., Currie, S., Schlijper, R., Bauman, G.S., Laba, J., Qu, X.M., Warner, A., Senan, S., 2020. Stereotactic Ablative Radiotherapy for the Comprehensive Treatment of Oligometastatic Cancers: Long-Term Results of the SABR-COMET Phase II Randomized Trial. J Clin Oncol 38, 2830–2838. https://doi.org/10.1200/JCO.20.00818

Papke, B., Der, C.J., 2017. Drugging RAS: Know the enemy. Science 355, 1158–1163. https://doi.org/10.1126/science.aam7622

Passiglia, F., Malapelle, U., Del Re, M., Righi, L., Pagni, F., Furlan, D., Danesi, R., Troncone, G., Novello, S., 2020. KRAS inhibition in non-small cell lung cancer: Past failures, new findings and upcoming challenges. Eur J Cancer 137, 57–68. https://doi.org/10.1016/j.ejca.2020.06.023

Patricelli, M.P., Janes, M.R., Li, L.-S., Hansen, R., Peters, U., Kessler, L.V., Chen, Y., Kucharski, J.M., Feng, J., Ely, T., Chen, J.H., Firdaus, S.J., Babbar, A., Ren, P.,

Liu, Y., 2016. Selective Inhibition of Oncogenic KRAS Output with Small Molecules Targeting the Inactive State. Cancer Discov 6, 316–329. https://doi.org/10.1158/2159-8290.CD-15-1105

Pawlik, T.M., Keyomarsi, K., 2004. Role of cell cycle in mediating sensitivity to radiotherapy. Int J Radiat Oncol Biol Phys 59, 928–942. https://doi.org/10.1016/j.ijrobp.2004.03.005

Peng, Y., Fu, S., Hu, W., Qiu, Y., Zhang, L., Tan, R., Sun, L.-Q., 2020a. Glutamine synthetase facilitates cancer cells to recover from irradiation-induced G2/M arrest. Cancer Biology & Therapy 21, 43–51. https://doi.org/10.1080/15384047.2019.1665394

Peng, Y., Fu, S., Hu, W., Qiu, Y., Zhang, L., Tan, R., Sun, L.-Q., 2020b. Glutamine synthetase facilitates cancer cells to recover from irradiation-induced G2/M arrest. Cancer Biol Ther 21, 43–51. https://doi.org/10.1080/15384047.2019.1665394

Phillips, T.M., McBride, W.H., Pajonk, F., 2006. The Response of CD24 −/low /CD44 + Breast Cancer–Initiating Cells to Radiation. JNCI: Journal of the National Cancer Institute 98, 1777–1785. https://doi.org/10.1093/jnci/djj495

Prior, I.A., Hood, F.E., Hartley, J.L., 2020a. The Frequency of Ras Mutations in Cancer. Cancer Res 80, 2969–2974. https://doi.org/10.1158/0008-5472.CAN-19-3682

Prior, I.A., Hood, F.E., Hartley, J.L., 2020b. The Frequency of Ras Mutations in Cancer. Cancer Research 80, 2969–2974. https://doi.org/10.1158/0008-5472.CAN-19-3682

Purvis, J.E., Karhohs, K.W., Mock, C., Batchelor, E., Loewer, A., Lahav, G., 2012. p53 dynamics control cell fate. Science 336, 1440–1444. https://doi.org/10.1126/science.1218351

Quinlan, M.P., Settleman, J., 2009. Isoform-specific ras functions in development and cancer. Future Oncology 5, 105–116. https://doi.org/10.2217/14796694.5.1.105

Rait, A., Pirollo, K., Will, D.W., Peyman, A., Rait, V., Uhlmann, E., Chang, E.H., 2000. 3'-End conjugates of minimally phosphorothioate-protected oligonucleotides with 1-O-hexadecylglycerol: synthesis and anti-ras activity in radiation-resistant cells. Bioconjug Chem 11, 153–160. https://doi.org/10.1021/bc990106n

Rait, Antonina, Pirollo, K., Will, D.W., Peyman, A., Rait, V., Uhlmann, E., Chang, E.H., 2000. 3`-End Conjugates of Minimally Phosphorothioate-Protected Oligonucleotides with 1- *O* -Hexadecylglycerol: Synthesis and Anti- *ras* Activity in Radiation-Resistant Cells. Bioconjugate Chem. 11, 153–160. https://doi.org/10.1021/bc990106n

Rakotomalala, A., Escande, A., Furlan, A., Meignan, S., Lartigau, E., 2021. Hypoxia in Solid Tumors: How Low Oxygenation Impacts the "Six Rs" of Radiotherapy. Front. Endocrinol. 12, 742215. https://doi.org/10.3389/fendo.2021.742215

Raleigh, D.R., Haas-Kogan, D.A., 2013. Molecular targets and mechanisms of radiosensitization using DNA damage response pathways. Future Oncology 9, 219–233. https://doi.org/10.2217/fon.12.185

Rascio, F., Spadaccino, F., Rocchetti, M.T., Castellano, G., Stallone, G., Netti, G.S., Ranieri, E., 2021. The Pathogenic Role of PI3K/AKT Pathway in Cancer Onset and Drug Resistance: An Updated Review. Cancers 13, 3949. https://doi.org/10.3390/cancers13163949

Ravanat, J.-L., Breton, J., Douki, T., Gasparutto, D., Grand, A., Rachidi, W., Sauvaigo, S., 2014. Radiation-mediated formation of complex damage to DNA: a chemical aspect overview. Br J Radiol 87, 20130715. https://doi.org/10.1259/bjr.20130715

Reaper, P.M., Griffiths, M.R., Long, J.M., Charrier, J.-D., Maccormick, S., Charlton, P.A., Golec, J.M.C., Pollard, J.R., 2011. Selective killing of ATM- or p53-deficient cancer cells through inhibition of ATR. Nat Chem Biol 7, 428–430. https://doi.org/10.1038/nchembio.573

Redon, C.E., Nakamura, A.J., Zhang, Y.-W., Ji, J.J., Bonner, W.M., Kinders, R.J., Parchment, R.E., Doroshow, J.H., Pommier, Y., 2010. Histone gammaH2AX and poly(ADP-ribose) as clinical pharmacodynamic biomarkers. Clin Cancer Res 16, 4532–4542. https://doi.org/10.1158/1078-0432.CCR-10-0523

Resnick, M.A., 1976. The repair of double-strand breaks in DNA; a model involving recombination. J Theor Biol 59, 97–106. https://doi.org/10.1016/s0022-5193(76)80025-2

Rey, S., Schito, L., Koritzinsky, M., Wouters, B.G., 2017. Molecular targeting of hypoxia in radiotherapy. Advanced Drug Delivery Reviews 109, 45–62. https://doi.org/10.1016/j.addr.2016.10.002

Reynders, K., Illidge, T., Siva, S., Chang, J.Y., De Ruysscher, D., 2015. The abscopal effect of local radiotherapy: using immunotherapy to make a rare event clinically relevant. Cancer Treat Rev 41, 503–510. https://doi.org/10.1016/j.ctrv.2015.03.011

Riabinska, A., Daheim, M., Herter-Sprie, G.S., Winkler, J., Fritz, C., Hallek, M., Thomas, R.K., Kreuzer, K.-A., Frenzel, L.P., Monfared, P., Martins-Boucas, J., Chen, S., Reinhardt, H.C., 2013. Therapeutic targeting of a robust non-oncogene addiction to PRKDC in ATM-defective tumors. Sci Transl Med 5, 189ra78. https://doi.org/10.1126/scitranslmed.3005814

Riely, G.J., Ou, S.-H.I., Rybkin, I., Spira, A., Papadopoulos, K., Sabari, J.K., Johnson, M., Heist, R.S., Bazhenova, L., Barve, M., Pacheco, J.M., Velastegui, K., Cilliers, C., Olson, P., Christensen, J.G., Kheoh, T., Chao, R.C., Jänne, P.A., 2021. 99O_PR KRYSTAL-1: Activity and preliminary pharmacodynamic (PD) analysis of adagrasib (MRTX849) in patients (Pts) with advanced non–small cell lung cancer (NSCLC) harboring KRASG12C mutation. Journal of Thoracic Oncology 16, S751–S752. https://doi.org/10.1016/S1556-0864(21)01941-9

Rogakou, E.P. ;Plich, D.R.,Orr A.H., Bonner, W.M.,1998. DAN Double-stranded breaks induce histone H2AX phosphorylation on Serine 139. Journal of Biological Chemistry 273,5858-5868. https://doi.org/10.1074/jbc.273.10.5858

Roh, M.S., Colangelo, L.H., O'Connell, M.J., Yothers, G., Deutsch, M., Allegra, C.J., Kahlenberg, M.S., Baez-Diaz, L., Ursiny, C.S., Petrelli, N.J., Wolmark, N., 2009. Preoperative multimodality therapy improves disease-free survival in patients with carcinoma of the rectum: NSABP R-03. J Clin Oncol 27, 5124–5130. https://doi.org/10.1200/JCO.2009.22.0467

Roth, A.D., Tejpar, S., Delorenzi, M., Yan, P., Fiocca, R., Klingbiel, D., Dietrich, D., Biesmans, B., Bodoky, G., Barone, C., Aranda, E., Nordlinger, B., Cisar, L., Labianca, R., Cunningham, D., Van Cutsem, E., Bosman, F., 2010. Prognostic role of KRAS and BRAF in stage II and III resected colon cancer: results of the translational study on the PETACC-3, EORTC 40993, SAKK 60-00 trial. J Clin Oncol 28, 466–474. https://doi.org/10.1200/JCO.2009.23.3452

Roth, D.B., Porter, T.N., Wilson, J.H., 1985. Mechanisms of nonhomologous recombination in mammalian cells. Mol Cell Biol 5, 2599–2607. https://doi.org/10.1128/mcb.5.10.2599-2607.1985

Roux, P.P., Blenis, J., 2004. ERK and p38 MAPK-activated protein kinases: a family of protein kinases with diverse biological functions. Microbiol Mol Biol Rev 68, 320–344. https://doi.org/10.1128/MMBR.68.2.320-344.2004

Ruers, T., Punt, C., Van Coevorden, F., Pierie, J.P.E.N., Borel-Rinkes, I., Ledermann, J.A., Poston, G., Bechstein, W., Lentz, M.A., Mauer, M., Van Cutsem, E., Lutz, M.P., Nordlinger, B., EORTC Gastro-Intestinal Tract Cancer Group, Arbeitsgruppe Lebermetastasen und—tumoren in der Chirurgischen Arbeitsgemeinschaft Onkologie (ALM-CAO) and the National Cancer Research Institute Colorectal Clinical Study Group (NCRI CCSG), 2012. Radiofrequency ablation combined with systemic treatment versus systemic treatment alone in patients with non-resectable colorectal liver metastases: a randomized EORTC Intergroup phase II study (EORTC 40004). Ann Oncol 23, 2619–2626. https://doi.org/10.1093/annonc/mds053

Ruppert, R., Junginger, T., Ptok, H., Strassburg, J., Maurer, C.A., Brosi, P., Sauer, J., Baral, J., Kreis, M., Wollschlaeger, D., Hermanek, P., Merkel, S., OCUM group, 2018. Oncological outcome after MRI-based selection for neoadjuvant chemoradiotherapy in the OCUM Rectal Cancer Trial. Br J Surg 105, 1519–1529. https://doi.org/10.1002/bjs.10879

Russell, J.S., Lang, F.F., Huet, T., Janicot, M., Chada, S., Wilson, D.R., Tofilon, P.J., 1999a. Radiosensitization of human tumor cell lines induced by the adenovirus-mediated expression of an anti-Ras single-chain antibody fragment. Cancer Res 59, 5239–5244.

Russell, J.S., Lang, F.F., Huet, T., Janicot, M., Chada, S., Wilson, D.R., Tofilon, P.J., 1999b. Radiosensitization of human tumor cell lines induced by the adenovirus-mediated expression of an anti-Ras single-chain antibody fragment. Cancer Res 59, 5239–5244.

Russo, A.L., Ryan, D.P., Borger, D.R., Wo, J.Y., 2014. Mutational and clinical predictors of pathologic complete response in the treatment of locally advanced rectal cancer. J Gastrointest Cancer 45, 34–39. https://doi.org/10.1007/s12029-013-9546-y

Sage, E., Shikazono, N., 2017. Radiation-induced clustered DNA lesions: Repair and mutagenesis. Free Radic Biol Med 107, 125–135. https://doi.org/10.1016/j.freeradbiomed.2016.12.008

Sakamoto, K., Lin, B., Nunomura, K., Izawa, T., Nakagawa, S., 2022. The K-Ras(G12D)-inhibitory peptide KS-58 suppresses growth of murine CT26 colorectal cancer cell-derived tumors. Sci Rep 12, 8121. https://doi.org/10.1038/s41598-022-12401-3

Santivasi, W.L., Xia, F., 2014. Ionizing Radiation-Induced DNA Damage, Response, and Repair. Antioxidants & Redox Signaling 21, 251–259. https://doi.org/10.1089/ars.2013.5668

Sato, H., Niimi, A., Yasuhara, T., Permata, T.B.M., Hagiwara, Y., Isono, M., Nuryadi, E., Sekine, R., Oike, T., Kakoti, S., Yoshimoto, Y., Held, K.D., Suzuki, Y., Kono, K., Miyagawa, K., Nakano, T., Shibata, A., 2017. DNA double-strand break repair pathway regulates PD-L1 expression in cancer cells. Nat Commun 8, 1751. https://doi.org/10.1038/s41467-017-01883-9

Sauer, R., Liersch, T., Merkel, S., Fietkau, R., Hohenberger, W., Hess, C., Becker, H., Raab, H.-R., Villanueva, M.-T., Witzigmann, H., Wittekind, C., Beissbarth, T., Rödel, C., 2012. Preoperative versus postoperative chemoradiotherapy for locally advanced rectal cancer: results of the German CAO/ARO/AIO-94 randomized phase III trial after a median follow-up of 11 years. J Clin Oncol 30, 1926–1933. https://doi.org/10.1200/JCO.2011.40.1836

Schiller, J.H., Adak, S., Feins, R.H., Keller, S.M., Fry, W.A., Livingston, R.B., Hammond, M.E., Wolf, B., Sabatini, L., Jett, J., Kohman, L., Johnson, D.H., 2001. Lack of prognostic significance of p53 and K-ras mutations in primary resected non-small-cell lung cancer on E4592: a Laboratory Ancillary Study on an Eastern Cooperative Oncology Group Prospective Randomized Trial of Postoperative Adjuvant Therapy. J Clin Oncol 19, 448–457. https://doi.org/10.1200/JCO.2001.19.2.448

Schlesinger, T.K., Fanger, G.R., Yujiri, T., Johnson, G.L., 1998. The TAO of MEKK. Front Biosci 3, D1181-1186. https://doi.org/10.2741/a354

Schmukler, E., Grinboim, E., Schokoroy, S., Amir, A., Wolfson, E., Kloog, Y., Pinkas-Kramarski, R., 2013. Ras inhibition enhances autophagy, which partially protects cells from death. Oncotarget 4, 142–152. https://doi.org/10.18632/oncotarget.703

Schuch, A.P., Garcia, C.C.M., Makita, K., Menck, C.F.M., 2013. DNA damage as a biological sensor for environmental sunlight. Photochem Photobiol Sci 12, 1259–1272. https://doi.org/10.1039/c3pp00004d

Sebag-Montefiore, D., Stephens, R.J., Steele, R., Monson, J., Grieve, R., Khanna, S., Quirke, P., Couture, J., de Metz, C., Myint, A.S., Bessell, E., Griffiths, G., Thompson, L.C., Parmar, M., 2009. Preoperative radiotherapy versus selective postoperative chemoradiotherapy in patients with rectal cancer (MRC CR07 and NCIC-CTG C016): a multicentre, randomised trial. Lancet 373, 811–820. https://doi.org/10.1016/S0140-6736(09)60484-0

Serna-Blasco, R., Sanz-Álvarez, M., Aguilera, Ó., García-Foncillas, J., 2019. Targeting the RAS-dependent chemoresistance: The Warburg connection. Semin Cancer Biol 54, 80–90. https://doi.org/10.1016/j.semcancer.2018.01.016

Seymour, C.B., Mothersill, C., 1997. Delayed expression of lethal mutations and genomic instability in the progeny of human epithelial cells that survived in a bystander-killing environment. Radiat Oncol Investig 5, 106–110. https://doi.org/10.1002/(SICI)1520-6823(1997)5:3<106::AID-ROI4>3.0.CO;2-1

Sharda, N., Yang, C.-R., Kinsella, T., Boothman, D., 2002. Radiation Resistance, in: Encyclopedia of Cancer. Elsevier, pp. 1–11. https://doi.org/10.1016/B0-12-227555-1/00519-0
Shields, J.M., Pruitt, K., McFall, A., Shaub, A., Der, C.J., 2000. Understanding Ras: 'it ain't over "til it's over." Trends Cell Biol 10, 147–154. https://doi.org/10.1016/s0962-8924(00)01740-2
Siddiqui, M.S., François, M., Fenech, M.F., Leifert, W.R., 2015. Persistent γH2AX: A promising molecular marker of DNA damage and aging. Mutat Res Rev Mutat Res 766, 1–19. https://doi.org/10.1016/j.mrrev.2015.07.001
Simanshu, D.K., Nissley, D.V., McCormick, F., 2017. RAS Proteins and Their Regulators in Human Disease. Cell 170, 17–33. https://doi.org/10.1016/j.cell.2017.06.009
Sinclair, W.K., 2012. Cyclic X-ray responses in mammalian cells in vitro. 1968. Radiat Res 178, AV112-124. https://doi.org/10.1667/rrav09.1
Sinclair, W.K., 1967. Hydroxyurea: effects on Chinese hamster cells grown in culture. Cancer Res 27, 297–308.
Sinclair, W.K., Morton, R.A., 1966. X-ray sensitivity during the cell generation cycle of cultured Chinese hamster cells. Radiat Res 29, 450–474.
Sinclair, W.K., Morton, R.A., 1963. VARIATIONS IN X-RAY RESPONSE DURING THE DIVISION CYCLE OF PARTIALLY SYNCHRONIZED CHINESE HAMSTER CELLS IN CULTURE. Nature 199, 1158–1160. https://doi.org/10.1038/1991158a0
Sklar, M. D., 1988a. The ras oncogenes increase the intrinsic resistance of NIH 3T3 cells to ionizing radiation. Science 239, 645–647. https://doi.org/10.1126/science.3277276
Sklar, M. D., 1988b. Increased resistance to cis-diamminedichloroplatinum(II) in NIH 3T3 cells transformed by ras oncogenes. Cancer Res 48, 793–797.
Sklar, Marshall D., 1988. The *ras* Oncogenes Increase the Intrinsic Resistance of NIH 3T3 Cells to Ionizing Radiation. Science 239, 645–647. https://doi.org/10.1126/science.3277276
Skoulidis, F., Byers, L.A., Diao, L., Papadimitrakopoulou, V.A., Tong, P., Izzo, J., Behrens, C., Kadara, H., Parra, E.R., Canales, J.R., Zhang, Jianjun, Giri, U., Gudikote, J., Cortez, M.A., Yang, C., Fan, Y., Peyton, M., Girard, L., Coombes, K.R., Toniatti, C., Heffernan, T.P., Choi, M., Frampton, G.M., Miller, V., Weinstein, J.N., Herbst, R.S., Wong, K.-K., Zhang, Jianhua, Sharma, P., Mills, G.B., Hong, W.K., Minna, J.D., Allison, J.P., Futreal, A., Wang, J., Wistuba, I.I., Heymach, J.V., 2015. Co-occurring Genomic Alterations Define Major Subsets of *KRAS* -Mutant Lung Adenocarcinoma with Distinct Biology, Immune Profiles, and Therapeutic Vulnerabilities. Cancer Discovery 5, 860–877. https://doi.org/10.1158/2159-8290.CD-14-1236
Skoulidis, F., Heymach, J.V., 2019. Co-occurring genomic alterations in non-small-cell lung cancer biology and therapy. Nat Rev Cancer 19, 495–509. https://doi.org/10.1038/s41568-019-0179-8
Slebos, R.J., Kibbelaar, R.E., Dalesio, O., Kooistra, A., Stam, J., Meijer, C.J., Wagenaar, S.S., Vanderschueren, R.G., van Zandwijk, N., Mooi, W.J., 1990. K-ras oncogene activation as a prognostic marker in adenocarcinoma of the lung. N Engl J Med 323, 561–565. https://doi.org/10.1056/NEJM199008303230902

Slebos, R.J.C., Kibbelaar, R.E., Dalesio, O., Kooistra, A., Stam, J., Meijer, C.J.L.M., Wagenaar, S.S., Vanderschueren, R.G.J.R.A., van Zandwijk, N., Mooi, W.J., Bos, J.L., Rodenhuis, S., 1990. K- *ras* Oncogene Activation as a Prognostic Marker in Adenocarcinoma of the Lung. N Engl J Med 323, 561–565. https://doi.org/10.1056/NEJM199008303230902

Smith, T.A., Kirkpatrick, D.R., Smith S., Smith, T.K., 2017. Radioprotective agents to prevent cellular damage due to ionizing radiation. Journal of Translational Medicine 15, 232. https://doi.org/10.1186/s12967-017-1338-x

Soh, J., Okumura, N., Lockwood, W.W., Yamamoto, H., Shigematsu, H., Zhang, W., Chari, R., Shames, D.S., Tang, X., MacAulay, C., Varella-Garcia, M., Vooder, T., Wistuba, I.I., Lam, S., Brekken, R., Toyooka, S., Minna, J.D., Lam, W.L., Gazdar, A.F., 2009. Oncogene Mutations, Copy Number Gains and Mutant Allele Specific Imbalance (MASI) Frequently Occur Together in Tumor Cells. PLoS ONE 4, e7464. https://doi.org/10.1371/journal.pone.0007464

Spira, A.I., Riely, G.J., Gadgeel, S.M., Heist, R.S., Ou, S.-H.I., Pacheco, J.M., Johnson, M.L., Sabari, J.K., Leventakos, K., Yau, E., Bazhenova, L., Negrao, M.V., Pennell, N.A., Zhang, J., Velastegui, K., Christensen, J.G., yan, xiaohong, Anderes, K.L., Chao, R.C., Janne, P.A., 2022. KRYSTAL-1: Activity and safety of adagrasib (MRTX849) in patients with advanced/metastatic non–small cell lung cancer (NSCLC) harboring a KRAS ^{G12C} mutation. JCO 40, 9002–9002. https://doi.org/10.1200/JCO.2022.40.16_suppl.9002

Srivastava, M., Nambiar, M., Sharma, S., Karki, S.S., Goldsmith, G., Hegde, M., Kumar, S., Pandey, M., Singh, R.K., Ray, P., Natarajan, R., Kelkar, M., De, A., Choudhary, B., Raghavan, S.C., 2012. An inhibitor of nonhomologous end-joining abrogates double-strand break repair and impedes cancer progression. Cell 151, 1474–1487. https://doi.org/10.1016/j.cell.2012.11.054

Steel, G.G., 1994. Cell synchronization unfortunately may not benefit cancer therapy. Radiother Oncol 32, 95–97. https://doi.org/10.1016/0167-8140(94)90094-9

Steel, G.G., McMillan, T.J., Peacock, J.H., 1989. The 5Rs of radiobiology. Int J Radiat Biol 56, 1045–1048. https://doi.org/10.1080/09553008914552491

Stewart, G.S., Wang, B., Bignell, C.R., Taylor, A.M.R., Elledge, S.J., 2003. MDC1 is a mediator of the mammalian DNA damage checkpoint. Nature 421, 961–966. https://doi.org/10.1038/nature01446

Stewart, R.D., 2018. Induction of DNA Damage by Light Ions Relative to 60Co γ-rays. Int J Part Ther 5, 25–39. https://doi.org/10.14338/IJPT-18-00030

Strauss, L., Mahmoud, M.A.A., Weaver, J.D., Tijaro-Ovalle, N.M., Christofides, A., Wang, Q., Pal, R., Yuan, M., Asara, J., Patsoukis, N., Boussiotis, V.A., 2020. Targeted deletion of PD-1 in myeloid cells induces antitumor immunity. Sci. Immunol. 5, eaay1863. https://doi.org/10.1126/sciimmunol.aay1863

Sun, R., Sbai, A., Ganem, G., Boudabous, M., Collin, F., Marcy, P.-Y., Doglio, A., Thariat, J., 2014. [Non-targeted effects (bystander, abscopal) of external beam radiation therapy: an overview for the clinician]. Cancer Radiother 18, 770–778. https://doi.org/10.1016/j.canrad.2014.08.004

Tanaka, H., Deng, G., Matsuzaki, K., Kakar, S., Kim, G.E., Miura, S., Sleisenger, M.H., Kim, Y.S., 2006. BRAF mutation, CpG island methylator phenotype and microsatellite instability occur more frequently and concordantly in mucinous

than non-mucinous colorectal cancer. Int J Cancer 118, 2765–2771. https://doi.org/10.1002/ijc.21701
Taylor, F.G.M., Quirke, P., Heald, R.J., Moran, B.J., Blomqvist, L., Swift, I.R., Sebag-Montefiore, D., Tekkis, P., Brown, G., Magnetic Resonance Imaging in Rectal Cancer European Equivalence Study Study Group, 2014. Preoperative magnetic resonance imaging assessment of circumferential resection margin predicts disease-free survival and local recurrence: 5-year follow-up results of the MERCURY study. J Clin Oncol 32, 34–43. https://doi.org/10.1200/JCO.2012.45.3258
Terasima, T., Tolmach, L.J., 1963a. X-ray sensitivity and DNA synthesis in synchronous populations of HeLa cells. Science 140, 490–492. https://doi.org/10.1126/science.140.3566.490
Terasima, T., Tolmach, L.J., 1963b. Variations in several responses of HeLa cells to x-irradiation during the division cycle. Biophys J 3, 11–33. https://doi.org/10.1016/s0006-3495(63)86801-0
Toulany, M., Rodemann, H.P., 2015. Phosphatidylinositol 3-kinase/Akt signaling as a key mediator of tumor cell responsiveness to radiation. Semin Cancer Biol 35, 180–190. https://doi.org/10.1016/j.semcancer.2015.07.003
Trujillo, K.M., Yuan, S.-S.F., Lee, E.Y.-H.P., Sung, P., 1998. Nuclease Activities in a Complex of Human Recombination and DNA Repair Factors Rad50, Mre11, and p95. Journal of Biological Chemistry 273, 21447–21450. https://doi.org/10.1074/jbc.273.34.21447
Tsao, M.-S., Aviel-Ronen, S., Ding, K., Lau, D., Liu, N., Sakurada, A., Whitehead, M., Zhu, C.-Q., Livingston, R., Johnson, D.H., Rigas, J., Seymour, L., Winton, T., Shepherd, F.A., 2007. Prognostic and predictive importance of p53 and RAS for adjuvant chemotherapy in non small-cell lung cancer. J Clin Oncol 25, 5240–5247. https://doi.org/10.1200/JCO.2007.12.6953
Tseng, M., Soon, Y.Y., Vellayappan, B., Ho, F., Tey, J., 2019. Radiation therapy for rectal cancer. J Gastrointest Oncol 10, 1238–1250. https://doi.org/10.21037/jgo.2018.12.04
Turan, V., Oktay, K., 2020. BRCA-related ATM-mediated DNA double-strand break repair and ovarian aging. Hum Reprod Update 26, 43–57. https://doi.org/10.1093/humupd/dmz043
Tutt, A., Connor, F., Bertwistle, D., Kerr, P., Peacock, J., Ross, G., Ashworth, A., 2003. Cell cycle and genetic background dependence of the effect of loss of BRCA2 on ionizing radiation sensitivity. Oncogene 22, 2926–2931. https://doi.org/10.1038/sj.onc.1206522
Ulkü, A.S., Der, C.J., 2003. Ras signaling, deregulation of gene expression and oncogenesis. Cancer Treat Res 115, 189–208.
Vaupel, P., 2004. Tumor microenvironmental physiology and its implications for radiation oncology. Semin Radiat Oncol 14, 198–206. https://doi.org/10.1016/j.semradonc.2004.04.008
Vaupel, P., Schmidberger, H., Mayer, A., 2019. The Warburg effect: essential part of metabolic reprogramming and central contributor to cancer progression. Int J Radiat Biol 95, 912–919. https://doi.org/10.1080/09553002.2019.1589653

Vigil, D., Cherfils, J., Rossman, K.L., Der, C.J., 2010. Ras superfamily GEFs and GAPs: validated and tractable targets for cancer therapy? Nat Rev Cancer 10, 842–857. https://doi.org/10.1038/nrc2960
Vivanco, I., Sawyers, C.L., 2002. The phosphatidylinositol 3-Kinase AKT pathway in human cancer. Nat Rev Cancer 2, 489–501. https://doi.org/10.1038/nrc839
Vlatkovic, T., Veldwijk, M.R., Giordano, F.A., Herskind, C., 2022. Targeting Cell Cycle Checkpoint Kinases to Overcome Intrinsic Radioresistance in Brain Tumor Cells. Cancers (Basel) 14, 701. https://doi.org/10.3390/cancers14030701
Voicu, P.-M., Petrescu-Danila, E., Poitelea, M., Watson, A.T., Rusu, M., 2007. In Schizosaccharomyces pombe the 14-3-3 protein Rad24p is involved in negative control of pho1 gene expression. Yeast 24, 121–127. https://doi.org/10.1002/yea.1433
Wang, G.L., Jiang, B.H., Rue, E.A., Semenza, G.L., 1995. Hypoxia-inducible factor 1 is a basic-helix-loop-helix-PAS heterodimer regulated by cellular O2 tension. Proc Natl Acad Sci U S A 92, 5510–5514. https://doi.org/10.1073/pnas.92.12.5510
Wang, H., Zhang, X., Teng, L., Legerski, R.J., 2015. DNA damage checkpoint recovery and cancer development. Experimental Cell Research 334, 350–358. https://doi.org/10.1016/j.yexcr.2015.03.011
Wang, Y., Cortez, D., Yazdi, P., Neff, N., Elledge, S.J., Qin, J., 2000. BASC, a super complex of BRCA1-associated proteins involved in the recognition and repair of aberrant DNA structures. Genes Dev 14, 927–939.
Ward, J.F., 1994. The complexity of DNA damage: relevance to biological consequences. Int J Radiat Biol 66, 427–432. https://doi.org/10.1080/09553009414551401
Wennerberg, K., Rossman, K.L., Der, C.J., 2005. The Ras superfamily at a glance. J Cell Sci 118, 843–846. https://doi.org/10.1242/jcs.01660
West, C.M., Davidson, S.E., Hunter, R.D., 1989. Evaluation of surviving fraction at 2 Gy as a potential prognostic factor for the radiotherapy of carcinoma of the cervix. Int J Radiat Biol 56, 761–765. https://doi.org/10.1080/09553008914552011
West, C.M., Davidson, S.E., Roberts, S.A., Hunter, R.D., 1993. Intrinsic radiosensitivity and prediction of patient response to radiotherapy for carcinoma of the cervix. Br J Cancer 68, 819–823. https://doi.org/10.1038/bjc.1993.434
Williams, T.M., Flecha, A.R., Keller, P., Ram, A., Karnak, D., Galbán, S., Galbán, C.J., Ross, B.D., Lawrence, T.S., Rehemtulla, A., Sebolt-Leopold, J., 2012a. Cotargeting MAPK and PI3K signaling with concurrent radiotherapy as a strategy for the treatment of pancreatic cancer. Mol Cancer Ther 11, 1193–1202. https://doi.org/10.1158/1535-7163.MCT-12-0098
Williams, T.M., Flecha, A.R., Keller, P., Ram, A., Karnak, D., Galbán, S., Galbán, C.J., Ross, B.D., Lawrence, T.S., Rehemtulla, A., Sebolt-Leopold, J., 2012b. Cotargeting MAPK and PI3K Signaling with Concurrent Radiotherapy as a Strategy for the Treatment of Pancreatic Cancer. Molecular Cancer Therapeutics 11, 1193–1202. https://doi.org/10.1158/1535-7163.MCT-12-0098
Wilson, W.R., Hay, M.P., 2011. Targeting hypoxia in cancer therapy. Nat Rev Cancer 11, 393–410. https://doi.org/10.1038/nrc3064
Withers, H.R., 1975. The Four R's of Radiotherapy, in: Advances in Radiation Biology. Elsevier, pp. 241–271. https://doi.org/10.1016/B978-0-12-035405-4.50012-8

Wlodek, D., Hittelman, W.N., 1988. The relationship of DNA and chromosome damage to survival of synchronized X-irradiated L5178Y cells. I. Initial damage. Radiat Res 115, 550–565.

Wo, J.Y., Anker, C.J., Ashman, J.B., Bhadkamkar, N.A., Bradfield, L., Chang, D.T., Dorth, J., Garcia-Aguilar, J., Goff, D., Jacqmin, D., Kelly, P., Newman, N.B., Olsen, J., Raldow, A.C., Ruiz-Garcia, E., Stitzenberg, K.B., Thomas, C.R., Wu, Q.J., Das, P., 2021. Radiation Therapy for Rectal Cancer: Executive Summary of an ASTRO Clinical Practice Guideline. Practical Radiation Oncology 11, 13–25. https://doi.org/10.1016/j.prro.2020.08.004

Wohlgemuth, S., Kiel, C., Krämer, A., Serrano, L., Wittinghofer, F., Herrmann, C., 2005. Recognizing and Defining True Ras Binding Domains I: Biochemical Analysis. Journal of Molecular Biology 348, 741–758. https://doi.org/10.1016/j.jmb.2005.02.048

Wu, Q., Paul, A., Su, D., Mehmood, S., Foo, T.K., Ochi, T., Bunting, E.L., Xia, B., Robinson, C.V., Wang, B., Blundell, T.L., 2016. Structure of BRCA1-BRCT/Abraxas Complex Reveals Phosphorylation-Dependent BRCT Dimerization at DNA Damage Sites. Molecular Cell 61, 434–448. https://doi.org/10.1016/j.molcel.2015.12.017

Xue, J., Kubicek, G., Patel, A., Goldsmith, B., Asbell, S.O., LaCouture, T.A., 2016. Validity of Current Stereotactic Body Radiation Therapy Dose Constraints for Aorta and Major Vessels. Seminars in Radiation Oncology 26, 135–139. https://doi.org/10.1016/j.semradonc.2015.11.001

Yaeger, R., Weiss, J., Pelster, M.S., Spira, A.I., Barve, M., Ou, S.-H.I., Leal, T.A., Bekaii-Saab, T.S., Paweletz, C.P., Heavey, G.A., Christensen, J.G., Velastegui, K., Kheoh, T., Der-Torossian, H., Klempner, S.J., 2023. Adagrasib with or without Cetuximab in Colorectal Cancer with Mutated *KRAS* G12C. N Engl J Med 388, 44–54. https://doi.org/10.1056/NEJMoa2212419

Yagishita, S., Horinouchi, H., Sunami, K.S., Kanda, S., Fujiwara, Y., Nokihara, H., Yamamoto, N., Sumi, M., Shiraishi, K., Kohno, T., Furuta, K., Tsuta, K., Tamura, T., Ohe, Y., 2015. Impact of KRAS mutation on response and outcome of patients with stage III non-squamous non-small cell lung cancer. Cancer Sci 106, 1402–1407. https://doi.org/10.1111/cas.12740

Yamashita, Y.M., Yuan, H., Cheng, J., Hunt, A.J., 2010. Polarity in Stem Cell Division: Asymmetric Stem Cell Division in Tissue Homeostasis. Cold Spring Harbor Perspectives in Biology 2, a001313–a001313. https://doi.org/10.1101/cshperspect.a001313

Young, A., Berry, R., Holloway, A.F., Blackburn, N.B., Dickinson, J.L., Skala, M., Phillips, J.L., Brettingham-Moore, K.H., 2014. RNA-seq profiling of a radiation resistant and radiation sensitive prostate cancer cell line highlights opposing regulation of DNA repair and targets for radiosensitization. BMC Cancer 14, 808. https://doi.org/10.1186/1471-2407-14-808

Yu, C.-C., Hung, S.-K., Lin, H.-Y., Chiou, W.-Y., Lee, M.-S., Liao, H.-F., Huang, H.-B., Ho, H.-C., Su, Y.-C., 2017. Targeting the PI3K/AKT/mTOR signaling pathway as an effectively radiosensitizing strategy for treating human oral squamous cell carcinoma *in vitro* and *in vivo*. Oncotarget 8, 68641–68653. https://doi.org/10.18632/oncotarget.19817

Zdrowowicz, M., Spisz, P., Hav, A., Herman-Antosie, A., Rak, J. 2022. Radiotherapy is a crucial cancer treatment. International Journal of Molecular Sciences, 23, 1429. https://doi.org/10.3390/ijms23031429

Zhang, X.F., Settleman, J., Kyriakis, J.M., Takeuchi-Suzuki, E., Elledge, S.J., Marshall, M.S., Bruder, J.T., Rapp, U.R., Avruch, J., 1993. Normal and oncogenic p21ras proteins bind to the amino-terminal regulatory domain of c-Raf-1. Nature 364, 308–313. https://doi.org/10.1038/364308a0

Zheng, Y., Liu, Y., Zhang, F., Su, C., Chen, X., Zhang, M., Sun, M., Sun, Y., Xing, L., 2023. Radiation combined with KRAS-MEK inhibitors enhances anticancer immunity in KRAS-mutated tumor models. Translational Research 252, 79–90. https://doi.org/10.1016/j.trsl.2022.08.005

Zhong, Q., Chen, C.-F., Li, S., Chen, Y., Wang, C.-C., Xiao, J., Chen, P.-L., Sharp, Z.D., Lee, W.-H., 1999. Association of BRCA1 with the hRad50-hMre11-p95 Complex and the DNA Damage Response. Science 285, 747–750. https://doi.org/10.1126/science.285.5428.747

Zhou, B.-B.S., Bartek, J., 2004. Targeting the checkpoint kinases: chemosensitization versus chemoprotection. Nat Rev Cancer 4, 216–225. https://doi.org/10.1038/nrc1296

Zhou, Y., Hancock, J.F., 2015. Ras nanoclusters: versatile lipid-based signaling platforms. 2015, Biochim Biophys Acta, 1853, 841-849. https://doi.org/10.1016/j.bbamcr.2014.09.008

Zhu, G., Pei, L., Xia, H., Tang., Q., Bu, F. 2021 Role of oncogenic KRAS in the prognosis, diagnosis and treatment of colorectal cancer. Mol Cancer, 20-143. https://doi.org/10.1186/s12943-021-01441-4

Zoli, W., Ricotti, L., Barzanti, F., Dal Susino, M., Frassineti, G.L., Milandri, C., Casadei Giunchi, D., Amadori, D., 1999. Schedule-dependent interaction of doxorubicin, paclitaxel and gemcitabine in human breast cancer cell lines. Int J Cancer 80, 413–416. https://doi.org/10.1002/(sici)1097-0215(19990129)80:3<413::aid-ijc13>3.0.co;2-i